Hippocampal Diffusion Tensor Imaging in Parkinson's Disease and Associations with Non-Motor Symptoms

by

Alexandra Sarah Budd

A thesis submitted in partial fulfillment of the requirements for the degree of

Master of Science

Centre of Neuroscience

University of Alberta

Abstract

Parkinson's disease (PD) is the second most common neurodegenerative disorder and causes not only well-characterised motor symptoms, but also a host of non-motor symptoms that greatly impact quality of life. PD exists within a larger spectrum of disorders caused by the accumulation of Lewy bodies within the brain. This spectrum also includes Dementia with Lewy Bodies (DLB), and different cognitive subtypes of PD, such as PD with mild cognitive impairment (PD-MCI) and PD with dementia (PDD). There is still much to be learnt about non-motor symptoms and progression in the brains of patients with diseases within the Lewy body spectrum. One region of the brain that may be implicated in non-motor symptoms is the hippocampus, which is a site that develops marked pathology as the disease spreads through the brain. However, few studies prior to this time have been able to investigate the microstructure of the hippocampus in PD and DLB patients in vivo, making it difficult to characterize ongoing non-motor symptoms and their relationship to non-motor symptoms in living patients.

Recently, a novel diffusion tensor imaging (DTI) technique has been developed to allow high resolution diffusion imaging of the hippocampus. In this project, high resolution imaging was used to first investigate hippocampal changes in 38 patients with Lewy body spectrum diseases relative to 40 healthy older adult controls. After an initial visual inspection of the hippocampi and counting of the hippocampal digitations, no overt differences between groups were apparent. Next, we determined the association between hippocampal measures and non-motor symptoms in participants with PD and DLB. We found that fractional anisotropy (FA), but not mean diffusivity (MD) or volume (as derived from DTI), was altered in the hippocampus of patients with PD and DLB, and that FA was decreased in patients with PD and DLB when compared to controls. Furthermore, diffusion measures were correlated with age, with FA and

volume decreasing and MD increasing with age as expected, but not all results were statistically significant across groups. In participants with PD and DLB, we found that patients with worse depression or sleep disturbances had higher FA than those who were less affected.

Using the new improved method of DTI for imaging the hippocampus has allowed a more in-depth look into the hippocampal structure of living patients with PD and DLB. However, further studies are needed to understand the reasons for the direction of diffusion changes uncovered. Further studies that examine the relationship between non-motor symptoms in regions and diffusion changes beyond the hippocampus proper are also needed.

Preface

This thesis is an original work by Alexandra Budd. The research project, of which this thesis is a part, received research ethics approval from the University of Alberta Research Ethics Board, project name: “Hippocampal Changes and Non-Motor Symptoms in Neurodegeneration and Aging.” Pro00106834, June 3, 2021.

Acknowledgements

This thesis would not have been possible without the contributions of several exceptional people. I am extremely grateful to my supervisor Dr. Richard Camicioli, who has been an incredible source of support and knowledge throughout this journey. I would also like to sincerely thank my committee members, Dr. Christian Beaulieu and Dr. Sanjay Kalra, as well as Dr. Myrlene Gee, who have all provided me with guidance and advice that has been crucial to my success in completing this thesis. I must also provide special thanks to Kevin Solar, who taught me the method for segmenting the hippocampus that is central to this thesis, as well as Dr. Zahinoor Ismail for his input on converting neuropsychiatric scores to the domains of mild behavioural impairment, and members of Dr. Camicioli's lab, including Krista Nelles, Brooklyn Mankasingh, and Lori Piquette, who helped obtain the clinical data used in this study and provided me with great feedback along the way. Finally, I would like to thank my fiancé Josh who has been a constant source of support and love throughout this entire process.

Table of Contents

List of Tables

List of Figures

List of Abbreviations

ACC	Anterior Cingulate Cortex
AD	Alzheimer's Disease
ADLs	Activities of Daily Living
ANOVA	Analysis of Variance
ATR	Anterior Thalamic Radiation
BG	Basal Ganglia
BVMT-R	Brief Visuospatial Memory Test – Revised
BW	Bandwidth
CA	Cornu Ammonis
CANTAB	Cambridge Neuropsychological Test Automated Battery
CB	Cingulate Bundle
CC	Corpus Callosum
CCNA	Canadian Consortium on Neurodegeneration in Aging
CDIP	Canadian Dementia Imaging Protocol
CERAD	Consortium to Establish a Registry for Alzheimer's Disease
CG	Cingulate Gyrus
COMPASS-ND	Comprehensive Assessment of Neurodegeneration and Dementia
CR	Corona Radiata
CSF	Cerebrospinal Fluid
CST	Corticospinal Tract
D_a	Axial Diffusivity
DG	Dentate Gyrus
D-KEFS	Delis-Kaplan Executive Function System
DLB	Dementia with Lewy Bodies
D_r	Radial Diffusivity
DSM-5	Diagnostic and Statistical Manual of Mental Disorders - Fifth Edition
DTI	Diffusion Tensor Imaging
DWI	Diffusion-Weighted Image
EC	External Capsule
EDS	Excessive Daytime Sleepiness
EF	Executive Function
EPI	Echo-Planar Imaging
ESS	Epworth Sleepiness Scale
FA	Fractional Anisotropy
FAVR	Functional Assessment of Vascular Reactivity

FCSRT	Free and Cued Selective Reminding Test
FDR	False Discovery Rate
FMa	Forceps Major
FMi	Forceps Minor
FRS	Framingham Risk Score
GAD	Generalized Anxiety Disorder
GAD-7	Generalized Anxiety Disorder 7-Item Scale
GDS-15	Geriatric Depression 15-Item Scale
GDS-30	Geriatric Depression 30-Item Scale
GM	Gray Matter
GP	Globus Pallidus
GRAPPA	Generalized Autocalibrating Partially Parallel Acquisition
HAMA	Hamilton Anxiety Rating Scale
HAMD	Hamilton Depression Rating Scale
HC	Healthy Control
HSD	Honestly Significant Difference
IC	Internal Capsule
ICC	Intra-class Correlation Coefficient
ICD	Impulse Control Disorder
ICP	Inferior Cerebellar Peduncle
IFG	Inferior Frontal Gyrus
IFOF	Inferior Fronto-Occipital Fasciculus
ILF	Inferior Longitudinal Fasciculus
IPG	Inferior Parietal Gyrus
LB	Lewy Body
LBD	Lewy Body Dementia
LED	Levodopa Equivalent Dose
LN	Lewy Neurite
LORIS	Longitudinal Online Research and Imaging System
MBI	Mild Behavioural Impairment
MCI	Mild Cognitive Impairment
MCP	Middle Cerebellar Peduncle
MD	Mean Diffusivity
MDS-UPDRS	Movement Disorder Society-Sponsored Revision of the Unified Parkinson's Disease Rating Scale
MFG	Middle Frontal Gyrus
MMSE	Mini-Mental State Examination
MoCA	Montreal Cognitive Assessment
MRI	Magnetic Resonance Imaging
NBM	Nucleus Basalis of Meynert
NMSS	Non-Motor Symptoms Scale

NODDI	Neurite Orientation Dispersion and Density Imaging
NPI	Neuropsychiatric Inventory
OFC	Orbitofrontal Cortex
PASE	Physical Activity Scale for the Elderly
PD	Parkinson's Disease
PD-CRS	Parkinson's Disease - Cognitive Rating Scale
PDD	Parkinson's Disease with Dementia
PD-MCI	Parkinson's Disease with Mild Cognitive Impairment
PDQ-39	Parkinson’s Disease Questionnaire (39 items)
PDSS	Parkinson's Disease Sleep Scale
PPF	Phase Partial Fourier
PPN	Pedunculopontine Nucleus
PTR	Posterior Thalamic Radiation
QoL	Quality of Life
RAVLT	Rey’s Auditory Verbal Learning Test
RBANS	Repeatable Battery for the Assessment of Neuropsychological Status
RBD	Rapid Eye Movement Sleep Behaviour Disorder
RCFT	Rey Complex Figure Test
REM	Rapid Eye Movement
ROI	Region of Interest
SCP	Superior Cerebellar Peduncle
SD	Standard Deviation
SFG	Superior Frontal Gyrus
SFOF	Superior Fronto-Occipital Fasciculus
SI	Summary Index
SLF	Superior Longitudinal Fasciculus
SN	Substantia Nigra
SWS	Slow Wave Sleep
TE	Time to Echo
TMT	Trail Making Test
TR	Repetition Time
UF	Uncinate Fasciculus
VH	Visual Hallucinations
WAIS-III	Wechsler Adult Intelligence Scale, Third Edition
WM	White Matter

Chapter 1 Introduction

An Introduction to Parkinson's Disease and the Lewy Body Spectrum

The Lewy Body Spectrum and its History

In 1817, James Parkinson published *An Essay of the Shaking Palsy* (1), in which he cautiously presented his preliminary observations of what has now come to be known as Parkinson's Disease (PD), stating:

> By these repeated observations, he hoped that he had been led to a probable conjecture as to the nature of the malady, and that analogy had suggested such means as might be productive of relief, and perhaps even of cure, if employed before the disease had been too long established. He therefore considered it to be a duty to submit his opinions to the examination of others, even in their present state of immaturity and imperfection. (p. 223)

Although he was the first to bring attention to PD as a distinct disorder accompanied by characteristic symptoms, Parkinson noted that he was not the first to observe such symptoms in patients. The disease had likely afflicted people for a long time before his publication (1).

Indeed, in Ancient Indian literature, the surgeon Susruta referred to symptoms such as slowness, akinesia, rigidity, and tremor in 600 BC (2), and writings in the 15th century refer to a disease called *kambavata* which was characterised by tremor (*kampa*) and rigidity (*stambha*) (3). Similarly, descriptions of symptoms characteristic of PD can be found in medical literature from Ancient China. In a collection of observations of medical providers from around 425-221 BC, a condition was described that caused a person to develop a stooped posture, rigidity in the legs, and tremor while walking (4). Another example dating from 220-228 AD includes a description

of fast walking that turns into running without the ability to slow down (4). Western medical texts that mention these characteristic symptoms have also been found, one of the first being from Galen in the 2nd century, who described uncontrollable movements accompanied by psychological distress and depression, as well as a condition in which people had trouble walking straight and raising their foot from the ground (5).

Today, our ability to identify Parkinson's Disease has allowed us to study this disease on a large scale, which is aided by the fact that PD is the second most common neurodegenerative disease, following Alzheimer's Disease (AD). We now know that the average age of onset for PD is 50-60 years (6). Around that time, the loss of dopaminergic neurons from the substantia nigra pars compacta and the presence of intracellular inclusions known as Lewy bodies can be seen in patient brains (7). Additionally, researchers have determined that Lewy bodies are composed mainly of the protein α-synuclein, which aggregates within neuronal cell bodies (8). Research has also shown that cognitive decline can accompany PD, manifesting into PD with Mild Cognitive Impairment (PD-MCI) and PD with dementia (PDD), and a related form of cognitive impairment, Dementia with Lewy Bodies (DLB), has also been identified (9). DLB, which is also characterised by the presence of Lewy bodies, was first described in a 1962 report the presence of Lewy body disease on autopsy for 27 individuals who had experienced cognitive decline, but for which the majority had not presented with parkinsonian symptoms (9). Subsequently, the primary component of Lewy bodies (α-synuclein) was uncovered in the 1990s, the term "dementia with Lewy Bodies" was introduced, and the diagnostic criteria for DLB were published (9).

The Lewy Body disease spectrum includes PD, PD-MCI, PDD, and DLB. DLB is distinguished clinically from PDD by the time at which cognitive impairment occurs relative to

motor dysfunction (10). Therefore, if motor dysfunction and cognitive impairment appear within one year of each other, a patient could be classified as having DLB; otherwise, PDD is diagnosed when motor symptoms present at least one year before cognitive symptoms (10).

According to the Movement Disorder Society Clinical Diagnostic Criteria for Parkinson's Disease (11), the essential feature required for diagnosing PD is parkinsonism, which includes bradykinesia and rest tremor, either with or without rigidity. For a diagnosis of clinically-established PD, at least two supportive features also need to be present (which include a positive response to dopaminergic therapy, levodopa-induced dyskinesia, rest tremor in a limb, and olfactory dysfunction or cardiac sympathetic denervation (11). Additionally, the patient should not meet any of the absolute exclusion criteria (which include cerebellar abnormalities, downward vertical supranuclear palsy or slow downward vertical saccades, primary progressive aphasia or the behavioural variant of frontotemporal dementia, parkinsonism in only the lower limbs for more than 3 years, drug-induced parkinsonism, normal functional imaging of the presynaptic dopaminergic system, lack of responsiveness to high doses of levodopa, cortical sensory loss, limb ideomotor apraxia, primary progressive aphasia, or other conditions that could cause parkinsonism), and should lack several other red flags (11).

For a diagnosis of PD-MCI, the inclusion criteria state that there must be an established diagnosis of PD (12). During this time, there must have been a gradual decline in cognition in at least two of five cognitive domains (attention and working memory, executive functioning, language, memory, and visuospatial) observed by the patient, informant, or clinician (12). Additionally, this cognitive decline must be measurable using neuropsychological testing or scales of global cognitive decline but not severe enough to impair the individual's functional independence (12). Exclusion criteria for PD-MCI include a diagnosis of PDD, other non-PD-

related reasons for cognitive impairment, and other PD-associated conditions that could interfere with cognitive testing (12).

There are two core features of PDD, both of which must be present for a diagnosis of probable PDD (13). Core features include a diagnosis of PD and slow-onset dementia that has developed during established PD, impacting the individual's daily activities (ADLs) (13).

The central feature required for diagnosing DLB is dementia (10). For patients with DLB, dementia is typically characterised by deficits in attention, visuospatial abilities, and executive function in the earlier stages, which can progress to deficits in memory (10). Core clinical features of DLB (two of which are required for a diagnosis of probable DLB) include fluctuations in cognition, visual hallucinations, rapid eye movement sleep behaviour disorder (RBD), and at least one of the cardinal features of parkinsonism (bradykinesia, resting tremor, and rigidity) (10).

Additionally, new research has identified MCI-DLB, which refers to the time when mild cognitive impairment is present before dementia occurs, and in which Lewy bodies are present in the brain (14). For a diagnosis of MCI-DLB, the patient must meet the criteria for MCI, which includes the observation of cognitive decline by the patient, informant, or clinician, objective measures of impairment in at least one cognitive domain (which can be any domain, but is more likely to include impairments in attention, visuospatial abilities, or executive function), and which does not significantly interfere with functional independence (14). Additionally, for a patient to be diagnosed with probable MCI-DLB, the patient must have at least two core clinical features (with or without a proposed biomarker), one core clinical biomarker, and at least one proposed biomarker (14). The core clinical features of MCI-DLB include cognitive fluctuations, visual hallucinations, RBD, and at least one cardinal feature of parkinsonism (14). Proposed

biomarkers include evidence of decreased dopamine transporter uptake in the basal ganglia, evidence of REM sleep without atonia using polysomnography, and decreased meta-iodobenzylguanidine uptake through myocardial scintigraphy (14).

Non-Motor Features of Lewy Body Diseases

Parkinson's disease is most recognised by its motor features, which include bradykinesia, muscular rigidity, and tremor (15). However, as shown in Table 1.1, there are also various non-motor features of PD, which can be categorised into neuropsychiatric symptoms (e.g., depression, anxiety, apathy, psychosis, and cognitive impairment), sleep disorders (e.g., RBD and excessive daytime sleepiness), autonomic symptoms (e.g., bladder disturbances, orthostatic hypotension, and sexual dysfunction), gastrointestinal symptoms (e.g., constipation), sensory symptoms (e.g., pain and olfactory disturbance), and other symptoms (e.g., fatigue as well as vision and weight changes) (16).

Table 1.1 Motor and Non-Motor Symptoms in Parkinson's Disease

Category	Symptoms
Motor symptoms	• Bradykinesia • Muscular rigidity • Rest tremor • Postural instability
Neuropsychiatric symptoms	• Depression, apathy, anxiety • Anhedonia • Attention deficit • Hallucinations, illusion, delusions • Dementia • Obsessional behaviour (usually drug induced), repetitive behaviour • Confusion • Delirium (could be drug induced) • Panic attacks
Sleep disorders	• Restless legs and periodic limb movements • Rapid eye movement sleep behaviour disorder (RBD) and REM loss of atonia

	• Non-REM-sleep related movement disorders • Excessive daytime somnolence • Vivid dreaming • Insomnia • Sleep disordered breathing

Autonomic symptoms	• Bladder disturbances
	  ○ Urgency
	  ○ Nocturia
	  ○ Frequency
	• Sweating
	• Orthostatic hypotension
	  ○ Falls related to orthostatic hypotension
	  ○ Coat-hanger pain
	• Sexual dysfunction
	  ○ Hypersexuality (likely to be drug induced)
	  ○ Erectile impotence
	• Dry eyes (xerostomia)

Gastrointestinal symptoms (overlaps with autonomic symptoms)	• Dribbling of saliva • Ageusia • Dysphagia and choking • Reflux, vomiting • Nausea • Constipation • Unsatisfactory voiding of bowel • Faecal incontinence
Sensory symptoms	• Pain • Paraesthesia • Olfactory disturbance
Other symptoms	• Fatigue • Diplopia • Blurred vision • Seborrhoea • Weight loss • Weight gain (possibly drug induced)

Motor symptoms adapted from Berardelli et al. (15) and non-motor symptoms adapted from Chaudhuri et al. (16)

Three significant psychiatric-related PD symptoms include depression, anxiety, and apathy, all of which can present before motor symptoms (17). These symptoms are common in PD, with 35% having clinically significant depression, 60% having anxiety, and 60% having apathy (17). According to the Diagnostic and Statistical Manual of Mental Disorders, Fifth

Edition (DSM-5) (18), depression can be diagnosed if, during two weeks, an individual meets at least five of the following criteria (including at least one of the first two symptoms listed, and which cause significant distress or impact in daily functioning): depressed mood, diminished interest or pleasure, weight change, insomnia or hypersomnia, psychomotor agitation or retardation, fatigue or loss of energy, feelings of worthlessness or guilt, diminished concentration or indecisiveness, and suicidal ideation or recurrent thoughts of death. The diagnostic criteria for Generalized Anxiety Disorder (GAD) include excessive anxiety and worry that occurs on over half of the days during at least a six-month period, which is difficult to control and is associated with at least three of the following symptoms: restlessness, being easily fatigued, difficulty concentrating, irritability, muscle tension, and disturbed sleep (18). Apathy, the third significant psychiatric-related symptom, often includes decreased motivation, goal-directed behaviours, and emotional responsiveness (18).

Aside from these features, a review by Hinkle and Potone (19) also highlighted cognitive impairment, psychosis, disrupted sleep, and impulse control disorders as being key non-motor features of PD. Most patients with PD experience non-motor and neuropsychiatric symptoms, with most patients reporting at least one symptom and the average patient reporting eight (19). Despite their ubiquity, Hinkle and Potone (19) state that relatively little focus has been given to these symptoms until recently. They theorise that this may be due to a shift in medical research towards an emphasis on quality of life (19). Indeed, non-motor symptoms can have a greater impact on a patient's quality of life than motor symptoms. Those with the worst impact include cognitive (e.g., attention, executive function, and memory) disturbances, sleep, and mood (20). As the research into non-motor symptoms within the Lewy body spectrum is still emerging and given the importance these symptoms play in quality of life, this remains a critical area of study.

Cognitive decline is an important non-motor aspect of PD. It usually occurs in the later stages of the disease and can progress to dementia, which is estimated to affect approximately 80% of surviving patients 20 years after diagnosis (21). In patients with PD, cognitive impairment typically impacts executive functioning or related cognitive processes, including cognitive flexibility, attention, and working memory (19). As mentioned previously, if cognitive decline occurs around the same time as the onset of motor symptoms, a patient may be diagnosed with Dementia with Lewy Bodies, which is separate from Parkinson's Disease Dementia, but both are grouped under the umbrella term Lewy Body Dementia (10). The related α-synucleinopathy, Dementia with Lewy Bodies, is additionally characterised by hallucinations and fluctuations in cognition (22). Therefore, for this project, we will be grouping both conditions together because they are each part of the spectrum of dementias characterised by the presence of Lewy Bodies.

Psychosis and sleep disturbances are other non-motor symptoms of PD and DLB that significantly impact quality of life (19). Psychosis is usually experienced as visual hallucinations (VH) or delusions and can be debilitating in the later stages of the disease (19). Sleep disturbances can manifest in several ways in PD and DLB. Over 50% of individuals with PD experience rapid eye movement sleep behaviour disorder (RBD), which is characterised by the inability to maintain the loss of muscle tone that usually accompanies sleep, and therefore results in the affected individuals acting out their dreams by moving and speaking, potentially causing injury to themselves or their partners (19). Interestingly, when confirmed through polysomnography, RBD is the most predictive biomarker of incipient Lewy Body Dementia (LBD) (19).

The final key non-motor feature is impulse control disorders (ICDs), which are characterised by disproportionate reward-directed behaviours (19), such as excessive gambling, shopping, eating, and sexual behaviours (23). In Lewy Body diseases, ICDs are thought to be the result of excess dopamine because patients with PD who are treated with dopamine receptor agonists (which increase the activity of dopamine in the brain) are at higher risk for ICDs (19). However, patients without PD who take dopamine agonists for conditions such as hyperprolactinemia and restless leg syndrome are at a much lower risk, which suggests that PD and dopamine agonists interact to increase the rate of ICDs in this population (19).

The Pathology of Lewy Body Diseases

The two most common neurodegenerative diseases, AD and PD, are both marked by the accumulation of misfolded proteins and the destruction of projection neurons (24). In AD, the misfolded proteins of note are Amyloid and Tau, whereas, in PD, α-synuclein aggregation occurs. Post-mortem studies of the brains of patients with PD, PDD, and DLB have long shown inclusions known as Lewy bodies (LBs) (25). A definitive diagnosis of Parkinson's Disease requires autopsy evidence of inclusion bodies such as the spherically shaped LBs and thread-like Lewy neurites (LNs) (27). Both inclusions consist primarily of aggregations of the hydrophilic protein α-synuclein (27). While the cause of most PD is unknown, there are less common familial forms of PD caused by mutations within the gene coding for α-synuclein, suggesting that abnormal α-synuclein is the driving force behind neurodegeneration (25). One hypothesis of the origin of sporadic PD proposes that a small amount of aberrant α-synuclein in one neuron acts as a template to induce α-synuclein misfolding in adjacent neurons, which then do the same, causing pathology to spread throughout the nervous system (25).

The neuropathology in PD is essential to understand how non-motor symptoms appear. Braak and colleagues, who developed the prevalent model for staging the spread of pathology in AD (26), also described a sequence of spread that occurs in PD (27). In PD, they have proposed that the pathology progresses in 6 stages, in which Lewy bodies first appear in the brainstem and spread to further brain regions (27-29). Stage 1 is marked by the appearance of a small number of thin LNs within the dorsal motor nucleus of the vagal nerve, which connects the enteric system with the central nervous system (29). More inclusions, including LBs, deposit in the vagal nerve as the disease progresses, and this pattern of pathological accumulation of LNs followed by LBs occurs in the other affected areas (29). In the second stage, inclusions appear in regions known collectively as the "gain setting" system, which is responsible for modulating pain perception and motor functions (29). Stage three is when the substantia nigra becomes affected (29). However, the loss of its melanoneurons has not yet occurred because the damage is just beginning to accumulate (29). During this stage, Lewy pathology also starts to appear in other regions, including within limbic regions such as the amygdala (29, 30). In stage four, LNs infiltrate the temporal mesocortex, which is directly connected to the hippocampal formation, and clinically significant symptoms develop (29). Other limbic white matter (WM) structures that may be involved in non-motor symptoms, including the cingulate cortex and fornix, develop pathology at this time (27). By stages five and six, the substantia nigra has lost most of its melanocytes, inclusion bodies have permeated the cortex and damage throughout the brain has led to a wide range of symptoms (29). See Figure 1-1 for immunohistochemistry showing Lewy bodies, as well as a depiction of Braak staging, and Figure 1-2 for staining showing lesions in the amygdala and cortex during the final three stages of the disease.

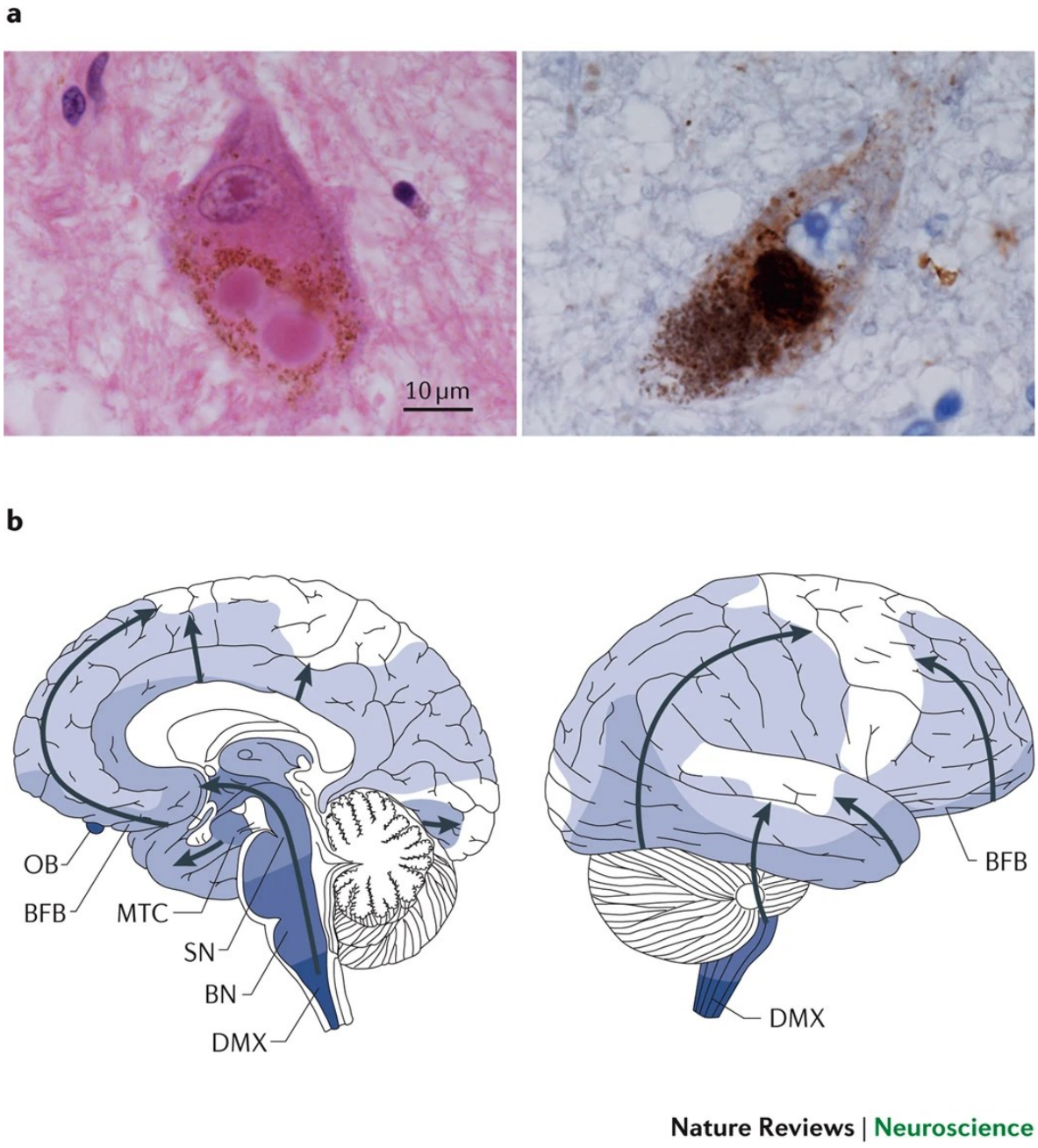

Figure 1-1 Lewy body immunohistochemistry and a depiction of Braak staging.

(A) the left panel, a Lewy body is highlighted using haematoxylin and eosin staining, and in the right panel, a Lewy body is shown using α-synuclein immunohistochemistry. (B) Darker shaded areas represent earlier pathology as described by the Braak hypothesis, and arrows demonstrate the direction of spread throughout the disease course. BFB: basal forebrain; BN: brainstem nuclei; DMX: dorsal motor nucleus of the vagus nerve; MTC: mesiotemporal cortex; OB: olfactory bulb; and SN: substantia nigra.
Figure from Schapira, A.H.V., Chaudhuri, K.R., & Jenner, P. (2017). Non-motor features of Parkinson disease. *Nature Reviews Neuroscience, 18*, 435-450. (17). Reproduced with permission from Springer Nature.

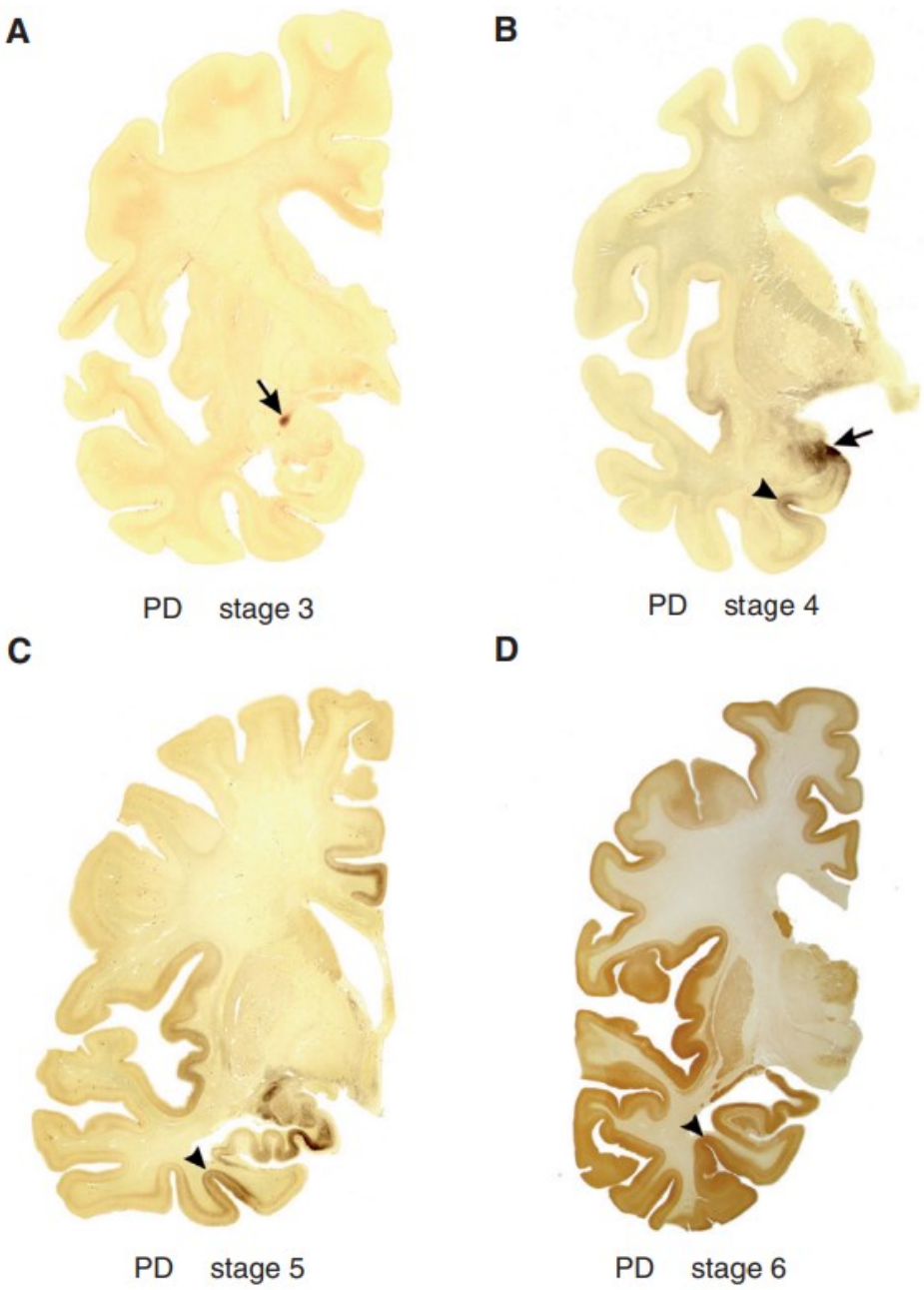

Figure 1-2 a-Synuclein immunohistochemistry showing Lewy pathology in stages 3–6 of sporadic Parkinson's disease.

(A) The arrow indicates the presence of lesions in the amygdala. (B) the arrow points to cortical and basolateral subnuclei, the arrowhead indicates involvement of the transentorhinal region. (C) Increasing pathology present in the transentorhinal region (shown by the arrowhead), as well as worsening inclusions in limbic cortex, hippocampal formation, and the amygdala gradually worsen. (D) Extensive involvement of the temporal, insular, and cingulate cortex. The arrowhead points to the transentorhinal region.

Figure from Braak, H., Del Tredici, K. (2016). Potential Pathways of Abnormal Tau and alpha-Synuclein Dissemination in Sporadic Alzheimer's and Parkinson's Diseases. *Cold Spring Harb Perspect Biol, 8*(11):a023630. (24). Reproduced with permission from Cold Spring Harbor Laboratory Press.

The Hippocampus

Structure

The hippocampus, which is critical to memory, is a small structure embedded within the limbic lobe (31). The term hippocampus, meaning sea horse, was first used by Arantius in 1587 because he believed it resembles the fish, which has a flexible, segmented body that progressively narrows from head to tail (32). An overview of the structure of the hippocampus can be seen in Figures 1-3 and 1-4, and Table 1.2.

The hippocampus is located within the temporal lobe and is part of the hippocampal formation, which includes the dentate gyrus, subiculum, and entorhinal cortex (31). The hippocampus can be divided into three main sections: the head, body, and tail. The head forms the widened portion at the anterior of the hippocampus. It typically bears three to four claw-like projections known as the digitationes hippocampi (or hippocampal digitations) (31). The middle portion of the hippocampus, the body, connects the head to the narrow tail at the posterior (31).

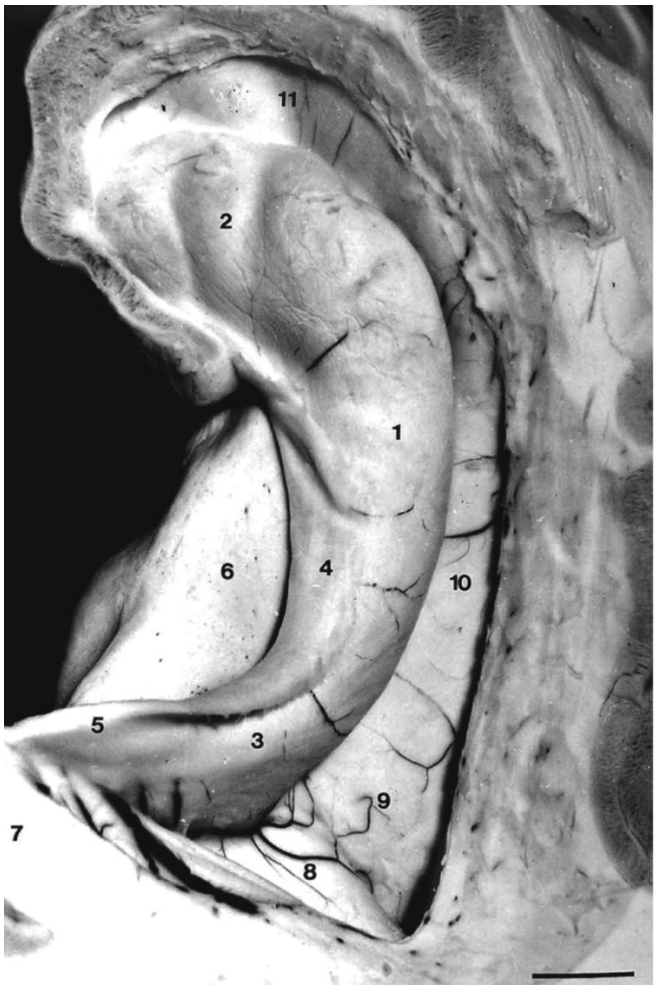

Figure 1-3 Intraventricular aspect of the right hippocampus.

Bar, 6.5 mm. *1* hippocampal body, *2* head and digitationes hippocampi, *3* hippocampal tail, *4* fimbria, *5* crus of fornix, *6* subiculum, *7* splenium of the corpus callosum, *8* calcar avis (hippocampus minor), *9* collateral trigone, *10* collateral eminence, *11* uncal recess of the temporal horn.
Figure from Duvernoy, H.M., Cattin, F., Risold, P.Y. (2013). *The human hippocampus: Functional anatomy, vascularization, and serial sections with MRI.* Berlin Heidelberg: Springer-Verlag. (31). Reproduced with permission from Springer Nature.

The hippocampus comprises two laminae: the cornu ammonus and the dentate gyrus (DG) (31). Both are allocortex, the primitive and more simplistic part of the cortex (31). The cornu ammonis (or Ammon's horn; CA) is also known as the hippocampus proper (31). It is composed of six layers: the *alveus* (contains efferent hippocampal axons), the *stratum oriens* (contains basket cells), the *stratum pyramidale* (contains pyramidal neurons), the *stratum radiatum* (contains apical dendrites of the pyramidal neurons), the *stratum lacunosum* (contains

perforant fibers and Schaffer collaterals), and the *stratum moleculare* (contains some interneurons and the apical dendrites of pyramidal neurons) (31). The cornu ammonis has four subfields: CA1 (where somata of pyramidal neurons are small and triangular), CA2 (where somata of pyramidal neurons are large, oval-shaped, and dense), CA3 (similar to CA2, but less dense and surrounded by mossy fibers), and CA4 (similar to CA3, but is folded into the dentate gyrus) (31).

The gyrus dentatus (or dentate gyrus; DG) is also known as the fascia dentata and has a more straightforward organization than the cornu ammonis, from which it is separated by the vestigial hippocampal sulcus (31). The dentate gyrus contains three layers: the *stratum molecular* (where preferent fibers enter the region closest to the hippocampal sulcus, and commissural and septal fibers enter the region bordering the septum granulosum), the *stratum granulosum* (contains the densely packed somata of granular neurons), and the *polymorphic layer* (where the axons from the stratum granulosum pass through into CA4) (31). Finally, the superficial part of the hippocampus (the intraventricular part) contains the cornu ammonis sections 1-3 (CA1, CA2, and CA3) (31).

Table 1.2 Structure of the Hippocampus

	Laminae	
	Cornu Ammonus (CA)	**Dentate Gyrus (DG)**
Layers	• alveus • stratum oriens • stratum pyramidale • stratum radiatum • stratum lacunosum • stratum moleculare	• stratum molecular • stratum granulosum • polymorphic layer
Subfields	• CA1 • CA2 • CA3 • CA4	_N/A

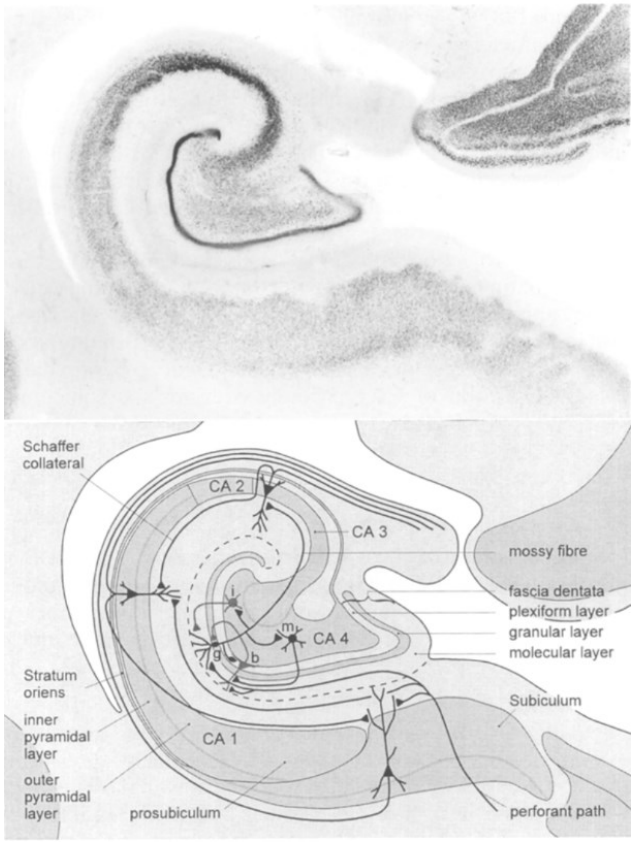

Figure 1-4 A micrograph and drawing of a frontal section through the hippocampus.

Above: A frontal section through the hippocampus. *Below*: Drawing of the same hippocampal section. *b* basket cell (interneuron) of the fascia dentata; *g* granule cell (projection neuron) of the fascia dentata; *i* a large interneuron of CA4; *m* the mossy cell (CA4 projection neuron).
Figure from Braak, H., Braak, E., Yilmazer, D., de Vos, R.A.I., Jansen, E.N.H., & Bohl, J. (1996). Pattern of brain destruction in Parkinson's and Alzheimer's diseases. *J Neural Transm, 103*, 455-490. (27). Reproduced with permission from Springer Nature.

Memory Functions

The hippocampus influences the rest of the brain by sending and receiving information through the entorhinal area (31). The hippocampus's most well-known function is its role in short-term memory, holding and sorting incoming information before transferring it to the neocortex to form a lasting impression (31). More specifically, the hippocampus is involved in forming declarative memories, which allows one to remember facts (semantic memory), events (episodic memory), and places (spatial memory) (31).

Episodic and spatial memory functions are mainly subserved by the *polysynaptic intrahippocampal pathway* (31). In this pathway, input from cortical regions such as the posterior parietal association cortex, which is involved in processing spatial information, is passed on to the entorhinal cortex and then through the subiculum to the gyrus dentatus via the perforant pathway (31). From there, mossy fibers of the gyrus dentatus primarily send signals to neurons within CA3, and to a lesser extent, CA4, which then synapse onto CA1 via their Schaffer collaterals. CA1 then passes information to the subiculum, which provides the output of the pathway, travelling to the alveus and then the fimbria (31). From the fimbria, impulses are passed onto the remaining areas within the limbic loop, beginning with the fornix and then the anterior thalamic nucleus. Finally, the thalamus disseminates information to the posterior and anterior cingulate cortex as well as the retrosplenial cortex (31).

Semantic memory functions are primarily performed through the *direct intrahippocampal pathway*. In this pathway, the inferior temporal cortex, which is involved in object recognition, passes information directly from the entorhinal cortex to CA1 neurons (31). The CA1 neurons then synapse onto the subiculum, passing information back to the entorhinal cortex, which sends output to the temporal association cortex, temporal pole, and prefrontal cortex (31). It is believed that the right hippocampus plays a more prominent role in spatial memory, while the left hippocampus is more involved in episodic memory (31).

As with CA1, CA2 neurons receive input from the entorhinal cortex (33). However, because it is smaller than the others, fewer studies have examined the functions of the CA2 subfield (33). Still, there is some evidence that CA2 is particularly sensitive to slight changes in familiar environments, encoding temporal order, and processing social memory (33), and that its neurons seem to display diminished plasticity and relative resistance to injury compared to those

in other subfields (33). Thus far, the main function ascribed to CA2 is its role in forming social memories (34).

Other Hippocampal Functions

The hippocampus is also implicated in emotional regulation (31). Emotional responses to pain are believed to be partially controlled by projections from the *intrahippocampal polysynaptic pathway* to the anterior cingulate cortex, which is involved in the perception of pain (31). Additionally, the hippocampus is believed to play a role in motor behaviour, including motor responses to emotional stimuli, as part of the *ventral striatal loop*, which is a limbic system component (31). Finally, the hippocampus is involved in the hypo-thalamo-hypophysial axis and may regulate the secretion of adrenocorticotropic hormone (31).

Impact of Lewy Body Diseases

Pathology in the brains of PD patients is seen initially in the dorsal motor nucleus of the glossopharyngeal and vagal nerves and the anterior olfactory nucleus before it spreads to cortical regions (28). During stage four, Lewy pathology begins to deposit within the temporal mesocortex, and a meshwork of LNs develops in CA2, extending to the adjacent CA1 and CA3 regions in stage five (29). As with the loss of the dark neurons within the substantia nigra, CA pathology is so distinctive of PD that a post-mortem diagnosis can be made by looking solely at this region (29). In Parkinson's disease, the most affected regions of the limbic system include the entorhinal region, CA2, and limbic nuclei within the thalamus, anterior cingulate cortex, insular cortex, and the amygdala (27). Figure 1-5 shows an example of LNs within CA2, a finding in most patients with PD (27).

As for the associated symptoms, there is evidence that the CA2-CA3 subregion may play a role in depression in drug-naïve patients with PD, as it was found to be atrophied in patients with depression, although this normalized after 24 weeks of treatment with levodopa (35). The destruction of neurons within the temporal mesocortex can lead to cognitive dysfunction due to this region's critical role in transmitting information between the prefrontal cortex and higher-order sensory cortex through the limbic system (29). However, co-pathology with misfolded proteins characteristic of AD, such as Amyloid-β, may also contribute to the development of dementia in PD (36). Although we cannot determine the extent of Amyloid-β pathology in the brains of the patients with PD in this study, and although all have met the criteria PD, we cannot rule out the presence of a co-pathology with AD (36).

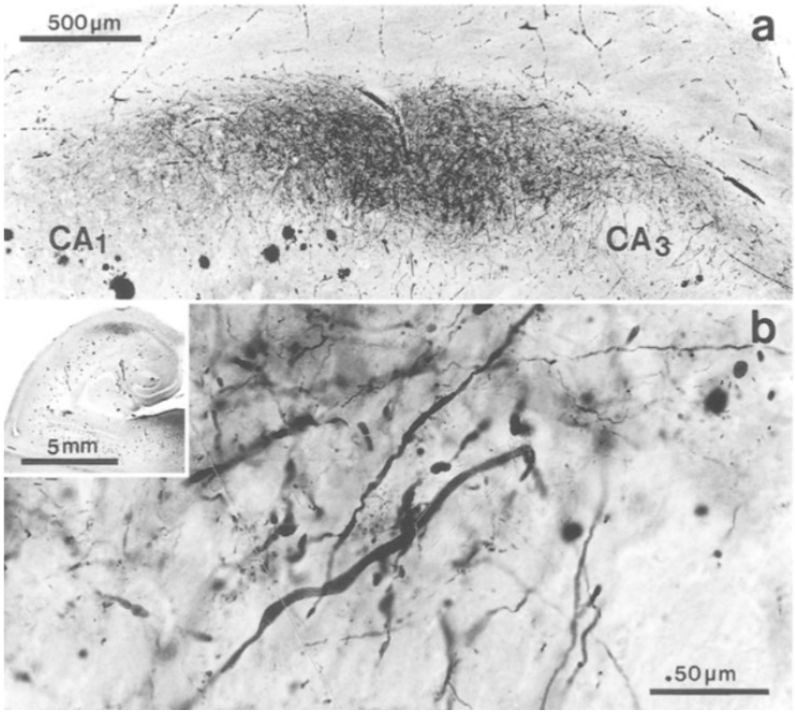

Figure 1-5 A dense network of Lewy neurites in CA2 in Parkinson's disease.

(A) Lewy neurites between sectors CA1 and CA3. (B) Higher magnification shows long Lewy neurites.
Figure from Braak, H., Braak, E., Yilmazer, D., de Vos, R.A.I., Jansen, E.N.H., & Bohl, J. (1996). Pattern of brain destruction in Parkinson's and Alzheimer's diseases. *J Neural Transm, 103*, 455-490. (27). Reproduced with permission from Springer Nature.

Magnetic Resonance Imaging

Magnetic Resonance Imaging in Lewy Body Diseases

Neuropathological changes in PD can only be directly examined in post-mortem studies of brain tissue. However, magnetic resonance imaging (MRI) is a valuable tool to characterize brain changes *in vivo*, aiding in diagnosis and facilitating the study of all disease stages and designing targeted interventions. There are many methods that have been applied to examine MRI data to quantify brain changes in individuals with Lewy Body diseases. These methods range from conventional measures of brain regions using structural MRI to other modalities such as iron and neuromelanin sensitive imaging, functional MRI, and diffusion MRI (37). Most studies thus far have focused on MRI within the motor regions of the brain, such as the substantia nigra, in association with the motor symptoms that are characteristic of PD, however as research is beginning to delve further into exploring the non-motor impacts of Lewy Body diseases, these techniques are being increasingly applied to limbic and neocortical regions of the brain (37).

Studies have used structural imaging to quantify hippocampal size in participants with LB diseases compared healthy controls and have varying results, reporting either no significant difference in overall hippocampal volume between groups (38, 39) or significant decreases in volume in participants with PD (40-42). Studies that have used iron-sensitive and neuromelanin-sensitive imaging have mainly done so within the substantia nigra, as this area has higher levels of iron and neuromelanin than others, and therefore this method may be less useful for studying regions associated with non-motor symptoms (37). Resting state functional MRI focuses on activity within the brain and has provided some interesting insights into cognitive changes within PD, finding a specific pattern of brain function related to cognition in PD (43), as well as a

reduction in functional connectivity within brain networks related to cognition (44). However, this method focuses on activity within the brain, rather than serving as an explicit measure of structure. One method that can measure structure of brain tissue at a microscopic level (as opposed to macroscopic measures provided by volumetric measures from structural imaging) is diffusion tensor imaging (DTI), which we use in this thesis to quantify changes within the hippocampus.

Diffusion Tensor Imaging as a Tool

Diffusion tensor imaging takes advantage of the diffusion of water in the brain to provide estimates of microstructural tissue integrity that would otherwise be unachievable *in vivo* (45). Diffusion tensor imaging makes use of the Einstein diffusion equation to describe the movement of water molecules from one location to another over time (45). In this equation, *D* (the diffusion coefficient in mm^2/s) is proportional to Δr^2 (the mean squared displacement), and divided by *n* (the number of dimensions along which displacement is occurring) multiplied by Δt (diffusion time):

$$D = \frac{(\Delta r)^2}{2n\Delta t}$$

Equation 1

At room temperature (i.e., 20 °C), the diffusion coefficient of water is 2.0×10^{-3} mm^2/s, and this coefficient increases as temperature increases (45). Diffusion is useful for studying tissue structure because components of tissues within the body hinder diffusion, and these changes can be measured and compared across subjects and brain regions. For example, when water is impeded by cellular membranes, this will cause the water molecules to deviate from a straight path, thereby decreasing the average displacement (45).

Diffusion tensor imaging is typically acquired using echo-planar imaging (EPI) sequence wherein two gradient pulses, which are described by a *b*-value, are applied before and after a 180° radiofrequency pulse (45). The application of this sequence results in stationary water molecules producing no signal attenuation, whereas water molecules that are moving produce a measurable loss in signal (45). To measure a diffusion tensor, gradients with high *b*-values (usually ranging from b = 700-1000 s/mm^2) are applied along at least 6 directions, with at least one additional image (the b_0 image) acquired without any diffusion gradients (46). The images are then visually inspected for quality and go through several preprocessing steps, which include registering the diffusion-weighted data to the b_0 image, to minimize the motion and eddy current artifacts to which DTI is prone (46). After preprocessing, the images are fitted to estimate the diffusion tensor at each voxel. The diffusion tensor may be visualized as an ellipsoid, characterized by three eigenvectors (e1, e2, e3) that define the principal axes and three eigenvalues ($\lambda_1, \lambda_2, \lambda_3$) which represent the magnitude of diffusion in each principal axis (46). Using these values, certain parameters can be calculated that describe aspects of diffusion within the tissue of interest. Mean diffusivity (MD) is one such parameter, and can be calculated by taking the average of the three eigenvalues (45, 46):

$$MD = \frac{\lambda_1 + \lambda_2 + \lambda_3}{3}$$

Equation 2

Mean diffusivity describes the overall diffusion and is not directionally dependent. A higher MD value indicates greater mobility of water molecules (45). Mean diffusivity is influenced by axial diffusivity (D_a) which is equivalent to λ_1 and radial diffusivity (D_r) which can be described by $(\lambda_2 + \lambda_3)/2$ (45). In terms of how these values characterize the movement of water molecules in the brain, D_a functions as a measure of diffusivity parallel to fiber tracts,

while D_r represents diffusivity perpendicular to fiber tracts (47). While dysmyelination affects D_r, it does not seem to alter D_a (47), and instead, D_a may reflect axonal damage (48). Previous studies have interpreted increasing MD as reflecting atrophy, cell damage, edema, and necrosis (49). Unlike MD, fractional anisotropy (FA) describes the non-uniformity of diffusion and is calculated using the following equation:

$$FA = \sqrt{\frac{(\lambda_1 - MD)^2 + (\lambda_2 - MD)^2 + (\lambda_3 - MD)^2}{2({\lambda_1}^2 + {\lambda_2}^2 + {\lambda_3}^2)}}$$

Equation 3

For FA, a value of 0 means that diffusion occurs equally in all directions, whereas a value of 1 indicates that diffusion occurs exclusively in one direction (45). In general, decreased FA may reflect reduced integrity, axonal loss, and demyelination, while increased FA may reflect improved axonal alignment, re-myelination, and crossing fibres (fibres of different orientations within a voxel) (49). It is important to remember that these measures hint at the underlying tissue structure, so care is needed with respect to interpretation.

Several methods of acquiring and analyzing DTI data can be employed depending on the questions a researcher wants to address. Figure 1-6 demonstrates that analysis methods can generally be grouped into three main categories: whole-brain, region-specific, and voxel-based (50). Whole-brain analyses summarize and compare diffusion measures across the entire brain, usually obtaining average whole-brain values for diffusion metrics (50). However, if a researcher wants to focus on specific brain structures, region-specific analyses can be used to compare diffusion measures in select regions of interest (ROIs). Region-specific analyses can include tractography, which is a method used to isolate WM tracts in the brain, or the delineation of GM regions, which can be done through automated or manual segmentation (50).

In this thesis, we used manual segmentation to trace the hippocampi of each participant before extracting diffusion metrics from this ROI. The final category of DTI techniques, voxel-based analyses, involve comparing diffusion measures at the smallest scale of the image (a voxel), and can include investigating diffusion metrics in each voxel across the brain's entire WM, GM, or both (50). For example, a study by Andica and colleagues (52) used tract-based and GM-based spatial statistics to explore diffusion across the entire brain in participants with PD to determine which voxels were significantly different from healthy controls and if they were associated with clinical measures (see Appendix Tables A1-A2). For this project, we decided to use region-specific analysis because we were interested in characterizing hippocampal changes in patients with PD and were able to utilize a novel DTI protocol designed specifically to acquire ultra-high-resolution imaging of the hippocampus (53).

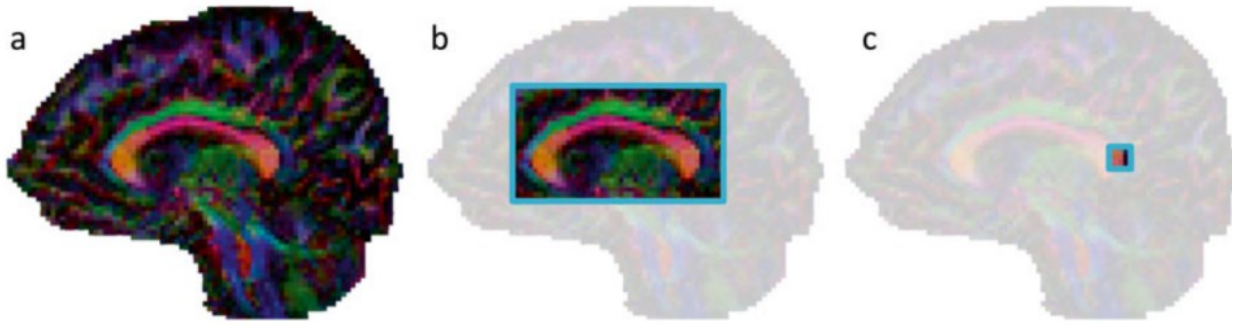

Figure 1-6 DTI analysis methods.

Overlying a color-coded FA map (red indicates diffusion in the transverse direction, blue indicated cranio-caudal diffusion, and green indicates anterior-posterior diffusion) are examples of the regions used in different analysis methods. (A) Whole-brain analysis, (B) region-specific analysis, and (C) voxel-based analysis.
Figure from Van Hecke, W., Emsell, L., & Sunaert, S. (2016). *The human hippocampus: Functional anatomy, vascularization, and serial sections with MRI*. New York Heidelberg: Springer. (50). Reproduced with permission from Springer Nature.

Diffusion Imaging of the Hippocampus

A novel method of high-resolution DTI has been developed to allow for diffusion imaging of the hippocampus (53). Because of this new method, DTI in the hippocampus can now be acquired with higher resolution and decreased partial volume effects, which limit investigations of hippocampal diffusion using standard DTI protocols (53). This method has already been successfully implemented in a study of temporal lobe epilepsy (128) and to characterize age-related hippocampal changes (129). In this project, we used high-resolution DTI to expand the literature on hippocampal changes in PD and their associations with non-motor symptoms.

Studies that have looked at the hippocampus in participants with Lewy body diseases have had voxel volumes ranging from 2.5 – 12 mm^3 (39, 52, 54-65). With the new protocol utilized in this thesis, we have been able to achieve a resolution of 1 mm^3 in a short scan time of around 6 minutes by acquiring 20 slices along the hippocampus and using a lower *b*-value of 500 s/mm^2 to lessen the loss in signal-to-noise ratio that occurs with decreased voxel volumes, while still maintaining adequate contrast (53). Furthermore, the smaller number of slices used also allowed for a shorter repetition time (TR), allowing for more images per slice per unit time, also improving SNR (53). Overall, the use of this sequence enabled us to look at the hippocampus in higher detail than has been previously used in diffusion studies of Lewy body diseases and allowed better delineation of the hippocampal boundaries during manual segmentation.

In this study, we also used the same MR images to measure hippocampal volume. Other studies have shown that hippocampal volumes are smaller in patients with PD when compared to healthy controls, especially for patients with more advanced disease (40, 66). However, hippocampal atrophy due to PD will only be measurable when enough neurons have

accumulated enough damage to die off. Because DTI is a microscopic measure, it may be able to detect damage before significant atrophy occurs.

Diffusion Tensor Imaging Studies of the Lewy Body Spectrum

Few studies have looked at differences in DTI measures of the hippocampus between participants with Lewy Body Spectrum diseases and healthy controls. For the studies that have, findings have shown either no significant difference (57, 62, 63) or significant increases in hippocampal MD bilaterally (39), on the left side (60, 61), and averaged between both sides (58) in participants with PD when compared to healthy controls, and no significant difference (58, 60-63) in hippocampal FA between participants with PD and healthy controls.

Since the focus of this thesis was on the use of DTI to investigate non-motor symptoms in Lewy body diseases, a review of the literature in this area was performed. Summary tables of the literature on DTI and non-motor symptoms in the Lewy body spectrum can be found in Appendix A, and show the FA and MD findings relating to cognitive and other non-motor symptoms in patients with PD can be found in Appendix A. The broadest group of studies investigating non-motor symptoms in PD have included analyses of measures relating to cognition, which can be classified into measures relating to global cognition, memory, attention/working memory, executive function, processing speed, verbal/language, visuospatial, and other cognitive functions (see Table A1). DTI studies using measures of other non-motor symptoms (i.e., non-cognitive non-motor symptoms) in PD are shown in Table A2. Here, other non-motor symptoms could be classified into overall non-motor symptom scores, depression, anxiety, apathy, other mood, sleep/fatigue, QoL/ADL, psychosis/hallucinations, other

psychiatric/behavioural, olfaction, bladder/urinary symptoms, gastrointestinal symptoms, pain, cardiovascular and respiratory measures, and other non-motor symptoms.

Imaging of Cognitive Symptoms in the Lewy Body Spectrum

In this thesis, for measures of cognitive function, we compared patients classified into different cognitive domains (PD without cognitive impairment, PD-MCI, and PDD/DLB), assessing global cognition and specific cognitive domains, including memory, executive function, and cognitive speed. Brain regions included in these studies were extensive and have therefore been listed in Table A1. Previous studies investigating WM structures have typically shown either decreased FA, increased MD, or both. Notably, these results were seen in patients with PD-MCI compared to HC (51, 67-72) and PD without cognitive impairment (51, 67-69, 72), and when comparing patients with PDD to HC (67, 69, 71-77), PD without cognitive impairment (67, 69, 71-73, 75, 77-79), and PD-MCI (72, 79). Studies have also associated diffusion measures with MoCA scores, although none have looked at the hippocampus specifically (77, 80-93). Two of these studies (77, 87) found that lower scores on the MoCA were associated with decreased FA, and four studies (77, 80, 84, 87) found that lower scores were associated with increased MD. Studies that have looked at the association between aggregate memory scores and diffusion measures have exclusively investigated WM structures (51, 67, 75, 79, 94). They have found positive associations between memory scores and FA (75, 79) and negative associations with MD (67, 79, 94). Investigations of composite scores of executive function have again only focused on WM (51, 67, 79, 94-99). These studies have found that better performance on tests of executive function was associated with higher FA (79, 94, 97) and lower MD (51, 79, 94).

Finally, one study (99) looked at the relationship between a composite measure of processing speed and FA in WM regions and found no significant association.

Imaging of Non-Cognitive Non-Motor Symptoms in the Lewy Body Spectrum

Few studies appear to have looked at non-motor symptoms other than cognitive impairment. In this thesis, we specifically investigated overall neuropsychiatric symptom severity, depression, anxiety, apathy, health-related QoL, disordered sleep, and mild behavioural impairment (MBI). See Table A2 for comprehensive descriptions of the brain regions included in these studies. Only two prior studies (100, 101) investigated the difference in WM diffusivity in patients with PD and depression compared to HC, with one (101) finding significant increases in MD in patients with depression. More studies have investigated diffusion differences, in regions other than the hippocampus, between patients with PD and depression and patients without depression, finding decreases in FA (102-105) and increased MD in patients with depression relative to those without (101). In terms of associations between depression severity and diffusion measures, three studies (92, 106, 107) have looked at the association between GDS-15 scores and WM in patients with PD, with one study (107) showing a significant positive association with MD. Studies employing other depression scales (52, 70, 82, 102, 103, 105, 108-111) have not specifically looked at the hippocampus but have found associations between higher depression scores and lower FA (102, 103, 105, 110, 111). Compared to depression which has been relatively well studied, only three papers have examined anxiety (52, 109, 110), with one finding a positive association between anxiety and MD (109).

Research that has explored the relationship between apathy and diffusion in patients with PD has yet to specifically examine the hippocampus (52, 70, 82, 110, 112, 113). Apathy has been associated with decreased FA (110, 113) and both increased (110, 112) and decreased (112) MD.

For QoL, one paper (65) found that higher PDQ-39 SI scores were associated with lower FA and higher and lower MD in several GM structures.. Literature has also covered the associations between diffusion and different aspects of disordered sleep in patients with PD (52, 57, 82, 107, 108, 114-122). Daytime sleepiness was associated with decreased FA (120). Fatigue was associated with increased FA and decreased MD (117), and patients with PD and RBD were found to have decreased (115, 116, 119) and increased (115, 116) FA and increased MD (57, 115, 119) relative to HCs and patients without RBD.

Other findings of note include decreased FA and increased MD in patients with DLB with visual hallucinations compared to patients with DLB without visual hallucinations (123). Decreased FA (124) and increased MD (59, 124, 125) were found in patients with PD and visual hallucinations when compared to HCs, and increased MD was found in patients with PD and visual hallucinations compared to patients without visual hallucinations (59, 124, 125). Similarly, patients with PD and psychosis were found to have reduced FA compared to patients without psychosis (56, 126). Finally, PD patients with impulse control disorders (ICD) were found to have increased FA compared to HCs (115, 127) and patients without ICD (127), and decreased MD compared to HCs (115).

Hippocampal Imaging and Non-Motor Symptoms in the Lewy Body Spectrum

Studies that have looked at non-motor symptoms of PD in association with diffusion measures (FA or MD) in whole-brain GM using brain atlases that included the hippocampus (52,

55, 64, 65) or the hippocampus specifically as a region of interest (39, 54, 56-59, 62, 121) have been highlighted in Tables 1.3 and 1.4. The papers in the tables below describe either no significant difference in hippocampal FA (52, 55, 64, 65, 121) or MD (52, 54, 55, 57-59, 64, 65), decreased hippocampal FA (56, 62, 121), or increased hippocampal MD (39, 54, 59, 62, 65) in the hippocampus associated with cognitive decline (Table 1.3) and other non-motor symptoms (Table 1.4). Overall, several approaches have been used with varying results, and the question of how, or if, hippocampal structure in LB diseases changes in association with non-motor symptoms unanswered. In this thesis, we hope to provide further clarity into these changes using higher resolution DTI than has been used in these studies.

Table 1.3 DTI literature on cognitive impairment in PD and the hippocampus

Cognitive Impairment							
Measure	Author (Year)	Groups	Regions Analyzed	FA	FA-Location	MD	MD-Location
Global Cognition – Group Comparisons							
PD with MoCA <=25 (vs. PD with MoCA >=26)	Schulz (2018)(62)	72 PD with MoCA <=25, 232 PD with MoCA >=26	Amygdala, entorhinal cortex, hippocampus, insula, NBM, primary somatosensory cortex, thalamus	↓	Amygdala^{avg}, hippocampus^{avg}, thalamus^{avg}	↑	Entorhinal cortex^{avg}, hippocampus^{avg} , insula^{avg}, NBM^{avg}, thalamus^{avg}
Global Cognition – Rating Scales							
MMSE	Lu (2016)(64)	126 PD	Whole-brain GM	n.s.	-	n.s.	-
	Wei (2016)(121)	43 PD	BG, frontal WM, hippocampus, occipital WM, parietal WM, SN, temporal WM	n.s.	-	N/A	-
PD-CRS Total Score	Grothe (2021)(54)	73 PD	Basal forebrain, hippocampus	N/A	N/A	⊖	Hippocampus^{avg}
UPDRS-I – Cognitive Impairment	Andica (2019)(52)	20 PD	Whole-brain WM and GM	n.s.	-	n.s.	-
Memory							
Delayed Recall (15-Word List)	Carlesimo (2012)(39)	25 PD	Hippocampus	N/A	N/A	⊖	Hippocampus^{b}
Delayed Verbal Memory (PD-CRS)	Grothe (2021)(54)	73 PD	Basal forebrain, hippocampus	N/A	N/A	⊖	Hippocampus^{avg}
Immediate Recall (15-Word List)	Carlesimo (2012)(39)	25 PD	Hippocampus	N/A	N/A	⊖	Hippocampus^{r}
Immediate Verbal Memory (PD-CRS)	Grothe (2021)(54)	73 PD	Basal forebrain, hippocampus	N/A	N/A	n.s.	-

Cognitive Impairment							
Measure	Author (Year)	Groups	Regions Analyzed	FA	FA-Location	MD	MD-Location
Paired Associates Learning (CANTAB)	Yao (2016)(59)	12 PD with VH	Hippocampus	N/A	N/A	n.s.	-
Attention/Working Memory							
Attention/Memory (NMSS)	Wei (2016)(121)	43 PD	BG, frontal WM, hippocampus, occipital WM, parietal WM, SN, temporal WM	n.s.	-	N/A	N/A
Working Memory (PD-CRS)	Grothe (2021)(54)	73 PD	Basal forebrain, hippocampus	N/A	N/A	⊖	Hippocampus^{avg}
Sustained Attention (PD-CRS)				N/A	N/A	n.s.	-
Verbal/Language – Rating Scales							
Action Verbal Fluency (PD-CRS)	Grothe (2021)(54)	73 PD	Basal forebrain, hippocampus	N/A	N/A	⊖	Hippocampus^{avg}
Alternating Verbal Fluency (PD-CRS)				N/A	N/A	⊖	Hippocampus^{avg}
Confrontation Naming (PD-CRS)				N/A	N/A	n.s.	-
Visuospatial							
Clock Copying Task	Grothe (2021)(54)	73 PD	Basal forebrain, hippocampus	N/A	N/A	⊖	Hippocampus^{avg}
Rey Complex Figure Test	Carlesimo (2012)(39)	25 PD	Hippocampus	N/A	N/A	⊖	Hippocampus^{r}

WM: white matter; CB: Cingulate bundle; ILF: inferior longitudinal fasciculus; SLF: superior longitudinal fasciculus, IFOF: inferior fronto-occipital fasciculus, UF: uncinate fasciculus, CC: corpus callosum; IC: internal capsule; SN: substantia nigra; EC: external capsule; CST: corticospinal tract; SCP: superior cerebellar peduncle; CR: corona radiata; ATR: anterior thalamic radiation; CG: cingulate gyrus; SFOF: superior fronto-occipital fasciculus; Fmi: forceps minor; MFG: middle frontal gyrus; IFG: inferior frontal gyrus; OFC: orbitofrontal cortex; IPG: inferior parietal gyrus; GP: globus pallidus; BG: basal ganglia; Fma: forceps major; NBM: nucleus basalis of Meynert; PTR: posterior thalamic radiation; ACC: anterior cingulate cortex; PPN: pedunculopontine nucleus; ICP: inferior cerebellar peduncle; MCP: middle cerebellar peduncle.

↓ = significant decrease; ↑ = significant increase; ⊖ = significant negative association; N/A = the study did not report or measure the parameter.

Table 1.4 DTI literature on other non-motor symptoms in PD in the hippocampus

Other Non-Motor Symptoms							
Measure	Author (Year)	Groups	Regions Analyzed	FA	FA-Location	MD	MD-Location
Overall Non-Motor Scores							
NMSS-Total	Wei (2016)(121)	43 PD	BG, frontal WM, hippocampus, occipital WM, parietal WM, SN, temporal WM	⊖	Hippocampus (contralateral to more symptomatic side)	N/A	N/A
UPDRS-I	Tsai (2020)(65)	82 PD	Whole-brain GM	⊖	IFG (orbital^{r}), IPG^{r}, Rolandic operculum^{l}, temporal pole^{r} (superior)	⊖	Cerebellum^{uns}, SFG (medial^{r} and orbital^{l})

Other Non-Motor Symptoms							
Measure	Author (Year)	Groups	Regions Analyzed	FA	FA-Location	MD	MD-Location
	Wei (2016)(121)	43 PD	BG, frontal WM, hippocampus, occipital WM, parietal WM, SN, temporal WM	⊖	Hippocampus^{avg} (and contralateral to more symptomatic side)	N/A	N/A
	Tsai (2020)(65)	82 PD	Whole-brain GM	⊕	Cerebellum^{r}, olfactory cortex^{r}	⊕	Hippocampus^{l}, thalamus^{r}
	Andica (2019)(52)	20 PD	Whole-brain WM and GM	n.s.	-	n.s.	-
Depression – Rating Scales							
UPDRS-I – Depression	Andica (2019)(52)	20 PD	Whole-brain WM and GM	n.s.	-	n.s.	-
Anxiety							
UPDRS-I – Anxiety	Andica (2019)(52)	20 PD	Whole-brain WM and GM	n.s.	-	n.s.	-
Apathy – Rating Scales							
UPDRS-I – Apathy	Andica (2019)(52)	20 PD	Whole-brain WM and GM	n.s.	-	n.s.	-
Other Mood							
NMSS – Mood	Wei (2016)(121)	43 PD	BG, frontal WM, hippocampus, occipital WM, parietal WM, SN, temporal WM	⊖	Hippocampus^{avg} (and hemisphere contralateral to more symptomatic side, and hemisphere contralateral to less symptomatic side)	N/A	N/A
Sleep/Fatigue – Group Comparisons							
PD with RBD (vs. HC)	Pyatigorskaya (2021)(57)	34 PD with RBD, 25 HC	Amygdala, brainstem, hippocampus, NBM, PPN, prefrontal cortex, SN	N/A	N/A	↑	Medulla oblongata^{avg}, NBM^{avg}
PD with RBD (vs. PD without RBD)		34 PD with RBD, 20 PD without RBD		N/A	N/A	n.s.	-
Sleep/Fatigue – Rating Scales							
NMSS – Sleep/Fatigue	Wei (2016)(121)	43 PD	BG, frontal WM, hippocampus, occipital WM, parietal WM, SN, temporal WM	n.s.	-	N/A	N/A
UPDRS-I – Daytime Sleepiness	Andica (2019)(52)	20 PD	Whole-brain WM and GM	n.s.	-	n.s.	-
UPDRS-I – Fatigue				n.s.	-	n.s.	-
UPDRS-I – Sleep Problems				n.s.	-	n.s.	-
QoL/ADL							
PDQ-39 SI	Tsai (2020)(65)	82 PD	Whole-brain GM	⊕	Cerebellum^{r}, Rolandic operculum^{r}, SFG^{r} (medial)	⊕	Cerebellum^{uns}, CB^{r} (anterior and posterior), paracentral lobule^{l}, temporal gyrus^{r} (superior)
				n.s.	-	⊖	Caudate^{l}, cerebellum^{l}, insula^{r}, occipital gyrus^{l} (middle)
S&E	Lu (2016)(64)	126 PD	Whole-brain GM	n.s.	-	⊖	CG (posterior) (ipsilateral to side of disease onset)
Psychosis/Hallucinations – Group Comparisons							
PD with VH (vs. HC)	Yao (2016)(59)	12 PD with VH, 14 HC	Hippocampus	N/A	N/A	↑	Hippocampus (entire^{b}, body^{b}, and posterior^{r})
PD with VH (vs. PD without VH)		12 PD with VH, 15 PD without VH		N/A	N/A	↑	Hippocampus^{r} (entire and posterior)

Other Non-Motor Symptoms							
Measure	Author (Year)	Groups	Regions Analyzed	FA	FA-Location	MD	MD-Location
PD with Psychosis (vs. PD without Psychosis)	Zhong (2013)(56)	18 PD with Psychosis, 48 PD without Psychosis	BG, CG, frontal lobe, hippocampus, occipital lobe, SN	↓	CG[b], frontal lobe[b], hippocampus[l], occipital lobe[b]	N/A	N/A
Psychosis/Hallucinations – Rating Scales							
UPDRS-I – Hallucinations	Andica (2019)(52)	20 PD	Whole-brain WM and GM	n.s.	-	n.s.	-
Olfaction – Rating Scales							
Five Odor Olfactory Detection Array: Thresholds of Olfactory Detection	Zhang (2011)(55)	25 PD	Whole-brain WM and GM	n.s.	-	⊖	Parietal WM[l] (inferior)
Five Odor Olfactory Detection Array: Thresholds of Olfactory Identification				⊕	Cerebellum[l] (medial)	⊖	Cerebellum[r]
Bladder/Urinary Symptoms							
NMSS – Urinary	Wei (2016)(121)	43 PD	BG, frontal WM, hippocampus, occipital WM, parietal WM, SN, temporal WM	n.s.	-	N/A	N/A
UPDRS-I – Urinary problems	Andica (2019)(52)	20 PD	Whole-brain WM and GM	n.s.	-	n.s.	-
Gastrointestinal Symptoms							
NMSS – Gastrointestinal	Wei (2016)(121)	43 PD	BG, frontal WM, hippocampus, occipital WM, parietal WM, SN, temporal WM	n.s.	-	N/A	N/A
UPDRS-I – Constipation	Andica (2019)(52)	20 PD	Whole-brain WM and GM	n.s.	-	n.s.	-
Pain – Rating Scales							
UPDRS-I – Pain	Andica (2019)(52)	20 PD	Whole-brain WM and GM	n.s.	-	n.s.	-
Cardiovascular and Respiratory Measures							
Heart Rate Variability during REM Sleep: High Frequency Components	Pyatigorskaya (2016)(58)	52 PD	Brainstem, hippocampus	N/A	N/A	⊕	Medulla oblongata[avg]
Heart Rate Variability during REM Sleep: Low Frequency Components				N/A	N/A	⊖	Medulla oblongata[avg]
Heart Rate Variability during REM				N/A	N/A	⊖	Medulla oblongata[avg]

Other Non-Motor Symptoms							
Measure	Author (Year)	Groups	Regions Analyzed	FA	FA-Location	MD	MD-Location
Sleep: Low Frequency/High Frequency Ratio							
Heart Rate Variability during SWS Sleep: High Frequency Components				N/A	N/A	n.s.	-
Heart Rate Variability during SWS Sleep: Low Frequency Components				N/A	N/A	n.s.	-
Heart Rate Variability during SWS Sleep: Low Frequency/High Frequency Ratio				N/A	N/A	n.s.	-
NMSS – Cardiovascular	Wei (2016)(121)	43 PD	BG, frontal WM, hippocampus, occipital WM, parietal WM, SN, temporal WM	n.s.	-	N/A	N/A
Respiratory Variability during REM Sleep	Pyatigorskaya (2016)(58)	52 PD	Brainstem, hippocampus	N/A	N/A	⊖	Medulla oblongata[avg]
Respiratory Variability during SWS Sleep				N/A	N/A	n.s.	-
Other Non-Motor Symptoms							
NMSS – Miscellaneous	Wei (2016)(121)	43 PD	BG, frontal WM, hippocampus, occipital WM, parietal WM, SN, temporal WM	n.s.	-	N/A	N/A
NMSS – Sexual Function				n.s.	-	N/A	N/A
UPDRS-I – Light-Headedness on Standing	Andica (2019)(52)	20 PD	Whole-brain WM and GM	n.s.	-	n.s.	-

WM: white matter; CB: Cingulate bundle; ILF: inferior longitudinal fasciculus; SLF: superior longitudinal fasciculus, IFOF: inferior fronto-occipital fasciculus, UF: uncinate fasciculus, CC: corpus callosum; IC: internal capsule; SN: substantia nigra; EC: external capsule; CST: corticospinal tract; SCP: superior cerebellar peduncle; CR: corona radiata; ATR: anterior thalamic radiation; CG: cingulate gyrus; SFOF: superior fronto-occipital fasciculus; Fmi: forceps minor; MFG: middle frontal gyrus; IFG: inferior frontal gyrus; OFC: orbitofrontal cortex; IPG: inferior parietal gyrus; GP: globus pallidus; BG: basal ganglia; Fma: forceps major; NBM: nucleus basalis of Meynert; PTR: posterior thalamic radiation; ACC: anterior cingulate cortex; PPN: pedunculopontine nucleus; SFG: superior frontal gyrus; ICP: inferior cerebellar peduncle; MCP: middle cerebellar peduncle.

↓ = significant decrease; ↑ = significant increase; ⊕ = significant positive association; ⊖ = significant negative association; N/A = the study did not report or measure the parameter.

Research Aims

Because the role the hippocampus plays in non-motor symptoms of Lewy Body diseases, and the conflicting literature, we aimed to investigate this area using a new high-resolution DTI technique to study participants that have been recruited through the Canadian Consortium on Neurodegeneration in Aging (CCNA), with data collected using CCNA methods. The current research project will use this method to 1) examine the difference in hippocampal microstructure (without the subiculum) between patients with PD and HC, and 2) determine the associations between hippocampal diffusion metrics and non-motor symptoms of PD, especially neuropsychiatric symptoms. We hypothesized that MD and FA changes would occur in patients with PD relative to HC and reflect changes associated with neurodegeneration through increased MD and decreased FA. We also hypothesize that non-motor symptoms (i.e., global cognitive function, memory, executive function, cognitive speed, neuropsychiatric symptom severity, depression, anxiety, apathy, decreased health-related quality of life, disordered sleep, and symptoms associated with mild behavioural impairment) would be associated with these changes.

Chapter 2 Methods

Overview of Study Design

Research records were obtained through the CCNA Longitudinal Online Research and Imaging System (LORIS) (130). Through this database, we collected participant demographics, clinical descriptors, measures of non-motor symptoms, and neuroimaging data.

Data for the study is being collected as part of the national Comprehensive Assessment of Neurodegeneration and Dementia (COMPASS-ND) study (131), the Functional Assessment and Vascular Reactivity (FAVR)-II study, (132-134), or CB Brain (129). In brief, the COMPASS-ND study is a Canada-wide study that has recruited approximately one thousand individuals experiencing a range of neurodegenerative disorders, as well as cognitively intact older adults, and seeks to address hypotheses around neurodegeneration and age-related cognitive changes that have been developed by CCNA-affiliated research teams around the country (131). We also used healthy control data from phase two of the FAVR study (134), which is a study that recruits participants with cerebral amyloid angiopathy, MCI, mild AD and healthy older adult controls at the University of Calgary and University of Alberta (132, 133). The other study from which imaging data was collected images is CB Brain, which is based at the University of Alberta and recruits healthy volunteers across the lifespan for neuroimaging in order to characterize age-related changes in the brain (129).

Study Sample

All participants in this study have provided informed consent for the collection and use of their data by the COMPASS-ND study. The research project, of which this thesis is a part, received

research ethics approval from the University of Alberta Research Ethics Board, project name: "Hippocampal Changes and Non-Motor Symptoms in Neurodegeneration and Aging." Pro00106834, June 3, 2021. The initial data for this study was obtained through the COMPASS-ND and FAVR studies, including 40 participants with neurodegenerative diseases (24 PD, 10 PD-MCI, 6 LBD [3 DLB/3 PDD]) who were assessed at the University of Alberta. Healthy controls recruited through the same program (7 through FAVR and 8 through COMPASS-ND) included spouses, friends, and family of the participants with PD. An additional 20 healthy control subjects, who underwent an identical diffusion imaging protocol, were recruited through the laboratory of Dr. Christian Beaulieu as part of CB Brain.

Participants with Parkinson's Disease were recruited through the University of Alberta Movement Disorders Program or community referral. At the time of recruitment, 40 PD participants met the criteria for Parkinson's Disease; however, since this was a longitudinal study without imaging two years after baseline, disease status was re-assessed at this visit and two participants were reclassified into other non-PD disorders (progressive supranuclear palsy and multiple system atrophy) and excluded from the current study. Other exclusion criteria for participants in the COMPASS-ND study included the previous traumatic brain injury or the presence of other diseases that significantly impact brain function, (e.g., multiple sclerosis, Huntington's, or brain malignancies), symptomatic stroke within the past year, current substance use disorder, the lack of a study partner, lack of proficiency in either English or French, a Montreal Cognitive Assessment (MoCA) score < 13, and any contraindications to MRI scanning (131). Exclusion criteria for HC also included a family history of PD and the presence of significant medical, psychiatric, or neurological conditions.

For this project, hippocampal segmentations were performed on all participants (see Appendix B), and the final analyses included 38 participants in the group and 35 in the HC group.

Clinical Data Collection

Procedure

Several measures of non-motor symptoms were chosen for analysis based on their abilities to discriminate PD from HC or other neurodegenerative diseases, or their known associations with hippocampal structure and function. Available data were collected from each participant, however, control participants within the CB brain group (n = 20) did not have neurocognitive data, since these assessments were performed through the COMPASS-ND and FAVR studies only.

Demographics and Clinical Descriptors

Age rounded to the nearest year at the time of the baseline MRI scan, and sex was recorded for all participants. Additionally, for all individuals within the LB group (and HCs with available data), years of education, general measures of health and cognition, such as cardiovascular risk measured using the Framingham Cardiovascular Risk Score (135), the Physical Activity Scale for the Elderly (PASE) score (136), and cognitive fluctuations as measured by the Mayo Fluctuations Scale (137). Additionally, we included a measure of olfactory score using the Brief Smell Identification Test (138), because of the association between the olfaction and hippocampal function (139), and we used nutrition risk, measured

using the Seniors in the Community: Risk Evaluation for Eating and Nutrition, Version II (140), which has been also been found to have an effect on hippocampal function (141).

For individuals within the LB group, we obtained disease duration in years, age at disease onset in years, the third section of the Movement Disorder Society-sponsored revision of the Unified Parkinson's Disease Rating Scale (MDS-UPDRS-III) including total as well as an axial symptoms score (142), Levodopa Equivalent Dose (LED) in mg (143), side of disease onset (bilateral, left-, or right-sided) calculated using the asymmetric index score (144), and Hoehn and Yahr stage (145).

Measuring Non-Motor Symptoms

Global cognitive function, memory, executive function, and cognitive speed were assessed using a comprehensive neuropsychological test battery and participant ratings of subjective cognitive impairment and functional capacity. Using this data, we examined the association between hippocampal measures and cognition.

To determine the presence of other non-motor and neuropsychiatric symptoms, we measured the following: overall neuropsychiatric symptom severity, depression, anxiety, apathy, health-related QoL, disordered sleep, and mild behavioural impairment (MBI). An overview of the measures used for non-motor symptoms can be found in Table 2.1.

Table 2.1 Measures of Cognition and Neuropsychiatric Symptoms

	Test	Criteria	Reference
Cognitive Symptoms			
Global Cognitive Function	MoCA	Higher score indicates better function; < 26 classified as PD-MCI	(146)
Memory Z-Score	Average z-scores from RAVLT – Delayed Recall and BVMT-R	Higher score indicates better function	(147)
Executive Function Z-Score	Average z-scores from D-KEFS – Letter Fluency and TMT-B		
Cognitive Speed Z-Score	Average z-scores from TMT-A and WAIS-III – Digit Substitution		
Neuropsychiatric Symptoms			
Neuropsychiatric Symptom Severity	NPI Severity Score	Higher score indicates increased symptom severity	(148)
Depression	GDS-30	Higher score indicates increased symptoms of depression; > 11 classified as depression	(149)
Anxiety	GAD-7	Higher score indicates increased symptoms of anxiety; > 10 classified as anxiety	(150)
Apathy	Apathy Inventory	Higher score indicates increased symptoms of apathy; > 1 classified as apathy	(151)
QoL and Sleep Symptoms			
Health-Related QoL	PDQ-39 SI Score	Higher score indicates worse health-related QoL	(152)
Disordered Sleep	COMPASS-ND Sleep Questionnaire	Higher score indicates worse sleep	(153)
Behavioural Symptoms – MBI			
Abnormal Perception or Thought Content	Presence of delusions with or without hallucinations on NPI	Score of 1 indicates symptom is present, score of 0 indicates symptom is absent	(154)
Decreased Motivation	Presence of apathy/indifference on NPI		
Emotional / Affective Dysregulation	Presence of depression/dysphoria, anxiety, with or without elation/euphoria on NPI		
Impulse Dyscontrol	Presence of agitation/aggression, irritability/lability, with or without aberrant motor behaviour on NPI		
Social Inappropriateness	Presence of apathy/indifference on NPI		

MoCA: Montreal Cognitive Assessment; PD-MCI: Parkinson's Disease with Mild Cognitive Impairment; RAVLT: Rey's Auditory Verbal Learning Test; BVMT-R: Brief Visuospatial Memory Test – Revised; D-KEFS: Delis-Kaplan Executive Function System; TMT: Trail Making Test; WAIS-III: Wechsler Adult Intelligence Scale, Third Edition; NPI: Neuropsychiatric Inventory; GDS-30: Geriatric Depression 30-Item Scale; GAD-7: Generalized Anxiety Disorder 7-Item Scale; PDQ-39: Parkinson's Disease Questionnaire (39 items); SI: Summary Index; COMPASS-ND: Comprehensive Assessment of Neurodegeneration and Dementia; MBI: Mild Behavioural Impairment.

Cognitive Measures

As shown above, global cognition and cognitive function in several domains (including visuospatial, executive function, learning and memory, attention, and language) were assessed using a comprehensive neuropsychological test battery, as well as participant ratings of subjective cognitive impairment and functional capacity. To associate general cognition with hippocampal measures, we used a measure of global cognition and aggregate z-scores spanning the domains of memory, executive function, and cognitive speed from the data available through the test battery. Cognitive domain z-scores were calculated by converting raw neuropsychological test scores to z-scores based on published age-stratified normative data (147).

To measure global cognitive function, we used the Montreal Cognitive Assessment (MoCA), which was developed as a quick way to detect MCI (146). We used this measure PD to classify PD participants as having MCI when their MoCA scores were below 26 (146). The MoCA has been validated for use in PD and is more sensitive for detecting cognitive impairment in these patients than similar tests such as the Mini-Mental State Examination (155).

Memory z-scores were calculated by averaging the z-scores from the delayed recall portion of Rey's Auditory Verbal Learning Test (RAVLT) and the Brief Visuospatial Memory Test – Revised (BVMT-R) (156). The RAVLT has been shown to be helpful in exploring hippocampal structure in patients with neurodegenerative diseases. For instance, delayed recall as measured by the RAVLT has been associated with DTI-measured degradation of the perforant pathway in healthy older adults (157, 158) and has been predicted by structural changes in the hippocampus and amygdala of patients with Alzheimer's disease (159) and hippocampal subfield volumes in patients with PD (160). The BVMT-R (156) has been associated with hippocampal volume in

patients with amnestic MCI (161) and detected visuospatial deficits in patients with PD-MCI (162).

We calculated executive function z-scores by averaging the z-scores from the letter fluency section of the Delis-Kaplan Executive Function System (D-KEFS) and part B of the Trail Making Test (TMT-B). Letter fluency, also known as phonemic fluency, is known to be impaired in patients with PD compared to HCs (163). The TMT-B (164) has been correlated with functional connectivity between the hippocampus and other parts of the brain in individuals with amnestic MCI (165).

Finally, we calculated cognitive speed z-scores by using the average z-scores from part A of the Trail Making Test (TMT-A) and the digit substitution portion of the Wechsler Adult Intelligence Scale, Third Edition (WAIS-III) (166, 167). The TMT-A (164) has also been associated with functional connectivity between the hippocampus and other regions of the brain in individuals with amnestic MCI (165). Compared to healthy HC, individuals with PD have also been found to have marked impairments in digit symbol substitution, also known as digit symbol coding (168).

Non-Cognitive Measures

Neuropsychiatric and Behavioural Raw Scores

First, an overall measure of neuropsychiatric symptoms, as measured by the Neuropsychiatric Inventory (NPI) severity score (148) was used, followed by the Geriatric Depression Scale 30-item scale (GDS-30) to assess depression (149), the Generalized Anxiety Disorder 7-item scale (GAD-7) to identify anxiety (150), and the Apathy Inventory to measure apathy (151).

Quality of Life and Sleep

Parkinson's Disease Questionnaire 39 (PDQ-39) Summary Index (SI) score (152) was used as a measure of health-related quality of life. Disordered sleep was measured using the sleep questionnaire from COMPASS-ND (131) based on the Pittsburgh Sleep Quality Index (153).

Neuropsychiatric and Behavioural Groupings

Study participants were categorised into having depression or no depression based on the suggested cut-off of 11 on the GDS-30 (149). Similarly, patients were characterised as having a generalized anxiety disorder or not, using the suggested cut-off of 10 on the GAD-7 (150). Participants with a score of 1 or higher on the Apathy Inventory (151) were categorised as having apathy. Finally, following the methods of a previous study (154), responses to questions on the NPI were used to determine the presence of behavioural symptoms in five domains of Mild Behavioural Impairment (MBI): Abnormal perception or thought content (presence of delusions with or without hallucinations on the NPI), decreased motivation (presence of apathy/indifference on the NPI), emotional/affective dysregulation (presence of depression/dysphoria, anxiety, with or without elation/euphoria on the NPI), impulse dyscontrol (presence of agitation/aggression, irritability/lability, with or without aberrant motor behaviour on the NPI), and social inappropriateness (presence of apathy/indifference on the NPI) (154). The MBI index measures neuropsychiatric symptoms in individuals with MCI and can indicate a risk for further cognitive decline (154). The authors of one study (154) have developed a method to translate responses on the Neuropsychiatric Inventory to MBI categories, which is the method we have implemented here.

Neuroimaging

Image Acquisition

High-resolution hippocampal imaging was obtained for all participants using a protocol designed by Treit and colleagues (53), and the acquired data was processed using MRTrix (129). MRI images through a section of the brain that containing the hippocampus were acquired at Peter S. Allen MRI Research Centre at the University of Alberta on a 3T Siemens Prisma (Erlangen, Germany) using a 64-channel head coil. DTI images of the hippocampus were acquired using a single-shot 2D EPI sequence (GRAPPA factor 2, 6/8 PPF, A/P phase encode), with FoV = 220 mm x 216 mm, matrix = 220 x 216, BW = 1420 Hz/px, 20 axial-oblique slices parallel to the long axis of the hippocampus with 1 mm thickness and no gap, 1 mm x 1 mm x 1 mm with no interpolation, TE = 72 ms, TR = 2,800 ms, diffusion time = 29 ms, b =500 s/mm^2 with 10 monopolar gradient directions with 10 averages, and 10 non-diffusion-weighted image (DWI) volumes acquired in 5:18 min (53). Pre-scan normalize was used to correct for B1 inhomogeneity and provide better visualization of the hippocampus (53). See Figures 2-1 and 2-2 for representations of diffusion maps acquired and representative slices of the hippocampus before segmentation, respectively.

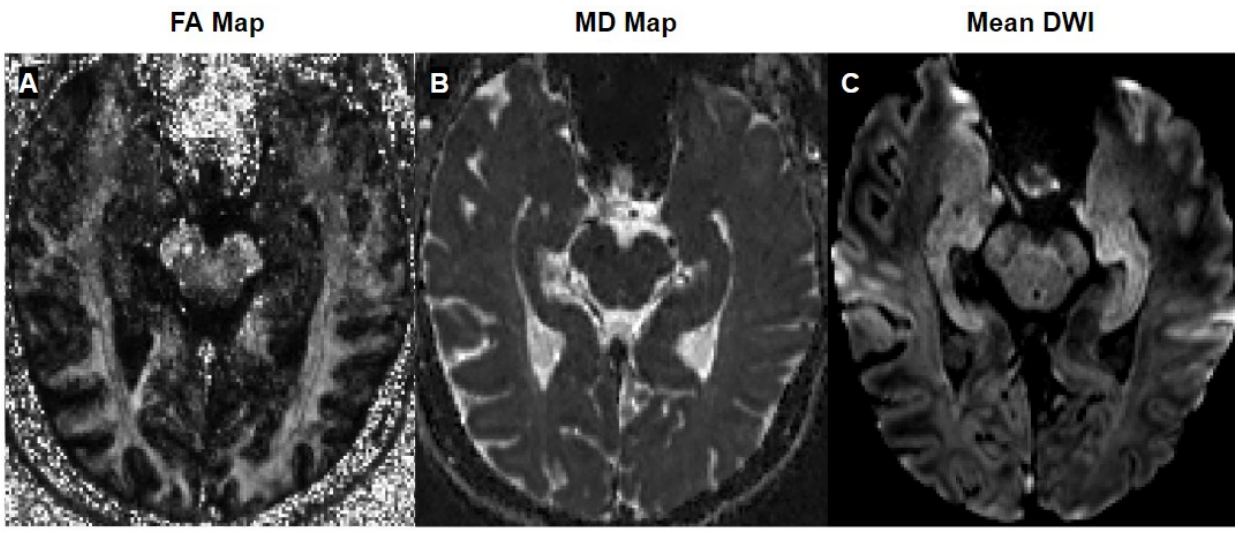

Figure 2-1 Axial maps obtained from diffusion imaging.

(A) Fractional anisotropy (FA) map, (B) mean diffusivity (MD) map, (C) and mean diffusion-weighted image (DWI).

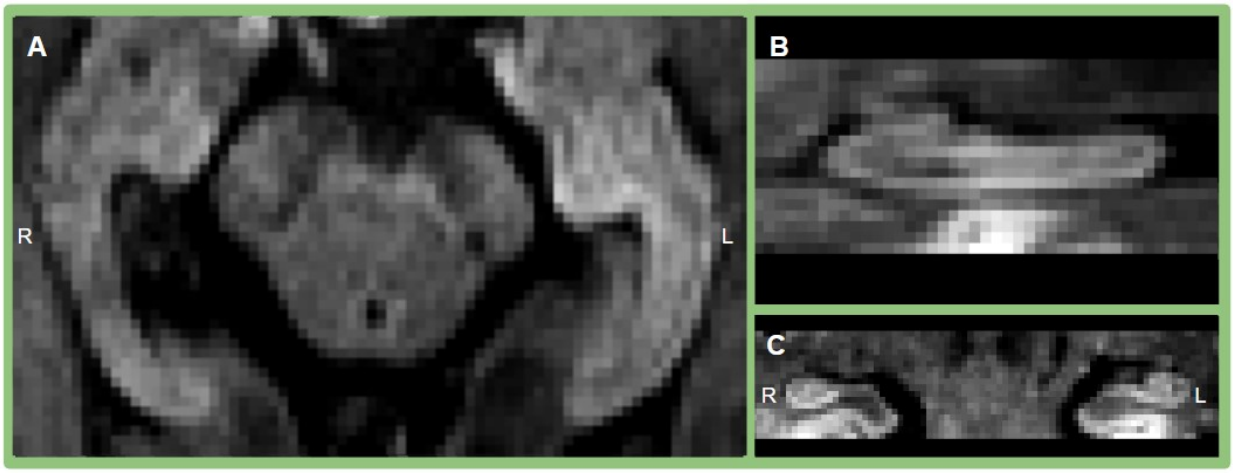

Figure 2-2 Sample of hippocampal slices before tracing in three planes.

(A) Transverse view of both hippocampi, (B) sagittal view of the left hippocampus, and (C) coronal view of both hippocampi.

Hippocampal Segmentation

Maps of MD obtained from hippocampal segmentations are shown in Appendix B (Figures B1-B2). The right and left hippocampi were segmented in a blinded manner for all participants by performing manual hippocampal tracing on high-resolution mean DWI images as described in

previous studies (53, 129). For each subject, hippocampi were manually segmented by a single rater (AB) on anonymized images using ITK-SNAP software (169). Images were segmented according to the European Alzheimer's Disease Consortium and Alzheimer's Disease Neuroimaging Initiative Harmonized protocol (170, 171), including the fimbria, alveus, and tail of the hippocampi, but excluding the subiculum (129). The hippocampi were first traced along the axial-oblique plane and then adjusted in the sagittal and coronal planes to ensure the hippocampi were segmented accurately in all planes (see Figure 2-3). After all segmentations were complete, the same rater reviewed each anonymized segmentation individually and adjusted as needed to ensure the hippocampi were segmented accurately and consistently across all participants. Once this was complete, the volumes and the average FA and MD of each left and right hippocampus were extracted for further analysis. The number of digitations on the hippocampal head were also determined following methods used in a previous study (129).

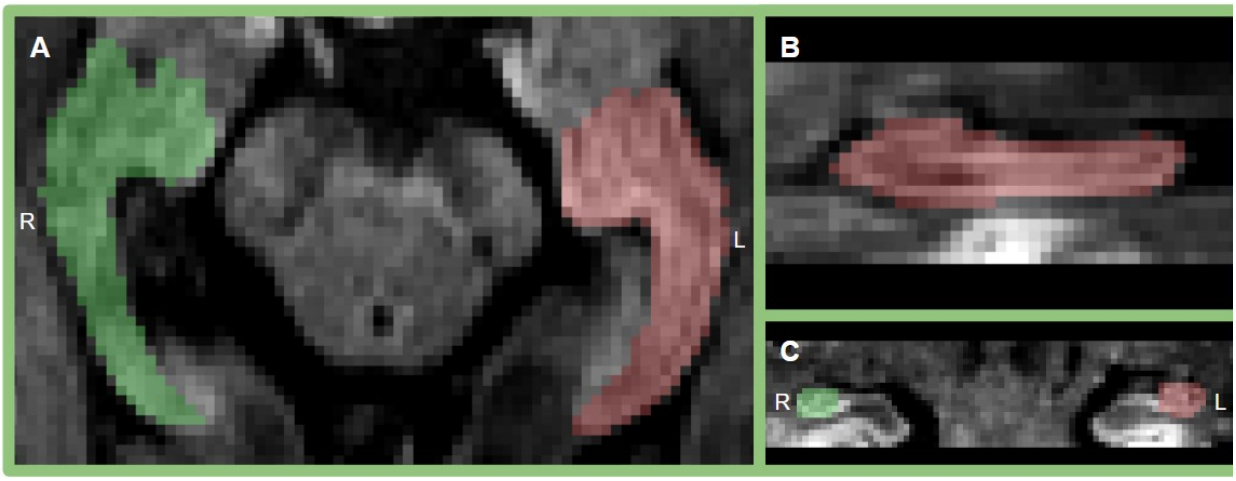

Figure 2-3 Sample of hippocampal tracing in three planes.

(A) Transverse view of both hippocampi, (B) sagittal view of the left hippocampus, and (C) coronal view of both hippocampi. Tracing of the right hippocampus is shown in green (on the left side of panel a), and the tracing of the left hippocampus is shown in red (on the right side of panel a). Left and right sides were identified using a vitamin E capsule that was taped to the participant's right temple at the time of imaging.

Reliability Analysis

To ensure the hippocampi were properly segmented, segmentations from another experienced rater were obtained to determine intra-rater reliability and inter-rater reliability. Intra-class correlation coefficients (ICC) for two raters were obtained using software designed for evaluating medical image segmentations (172). ICC values obtained over 14 segmentations indicate good inter-rater (ICC = 0.862) and intra-rater (ICC = 0.853) reliability (173). See Figure 2-4 for an example of 3D-rendered segmentations for rater 1 and rater 2.

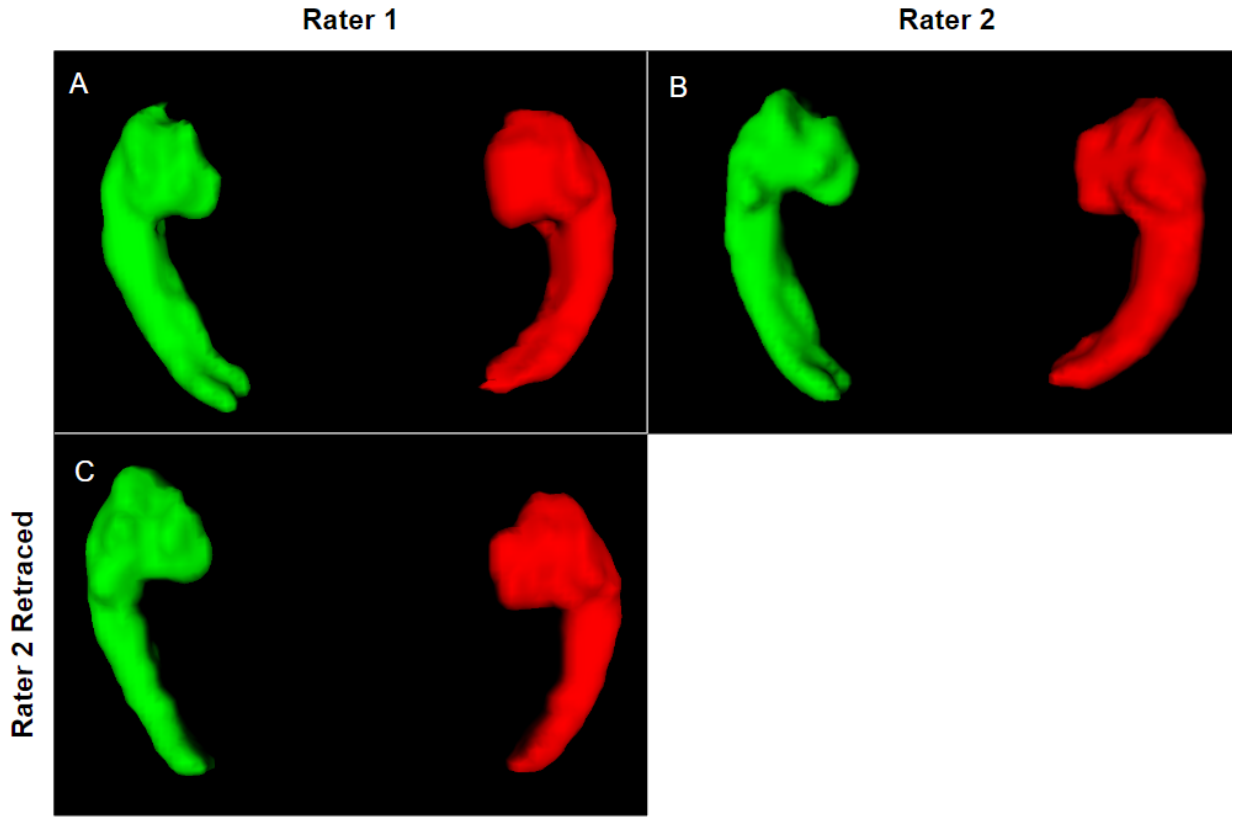

Figure 2-4 3D representation of segmentations obtained from two raters.

(A) A segmentation performed by rater 1 (Kevin Solar). (B) The first segmentation on the same subject, performed by rater 2 (Alexandra Budd). (C) The second segmentation on the same subject, performed by rater 2. Tracing of the right hippocampus is shown in green, and tracing of the left hippocampus is shown in red.

Statistical Analysis

For analyses of continuous data, we first checked that the data was normally distributed within each group by testing the significance of the skewness, kurtosis, and Shapiro-Wilk normality test. If the data were found to be not normally distributed within any of the groups, we then transformed the data by taking the square root and re-checking normality (174). Transforming the data rather than using a non-parametric approach on raw data has been shown to be more powerful, especially in samples that are quite non-normally distributed (175). If the transformation corrected the distribution, we used the transformed data for parametric comparisons (t-tests and ANOVAs). However, if applying the transformation did not correct the distribution, we used non-parametric tests (Wilcoxon-Signed Rank and Kruskal-Wallis) on the untransformed data.

Our first objective was to characterize any differences in demographic or general health variables and to determine whether there were differences in hippocampal volume and diffusivity metrics (i.e., FA and MD) between patients with LB spectrum diseases and healthy HC. To address this objective, we performed 2-tailed independent samples t-tests or Wilcoxon-Signed Rank tests. Additionally, we tested for differences between healthy HC, the LB-Unimpaired group, and the LB-Impaired groups using one-way ANOVAs with Tukey-HSD post-hoc analyses or Kruskal-Wallis tests with Dunn post-hoc analyses, and for measures that were not available in the control group, we compared the values between the two LB groups using 2-tailed independent samples t-tests or Wilcoxon-Signed Rank tests. Finally, we performed t-tests on normally distributed age- and sex-adjusted MRI measures and Wilcoxon-Signed Rank tests on non-normally distributed measures and then applied False Discovery Rate (FDR) corrections. Additionally, power calculations on the hippocampal volumes, MD, and FA were done by using

a post-hoc power analysis for independent samples t-tests using α, sample size, and effect size in G*Power 3.1 (176).

To meet our second objective, which was to determine the relationship between hippocampal diffusion metrics (i.e., FA and MD), volume, and neuropsychiatric symptoms, we first determined which neuropsychiatric symptoms were associated with DTI metrics using Kendall's Tau correlation tests with diffusion metrics adjusted for age and sex as covariates because age is known to be associated with diffusion metrics in the hippocampus (129), and there is some suggestion that sex may also affect diffusion measures (177) (see Appendix Tables C1-C2 for correlations between diffusion metrics and potential confounding variables). Afterwards, as a confirmatory analysis we compared diffusion metrics across LB participants grouped based on clinically significant symptoms of depression, anxiety, apathy, and MBI symptoms, using Wilcoxon Signed-Rank tests for FA and MD (since FA and MD were not normally distributed across all groups and square root transformation of their values did not make them normally distributed) and independent sample t-tests for volume (which was normally distributed in all groups). As before, we then performed t-tests on normally distributed age- and sex-adjusted MRI measures and Wilcoxon-Signed Rank tests on non-normally distributed measures and then applied FDR corrections. Results with a p-value ≤ 0.05 after FDR correction were considered significant.

Chapter 3 Findings

Participants

In total, 38 individuals with LB diagnoses were included in the analysis. Within this group, 12 (31.6%) were female and 26 (68.4%) were male, and ages ranged from 58 to 87 (mean: 69.5) years old at the time of the baseline MRI scan (Table 3.1). In the control group, there were 35 individuals, of which 19 (54.3%) were female and 16 (45.7%) were male. Ages in the control group ranged from 50 to 83 (mean: 67) years old at the time of the baseline MRI scan. Sex distribution for both LB-Unimpaired (LB-U) and LB-Impaired (LB-I) cognition groups was significantly different from HCs ($X^2 = 8$; $p = .02$), and the LB-I group had a significantly higher age than LB-U and HCs ($F = 6$; $p = .004$). Other demographics within these groups are also presented in Tables 3.1 and 3.2.

Table 3.1 Demographics and descriptors for study participants in the control and LB groups.

Measure	HC Group (n=35)			LB Group						Group Comparisons	
				LB-All (n=38)		LB-U (n=22)		LB-I (n=16)		Test Statistic (*p*)	
	n	Value	Min-Max	Value	Min-Max	Value	Min-Max	Value	Min-Max	HC vs. LB-All	HC vs. LB-U vs. LB-I
Age (years)	35	66.7[a] (6.8)	50-83	69.5 (7.2)	58-87	66.8[a] (6.2)	58-78	73.3[b] (7.0)	62-87	*t*=-1.8 (.09)	*F*=6 (**.004**)§
Sex, count (percent)											
Male	35	16[a] (45.7)	-	26 (68.4)	-	12[b] (54.5)	-	14[b] (87.5)	-	X^2 =3.8 (.05)	X^2=8 (**.02**)§
Female		19[a] (54.3)	-	12 (31.6)	-	10[b] (45.5)	-	2[b] (12.5)	-		
Education (years)	31	16.7	10-25	15.7 (3.6)	3-23	16.5 (3)	12-23	14.6 (4.3)	3-21	*W*=663 (.4)	*F*=2.1 (.1)
FRS*	14	21.7[a] (16)	4.4-65.5	28 (15.2)	5.7-60.4	23.1[a] (15.6)	5.7-60.4	34.7[b] (12.1)	11.6-54.4	*t*=-1.4 (.2)	*F*=4.6 (**.01**)§
Fluctuations	8	0.4 (0.5)	0-1	1.1 (1.1)	0-4	1 (1.1)	0-4	1.3 (1.1)	0-3	*W*=89.5 (.06)	*H*=4.7 (.1)
Olfactory	8	10.3[a] (0.9)	9-11	5.9 (3.1)	1-12	6.7[b] (3.0)	2-12	4.8[b] (3.0)	1-11	*W*=261 (**.001**)§	*H*=13.4 (**.001**)§
PASE (x10)*	15	12.4 (6)	3.6-25.3	11.3 (6.4)	1.2-30.8	12.5 (6.8)	3.8-30.8	9.6 (5.5)	1.2-23.4	*t*=0.7 (.5)	*F*=1.5 (.2)
Nutrition Risk*	15	35.7 (7.6)	18-44	35.3 (8.2)	7-46	36.9 (5.7)	23-45	33.1 (10.6)	7-46	*t*=0.02 (1)	*F*=1.1 (.4)

Note: Group comparisons were performed across two groups (HC vs, LB-All) and three groups (HC vs. LB-U vs. LB-I). Values shown in mean (SD) unless otherwise noted. Different superscript letters within a row denote FDR-corrected significantly different values after conducting Tukey-HSD (for ANOVA), Dunn (for Kruskal-Wallis) post-hoc tests, or between-group chi-squared tests (values for between-group comparisons were considered significantly different if $p < .017$). FRS measures risk of cardiovascular disease (135).

*Although raw values are presented in the table, group comparisons were conducted using square root-transformed values (for nutrition risk, the control group and LB subgroups were normally distributed, so raw values were used in the 3-group comparison).

§ Comparison between demographic and descriptive measures across both groups remained significant after FDR correction (when run across *p*-values for HC vs. LB-All and HC vs. LB-U vs. LB-I comparisons separately).

Values of $p < .05$ are bolded.

HC: Healthy control; LB: Lewy Body; LB-U: LB-Unimpaired cognition subgroup; LB-I: LB-Impaired cognition subgroup; FRS: Framingham Risk Score; PASE: Physical Activity Scale for the Elderly.

Table 3.2 Demographics and descriptors for participants in the LB group.

Measure	LB Group - All (n=38)		LB-Unimpaired Subgroup (n=22)		LB-Impaired Subgroup (n=16)		Subgroup Comparison
	Value	Min-Max	Value	Min-Max	Value	Min-Max	Test Statistic (*p*)
Disease Duration (years)	6.3 (4.4)	0.8-19.7	6 (3.8)	0.8-19	6.6 (5.1)	1.1-19.7	W=179.5 (.9)
Disease Onset (years)	63.3 (7.5)	47.2-78.9	60.9 (7.2)	47.2-72.3	66.6 (6.7)	55.9-78.9	t=2.5 (**.02**)
MDS-UPDRS-III*	19.7 (7.6)	7-44	18.4 (8.6)	7-44	21.4 (5.9)	12-33	t=1.5 (.2)
Axial Score	3.6 (1.8)	0-8	3 (1.6)	0-8	4.3 (1.9)	2-7	t=2.3 (**.03**)
LED (x10^2 mg)	6.1 (3.7)	0-15.3	6 (3.4)	0-13	6.3 (4.1)	0-15.3	t=0.2 (.8)
Disease Laterality, count (percent)							
Bilateral	13 (34.2)	-	8 (36.4)	-	5 (31.3)	-	X^2=0.45 (.8)
Left	12 (31.6)	-	6 (27.3)	-	6 (37.5)	-	
Right	13 (34.2)	-	8 (36.4)	-	5 (31.3)	-	
Hoehn and Yahr Stage, count (percent)							
1	4 (10.5)	-	4 (18.2)	-	0 (0)	-	X^2=6.6 (**.04**)
2	26 (68.4)	-	16 (72.7)	-	10 (62.5)	-	
3	8 (21.1)	-	2 (9.1)	-	6 (37.5)	-	

Note: Values shown in mean (SD) unless otherwise noted.
*Although raw values are presented in the table, group comparisons were conducted using square root-transformed values.
§ Comparison between demographic and descriptive measures in the LB group remained significant after FDR correction (when run across all *p*-values).
Values of p <.05 are bolded.
HC: Healthy control; LB: Lewy Body; LB-U: LB-Unimpaired cognition subgroup; LB-I: LB-Impaired cognition subgroup; MDS-UPDRS-III: Movement Disorders Society - Unified Parkinson's Disease Rating Scale Part III; LED: Levodopa Equivalent Dose.

Cognitive Measures

Within the LB group, participants with PD-MCI, PDD, or DLB were categorised as LB with cognitive impairment (LB-Impaired; n=16), and the rest were categorised as LB-Unimpaired (n=22).

As shown in Table 3.3, the LB-Impaired group had significantly lower MoCA scores (mean: 20.06 ± 4.12) than both the control group (mean: 27.07 ± 1.58) and the LB-Unimpaired group (mean: 27.77 ± 1.31; p < .001). Furthermore, the entire LB group had decreased memory (mean: -0.59 ± 1.11), executive function (mean: -0.45 ± 1.27), and cognitive speed (mean: -0.30 ± 1.12) z-scores compared to HC (means: 0.72 ± 0.98, 0.60 ± 0.75, and 0.86 ± 0.70, respectively; all p <.01). All values remained significant when FDR-corrected.

Table 3.3 Cognitive measures for study participants.

Measure	HC Group (n=15)		LB Group						Group Comparisons	
			LB-All (n=38)		LB-U (n=22)		LB-I (n=16)		Test Statistic (*p*)	
	Mean (SD)	**Min-Max**	**Mean (SD)**	**Min-Max**	**Mean (SD)**	**Min-Max**	**Mean (SD)**	**Min-Max**	**HC vs. LB-All**	**HC vs. LB-U vs. LB-I**
MoCA	27.07[a] (1.58)	25-30	24.53 (4.77)	10-30	27.77[a] (1.31)	26-30	20.06[b] (4.12)	10-24	*W*=361 (.1)	*H*=34.6 (**<.001**)§
Cognitive z-scores										
Memory	0.72[a] (0.98)	-1.31-2.32	-0.59 (1.11)	-2.8-1.69	0.06[b] (0.76)	-1.25-1.69	-1.49[c] (0.85)	-2.80- -0.22	*t*=4 (**<.001**)§	*F*=28.1 (**<.001**)§
Executive*	0.60[a] (0.75)	-0.41-2.26	-0.45 (1.27)	-2.67-2.05	0.08[a] (1.08)	-2.17-2.05	-1.18[b] (1.16)	-2.66 – 0.70	*W*=420.5 (**.008**)§	*F*=13.3 (**<.001**)§
Speed	0.86[a] (0.70)	-0.48-1.98	-0.3 (1.12)	-3-1.68	0.29[b] (0.81)	-0.99-1.68	-1.11[c] (0.98)	-3.00 – 0.74	*t*=3.7 (**<.001**)§	*F*=23.5 (**<.001**)§

Note: Group comparisons were performed across two groups (HC vs, LB-All) and three groups (HC vs. LB-U vs. LB-I). Different superscript letters within a row denote FDR-corrected significantly different values after conducting Tukey-HSD (for ANOVA) or Dunn (for Kruskal-Wallis) post-hoc tests.
*Although raw values are presented in the table, the 3-group comparison was conducted using square root-transformed values.
§ Comparison between cognitive measures remained significant after FDR correction (when run across *p*-values for HC vs. LB-All and HC vs. LB-U vs. LB-I comparisons separately).
Values of $p < .05$ are bolded.
HC: Healthy control; LB: Lewy Body; LB-U: LB-Unimpaired cognition subgroup; LB-I: LB-Impaired cognition subgroup; MoCA: Montreal Cognitive Assessment.

Non-Cognitive Measures

As shown in Table 3.4, NPI severity scores were also significantly increased in the LB (mean: 4.8 ± 5.2) compared to the control group (mean: 0.3 ± 0.8; $p < .001$). Additionally, although GAD-7 scores were not significantly different between groups, GDS-30 scores were significantly higher in the LB group (mean: 8.5 ± 5.8) than in HC (mean: 3.9 ± 3.6; $p = .002$). Apathy Inventory scores were significantly increased in the LB group (mean: 1.9 ± 4.0) compared to the control group (mean: 0 ± 0; $p = .008$), as were average sleep scores (LB: 8.1 ± 3.7; Control: 4.7 ± 2.5; $p = .003$). PDQ-39 SI scores were not significantly different between LB subgroups. All values remained significant when FDR-corrected.

Table 3.4 Non-cognitive scores for study participants.

Measure	HC (n=15)†		LB Group						Group Comparisons	
			LB-All (n=38)		LB-U (n=22)		LB-I (n=16)		Test Statistic (*p*)	
	Value	Min-Max	Value	Min-Max	Value	Min-Max	Value	Min-Max	HC vs. LB-All	HC vs. LB-U vs. LB-I
NPI Severity	0.3[a] (0.8)	0-3	4.8 (5.2)	0-28	3.2[b] (2)	0-6	7[b] (7.2)	0-28	*W*=39.5 (**<.001**)§	*H*=26.6 (**<.001**)§
GDS-30*	3.9[a] (3.6)	0-13	8.5 (5.8)	0-21	8.5[b] (6.4)	0-21	8.6[b] (5.1)	3-21	*t*=-3.2 (**.002**)§	*F*=5.1 (**.009**)§
GAD-7	1.7 (1.9)	0-6	4.7 (5.1)	0-16	4.2 (4.1)	0-16	5.5 (6.3)	0-16	*W*=187.5 (.05)	*H*=3.8 (.1)
Apathy	0[a] (0)	0-0	1.9 (4)	0-19	0.3[a] (0.8)	0-3	4.1[b] (5.4)	0-19	*W*=180 (**.008**)§	*H*=18.4 (**<.001**)§
Sleep	4.7[a] (2.5)	1-10	8.1 (3.7)	2-17	7.4[b] (2.9)	2-13	9[b] (4.5)	3-17	*t*=-3.2 (**.003**)§	*F*=6.1 (**.004**)§
Measure available in LB Group only										
			LB-All (n=37)		LB-U (n=22)		LB-I (n=16)		Comparison Between Subgroups	
PDQ-39 SI*	-	-	19.5 (12.7)	2.4-50.5	16.2 (9.8)	2.6-35.4	24.3 (15.3)	2.4-50.5	*t*=1.7 (.1)	

Note: Group comparisons were performed across two groups (HC vs, LB-All) and three groups (HC vs. LB-U vs. LB-I). Different superscript letters within a row denote FDR-corrected significantly different values after conducting Tukey-HSD (for ANOVA) or Dunn (for Kruskal-Wallis) post-hoc tests.
*Although raw values are presented in the table, the 3-group comparison was conducted using square root-transformed values.
†n=14 in the control group for sleep.
§ Comparison between non-cognitive measures remained significant after FDR correction (when run across *p*-values for HC vs. LB-All and HC vs. LB-U vs. LB-I comparisons separately).
Values of $p < .05$ are bolded.
HC: Healthy control; LB: Lewy Body; LB-U: LB-Unimpaired cognition subgroup; LB-I: LB-Impaired cognition subgroup; NPI: Neuropsychiatric Inventory; GDS-30: Geriatric Depression Scale (30 items); GAD-7: Generalized Anxiety Disorder (7 items); PDQ-39 SI: Parkinson's Disease Questionnaire (39 items) Summary Index.

As shown in Table 3.5, 26.3% of the LB group had met the cut-off for depression, compared to only 6.7% in the control group, although this difference was not statistically significant. Similarly, a higher percentage of participants in the LB group met the cut-off for GAD compared to HC (LB: 15.8%, HC: 0%), though this difference was not statistically significant. However, the presence of apathy was significantly different between groups (LB: 46.8%, HC: 0%; $p = .006$). The MBI domains with significant difference between groups were decreased motivation (LB: 39.5%, HC: 0%; $p = .004$), emotional dysregulation (LB: 65.8%, HC: 6.7%; $p < .001$), and impulse dyscontrol (LB: 39.5%, HC: 6.7%; $p = .02$). All comparisons remained significant when FDR-corrected.

Table 3.5 Study participants meeting criteria for clinically significant depression, anxiety, apathy, and mild behavioural impairment.

Measure	HC (n=15)	LB Groups			Group Comparisons	
		LB-All (n=38)	LB-U (n=22)	LB-I (n=16)	X^2 Statistic (p)	
	Count (%)	Count (%)	Count (%)	Count (%)	HC vs. LB-All	HC vs. LB-U vs. LB-I
Depression	1 (6.7)	10 (26.3)	6 (27.3)	4 (25)	2.5 (.1)	2.6 (.3)
Anxiety	0 (0)	6 (15.8)	2 (9.1)	4 (25)	2.7 (.1)	5 (.08)
Apathy	0^a (0)	14 (36.8)	4^a (18.2)	10^b (62.5)	7.5 (**.006**)§	16.9 (**<.001**)§
MBI Domains						
Abnormal Thoughts	0 (0)	5 (13.2)	2 (9.1)	3 (18.8)	2.2 (.1)	3.2 (.2)
Decreased Motivation	0^a (0)	15 (39.5)	$6^{a,b}$ (27.3)	9^b (56.3)	8.3 (**.004**)§	12.1 (**.002**)§
Emotional Dysregulation	1^a (6.7)	25 (65.8)	$14^{a,b}$ (63.6)	11^b (68.8)	15 (**<.001**)§	15.14 (**<.001**)§
Impulse Dyscontrol	1^a (6.7)	15 (39.5)	$6^{a,b}$ (27.3)	9^b (56.3)	5.5 (**.02**)§	9.2 (**.01**)§
Social Inappropriateness	0 (0)	4 (10.5)	1 (4.5)	3 (18.8)	1.7 (.2)	4.4 (.1)

Note: Group comparisons were performed across two groups (HC vs, LB-All) and three groups (HC vs. LB-U vs. LB-I). Different superscript letters within a row denote significantly different values after conducting between-group chi-squared tests (values for between-group comparisons were considered significantly different if $p < .017$). Participants were determined as having clinically significant symptoms if questionnaire scores were: above 11 on the GDS-30 (for clinically significant depression), above 10 on the GAD-7 (for clinically significant anxiety), and 1 or higher on the Apathy Inventory (for clinically significant apathy). Responses to questions on the NPI were used to determine the presence of behavioural symptoms in the five MBI domains.
*Although raw values are presented in the table, the 3-group comparison was conducted using square root-transformed values.
§ Comparisons between symptom grouping remained significant after FDR correction (when run across p-values for HC vs. LB-All and HC vs. LB-U vs. LB-I comparisons separately).
Values of $p < .05$ are bolded.
HC: Healthy control; LB: Lewy Body; LB-U: LB-Unimpaired cognition subgroup; LB-I: LB-Impaired cognition subgroup; MBI: Mild Behavioral Impairment; GDS-30: Geriatric Depression Scale (30 items); GAD-7: Generalized Anxiety Disorder (7 items); NPI: Neuropsychiatric Inventory.

MRI Measures

All MD maps obtained from segmentations of the HC and LB groups are shown in Appendix Figures B1 (axial view) and B2 (sagittal and coronal views). Upon visual inspection of the maps, the hippocampi were quite heterogenous in size and regions of increased MD from participant to participant, and the HC groups and LB groups did not appear to vary significantly from one group to another overall. Hippocampal digitations were also counted (see Table 3.6) and were not significantly different between groups.

Table 3.6 Hippocampal digitations.

Measure	HC (n=35)	LB Groups			Group Comparisons	
		LB-All (n=38)	LB-U (n=22)	LB-I (n=16)	X^2 Statistic (p)	
	Count (%)	Count (%)	Count (%)	Count (%)	HC vs. LB-All	HC vs. LB-U vs. LB-I
Digitations - Right						
0 to 1	6 (17.1)	8 (21.1)	3 (13.6)	5 (31.3)		
2	19 (54.3)	18 (47.4)	13 (59.1)	5 (31.3)	0.4 (.8)	3.6 (.5)
3 to 4	10 (28.6)	12 (31.6)	6 (27.3)	6 (37.5)		
Digitations – Left						
0 to 1	11 (31.4)	15 (39.5)	7 (31.8)	8 (50)		
2	14 (40)	11 (28.9)	7 (31.8)	4 (25)	1.0 (.6)	2.4 (.7)
3 to 4	10 (28.6)	12 (31.6)	8 (36.4)	4 (25)		

Note: Group comparisons were performed across two groups (HC vs, LB-All) and three groups (HC vs. LB-U vs. LB-I). Different superscript letters within a row denote significantly different values after conducting between-group chi-squared tests (values for between-group comparisons were considered significantly different if $p < .017$). Number of digitations on the hippocampal head were determined following methods used in a previous study (129).
§ Comparisons remained significant after FDR correction (when run across p-values for HC vs. LB-All and HC vs. LB-U vs. LB-I comparisons separately). Values of $p < .05$ are bolded.
HC: Healthy control; LB: Lewy Body; LB-U: LB-Unimpaired cognition subgroup; LB-I: LB-Impaired cognition subgroup

As shown in Table 3.7, the average hippocampal FA was significantly lower in the LB group compared to HC (LB: 0.17 ± 0.01, HC: 0.18 ± 0.02; $p = .02$), when values were adjusted for age and sex the results were similar, and these comparisons remained significant when FDR-corrected. Neither the average hippocampal volume (LB: 2.13 ± 0.34 x 10^3 mm^3, HC: 2.05 ± 0.30 x 10^3 mm^3; $p = .3$) nor the average hippocampal MD (LB: 0.80 ± 0.07 x 10^{-3} mm^2/s, HC: 0.80 ± 0.03 x 10^{-3} mm^2/s; $p = .5$) differed between groups. Figure 3-1 shows violin plots of average MRI values (raw and adjusted for age and sex) for the LB-All and HC groups, and Figures 3-2 to 3-4 show scatterplots of volume, MD, and FA values by age across group and sex.

Table 3.7 MRI measures for study participants

Measure	HC (n=35)		LB Groups						Group Comparisons	
			LB-All (n=38)		LB-U (n=22)		LB-I (n=16)		Test Statistic (*p*)	
	Mean (SD)	**Min-Max**	**Mean (SD)**	**Min-Max**	**Mean (SD)**	**Min-Max**	**Mean (SD)**	**Min-Max**	**HC vs. LB-All**	**HC vs. LB-U vs. LB-I**
Hippocampal Volume (x10^3 mm^3)										
Average	2.05 (0.30)	1.49-2.82	2.13 (0.34)	1.54-2.87	2.17 (0.32)	1.54-2.87	2.07 (0.36)	1.60-2.79	*t*=-1(.3)	*F*=1.0(.4)
Right	2.13 (0.31)	1.63-2.86	2.20 (0.36)	1.57-3.02	2.24 (0.33)	1.59-3.02	2.14 (0.40)	1.57-2.87	*t*=-0.9(.4)	*F*=0.7(.5)
Left	1.98 (0.32)	1.34-2.99	2.06 (0.34)	1.40-2.74	2.11 (0.33)	1.49-2.72	2.00 (0.35)	1.40-2.74	*t*=-1.1(.3)	*F*=1.1(.3)
Hippocampal MD (x10^{-3} mm^2/s)										
Average	0.80 (0.03)	0.73-0.86	0.80 (0.07)	0.69-1.07	0.79 (0.03)	0.69-0.89	0.83 (0.09)	0.71-1.07	*W*=729(.5)	*H*=1.4(.5)
Right	0.81 (0.03)	0.75-0.88	0.82 (0.06)	0.67-1.02	0.80 (0.04)	0.67-0.87	0.84 (0.08)	0.71-1.02	*W*=641(.8)	*H*=2.1(.4)
Left	0.78 (0.03)	0.70-0.88	0.79 (0.07)	0.72-1.12	0.77 (0.04)	0.72-0.9	0.81 (0.11)	0.72-1.12	*W*=775(.2)	*H*=1.6(.5)
Hippocampal FA*										
Average	0.18[a] (0.02)	0.15-0.21	0.17 (0.01)	0.14-0.19	0.17[a] (0.01)	0.15-0.19	0.17[a] (0.01)	0.14-0.19	*t*=2.5(**.02**)‡§	*F*=3.2(**.046**)
Right	0.18 (0.02)	0.14-0.21	0.17 (0.01)	0.14-0.20	0.17 (0.01)	0.14-0.20	0.17 (0.01)	0.14-0.19	*t*=2.5(**.02**)‡	*F*=2.8(.07)
Left	0.18 (0.02)	0.15-0.22	0.17 (0.01)	0.15-0.20	0.17 (0.01)	0.15-0.19	0.17 (0.01)	0.15-0.20	*t*=2.3(**.03**)‡	*F*=2.8(.07)

Note: Group comparisons were performed across two groups (HC vs, LB-All) and three groups (HC vs. LB-U vs. LB-I). Different superscript letters within a row denote FDR-corrected significantly different values after conducting Tukey-HSD (for ANOVA) or Dunn (for Kruskal-Wallis) post-hoc tests.
*Although raw values are presented in the table, group comparisons were conducted using square root-transformed values.
‡ Comparison is significant when using age- and sex-adjusted standardized MRI measures.
§ Comparison between age- and sex-adjusted standardized MRI measures remained significant after FDR correction (when run across *p*-values for HC vs. LB-All and HC vs. LB-U vs. LB-I comparisons for average, right, and left hippocampal values separately).
Values of $p < .05$ are bolded.
HC: Healthy control; LB: Lewy Body; LB-U: LB-Unimpaired cognition subgroup; LB-I: LB-Impaired cognition subgroup; MD: Mean Diffusivity; FA: Fractional Anisotropy.

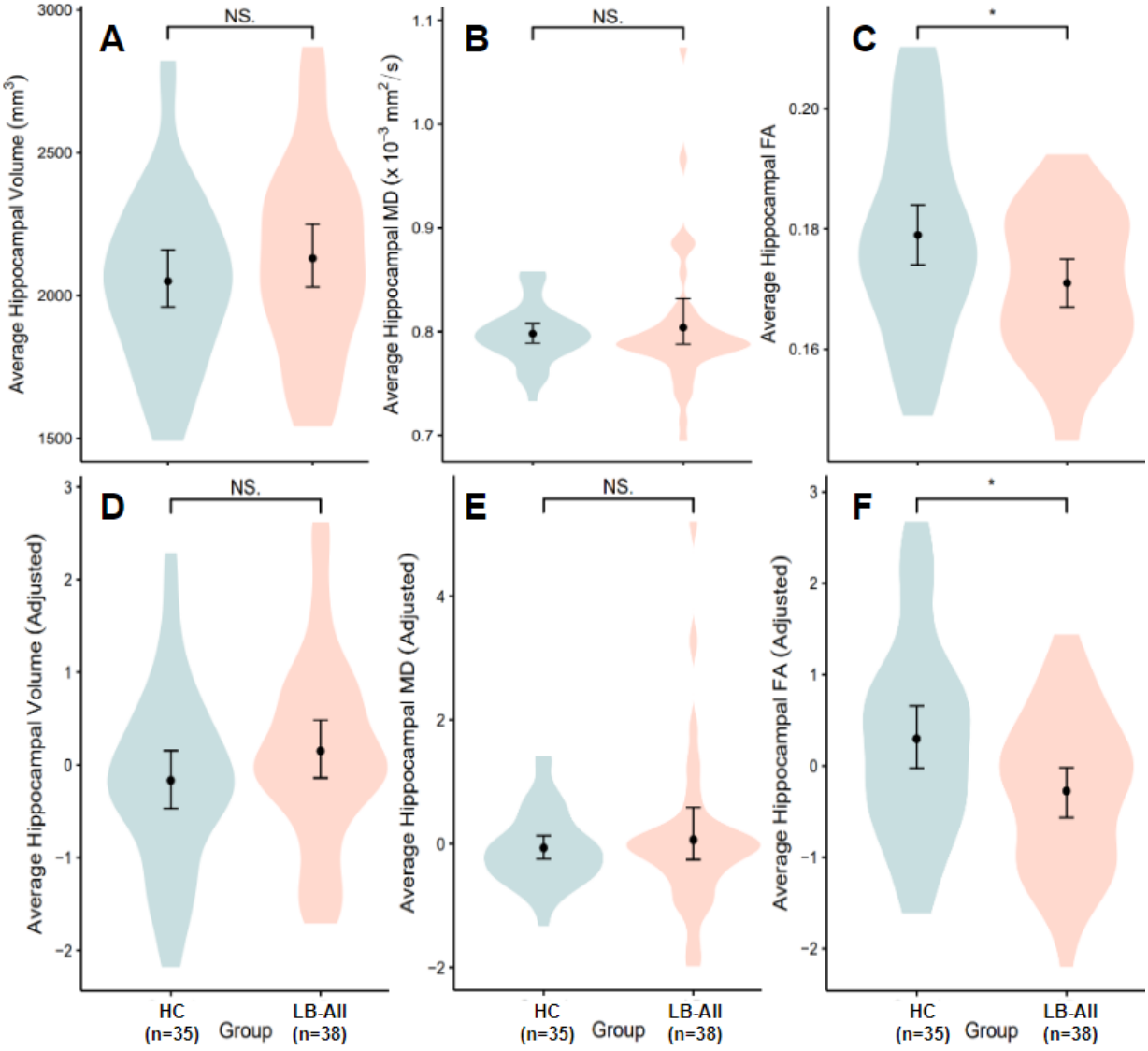

Figure 3-1 Violin plots showing raw and adjusted MRI-derived hippocampal measures for HC and LB-All.

A-C: Average raw hippocampal volume (A), MD (B), and FA (C); **D-F**: age- and sex-adjusted standardized average hippocampal volume (D), MD (E), and FA (F).
Note: The asterisk indicates significance at $p < 0.05$.
FA: Fractional Anisotropy, HC: Healthy Controls, LB: Lewy Body, MD: Mean Diffusivity, MRI: Magnetic Resonance Imaging, NS: Not Significant.

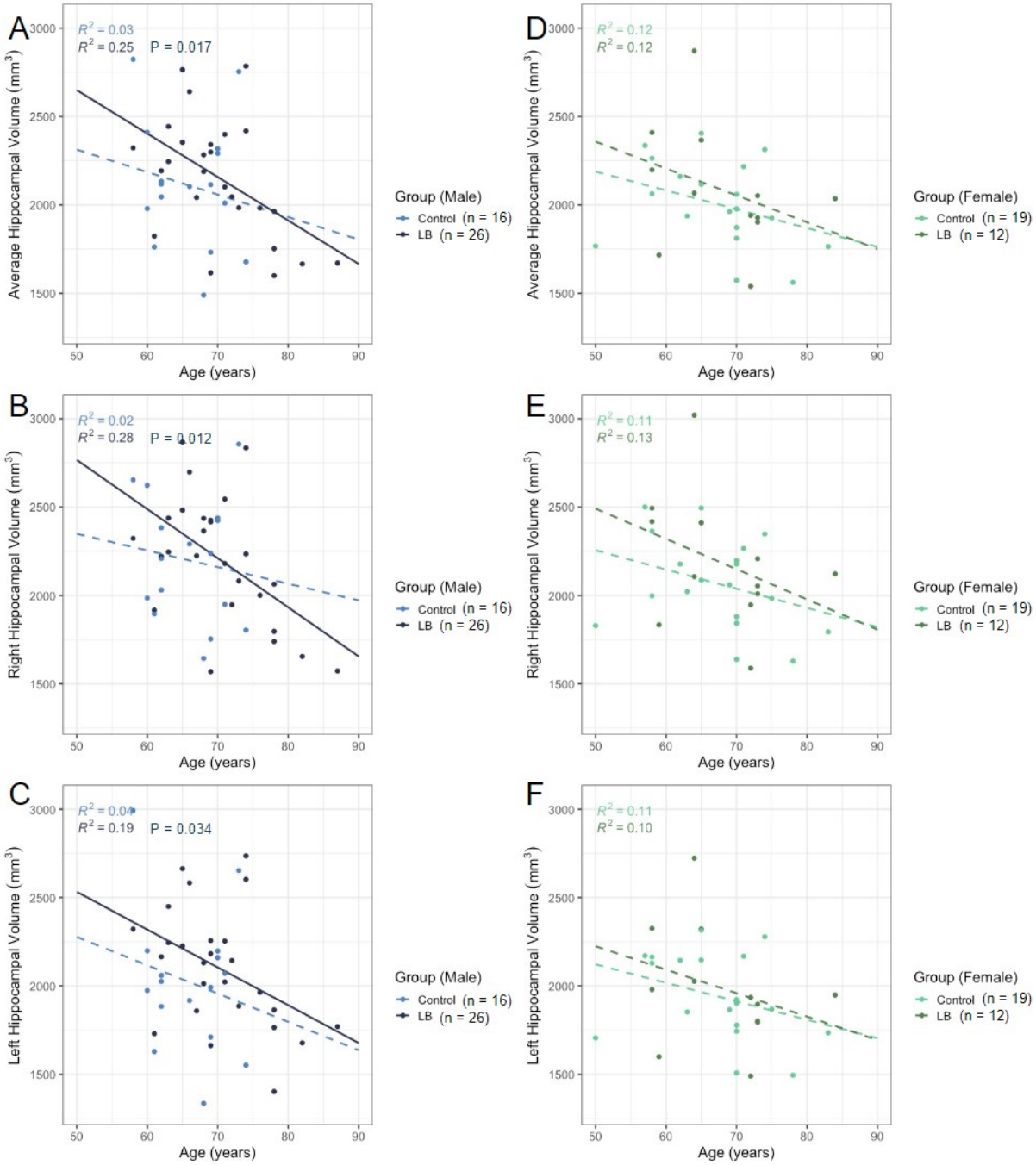

Figure 3-2 Scatter plots showing hippocampal volume by age for males and females in the HC and LB groups.

(A) Average hippocampal volume for males, (B) right hippocampal volume for males, and (C) left hippocampal volume for males. (D) average hippocampal volume for females, (E) right hippocampal volume for females, and (F) left hippocampal volume for females. Light blue indicates males in the HC group, dark blue indicates males in the LB-All group, light green indicates females in the HC group, and dark green indicates females in the LB-All group. Solid lines indicate a significant correlation at $p < .05$.

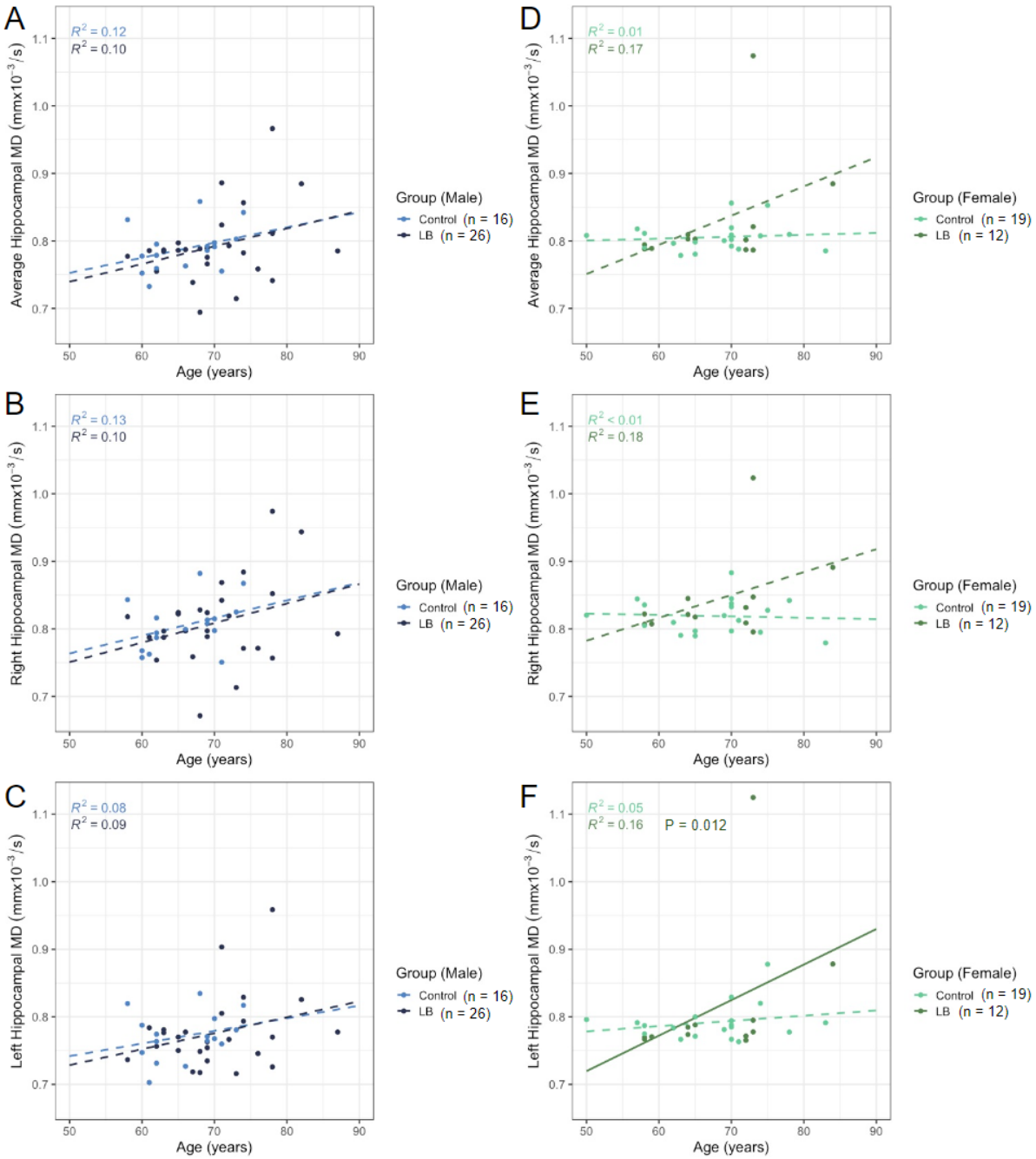

Figure 3-3 Scatter plots showing hippocampal MD by age for males and females in the HC and LB groups.

(A) Average hippocampal MD for males, (B) right hippocampal MD for males, and (C) left hippocampal MD for males. (D) average hippocampal MD for females, (E) right hippocampal MD for females, and (F) left hippocampal MD for females. Light blue indicates males in the HC group, dark blue indicates males in the LB-All group, light green indicates females in the HC group, and dark green indicates females in the LB-All group. Solid lines indicate a significant correlation at $p < .05$.

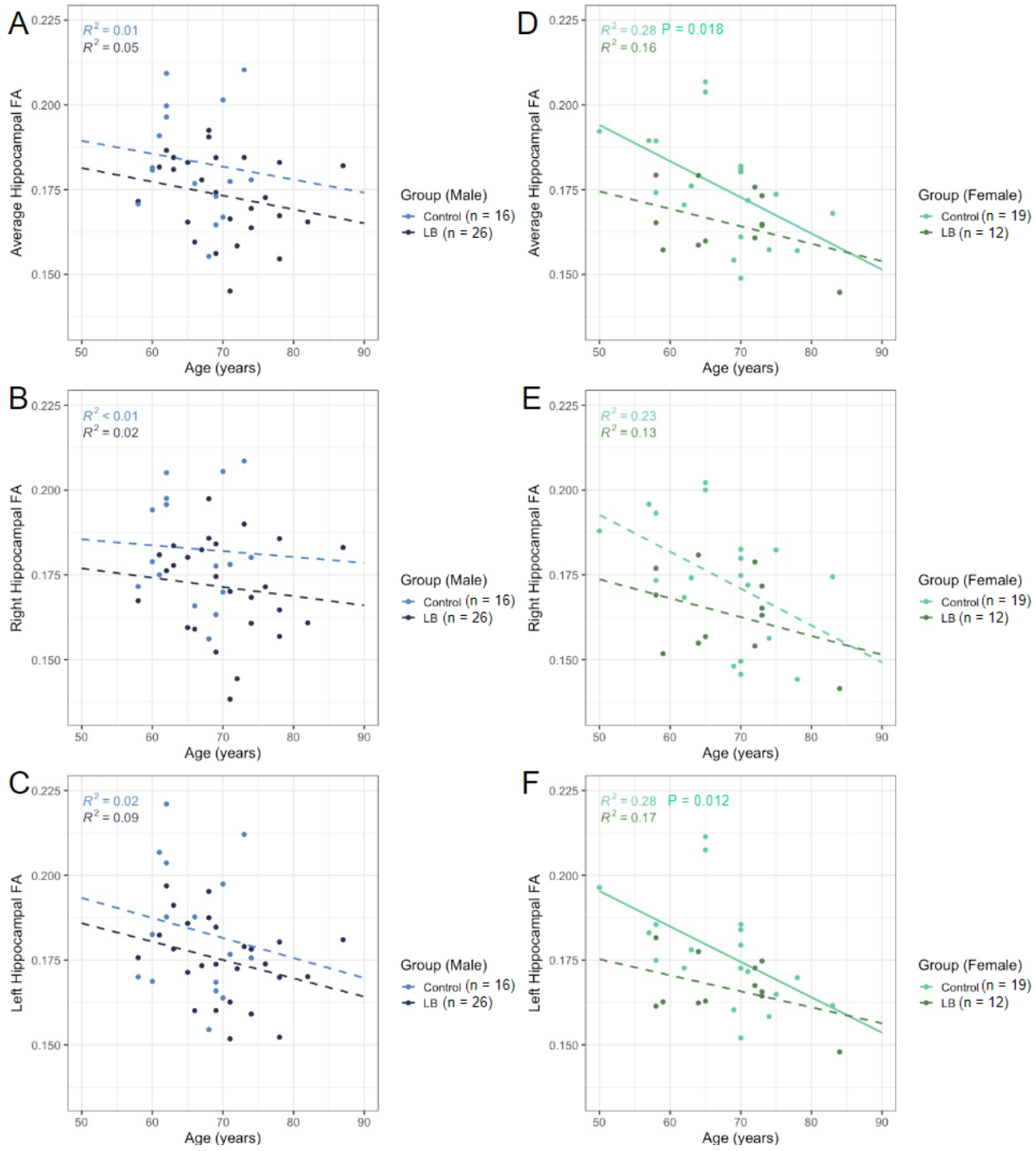

Figure 3-4 Scatter plots showing hippocampal FA by age for males and females in the HC and LB groups.

(A) Average hippocampal FA for males, (B) right hippocampal FA for males, and (C) left hippocampal FA for males. (D) Average hippocampal FA for females, (E) right hippocampal FA for females, and (F) left hippocampal FA for females. Light blue indicates males in the HC group, dark blue indicates males in the LB-All group, light green indicates females in the HC group, and dark green indicates females in the LB-All group. Solid lines indicate a significant correlation at $p < .05$.
FA: Fractional Anisotropy, HC: Healthy Controls, LB: Lewy Body.

The results of the power calculations are shown in Table 3.8. Power calculations were performed using α, sample size, and effect size, and indicate that the statistical power for MD was lower than that of volume and FA.

Table 3.8 Results of post-hoc power calculations for hippocampal volume, MD, and FA

Measure	**Power (1-β)**
Average Volume	0.18
Right Volume	0.16
Left Volume	0.19
Average MD	0.05
Right MD	0.11
Left MD	0.10
Average FA	0.99
Right FA	0.99
Left FA	0.99

Correlations between MRI and Clinical Measures

Correlations between FA and age were not significant for the LB group (Appendix Table C1); however, in HC, average (T = -0.24; p = .05) and left-sided (T = -0.25; p = .04) FA were significantly negatively correlated with age (Appendix Table C2). For the LB group, sex was significantly negatively associated with average FA (T = -0.27; p = .04; Appendix Table C1). As

shown in Table 3.9, correlations were performed between demographic and clinical scores that were significantly different between groups (see Tables 3.1 and 3.2), and none of these scores showed significant correlations with age- and sex-adjusted FA within the LB group. Hippocampal volume and MD also did not have significant correlations with these scores (Appendix Table C3).

Table 3.9 Kendall rank correlations between general health measures and hippocampal FA for participants in the LB group (n=38).

	Average Adjusted FA	*Right Adjusted FA*	*Left Adjusted FA*	*Framingham Risk Score*	*Olfactory Score*	*Age of Onset (years)*	*MDS-UPDRS Axial Score*
Average Adjusted FA							
Right Adjusted FA	0.84 *(<.001)*						
Left Adjusted FA	0.72 *(<.001)*	0.56 *(<.001)*					
Framingham Risk Score	-0.07 *(.52)*	-0.03 *(.77)*	-0.11 *(.32)*				
Olfactory Score	-0.06 *(.59)*	-0.04 *(.73)*	-0.05 *(.68)*	-0.20 *(.10)*			
Age of Onset (years)	0.04 *(.75)*	0.06 *(.64)*	0.03 *(.78)*	0.19 *(.09)*	-0.19 *(.11)*		
MDS-UPDRS Axial Score	0.08 *(.51)*	0.09 *(.43)*	0.05 *(.69)*	0.37 *(<.001)*	-0.33 *(.01)*	0.27 *(.03)*	

Computed correlation used kendall-method with pairwise-deletion.

Values of $p < .05$ are shown in darker font. LB: Lewy Body; FA: Fractional Anisotropy; MDS-UPDRS: Movement Disorders Society - Unified Parkinson's Disease Rating Scale.

For the correlations with cognitive measures (Table 3.10), left-sided FA was significantly negatively associated with executive function (T = -0.23, p = .05) and cognitive speed z-score (T = -0.24, p = .04; see Figure 3-5). However, these correlations did not remain significant after FDR-correction. There were no significant correlations between FA and memory z-score or MoCA score or between cognitive scores and hippocampal volume and MD (Appendix Table C4).

Table 3.10 Kendall rank correlations between cognitive measures and hippocampal FA for participants in the LB group (n=38).

	Average Adjusted FA	*Right Adjusted FA*	*Left Adjusted FA*	*MoCA Score*	*Memory Z-Score*	*Executive Function Z-Score*	*Cognitive Speed Z-Score*
Average Adjusted FA							
Right Adjusted FA	0.84 *(<.001)*						
Left Adjusted FA	0.72 *(<.001)*	0.56 *(<.001)*					
MoCA Score	-0.07 *(.58)*	-0.02 *(.86)*	-0.11 *(.36)*				
Memory Z-Score	-0.15 *(.20)*	-0.12 *(.28)*	-0.15 *(.20)*	0.50 *(<.001)*			
Executive Function Z-Score	-0.18 *(.10)*	-0.15 *(.19)*	-0.23 *(.05)*	0.51 *(<.001)*	0.36 *(<.001)*		
Cognitive Speed Z-Score	-0.21 *(.06)*	-0.16 *(.16)*	-0.24 *(.04)*	0.47 *(<.001)*	0.42 *(<.001)*	0.44 *(<.001)*	

Computed correlation used kendall-method with pairwise-deletion.

§ Correlations between age- and sex-adjusted standardized FA and cognitive measures remained significant after FDR correction (when run average, right, and left hippocampal FA separately).

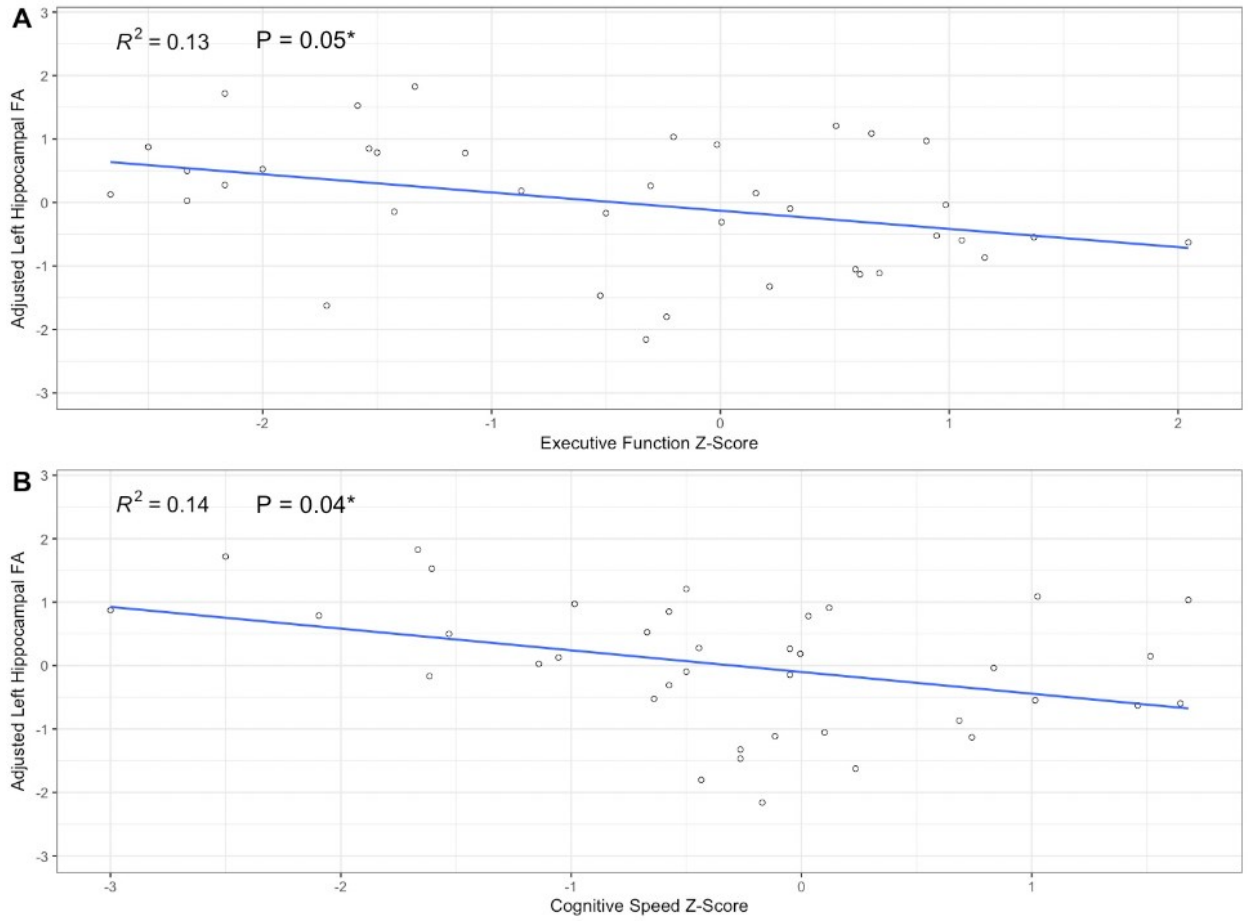

Figure 3-5 Scatter plots showing adjusted left hippocampal FA by executive function z-score and cognitive speed z-score.

(A) Left hippocampal FA adjusted by age and sex by executive function z-score for the LB group (n = 38), (B) left hippocampal FA adjusted by age and sex by and cognitive speed z-score for the LB group (n = 38). *Scores were only significant before FDR-correction.

As shown in Table 3.11, for associations with non-cognitive measures, average hippocampal FA was significantly positively correlated with GDS-30 score ($T = 0.28$, $p = .02$), NPI severity score ($T = 0.25$, $p = .03$), and PDQ-39 score ($T = 0.29$, $p = .01$). FA for the right hippocampus was significantly positively correlated with NPI severity score ($T = 0.29$, $p = .01$) and PDQ-39 score ($T = 0.24$, $p = .04$). Left-sided FA was significantly positively correlated with GDS-30 score ($T = 0.26$, $p = .02$), Apathy Inventory score ($T = 0.26$, $p = .04$), PDQ-39 score (T

= 0.34, $p < .001$), and sleep score ($T = 0.32$, $p = .01$). Only the correlations between average hippocampal FA and GDS-30, and between left hippocampal FA and PDQ-39 and sleep remained significant after FDR-correction (see Table 3.11 and Figure 3-6). The only significant association between other MRI measures and non-cognitive variables was between left hippocampal volume and NPI severity score ($T = -0.25$, $p = .03$), which did not remain significant after FDR-correction (Appendix Table C5).

Table 3.11 Kendall rank correlations between non-cognitive measures and hippocampal FA for participants in the LB group (n=38 for all variables except for sleep score [n=37]).

	Average Adjusted FA	*Right Adjusted FA*	*Left Adjusted FA*	*GDS Score*	*GAD Score*	*Apathy Inventory Score*	*NPI Severity Score*	*PDQ-39 SI Score*	*Sleep Score*
Average Adjusted FA									
Right Adjusted FA	0.84 *(<.001)*								
Left Adjusted FA	0.72 *(<.001)*	0.56 *(<.001)*							
GDS Score	0.28 § *(.02)*	0.22 *(.06)*	0.26 § *(.02)*						
GAD Score	0.15 *(.20)*	0.12 *(.29)*	0.15 *(.21)*	0.42 *(<.001)*					
Apathy Inventory Score	0.23 *(.06)*	0.19 *(.14)*	0.26 *(.04)*	0.26 *(.05)*	0.12 *(.36)*				
NPI Severity Score	0.25 *(.03)*	0.29 *(.01)*	0.18 *(.13)*	0.14 *(.24)*	0.26 *(.04)*	0.32 *(.01)*			
PDQ-39 SI Score	0.29 *(.01)*	0.24 *(.04)*	0.34 § *(<.001)*	0.47 *(<.001)*	0.32 *(.01)*	0.40 *(<.001)*	0.27 *(.02)*		
Sleep Score	0.22 *(.06)*	0.15 *(.20)*	0.32 § *(.01)*	0.24 *(.05)*	0.25 *(.04)*	0.18 *(.16)*	0.30 *(.01)*	0.29 *(.02)*	

Computed correlation used kendall-method with pairwise-deletion.

§ Correlations between age- and sex-adjusted standardized FA and non-cognitive measures remained significant after FDR correction (when run average, right, and left hippocampal FA separately).

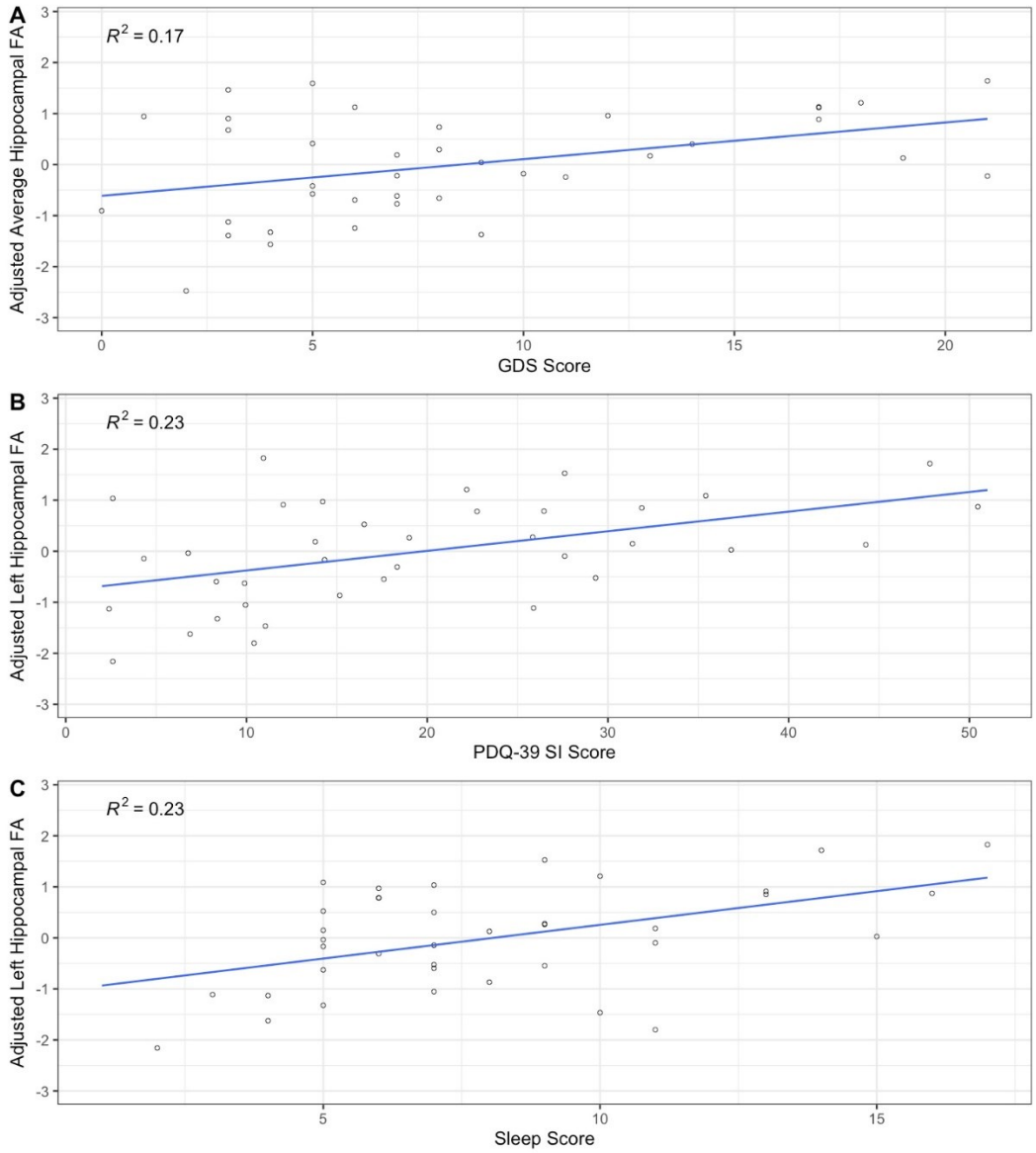

Figure 3-6 Scatter plots showing adjusted hippocampal FA by GDS score, PDQ-39 SI score, and sleep score.

(A) Average hippocampal FA adjusted by age and sex by GDS score for the LB group (n = 38), (B) left hippocampal FA adjusted by age and sex by PDQ-39 SI score for the LB group (n = 38), (C) average hippocampal FA adjusted by age and sex by sleep score for the LB group (n = 37).

In the analysis comparing FA across LB participants grouped by clinically significant symptoms (Table 3.12), those with depression had significantly higher average hippocampal FA (mean: 0.178 ± 0.010) and right-sided hippocampal FA (mean: 0.177 ± 0.011) than those without depression (Average FA: 0.168 ± 0.012, Right-Sided FA: 0.166 ± 0.014; $p = .03$ for both). Similarly, participants with decreased motivation had higher average and right-sided hippocampal FA (both means: 0.175 ± 0.012) than those without decreased motivation (Average FA: 0.168 ± 0.013, Right-Sided FA: 0.165 ± 0.014; $p = .04$ for both). The only comparison that remained significant after FDR-correction was average hippocampal FA between participants with and without clinically significant depression.

Additionally, as shown in Appendix C, the average and right- and left-sided hippocampal volumes were significantly lower in participants with emotional dysregulation compared to those without, however only the left-sided comparison remained significant after FDR-correction (Appendix Table C6). Finally, left-sided hippocampal MD was significantly lower in participants with decreased motivation, but this did not remain significant after FDR-correction (Appendix Table C7).

Table 3.12 FA comparisons between LB participants (n=38) with clinically significant non-cognitive symptoms.

Clinically Significant Symptom	Average FA			Right-Sided FA			Left-Sided FA		
	With	**Without**	***W* (p)**	**With**	**Without**	***W* (p)**	**With**	**Without**	***W* (p)**
Depression	0.178 (0.01)	0.168 (0.012)	76 (**.03**)‡§	0.177 (0.011)	0.166 (0.014)	75 (**.03**)‡	0.178 (0.01)	0.17 (0.012)	83 (.06)‡
Anxiety	0.178 (0.015)	0.169 (0.011)	58 (.1)	0.178 (0.015)	0.167 (0.014)	57 (.1)	0.178 (0.016)	0.171 (0.011)	63 (.2)
Apathy	0.175 (0.009)	0.168 (0.013)	110 (.08)	0.173 (0.01)	0.167 (0.016)	132 (.3)	0.177 (0.01)	0.17 (0.012)	109 (.08)
MBI Symptoms									
Abnormal Thoughts	0.169 (0.012)	0.171 (0.012)	90 (.8)	0.167 (0.015)	0.169 (0.014)	89 (.8)	0.171 (0.009)	0.173 (0.012)	92 (.7)
Decreased Motivation	0.175 (0.01)	0.168 (0.013)	104 (**.04**)	0.175 (0.012)	0.165 (0.014)	105 (**.04**)	0.176 (0.009)	0.17 (0.013)	124 (.2)
Emotional Dysregulation	0.172 (0.012)	0.168 (0.013)	135 (.4)	0.171 (0.014)	0.164 (0.014)	115 (.1)‡	0.172 (0.011)	0.172 (0.013)	155 (.8)
Impulse Dyscontrol	0.171 (0.012)	0.171 (0.012)	161 (.7)	0.169 (0.013)	0.169 (0.015)	169 (.9)	0.173 (0.014)	0.172 (0.011)	168 (.9)
Social Inappropriateness	0.177 (0.009)	0.17 (0.012)	45 (.3)	0.177 (0.008)	0.168 (0.014)	41 (.2)	0.177 (0.01)	0.172 (0.012)	48 (.4)

Note: Participants were determined as having clinically significant symptoms if questionnaire scores were: above 11 on the GDS-30 (for clinically significant depression; *n*=10 participants), above 10 on the GAD-7 (for clinically significant anxiety; *n*=6 participants), and 1 or higher on the Apathy Inventory (for clinically significant apathy; *n*=14 participants). Responses to questions on the NPI were used to determine the presence of behavioural symptoms in the five MBI domains: Abnormal thoughts (*n*=5 participants), decreased motivation (*n*=15 participants), emotional dysregulation (*n*=25 participants), impulse dyscontrol (*n*=15 participants), and social inappropriateness (*n*=4 participants).

Values of $p < .05$ are bolded.

FA: Fractional Anisotropy; LB: Lewy Body; MBI: Mild Behavioral Impairment; GDS-30: Geriatric Depression Scale (30 items); GAD-7: Generalized Anxiety Disorder (7 items); NPI: Neuropsychiatric Inventory.

‡ Comparison is significant when comparing age- and sex-adjusted standardized FA values.

§ Comparison between age- and sex-adjusted standardized MRI measures remained significant after FDR correction (when run separately across each set of *p*-values obtained for average, right-sided, and left-sided FA).

Chapter 4 Discussion

Non-motor symptoms play a crucial role in PD, and while many studies have looked at cognitive symptoms, others, such as apathy, depression, and anxiety, are essential contributors to quality of life with PD. After a review of the literature on DTI in PD, it was apparent that few studies had looked directly at the hippocampus in relation to non-motor symptoms. The hippocampus is a structure known to be impacted by PD pathology. While macro-structural imaging analyses such as volumetry often fail to show this impact, DTI allows us to identify changes at a microstructural level that may contribute to non-motor symptomatology. Studies using region-of-interest methods to examine hippocampal DTI changes in PD are scarce. This scarcity is likely because the lower spatial resolution afforded with diffusion imaging increases the difficulty of delineating smaller structures within the brain. However, with the novel high-resolution imaging technique used in this study, we were able to delineate the hippocampus and measure its unique diffusion properties successfully.

Our first objective for this study was to identify differences between hippocampal MRI measures, including volume, MD, and FA. In this analysis, our main finding was that average hippocampal FA was significantly decreased in participants within the LB group compared to HC. We did not find a difference in volume or MD between groups. Our second objective was to investigate the associations between hippocampal measures and non-motor symptoms for participants within the LB group. Here we focused primarily on FA, because this was the only measure showing a significant between-group difference. In this analysis, we found that average and left hippocampal FA were positively associated with GDS-30, and that left hippocampal FA was also positively associated with PDQ-39 and sleep scores. When grouping patients by

symptom, we also found that participants with LB and clinically significant depression had a higher average hippocampal FA than those without depression, confirming the results of our correlational analysis.

Between-Group Comparisons for Non-Motor Symptoms

For cognitive measures, the results were as expected, with the LB-Impaired group showing significant impairment compared to the HC and LB-unimpaired groups on all measures of cognition (i.e., the MoCA, memory, executive function, and cognitive speed). Additionally, the LB-Unimpaired group showed significant declines in memory and cognitive speed when compared to the HC group. However, it is worth noting here that the HC group had average z-scores ranging from 0.60 – 0.86 on the three cognitive domains measured, indicating that on average, participants in this group performed better than the average healthy individual at the same age based on normative data.

For non-cognitive non-motor symptoms, individuals in both the LB-Impaired and LB-Unimpaired groups had similar worsening of overall neuropsychiatric symptom burden (i.e., NPI severity), depression symptoms, and sleep disruption when compared to individuals in the HC group, which are known to impact individuals with LB diseases (16) . In terms of apathy, the LB-Impaired group was significantly had significantly more apathy than both the LB-Unimpaired and HC groups, which did not differ from each other. This finding agrees with other literature that has found that worse cognitive impairment is associated with higher levels of apathy in participants with PD (178). Quality of life (as measured by the PDQ-39 SI score) was not significantly different between the LB-Impaired and LB-Unimpaired groups, which contrasts with previous research conducted by Schonenberg and colleagues that has found that PDQ-39 SI score is significantly higher in participants with lower MoCA scores (179). However, in our

study, the average PDQ-39 SI score was still higher in the LB-Impaired group (average = 24.3 ± 15.3) when compared to the LB-Unimpaired group (average = 16.2 ± 9.8), and the difference between our studies may be due to the difference in MoCA cut-off to define cognitive impairment (< 26 for our study vs. < 21 for the Schonenberg study), as well as the lower number of participants in our study compared to theirs, which included 94 participants with cognitive impairment and 127 without (179).

Between-Group Comparisons for FA

The only measure to show differences between groups in our study was FA. While FA did not significantly differ between the LB-Impaired and LB-Unimpaired groups, the average hippocampal FA was significantly lower for participants in the LB group when compared to the HC group. To our knowledge, this is the first study reporting significant differences in hippocampal FA between patients with Lewy body diseases and healthy controls. The other studies looking at hippocampal FA between these groups have found no significant difference (58, 60-63), which could be because our method used a higher-resolution imaging protocol, enabling us to detect differences that had not been previously determined.

Between-Group Comparisons for MD

In this study, hippocampal MD did not differ between any of the groups. Previous studies looking at the difference between hippocampal MD between participants with Lewy body diseases and controls, either showed that MD was increased in those with Lewy body diseases (39, 58, 61), or that there was no difference between groups (60, 62). While the study Kim and

colleagues (61) does not report the exact values for MD, the study by Pyatigorskaya and colleagues (58) found that average hippocampal MD was increased by 7% in PD compared to HC and the study by Carlesimo and colleagues (39) showed that, for patients with PD, hippocampal MD was increased by approximately 6.5% (with the right side being significantly different) when compared to HC (39). In contrast, our results showed an increase of only about 1.2% in patients with PD compared to HC, which was not significantly different (39). Carlesimo (39) also conducted an additional voxel-wise MD analysis, which showed that their main cluster of difference was in the body of the hippocampus bilaterally. Our sample size (38 LB-All and 35 HC) was smaller than those used by Kim (61) (64 PD and 64 HC) and Pyatigorskaya (58) (52 PD and 24 HC). However, we still had a larger sample size than Carlesimo (39) (25 PD and 25 HC), with similar average participant ages (Carlesimo: 65 ± 8/9 years for PD/HC; our study: 67 ± 7 years for HC and 70 ± 6 years for LB-All). The average UPDRS-III score for the Carlesimo (39) cohort was 18.6 ± 8.7, compared to the MDS-UPDRS-III score for our cohort, which was 19.7 ± 7.6. One study suggests that a simplified conversion from the UPDRS-III score to the MDS-UPDRS-III score can be performed by adding 7 to the UPDRS-III score (180). Following this method, the MDS-UPDRS-III score for the Carlesimo cohort would be around 25.6, indicating that their participants were slightly more advanced than ours. On the other hand, disease duration was larger for our participants than Carlesimo's, but was still within one standard deviation (6.3 ± 4.4 for ours, compared to 4.4 ± 4.0 for Carlesimo's) (39).

The main difference between these studies and ours is likely the method used to delineate the hippocampus. All the studies previously mentioned used automated segmentation methods, whereas we manually segmented the hippocampus. For instance, both Carlesimo (39) and Kim (61) used an automated segmentation method in FSL (FIRST) (181) which relies on templates

created from manual segmentation from a range of participants ranging in age from 4 to 72 years, including healthy controls and participants with schizophrenia, AD, Attention Deficit Hyperactivity Disorder, and pre-natal cocaine exposure. See Figure 4-1 for a depiction of a hippocampal segmentation done using this method, which appears to include the subiculum in contrast to our method, which did not. Furthermore, manual segmentation is the gold standard for delineating the hippocampus on MRI (181). It has been determined that, when compared to manual segmentation, automated segmentation tends to largely overestimate the size of the hippocampus (182), and therefore, regions of the segmentation extend into adjacent non-hippocampal regions.

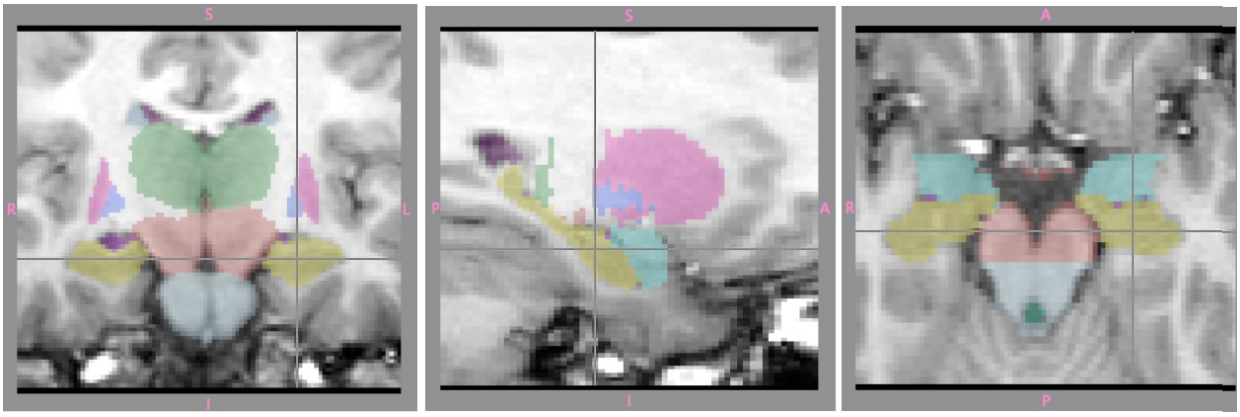

Figure 4-1 Depiction of automatic hippocampal segmentation.

Coronal, sagittal, and axial slices of the hippocampus (yellow) as delineated in FSL.
Figure from Patenaude, B. (2007). Bayesian statistical models of shape and appearance for subcortical brain segmentation [PhD thesis]. University of Oxford. (183).

In addition to manually segmenting the hippocampus (the gold standard to which automated segmentation is compared) that excluded the subiculum, we also used an imaging protocol explicitly designed to capture high-resolution diffusion tensor imaging of the hippocampus (53). Compared to lower resolution protocols, this method decreases the partial volume effects from the inadvertent inclusion of tissues and cerebrospinal fluid (CSF)

surrounding the hippocampus (53). Thus, the differences in MD between groups in studies using automated segmentation may have been partially due to atrophy of the hippocampus in the PD group, causing the inclusion of more CSF from the surrounding structure and leading to a higher average MD. Carlesimo and colleagues also looked at volume, but did not find any significant differences between groups (39). However, they calculated volume using the same automatically segmented masks with which they calculated MD (39). Therefore, if the masks were contaminated by surrounding CSF in atrophied areas, this may have inflated both volume and MD values in the PD group.

Correlations Between FA and Non-Motor Symptoms

In our study, FA was the only measure to show between-group differences. Therefore, we focused on analyses including FA for our second objective, which was to determine whether any relationships existed between MRI measures and non-motor symptoms of PD. After FDR correction, the average FA in both hippocampi and FA in the left hippocampus were positively correlated with GDS-30 scores. When we compared FA in participants with clinically significant depression to the hippocampal FA in those without depression, we also found that FA was higher in those with clinically significant depression, confirming the results of our correlational analysis. Additionally, left hippocampal FA was significantly positively correlated with PDQ-39 and sleep scores after FDR correction, and other non-significant correlations showed the same pattern of increased FA along with increased severity of non-motor symptoms.

To our knowledge, only one prior study has looked at correlations between non-motor symptoms and hippocampal FA using an ROI-based method (121). In this study, the authors looked at some variables that were similar to ours, such as global cognition (measured using the Mini-Mental State Examination [MMSE]), and scores from the Non-Motor Symptoms Scale

(NMSS), such as the attention/memory score, sleep/fatigue score, and mood score (121). Similar to our study, they found no significant association between hippocampal FA and global cognition and attention/memory (121). However, they found that hippocampal FA was negatively correlated with the NMSS mood score, whereas we found a positive correlation with GDS-30 score, and they found no significant correlation with the NMSS sleep/fatigue score while we found a positive correlation with sleep disturbance (121). The difference in scales used to measure the symptoms may have played a role in these contrasting results, as well as differences in participants between our studies. Wei and colleagues used a larger sample (43 PD) than ours, and the H&Y stages for their participants range from 1-4 while ours only ranged from 1-3, suggesting some of their participants may have been in a more advanced stage of disease. However, the average disease duration for their cohort is somewhat shorter than ours at 4.6 ± 4.1 years (121).

In our study, our results suggest that a higher non-motor symptom burden is associated with increased hippocampal FA. Typically, higher FA is interpreted as indicating increased neuronal integrity; hence we might expect those with higher non-motor symptoms, and particularly depression, to have decreased FA, which would correspond with the results of the study by Wei and colleagues (121). Though these findings appear counter-intuitive, our measurement method has good inter-rater reliability (see section 2.4.3), and our results show the expected relationships between FA and age, with FA decreasing as age increased in our HC group, following the same pattern shown in a study of healthy controls which used the same imaging methods (manual hippocampal segmentation on images acquired using the same high-resolution DTI protocol) (129).

To explain these counter-intuitive findings, we should consider that many studies using diffusion imaging have focused on WM structures, which consist mainly of bundles of neuronal axons, while the hippocampus is mostly composed of GM consisting of neuronal bodies and processes (184). Interpreting diffusion in GM structures is more complex. GM is particularly susceptible to partial volume effects because it contains convolutions filled with CSF, increasing the likelihood that a voxel will be contaminated with CSF, a problem that becomes more salient when atrophy occurs (184). Furthermore, it has been argued that, compared to FA, MD is a better (or at least more easily interpretable) measure for GM, which lacks the directionality present in WM (185). As mentioned above, our cohort's results suggest that a higher non-motor symptom (e.g., depression and disordered sleep) burden may be associated with higher FA in patients with Lewy body diseases. This finding is interesting because the LB group in our study had significantly lower FA than the HC group, which suggests that the hippocampi of patients in the LB group undergo a structural change that decreases FA relative to HCs, but within the LB group, a larger burden of non-motor symptoms is associated with an increase in FA. Another possible interpretation for our findings is that, among participants with the same disease severity, those who have less hippocampal damage may have more insight into the changes occurring in their bodies and the impact of these changes, thus resulting in higher levels of depression, sleep disturbance, and a worse perception of their quality of life.

While increased FA is often interpreted as showing less damage, our study suggests that higher FA values are associated with worse non-motor symptoms in patients with PD and LBD. This finding is not entirely unprecedented. Other studies, including a study of PD (186) and a rodent model of traumatic brain injury (187), have also found increased FA along with

worsening symptoms or pathology. Interpretations of this pattern have generally pointed to two mechanisms of interest which may cause this: neurodegeneration and neuroplasticity (186, 188).

While neurodegeneration is often believed to result in decreased FA, the relationship may be more complex. FA can reflect various aspects of tissue structure, including axon number, density, organization, and myelination (188). Increased FA may reflect increased axon number, density, and myelination, while decreased FA can occur when fibres of different orientations (e.g., axons travelling between different regions) are present in the same location (188). For this reason, the selective loss of a specific subset of axons or neuronal processes may increase FA, and measuring the mode of anisotropy is one method that could help us determine whether an increase in FA is due to anisotropy becoming more linear (188). A histological study (189) of the effects of Lewy body diseases on the brain showed that α-synuclein accumulation within the hippocampus leads to a loss of synaptic spines. The loss of synaptic spines could also potentially increase FA because, as shown in Figure 4-2, spines are oriented in different directions, which can cause fluid to flow around them, dispersing in different directions. A loss of synaptic spines may constitute the removal of one obstacle preventing linear fluid flow in GM.

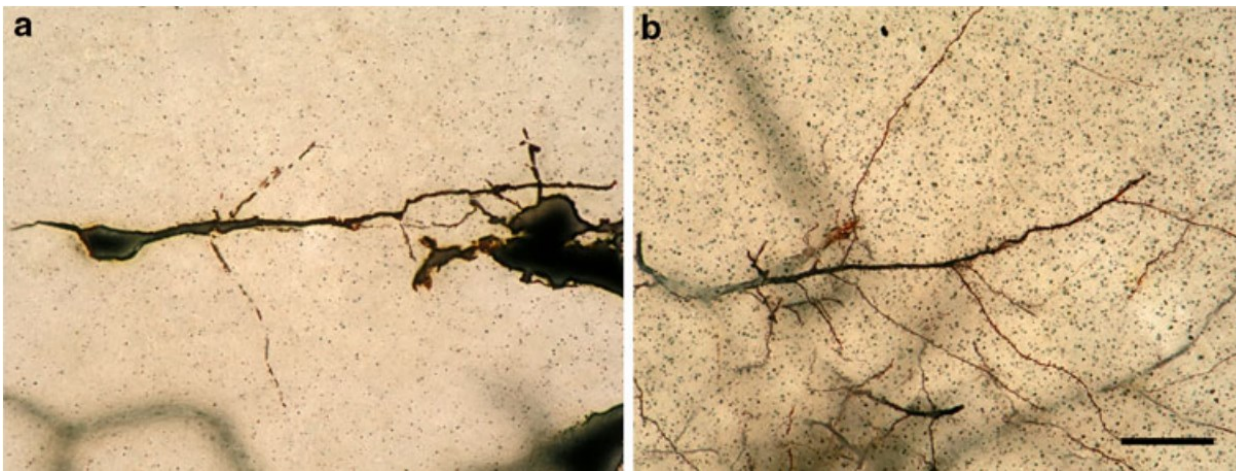

Figure 4-2 An almost complete loss of dendritic spines accompanies the presynaptic a-synuclein aggregates.

(A) Golgy–Cox–Davenport staining of a frontal cortex neuronal dendrite in a DLB patient, and (B) a control patient of the same age. *Bar* 50 lm,
Figure from Schulz-Schaeffer, W.J. (2010). The synaptic pathology of a-synuclein aggregation in dementia with Lewy bodies, Parkinson's disease and Parkinson's disease dementia. *Acta Neuropathol, 120*, 131-143. (189).

It is important to remember that FA is an indirect measure that reflects underlying tissue orientation, and further evidence is needed to determine the cause of any changes (190). FA changes are not exclusively due to changes in the orientation of neurons and neuronal processes. A study by Budde and colleagues (187) found that, in rat models of traumatic brain injury, astrocytes line up to form a glial scar in injured tissue, resulting in increased FA. This study suggests that elements recruited to the site of injury in an orderly fashion may increase FA. In PD, Lewy neurites, which are long and spindle-shaped, form within the hippocampus before the more spherical Lewy bodies deposit (27). Since few of our participants are in the late stages of PD, increased FA in patients with worse non-motor symptoms may represent a stage in which enough Lewy neurites have deposited within the hippocampus to induce a more linear flow of fluid around them. As time passes, FA may decrease as spherical Lewy bodies take over, obstructing the flow.

Neuroplasticity is another possible mechanism for increased FA. One study found increased FA in the motor pathways of patients with PD (186). The authors of this study argue that early compensation within those regions, such as axonal sprouting or neuronal re-routing in response to decreased input, leads to increased FA (186). Another study has found that white matter structures adjacent to the hippocampus (e.g., cingulum near the hippocampus) may also be affected in patients with PD and depression when compared to those without depression, with findings showing increased MD and decreased FA in these regions (191). However, PD cannot be diagnosed until symptoms become clinically apparent, long after pathology has appeared in the brain and compensatory mechanisms begin to break down (116). Consequently, while FA may be increased in early PD relative to HC, it could decline over time (116).

Strengths and Limitations

The use of validated measures for determining the presence of non-motor symptoms and the blinding of the tracer during manual segmentation of the hippocampus are two major strengths of this study. Additionally, the current study fills a gap in the literature regarding the knowledge of hippocampal diffusion and Parkinson's Disease. Since few studies have looked at how PD impacts hippocampal microstructure, this study identifies remodelling that may occur in individuals with PD. Furthermore, this study looks at the association between non-motor symptoms and diffusion, which only a small number of studies have investigated before, especially concerning non-cognitive symptoms of PD. Because non-motor symptoms broadly impact quality of life in individuals with PD, it is crucial to study their relationship with the brain, which, with continued research, could potentially lead to early identification of those predisposed to developing these symptoms and provide possibilities for early intervention.

Limitations of this study include the lack of power for detecting differences between groups, especially differences in MD. Power calculations showed that, for our sample size, power was much lower for hippocampal volume and MD ($\beta = 0.18$ and 0.05 for average hippocampal volume and MD, respectively) than it was for FA ($\beta = 0.99$ for average, left, and right hippocampal FA), indicating that, we had a much lower probability of detecting a significant difference between groups for volume and MD, but a better likelihood of detecting differences for FA. Because of this limitation, we may have failed to identify specific associations that might exist. However, since our sample size is similar to, or even larger than, some other studies in this area (39, 60, 121), we hope that our findings can be of use to further understand hippocampal changes in PD and DLB. Furthermore, we cannot determine whether there is co-pathology with Amyloid-β, which is characteristic of AD and may be associated with dementia in PD and DLB (36). Another limitation is that this is a cross-sectional study; therefore, we cannot make inferences about how non-motor symptoms and hippocampal changes evolve over time. However, this is an avenue we may be able to explore in the future, and it would be helpful to show how FA changes as patients progress. Changes over time could provide more evidence regarding whether increased FA with worse non-motor symptom burden was due to compensatory changes or Lewy neurite deposition (if FA decreased as the disease progressed) or the loss of synaptic spines (if FA increased over time). Additionally, it should be acknowledged that these findings may be an epiphenomenon, and that a higher severity of non-motor symptoms may not be related to changes within the hippocampus but instead due to generalized changes in brain function or other aspects of the illness experience that a cross-sectional study focused on the hippocampus may be unable to elucidate.

Concluding Remarks and Future Directions

Non-motor symptoms in Lewy body diseases have been relatively understudied compared to motor symptoms, despite their importance for QoL. Especially for hippocampal diffusion, few studies have looked at the associations between non-motor symptoms and hippocampal microstructure. Therefore, no similar literature can support our finding of increased hippocampal FA in individuals with worse non-motor symptoms. Future studies should continue this line of investigation and potentially use other methods to elucidate the mechanisms underlying FA changes. For example, one diffusion tensor imaging technique known as neurite orientation dispersion and density imaging (NODDI) can measure the density of dendrites and axons (i.e., neurites) (192). It may help further indicate whether the loss of dendric complexity contributes to increased FA in patients with worse non-motor symptoms. Another direction that could be taken is using measures of associated GM regions adjacent to the hippocampus proper, such as the entorhinal cortex and the subiculum, and associated limbic WM tracts (e.g., the fornix, cingulum, and uncinate fasciculus) (193) to compare any diffusion changes that may occur along with non-motor symptoms.

References

1. Parkinson J. An essay on the shaking palsy. 1817. J Neuropsychiatry Clin Neurosci. 2002;14(2):223-36; discussion 2.
2. Bhishagratna K. An English Translation of the Sushruta Samhita: Nidāna-sthāna, Śāriri-sthāna, Chikitsta-sthāna and Kalpa-sthāna: Chowkhamba Sanskrit series office; 1963.
3. Ovallath S, Deepa P. The history of parkinsonism: descriptions in ancient Indian medical literature. Mov Disord. 2013;28(5):566-8.
4. Zhang ZX, Dong ZH, Roman GC. Early descriptions of Parkinson disease in ancient China. Arch Neurol. 2006;63(5):782-4.
5. Stern G. Did parkinsonism occur before 1817? J Neurol Neurosurg Psychiatry. 1989;Suppl:11-2.
6. Beitz JM. Parkinson's disease: a review. Front Biosci (Schol Ed). 2014;6(1):65-74.
7. Forno LS. Neuropathology of Parkinson's disease. J Neuropathol Exp Neurol. 1996;55(3):259-72.
8. Lashuel HA, Overk CR, Oueslati A, Masliah E. The many faces of alpha-synuclein: from structure and toxicity to therapeutic target. Nat Rev Neurosci. 2013;14(1):38-48.
9. Mueller C, Ballard C, Corbett A, Aarsland D. Historical landmarks in dementia with Lewy bodies. Lancet Neurol. 2017;16(5):348.
10. Yamada M, Komatsu J, Nakamura K, Sakai K, Samuraki-Yokohama M, Nakajima K, et al. Diagnostic Criteria for Dementia with Lewy Bodies: Updates and Future Directions. J Mov Disord. 2020;13(1):1-10.
11. Postuma RB, Berg D, Stern M, Poewe W, Olanow CW, Oertel W, et al. MDS clinical diagnostic criteria for Parkinson's disease. Mov Disord. 2015;30(12):1591-601.
12. Litvan I, Goldman JG, Troster AI, Schmand BA, Weintraub D, Petersen RC, et al. Diagnostic criteria for mild cognitive impairment in Parkinson's disease: Movement Disorder Society Task Force guidelines. Mov Disord. 2012;27(3):349-56.
13. Emre M, Aarsland D, Brown R, Burn DJ, Duyckaerts C, Mizuno Y, et al. Clinical diagnostic criteria for dementia associated with Parkinson's disease. Mov Disord. 2007;22(12):1689-707; quiz 837.
14. McKeith IG, Ferman TJ, Thomas AJ, Blanc F, Boeve BF, Fujishiro H, et al. Research criteria for the diagnosis of prodromal dementia with Lewy bodies. Neurology. 2020;94(17):743-55.
15. Berardelli A, Wenning GK, Antonini A, Berg D, Bloem BR, Bonifati V, et al. EFNS/MDS-ES/ENS [corrected] recommendations for the diagnosis of Parkinson's disease. Eur J Neurol. 2013;20(1):16-34.
16. Chaudhuri KR, Healy DG, Schapira AH, National Institute for Clinical E. Non-motor symptoms of Parkinson's disease: diagnosis and management. Lancet Neurol. 2006;5(3):235-45.
17. Schapira AHV, Chaudhuri KR, Jenner P. Non-motor features of Parkinson disease. Nat Rev Neurosci. 2017;18(8):509.
18. American Psychiatric Association., American Psychiatric Association. DSM-5 Task Force. Diagnostic and statistical manual of mental disorders : DSM-5. 5th ed. Washington, D.C.: American Psychiatric Association; 2013. xliv, 947 p. p.

19. Hinkle JT, Pontone GM. Lewy Body Degenerations as Neuropsychiatric Disorders. Psychiatr Clin North Am. 2020;43(2):361-81.
20. Prakash KM, Nadkarni NV, Lye WK, Yong MH, Tan EK. The impact of non-motor symptoms on the quality of life of Parkinson's disease patients: a longitudinal study. Eur J Neurol. 2016;23(5):854-60.
21. Hely MA, Reid WG, Adena MA, Halliday GM, Morris JG. The Sydney multicenter study of Parkinson's disease: the inevitability of dementia at 20 years. Mov Disord. 2008;23(6):837-44.
22. Walker Z, Possin KL, Boeve BF, Aarsland D. Lewy body dementias. Lancet. 2015;386(10004):1683-97.
23. Weintraub D, Irwin D. Diagnosis and Treatment of Cognitive and Neuropsychiatric Symptoms in Parkinson Disease and Dementia With Lewy Bodies. Continuum (Minneap Minn). 2022;28(5):1314-32.
24. Braak H, Del Tredici K. Potential Pathways of Abnormal Tau and alpha-Synuclein Dissemination in Sporadic Alzheimer's and Parkinson's Diseases. Cold Spring Harb Perspect Biol. 2016;8(11).
25. Henderson MX, Trojanowski JQ, Lee VM. alpha-Synuclein pathology in Parkinson's disease and related alpha-synucleinopathies. Neurosci Lett. 2019;709:134316.
26. Braak H, Braak E. Neuropathological stageing of Alzheimer-related changes. Acta Neuropathol. 1991;82(4):239-59.
27. Braak H, Braak E, Yilmazer D, de Vos RA, Jansen EN, Bohl J. Pattern of brain destruction in Parkinson's and Alzheimer's diseases. J Neural Transm (Vienna). 1996;103(4):455-90.
28. Braak H, Del Tredici K, Rub U, de Vos RA, Jansen Steur EN, Braak E. Staging of brain pathology related to sporadic Parkinson's disease. Neurobiol Aging. 2003;24(2):197-211.
29. Braak H, Ghebremedhin E, Rub U, Bratzke H, Del Tredici K. Stages in the development of Parkinson's disease-related pathology. Cell Tissue Res. 2004;318(1):121-34.
30. Braak H, Braak E, Yilmazer D, de Vos RA, Jansen EN, Bohl J, et al. Amygdala pathology in Parkinson's disease. Acta Neuropathol. 1994;88(6):493-500.
31. Duvernoy HM, Cattin F, Risold P-Y, Vannson JL, Gaudron M. The human hippocampus : functional anatomy, vascularization and serial sections with MRI. Fourth edition. ed. Heidelberg ; New York: Springer; 2013. p. viii, 237 pages.
32. Lewis FT. The significance of the term Hippocampus. The Journal of Comparative Neurology. 1923;35(3):213-30.
33. Dudek SM, Alexander GM, Farris S. Rediscovering area CA2: unique properties and functions. Nat Rev Neurosci. 2016;17(2):89-102.
34. Benoy A, Dasgupta A, Sajikumar S. Hippocampal area CA2: an emerging modulatory gateway in the hippocampal circuit. Exp Brain Res. 2018;236(4):919-31.
35. Gyorfi O, Nagy H, Bokor M, Moustafa AA, Rosenzweig I, Kelemen O, et al. Reduced CA2-CA3 Hippocampal Subfield Volume Is Related to Depression and Normalized by l-DOPA in Newly Diagnosed Parkinson's Disease. Front Neurol. 2017;8:84.
36. Compta Y, Parkkinen L, O'Sullivan SS, Vandrovcova J, Holton JL, Collins C, et al. Lewy- and Alzheimer-type pathologies in Parkinson's disease dementia: which is more important? Brain. 2011;134(Pt 5):1493-505.
37. Ryman SG, Poston KL. MRI biomarkers of motor and non-motor symptoms in Parkinson's disease. Parkinsonism Relat Disord. 2020;73:85-93.

38. Kunst J, Marecek R, Klobusiakova P, Balazova Z, Anderkova L, Nemcova-Elfmarkova N, et al. Patterns of Grey Matter Atrophy at Different Stages of Parkinson's and Alzheimer's Diseases and Relation to Cognition. Brain Topogr. 2019;32(1):142-60.
39. Carlesimo GA, Piras F, Assogna F, Pontieri FE, Caltagirone C, Spalletta G. Hippocampal abnormalities and memory deficits in Parkinson disease: A multimodal imaging study. Neurology. 2012;78(24):1939-45.
40. Camicioli R, Moore MM, Kinney A, Corbridge E, Glassberg K, Kaye JA. Parkinson's disease is associated with hippocampal atrophy. Mov Disord. 2003;18(7):784-90.
41. Bruck A, Kurki T, Kaasinen V, Vahlberg T, Rinne JO. Hippocampal and prefrontal atrophy in patients with early non-demented Parkinson's disease is related to cognitive impairment. J Neurol Neurosurg Psychiatry. 2004;75(10):1467-9.
42. Tanner JJ, McFarland NR, Price CC. Striatal and Hippocampal Atrophy in Idiopathic Parkinson's Disease Patients without Dementia: A Morphometric Analysis. Front Neurol. 2017;8:139.
43. Vo A, Sako W, Fujita K, Peng S, Mattis PJ, Skidmore FM, et al. Parkinson's disease-related network topographies characterized with resting state functional MRI. Hum Brain Mapp. 2017;38(2):617-30.
44. Wolters AF, van de Weijer SCF, Leentjens AFG, Duits AA, Jacobs HIL, Kuijf ML. Resting-state fMRI in Parkinson's disease patients with cognitive impairment: A meta-analysis. Parkinsonism Relat Disord. 2019;62:16-27.
45. Alexander AL, Lee JE, Lazar M, Field AS. Diffusion tensor imaging of the brain. Neurotherapeutics. 2007;4(3):316-29.
46. Soares JM, Marques P, Alves V, Sousa N. A hitchhiker's guide to diffusion tensor imaging. Front Neurosci. 2013;7:31.
47. Song SK, Sun SW, Ramsbottom MJ, Chang C, Russell J, Cross AH. Dysmyelination revealed through MRI as increased radial (but unchanged axial) diffusion of water. Neuroimage. 2002;17(3):1429-36.
48. Budde MD, Xie M, Cross AH, Song SK. Axial diffusivity is the primary correlate of axonal injury in the experimental autoimmune encephalomyelitis spinal cord: a quantitative pixelwise analysis. J Neurosci. 2009;29(9):2805-13.
49. Zhang Y, Burock MA. Diffusion Tensor Imaging in Parkinson's Disease and Parkinsonian Syndrome: A Systematic Review. Front Neurol. 2020;11:531993.
50. Van Hecke W, Emsell L, Sunaert S. Diffusion tensor imaging : a practical handbook. New York ; Heidelberg: Springer; 2016. p. x, 441 pages.
51. Minett T, Su L, Mak E, Williams G, Firbank M, Lawson RA, et al. Longitudinal diffusion tensor imaging changes in early Parkinson's disease: ICICLE-PD study. J Neurol. 2018;265(7):1528-39.
52. Andica C, Kamagata K, Hatano T, Saito A, Uchida W, Ogawa T, et al. Free-Water Imaging in White and Gray Matter in Parkinson's Disease. Cells. 2019;8(8).
53. Treit S, Steve T, Gross DW, Beaulieu C. High resolution in-vivo diffusion imaging of the human hippocampus. Neuroimage. 2018;182:479-87.
54. Grothe MJ, Labrador-Espinosa MA, Jesús S, Macías-García D, Adarmes-Gómez A, Carrillo F, et al. In vivo cholinergic basal forebrain degeneration and cognition in Parkinson's disease: Imaging results from the COPPADIS study. Parkinsonism & Related Disorders. 2021;88:68-75.

55. Zhang K, Yu C, Zhang Y, Wu X, Zhu C, Chan P, et al. Voxel-based analysis of diffusion tensor indices in the brain in patients with Parkinson's disease. European Journal of Radiology. 2011;77(2):269-73.
56. Zhong JM, Wu SY, Zhao Y, Chen H, Zhao NW, Zheng KW, et al. Why psychosis is frequently associated with Parkinson's disease? Neural Regen Res. 2013;8(27):2548-56.
57. Pyatigorskaya N, Yahia-Cherif L, Valabregue R, Gaurav R, Gargouri F, Ewenczyk C, et al. Parkinson Disease Propagation Using MRI Biomarkers and Partial Least Squares Path Modeling. Neurology. 2021;96(3):e460-e71.
58. Pyatigorskaya N, Mongin M, Valabregue R, Yahia-Cherif L, Ewenczyk C, Poupon C, et al. Medulla oblongata damage and cardiac autonomic dysfunction in Parkinson disease. Neurology. 2016;87(24):2540-5.
59. Yao N, Cheung C, Pang S, Shek-kwan Chang R, Lau KK, Suckling J, et al. Multimodal MRI of the hippocampus in Parkinson's disease with visual hallucinations. Brain Structure & Function. 2016;221(1):287-300.
60. Kamagata K, Zalesky A, Hatano T, Ueda R, Di Biase MA, Okuzumi A, et al. Gray Matter Abnormalities in Idiopathic Parkinson's Disease: Evaluation by Diffusional Kurtosis Imaging and Neurite Orientation Dispersion and Density Imaging. Hum Brain Mapp. 2017;38(7):3704-22.
61. Kim HJ, Kim SJ, Kim HS, Choi CG, Kim N, Han S, et al. Alterations of mean diffusivity in brain white matter and deep gray matter in Parkinson's disease. Neurosci Lett. 2013;550:64-8.
62. Schulz J, Pagano G, Bonfante JAF, Wilson H, Politis M, Fernández Bonfante JA. Nucleus basalis of Meynert degeneration precedes and predicts cognitive impairment in Parkinson's disease. Brain: A Journal of Neurology. 2018;141(5):1501-16.
63. Hope TR, Selnes P, Rektorova I, Anderkova L, Nemcova-Elfmarkova N, Balazova Z, et al. Diffusion tensor and restriction spectrum imaging reflect different aspects of neurodegeneration in Parkinson's disease. PLoS One. 2019;14(5):e0217922.
64. Lu CS, Ng SH, Weng YH, Cheng JS, Lin WY, Wai YY, et al. Alterations of diffusion tensor MRI parameters in the brains of patients with Parkinson’s disease compared with normal brains: possible diagnostic use. Eur Radiol. 2016;26(11):3978-88.
65. Tsai CC, Lin YC, Ng SH, Chen YL, Cheng JS, Lu CS, et al. A Method for the Prediction of Clinical Outcome Using Diffusion Magnetic Resonance Imaging: Application on Parkinson's Disease. J Clin Med. 2020;9(3).
66. Laakso MP, Partanen K, Riekkinen P, Lehtovirta M, Helkala EL, Hallikainen M, et al. Hippocampal volumes in Alzheimer's disease, Parkinson's disease with and without dementia, and in vascular dementia: An MRI study. Neurology. 1996;46(3):678-81.
67. Melzer TR, Watts R, MacAskill MR, Pitcher TL, Livingston L, Keenan RJ, et al. White matter microstructure deteriorates across cognitive stages in Parkinson disease. Neurology. 2013;80(20):1841-9.
68. Galantucci S, Agosta F, Stefanova E, Basaia S, Van Den Heuvel MP, Stojković T, et al. Structural brain connectome and cognitive impairment in Parkinson disease. Radiology. 2017;283(2):515-25.
69. Gorges M, Müller HP, Liepelt-Scarfone I, Storch A, Dodel R, Hilker-Roggendorf R, et al. Structural brain signature of cognitive decline in Parkinson’s disease: DTI-based evidence from the LANDSCAPE study. Ther Adv Neurol Disord. 2019;12.

70. Inguanzo A, Segura B, Sala-Llonch R, Monte-Rubio G, Abos A, Campabadal A, et al. Impaired Structural Connectivity in Parkinson's Disease Patients with Mild Cognitive Impairment: A Study Based on Probabilistic Tractography. Brain Connectivity. 2021;11(5):380-92.
71. Hattori T, Orimo S, Aoki S, Ito K, Abe O, Amano A, et al. Cognitive status correlates with white matter alteration in Parkinson's disease. Hum Brain Mapp. 2012;33(3):727-39.
72. Deng B, Zhang Y, Wang L, Peng K, Han L, Nie K, et al. Diffusion tensor imaging reveals white matter changes associated with cognitive status in patients with Parkinson's disease. American Journal of Alzheimer's Disease and Other Dementias. 2013;28(2):154-64.
73. Kamagata K, Motoi Y, Tomiyama H, Abe O, Ito K, Shimoji K, et al. Relationship between cognitive impairment and white-matter alteration in Parkinson's disease with dementia: tract-based spatial statistics and tract-specific analysis. Eur Radiol. 2013;23(7):1946-55.
74. Kamagata K, Motoi Y, Abe O, Shimoji K, Hori M, Nakanishi A, et al. White matter alteration of the cingulum in Parkinson disease with and without dementia: Evaluation by diffusion tensor tract-specific analysis. Am J Neuroradiol. 2012;33(5):890-5.
75. Matsui H, Nishinaka K, Oda M, Niikawa H, Kubori T, Udaka F. Dementia in Parkinson's disease: Diffusion tensor imaging. Acta Neurologica Scandinavica. 2007;116(3):177-81.
76. Lee JE, Park HJ, Park B, Song SK, Sohn YH, Lee JD, et al. A comparative analysis of cognitive profiles and white-matter alterations using voxel-based diffusion tensor imaging between patients with Parkinson's disease dementia and dementia with Lewy bodies. Journal of Neurology, Neurosurgery & Psychiatry. 2010;81(3):320-6.
77. Chen B, Fan GG, Liu H, Wang S. Changes in anatomical and functional connectivity of Parkinson's disease patients according to cognitive status. European Journal of Radiology. 2015;84(7):1318-24.
78. Chondrogiorgi M, Astrakas LG, Zikou AK, Weis L, Xydis VG, Antonini A, et al. Multifocal alterations of white matter accompany the transition from normal cognition to dementia in Parkinson's disease patients. Brain Imaging & Behavior. 2019;13(1):232-40.
79. Bledsoe IO, Stebbins GT, Merkitch D, Goldman JG. White matter abnormalities in the corpus callosum with cognitive impairment in Parkinson disease. Neurology. 2018;91(24):e2244-e55.
80. Abbasi N, Fereshtehnejad SM, Zeighami Y, Larcher KM, Postuma RB, Dagher A. Predicting severity and prognosis in Parkinson's disease from brain microstructure and connectivity. Neuroimage (Amst). 2020;25:102111.
81. Arribarat G, Pasternak O, De Barros A, Galitzky M, Rascol O, Peran P. Substantia nigra locations of iron-content, free-water and mean diffusivity abnormalities in moderate stage Parkinson's disease. Parkinsonism Relat Disord. 2019;65:146-52.
82. Baumeister TR, Kim JL, Zhu M, McKeown MJ. White matter myelin profiles linked to clinical subtypes of Parkinson's disease. J Magn Reson Imaging. 2019;50(1):164-74.
83. Caspell-Garcia C, Simuni T, Tosun-Turgut D, Wu IW, Zhang Y, Nalls M, et al. Multiple modality biomarker prediction of cognitive impairment in prospectively followed de novo Parkinson disease. PLoS One. 2017;12(5):e0175674.
84. Guttuso T, Jr., Bergsland N, Hagemeier J, Lichter DG, Pasternak O, Zivadinov R. Substantia Nigra Free Water Increases Longitudinally in Parkinson Disease. AJNR Am J Neuroradiol. 2018;39(3):479-84.

85. Langley J, Huddleston DE, Merritt M, Chen X, McMurray R, Silver M, et al. Diffusion tensor imaging of the substantia nigra in Parkinson's disease revisited. Hum Brain Mapp. 2016;37(7):2547-56.
86. Le H, Zeng W, Zhang H, Li J, Wu X, Xie M, et al. Mean Apparent Propagator MRI Is Better Than Conventional Diffusion Tensor Imaging for the Evaluation of Parkinson's Disease: A Prospective Pilot Study. Frontiers in Aging Neuroscience. 2020;12:N.PAG-N.PAG.
87. Liu Z, Zhang Y, Wang H, Xu D, You H, Zuo Z, et al. Altered cerebral perfusion and microstructure in advanced Parkinson's disease and their associations with clinical features. Neurol Res. 2022;44(1):47-56.
88. Pelizzari L, Lagana MM, Di Tella S, Rossetto F, Bergsland N, Nemni R, et al. Combined assessment of diffusion parameters and cerebral blood flow within basal ganglia in early Parkinson's disease. Frontiers in Aging Neuroscience Vol 11 2019, ArtID 134. 2019;11.
89. Sampedro F, Martinez-Horta S, Marin-Lahoz J, Pagonabarraga J, Kulisevsky J. Longitudinal intracortical diffusivity changes in de-novo Parkinson's disease: A promising imaging biomarker. Parkinsonism Relat Disord. 2019;68:22-5.
90. Sampedro F, Perez-Gonzalez R, Martinez-Horta S, Marin-Lahoz J, Pagonabarraga J, Kulisevsky J. Serum neurofilament light chain levels reflect cortical neurodegeneration in de novo Parkinson's disease. Parkinsonism Relat Disord. 2020;74:43-9.
91. Surkont J, Joza S, Camicioli R, Martin W, Wieler M, Ba F. Subcortical microstructural diffusion changes correlate with gait impairment in Parkinson's disease. Parkinsonism & Related Disorders. 2021;87:111-8.
92. Wen MC, Heng HSE, Lu Z, Xu Z, Chan LL, Tan EK, et al. Differential White Matter Regional Alterations in Motor Subtypes of Early Drug-Naive Parkinson's Disease Patients. Neurorehabil Neural Repair. 2018;32(2):129-41.
93. Zhang Y, Wu IW, Tosun D, Foster E, Schuff N, the Parkinson's Progression Markers I. Progression of regional microstructural degeneration in Parkinson's disease: A multicenter diffusion tensor imaging study. PLoS ONE. 2016;11(10).
94. Zheng Z, Shemmassian S, Wijekoon C, Kim W, Bookheimer SY, Pouratian N. DTI correlates of distinct cognitive impairments in Parkinson's disease. Hum Brain Mapp. 2014;35(4):1325-33.
95. Auning E, Kjærvik VK, Selnes P, Aarsland D, Haram A, Bjørnerud A, et al. White matter integrity and cognition in Parkinson's disease: A cross-sectional study. BMJ Open. 2014;4(1).
96. Devignes Q, Viard R, Betrouni N, Carey G, Kuchcinski G, Defebvre L, et al. Posterior cortical cognitive deficits are associated with structural brain alterations in mild cognitive impairment in Parkinson's disease. Frontiers in Aging Neuroscience Vol 13 2021, ArtID 668559. 2021;13.
97. Gallagher C, Bell B, Bendlin B, Palotti M, Okonkwo O, Sodhi A, et al. White matter microstructural integrity and executive function in Parkinson's disease. J Int Neuropsychol Soc. 2013;19(3):349-54.
98. Koshimori Y, Segura B, Christopher L, Lobaugh N, Duff-Canning S, Mizrahi R, et al. Imaging changes associated with cognitive abnormalities in Parkinson's disease. Brain Struct Funct. 2015;220(4):2249-61.
99. Lucas-Jiménez O, Ojeda N, Peña J, Díez-Cirarda M, Cabrera-Zubizarreta A, Gómez-Esteban JC, et al. Altered functional connectivity in the default mode network is associated with

cognitive impairment and brain anatomical changes in Parkinson's disease. Parkinsonism & Related Disorders. 2016;33:58-64.
100. Surdhar I, Gee M, Bouchard T, Coupland N, Malykhin N, Camicioli R. Intact limbic-prefrontal connections and reduced amygdala volumes in Parkinson's disease with mild depressive symptoms. Parkinsonism & Related Disorders. 2012;18(7):809-13.
101. Li Z, Liu W, Xiao C, Wang X, Zhang X, Yu M, et al. Abnormal white matter microstructures in Parkinson's disease and comorbid depression: A whole-brain diffusion tensor imaging study. Neurosci Lett. 2020;735:135238.
102. Li W, Liu J, Skidmore F, Liu Y, Tian J, Li K. White matter microstructure changes in the thalamus in Parkinson disease with depression: A diffusion tensor MR imaging study. Am J Neuroradiol. 2010;31(10):1861-6.
103. Huang P, Xu X, Gu Q, Xuan M, Yu X, Luo W, et al. Disrupted white matter integrity in depressed versus non-depressed parkinson's disease patients: A tract-based spatial statistics study. Journal of the Neurological Sciences. 2014;346(1-2):145-8.
104. Matsui H, Nishinaka K, Oda M, Niikawa H, Komatsu K, Kubori T, et al. Depression in Parkinson's disease: Diffusion tensor imaging study. J Neurol. 2007;254(9):1170-3.
105. Wu J-Y, Zhang Y, Wu W-B, Hu G, Xu Y. Impaired long contact white matter fibers integrity is related to depression in Parkinson's disease. CNS Neuroscience & Therapeutics. 2018;24(2):108-14.
106. Gou L, Zhang W, Li C, Shi X, Zhou Z, Zhong W, et al. Structural brain network alteration and its correlation with structural impairments in patients with depression in de novo and drug-Naïve Parkinson's disease. Front Neurol. 2018;9(JUL).
107. Xiao Y, Peters TM, Khan AR. Characterizing white matter alterations subject to clinical laterality in drug-naive de novo Parkinson's disease. Hum Brain Mapp. 2021;42(14):4465-77.
108. Gargouri F, Gallea C, Mongin M, Pyatigorskaya N, Valabregue R, Ewenczyk C, et al. Multimodal magnetic resonance imaging investigation of basal forebrain damage and cognitive deficits in Parkinson's disease. Movement Disorders. 2019;34(4):516-25.
109. Jonkman LE, Fathy YY, Berendse HW, Schoonheim MM, van de Berg WDJ. Structural network topology and microstructural alterations of the anterior insula associate with cognitive and affective impairment in Parkinson's disease. Sci Rep. 2021;11(1).
110. Prange S, Metereau E, Maillet A, Lhommée E, Klinger H, Pelissier P, et al. Early limbic microstructural alterations in apathy and depression in de novo Parkinson's disease. Movement Disorders. 2019;34(11):1644-54.
111. Shen Q, Liu Y, Guo J, Zhang H, Xiang Y, Liao H, et al. Impaired white matter microstructure associated with severe depressive symptoms in patients with PD. Brain Imaging Behav. 2022;16(1):169-75.
112. Lucas-Jiménez O, Ojeda N, Peña J, Cabrera-Zubizarreta A, Díez-Cirarda M, Gómez-Esteban JC, et al. Apathy and brain alterations in Parkinson's disease: a multimodal imaging study. Ann Clin Transl Neurol. 2018;5(7):803-14.
113. Zhang Y, Wu J, Wu W, Liu R, Pang L, Guan D, et al. Reduction of white matter integrity correlates with apathy in Parkinson's disease. International Journal of Neuroscience. 2018;128(1):25-31.

114. Chondrogiorgi M, Tzarouchi LC, Zikou AK, Astrakas LG, Kosta P, Argyropoulou MI, et al. Multimodal imaging evaluation of excessive daytime sleepiness in Parkinson's disease. International Journal of Neuroscience. 2016;126(5):422-8.
115. Dolatshahi M, Ashraf-Ganjouei A, Wu IW, Zhang Y, Aarabi MH, Tosun D. White matter changes in drug-naive Parkinson's disease patients with impulse control & probable REM sleep behavior disorders. Journal of the Neurological Sciences Vol 430 2021, ArtID 120032. 2021;430.
116. Holtbernd F, Romanzetti S, Oertel WH, Knake S, Sittig E, Heidbreder A, et al. Convergent patterns of structural brain changes in rapid eye movement sleep behavior disorder and Parkinson's disease on behalf of the German rapid eye movement sleep behavior disorder study group. Sleep: Journal of Sleep and Sleep Disorders Research. 2021;44(3):1-12.
117. Kang SY, Bang M, Hong JY, Oh J, Kim JS, Han YM, et al. Neural and dopaminergic correlates of fatigue in Parkinson's disease. Journal of Neural Transmission. 2020;127(3):301-9.
118. Kluger BM, Zhao Q, Tanner JJ, Schwab NA, Levy SA, Burke SE, et al. Structural brain correlates of fatigue in older adults with and without Parkinson's disease. NeuroImage Clin. 2019;22.
119. Lim J-S, Shin SA, Lee J-Y, Nam H, Lee J-Y, Kim YK. Neural substrates of rapid eye movement sleep behavior disorder in Parkinson's disease. Parkinsonism & Related Disorders. 2016;23:31-6.
120. Matsui H, Nishinaka K, Oda M, Niikawa H, Komatsu K, Kubori T, et al. Disruptions of the fornix fiber in parkinsonian patients with excessive daytime sleepiness. Parkinsonism & Related Disorders. 2006;12(5):319-22.
121. Wei X, Yan R, Chen Z, Weng R, Liu X, Gao H, et al. Combined Diffusion Tensor Imaging and Arterial Spin Labeling as Markers of Early Parkinson's disease. Sci Rep. 2016;6:33762.
122. Wu J, Guo T, Zhou C, Guan X, Gao T, Xuan M, et al. Longitudinal Macro/Microstructural Alterations of Different Callosal Subsections in Parkinson's Disease Using Connectivity-Based Parcellation. Front Aging Neurosci. 2020;12:572086.
123. Zorzi G, Thiebaut de Schotten M, Manara R, Busse C, Corbetta M, Cagnin A. White matter abnormalities of right hemisphere attention networks contribute to visual hallucinations in dementia with Lewy bodies. Cortex. 2021;139:86-98.
124. Lee JY, Yoon EJ, Lee WW, Kim YK, Lee JY, Jeon B. Lateral geniculate atrophy in Parkinson's with visual hallucination: A trans-synaptic degeneration? Movement Disorders. 2016;31(4):547-54.
125. Hepp DH, Foncke EMJ, Berendse HW, Wassenaar TM, Olde Dubbelink KTE, Groenewegen HJ, et al. Damaged fiber tracts of the nucleus basalis of Meynert in Parkinson's disease patients with visual hallucinations. Sci Rep. 2017;7(1):10112.
126. Lenka A, Ingalhalikar M, Shah A, Saini J, Arumugham SS, Hegde S, et al. Abnormalities in the white matter tracts in patients with Parkinson disease and psychosis. Neurology. 2020;94(18):e1876-e84.
127. Yoo HB, Lee JY, Lee JS, Kang H, Kim YK, Song IC, et al. Whole-brain diffusion-tensor changes in parkinsonian patients with impulse control disorders. J Clin Neurol. 2015;11(1):42-7.
128. Treit S, Little G, Steve T, Nowacki T, Schmitt L, Wheatley BM, et al. Regional hippocampal diffusion abnormalities associated with subfield-specific pathology in temporal lobe epilepsy. Epilepsia Open. 2019;4(4):544-54.

129. Solar KG, Treit S, Beaulieu C. High resolution diffusion tensor imaging of the hippocampus across the healthy lifespan. Hippocampus. 2021;31(12):1271-84.
130. Mohaddes Z, Das S, Abou-Haidar R, Safi-Harab M, Blader D, Callegaro J, et al. National Neuroinformatics Framework for Canadian Consortium on Neurodegeneration in Aging (CCNA). Front Neuroinform. 2018;12:85.
131. Chertkow H, Borrie M, Whitehead V, Black SE, Feldman HH, Gauthier S, et al. The Comprehensive Assessment of Neurodegeneration and Dementia: Canadian Cohort Study. Can J Neurol Sci. 2019;46(5):499-511.
132. Peca S, McCreary CR, Donaldson E, Kumarpillai G, Shobha N, Sanchez K, et al. Neurovascular decoupling is associated with severity of cerebral amyloid angiopathy. Neurology. 2013;81(19):1659-65.
133. McCreary CR, Beaudin AE, Subotic A, Zwiers AM, Alvarez A, Charlton A, et al. Cross-sectional and longitudinal differences in peak skeletonized white matter mean diffusivity in cerebral amyloid angiopathy. Neuroimage Clin. 2020;27:102280.
134. Beaudin AE, McCreary CR, Mazerolle EL, Gee M, Sharma B, Subotic A, et al. Cerebrovascular Reactivity Across the Entire Brain in Cerebral Amyloid Angiopathy. Neurology. 2022;98(17):e1716-e28.
135. D'Agostino Sr RB, Vasan RS, Pencina MJ, Wolf PA, Cobain M, Massaro JM, et al. General cardiovascular risk profile for use in primary care: the Framingham Heart Study. Circulation. 2008;117(6):743-53.
136. Washburn RA, Smith KW, Jette AM, Janney CA. The Physical Activity Scale for the Elderly (PASE): development and evaluation. J Clin Epidemiol. 1993;46(2):153-62.
137. Ferman TJ, Smith GE, Boeve BF, Ivnik RJ, Petersen RC, Knopman D, et al. DLB fluctuations: specific features that reliably differentiate DLB from AD and normal aging. Neurology. 2004;62(2):181-7.
138. Menon C, Westervelt HJ, Jahn DR, Dressel JA, O'Bryant SE. Normative performance on the Brief Smell Identification Test (BSIT) in a multi-ethnic bilingual cohort: a Project FRONTIER study. Clin Neuropsychol. 2013;27(6):946-61.
139. Aqrabawi AJ, Kim JC. Hippocampal projections to the anterior olfactory nucleus differentially convey spatiotemporal information during episodic odour memory. Nat Commun. 2018;9(1):2735.
140. Keller HH, Goy R, Kane SL. Validity and reliability of SCREEN II (Seniors in the community: risk evaluation for eating and nutrition, Version II). Eur J Clin Nutr. 2005;59(10):1149-57.
141. Monti JM, Baym CL, Cohen NJ. Identifying and characterizing the effects of nutrition on hippocampal memory. Adv Nutr. 2014;5(3):337S-43S.
142. Goetz CG, Fahn S, Martinez-Martin P, Poewe W, Sampaio C, Stebbins GT, et al. Movement Disorder Society-sponsored revision of the Unified Parkinson's Disease Rating Scale (MDS-UPDRS): Process, format, and clinimetric testing plan. Mov Disord. 2007;22(1):41-7.
143. Tomlinson CL, Stowe R, Patel S, Rick C, Gray R, Clarke CE. Systematic review of levodopa dose equivalency reporting in Parkinson's disease. Mov Disord. 2010;25(15):2649-53.
144. Dawson BK, Fereshtehnejad SM, Anang JBM, Nomura T, Rios-Romenets S, Nakashima K, et al. Office-Based Screening for Dementia in Parkinson Disease: The Montreal Parkinson Risk of Dementia Scale in 4 Longitudinal Cohorts. JAMA Neurol. 2018;75(6):704-10.

145. Hoehn MM, Yahr MD. Parkinsonism: onset, progression and mortality. Neurology. 1967;17(5):427-42.
146. Nasreddine ZS, Phillips NA, Bedirian V, Charbonneau S, Whitehead V, Collin I, et al. The Montreal Cognitive Assessment, MoCA: a brief screening tool for mild cognitive impairment. J Am Geriatr Soc. 2005;53(4):695-9.
147. Subotic A, McCreary CR, Saad F, Nguyen A, Alvarez-Veronesi A, Zwiers AM, et al. Cortical Thickness and Its Association with Clinical Cognitive and Neuroimaging Markers in Cerebral Amyloid Angiopathy. J Alzheimers Dis. 2021;81(4):1663-71.
148. Cummings JL, Mega M, Gray K, Rosenberg-Thompson S, Carusi DA, Gornbein J. The Neuropsychiatric Inventory: comprehensive assessment of psychopathology in dementia. Neurology. 1994;44(12):2308-14.
149. Yesavage JA, Brink TL, Rose TL, Lum O, Huang V, Adey M, et al. Development and validation of a geriatric depression screening scale: a preliminary report. J Psychiatr Res. 1982;17(1):37-49.
150. Spitzer RL, Kroenke K, Williams JB, Lowe B. A brief measure for assessing generalized anxiety disorder: the GAD-7. Arch Intern Med. 2006;166(10):1092-7.
151. Robert PH, Clairet S, Benoit M, Koutaich J, Bertogliati C, Tible O, et al. The apathy inventory: assessment of apathy and awareness in Alzheimer's disease, Parkinson's disease and mild cognitive impairment. Int J Geriatr Psychiatry. 2002;17(12):1099-105.
152. Peto V, Jenkinson C, Fitzpatrick R, Greenhall R. The development and validation of a short measure of functioning and well being for individuals with Parkinson's disease. Qual Life Res. 1995;4(3):241-8.
153. Buysse DJ, Reynolds CF, 3rd, Monk TH, Berman SR, Kupfer DJ. The Pittsburgh Sleep Quality Index: a new instrument for psychiatric practice and research. Psychiatry Res. 1989;28(2):193-213.
154. Sheikh F, Ismail Z, Mortby ME, Barber P, Cieslak A, Fischer K, et al. Prevalence of mild behavioral impairment in mild cognitive impairment and subjective cognitive decline, and its association with caregiver burden. Int Psychogeriatr. 2018;30(2):233-44.
155. Gill DJ, Freshman A, Blender JA, Ravina B. The Montreal cognitive assessment as a screening tool for cognitive impairment in Parkinson's disease. Mov Disord. 2008;23(7):1043-6.
156. Benedict RH. Brief visuospatial memory test--revised: PAR; 1997.
157. Yassa MA, Muftuler LT, Stark CE. Ultrahigh-resolution microstructural diffusion tensor imaging reveals perforant path degradation in aged humans in vivo. Proc Natl Acad Sci U S A. 2010;107(28):12687-91.
158. Yassa MA, Mattfeld AT, Stark SM, Stark CE. Age-related memory deficits linked to circuit-specific disruptions in the hippocampus. Proc Natl Acad Sci U S A. 2011;108(21):8873-8.
159. Moradi E, Hallikainen I, Hanninen T, Tohka J, Alzheimer's Disease Neuroimaging I. Rey's Auditory Verbal Learning Test scores can be predicted from whole brain MRI in Alzheimer's disease. Neuroimage Clin. 2017;13:415-27.
160. Uribe C, Segura B, Baggio HC, Campabadal A, Abos A, Compta Y, et al. Differential Progression of Regional Hippocampal Atrophy in Aging and Parkinson's Disease. Front Aging Neurosci. 2018;10:325.
161. Bonner-Jackson A, Mahmoud S, Miller J, Banks SJ. Verbal and non-verbal memory and hippocampal volumes in a memory clinic population. Alzheimers Res Ther. 2015;7(1):61.

162. Havlik F, Mana J, Dusek P, Jech R, Ruzicka E, Kopecek M, et al. Brief Visuospatial Memory Test-Revised: normative data and clinical utility of learning indices in Parkinson's disease. J Clin Exp Neuropsychol. 2020;42(10):1099-110.
163. Obeso I, Casabona E, Bringas ML, Alvarez L, Jahanshahi M. Semantic and phonemic verbal fluency in Parkinson's disease: Influence of clinical and demographic variables. Behav Neurol. 2012;25(2):111-8.
164. Reitan RM. Validity of the Trail Making Test as an indicator of organic brain damage. Perceptual and motor skills. 1958;8(3):271-6.
165. Bai F, Zhang Z, Watson DR, Yu H, Shi Y, Yuan Y, et al. Abnormal functional connectivity of hippocampus during episodic memory retrieval processing network in amnestic mild cognitive impairment. Biol Psychiatry. 2009;65(11):951-8.
166. Jaeger J. Digit Symbol Substitution Test: The Case for Sensitivity Over Specificity in Neuropsychological Testing. J Clin Psychopharmacol. 2018;38(5):513-9.
167. Wechsler D. WAiS-iii: psychological Corporation; 1997.
168. Burdick DJ, Cholerton B, Watson GS, Siderowf A, Trojanowski JQ, Weintraub D, et al. People with Parkinson's disease and normal MMSE score have a broad range of cognitive performance. Mov Disord. 2014;29(10):1258-64.
169. Yushkevich PA, Piven J, Hazlett HC, Smith RG, Ho S, Gee JC, et al. User-guided 3D active contour segmentation of anatomical structures: significantly improved efficiency and reliability. Neuroimage. 2006;31(3):1116-28.
170. Boccardi M, Bocchetta M, Apostolova LG, Barnes J, Bartzokis G, Corbetta G, et al. Delphi definition of the EADC-ADNI Harmonized Protocol for hippocampal segmentation on magnetic resonance. Alzheimers Dement. 2015;11(2):126-38.
171. Frisoni GB, Jack CR, Jr., Bocchetta M, Bauer C, Frederiksen KS, Liu Y, et al. The EADC-ADNI Harmonized Protocol for manual hippocampal segmentation on magnetic resonance: evidence of validity. Alzheimers Dement. 2015;11(2):111-25.
172. Taha AA, Hanbury A. Metrics for evaluating 3D medical image segmentation: analysis, selection, and tool. BMC Med Imaging. 2015;15:29.
173. Koo TK, Li MY. A Guideline of Selecting and Reporting Intraclass Correlation Coefficients for Reliability Research. J Chiropr Med. 2016;15(2):155-63.
174. Field AP, Miles J, Field Z. Discovering statistics using R. London ; Thousand Oaks, Calif.: Sage; 2012. p. xxxiv, 957 p.
175. Rasmussen JL, Dunlap WP. Dealing with nonnormal data: Parametric analysis of transformed data vs nonparametric analysis. Educational and psychological measurement. 1991;51(4):809-20.
176. Faul F, Erdfelder E, Lang AG, Buchner A. G*Power 3: a flexible statistical power analysis program for the social, behavioral, and biomedical sciences. Behav Res Methods. 2007;39(2):175-91.
177. Abe O, Yamasue H, Yamada H, Masutani Y, Kabasawa H, Sasaki H, et al. Sex dimorphism in gray/white matter volume and diffusion tensor during normal aging. NMR Biomed. 2010;23(5):446-58.
178. Martin GP, McDonald KR, Allsop D, Diggle PJ, Leroi I. Apathy as a behavioural marker of cognitive impairment in Parkinson's disease: a longitudinal analysis. J Neurol. 2020;267(1):214-27.

179. Schonenberg A, Prell T. Measuring quality of life with the Parkinson's Disease Questionnaire-39 in people with cognitive impairment. PLoS One. 2022;17(4):e0266140.
180. Hentz JG, Mehta SH, Shill HA, Driver-Dunckley E, Beach TG, Adler CH. Simplified conversion method for unified Parkinson's disease rating scale motor examinations. Mov Disord. 2015;30(14):1967-70.
181. Patenaude B, Smith SM, Kennedy DN, Jenkinson M. A Bayesian model of shape and appearance for subcortical brain segmentation. Neuroimage. 2011;56(3):907-22.
182. Akudjedu TN, Nabulsi L, Makelyte M, Scanlon C, Hehir S, Casey H, et al. A comparative study of segmentation techniques for the quantification of brain subcortical volume. Brain Imaging Behav. 2018;12(6):1678-95.
183. Patenaude B. Bayesian statistical models of shape and appearance for subcortical brain segmentation: University of Oxford; 2007.
184. Weston PS, Simpson IJ, Ryan NS, Ourselin S, Fox NC. Diffusion imaging changes in grey matter in Alzheimer's disease: a potential marker of early neurodegeneration. Alzheimers Res Ther. 2015;7(1):47.
185. Chiapponi C, Piras F, Piras F, Fagioli S, Caltagirone C, Spalletta G. Cortical grey matter and subcortical white matter brain microstructural changes in schizophrenia are localised and age independent: a case-control diffusion tensor imaging study. PLoS One. 2013;8(10):e75115.
186. Mole JP, Subramanian L, Bracht T, Morris H, Metzler-Baddeley C, Linden DE. Increased fractional anisotropy in the motor tracts of Parkinson's disease suggests compensatory neuroplasticity or selective neurodegeneration. Eur Radiol. 2016;26(10):3327-35.
187. Budde MD, Janes L, Gold E, Turtzo LC, Frank JA. The contribution of gliosis to diffusion tensor anisotropy and tractography following traumatic brain injury: validation in the rat using Fourier analysis of stained tissue sections. Brain. 2011;134(Pt 8):2248-60.
188. Winston GP. The physical and biological basis of quantitative parameters derived from diffusion MRI. Quant Imaging Med Surg. 2012;2(4):254-65.
189. Schulz-Schaeffer WJ. The synaptic pathology of alpha-synuclein aggregation in dementia with Lewy bodies, Parkinson's disease and Parkinson's disease dementia. Acta Neuropathol. 2010;120(2):131-43.
190. Jones DK, Knosche TR, Turner R. White matter integrity, fiber count, and other fallacies: the do's and don'ts of diffusion MRI. Neuroimage. 2013;73:239-54.
191. Yang Y, Yang Y, Pan A, Xu Z, Wang L, Zhang Y, et al. Identifying Depression in Parkinson's Disease by Using Combined Diffusion Tensor Imaging and Support Vector Machine. Front Neurol. 2022;13:878691.
192. Zhang H, Schneider T, Wheeler-Kingshott CA, Alexander DC. NODDI: practical in vivo neurite orientation dispersion and density imaging of the human brain. Neuroimage. 2012;61(4):1000-16.
193. Pascalau R, Popa Stanila R, Sfrangeu S, Szabo B. Anatomy of the Limbic White Matter Tracts as Revealed by Fiber Dissection and Tractography. World Neurosurg. 2018;113:e672-e89.
194. Hanganu A, Houde JC, Fonov VS, Degroot C, Mejia-Constain B, Lafontaine AL, et al. White matter degeneration profile in the cognitive cortico-subcortical tracts in Parkinson's disease. Movement Disorders. 2018;33(7):1139-50.

195. Garcia-Diaz AI, Segura B, Baggio HC, Marti MJ, Valldeoriola F, Compta Y, et al. Structural Brain Correlations of Visuospatial and Visuoperceptual Tests in Parkinson's Disease. J Int Neuropsychol Soc. 2018;24(1):33-44.
196. Rossi ME, Ruottinen H, Saunamäki T, Elovaara I, Dastidar P. Imaging Brain Iron and Diffusion Patterns. A Follow-up Study of Parkinson's Disease in the Initial Stages. Acad Radiol. 2014;21(1):64-71.
197. Chen F, Wu T, Luo Y, Li Z, Guan Q, Meng X, et al. Amnestic mild cognitive impairment in Parkinson's disease: White matter structural changes and mechanisms. PLoS One. 2019;14(12):e0226175.
198. Shin NY, Shin YS, Lee PH, Yoon U, Han S, Kim DJ, et al. Different Functional and Microstructural Changes Depending on Duration of Mild Cognitive Impairment in Parkinson Disease. AJNR Am J Neuroradiol. 2016;37(5):897-903.
199. Wiltshire K, Concha L, Gee M, Bouchard T, Beaulieu C, Camicioli R. Corpus callosum and cingulum tractography in Parkinson's disease. Can J Neurol Sci. 2010;37(5):595-600.
200. Ota M, Sato N, Ogawa M, Murata M, Kuno S, Kida J, et al. Degeneration of dementia with Lewy bodies measured by diffusion tensor imaging. NMR Biomed. 2009;22(3):280-4.
201. Nicastro N, Mak E, Williams GB, Surendranathan A, Bevan-Jones WR, Passamonti L, et al. Correlation of microglial activation with white matter changes in dementia with Lewy bodies. Neuroimage Clin. 2020;25:102200.
202. Pardini M, Nobili F, Arnaldi D, Morbelli S, Bauckneht M, Rissotto R, et al. (123)I-FP-CIT SPECT validation of nigro-putaminal MRI tractography in dementia with Lewy bodies. Eur Radiol Exp. 2020;4(1):27.
203. Nedelska Z, Schwarz CG, Boeve BF, Lowe VJ, Reid RI, Przybelski SA, et al. White matter integrity in dementia with Lewy bodies: A voxel-based analysis of diffusion tensor imaging. Neurobiology of Aging. 2015;36(6):2010-7.
204. Delli Pizzi S, Maruotti V, Taylor J-P, Franciotti R, Caulo M, Tartaro A, et al. Relevance of subcortical visual pathways disruption to visual symptoms in dementia with Lewy bodies. Cortex: A Journal Devoted to the Study of the Nervous System & Behavior. 2014;59:12-21.
205. Delli Pizzi S, Franciotti R, Taylor JP, Thomas A, Tartaro A, Onofrj M, et al. Thalamic involvement in fluctuating cognition in dementia with lewy bodies: Magnetic resonance evidences. Cereb Cortex. 2015;25(10):3682-9.
206. Agosta F, Kostic VS, Davidovic K, Kresojevic N, Sarro L, Svetel M, et al. White matter abnormalities in Parkinson's disease patients with glucocerebrosidase gene mutations. Movement Disorders. 2013;28(6):772-8.
207. Youn J, Lee J-M, Kwon H, Kim JS, Son TO, Cho JW. Alterations of mean diffusivity of pedunculopontine nucleus pathway in Parkinson's disease patients with freezing of gait. Parkinsonism & Related Disorders. 2015;21(1):12-7.
208. Zhang Y, Huang B, Chen Q, Wang L, Zhang L, Nie K, et al. Altered microstructural properties of superficial white matter in patients with Parkinson's disease. Brain Imaging & Behavior. 2022;16(1):476-91.
209. Bingbing G, Yujing Z, Yanwei M, Chunbo D, Weiwei W, Shiyun T, et al. Diffusion Kurtosis Imaging of Microstructural Changes in Gray Matter Nucleus in Parkinson Disease. Front Neurol. 2020;11:252.

210. Surova Y, Lampinen B, Nilsson M, Latt J, Hall S, Widner H, et al. Alterations of Diffusion Kurtosis and Neurite Density Measures in Deep Grey Matter and White Matter in Parkinson's Disease. PLoS ONE [Electronic Resource]. 2016;11(6):e0157755.
211. Surova Y, Nilsson M, Lampinen B, Latt J, Hall S, Widner H, et al. Alteration of putaminal fractional anisotropy in Parkinson's disease: a longitudinal diffusion kurtosis imaging study. Neuroradiology. 2018;60(3):247-54.
212. Tang X, Zhang Y, Liu D, Hu Y, Jiang L, Zhang J. Association of Gyrification Pattern, White Matter Changes, and Phenotypic Profile in Patients With Parkinson Disease. Neurology. 2021;96(19):e2387-e94.
213. Guimaraes RP, Campos BM, de Rezende TJ, Piovesana L, Azevedo PC, Amato-Filho AC, et al. Is Diffusion Tensor Imaging a Good Biomarker for Early Parkinson's Disease? Front Neurol. 2018;9:626.
214. Duncan GW, Firbank MJ, Yarnall AJ, Khoo TK, Brooks DJ, Barker RA, et al. Gray and white matter imaging: A biomarker for cognitive impairment in early Parkinson's disease? Movement Disorders. 2016;31(1):103-10.
215. Lucas-Jimenez O, Diez-Cirarda M, Ojeda N, Pena J, Cabrera-Zubizarreta A, Ibarretxe-Bilbao N. Verbal memory in Parkinson's disease: A combined DTI and fMRI study. Journal of Parkinson's Disease. 2015;5(4):793-804.
216. Nazmuddin M, van Dalen J-W, Borra RJH, Stormezand GN, van der Horn HJ, van der Zee S, et al. Postural and gait symptoms in de novo Parkinson's disease patients correlate with cholinergic white matter pathology. Parkinsonism & Related Disorders. 2021;93:43-9.
217. Theilmann RJ, Reed JD, Song DD, Huang MX, Lee RR, Litvan I, et al. White-matter changes correlate with cognitive functioning in Parkinson's disease. Front Neurol. 2013;4:37.
218. Matsui H, Nishinaka K, Oda M, Niikawa H, Komatsu K, Kubori T, et al. Wisconsin Card Sorting Test in Parkinson's disease: Diffusion tensor imaging. Acta Neurologica Scandinavica. 2007;116(2):108-12.
219. Chen YS, Chen MH, Lu CH, Chen PC, Chen HL, Yang IH, et al. Associations among cognitive functions, plasma DNA, and white matter integrity in patients with early-onset Parkinson's disease. Front Neurosci. 2017;11(JAN).
220. Peterson DS, Smulders K, Mancini M, Nutt JG, Horak FB, Fling BW. Relating Response Inhibition, Brain Connectivity, and Freezing of Gait in People with Parkinson's Disease. J Int Neuropsychol Soc. 2021;27(7):733-43.
221. Jalakas M, Palmqvist S, Hall S, Svärd D, Lindberg O, Pereira JB, et al. A quick test of cognitive speed can predict development of dementia in Parkinson’s disease. Sci Rep. 2019;9(1).
222. Di Tella S, Baglio F, Pelizzari L, Cabinio M, Nemni R, Traficante D, et al. Uncinate fasciculus and word selection processing in Parkinson's disease. Neuropsychologia Vol 146 2020, ArtID 107504. 2020;146.
223. Yang Q, Nanivadekar S, Taylor PA, Dou Z, Lungu CI, Horovitz SG. Executive function network's white matter alterations relate to Parkinson's disease motor phenotype. Neurosci Lett. 2021;741:135486.
224. Bertrand JA, Bedetti C, Postuma RB, Monchi O, Genier Marchand D, Jubault T, et al. Color discrimination deficits in Parkinson's disease are related to cognitive impairment and white-matter alterations. Mov Disord. 2012;27(14):1781-8.

225. Lorio S, Sambataro F, Bertolino A, Draganski B, Dukart J. The Combination of DAT-SPECT, Structural and Diffusion MRI Predicts Clinical Progression in Parkinson's Disease. Front Aging Neurosci. 2019;11:57.
226. Lenfeldt N, Hansson W, Larsson A, Nyberg L, Birgander R, Forsgren L. Diffusion tensor imaging and correlations to Parkinson rating scales. J Neurol. 2013;260(11):2823-30.
227. Taylor KI, Sambataro F, Boess F, Bertolino A, Dukart J. Progressive decline in gray and white matter integrity in de novo Parkinson's Disease: An analysis of longitudinal parkinson progression markers initiative diffusion tensor imaging data. Frontiers in Aging Neuroscience Vol 10 2018, ArtID 318. 2018;10.
228. Baggio HC, Segura B, Ibarretxe-Bilbao N, Valldeoriola F, Marti MJ, Compta Y, et al. Structural correlates of facial emotion recognition deficits in Parkinson's disease patients. Neuropsychologia. 2012;50(8):2121-8.
229. Chiang PL, Chen HL, Lu CH, Chen PC, Chen MH, Yang IH, et al. White matter damage and systemic inflammation in Parkinson's disease. BMC Neurosci. 2017;18(1):48.
230. Yuki N, Yoshioka A, Mizuhara R, Kimura T. Visual hallucinations and inferior longitudinal fasciculus in Parkinson's disease. Brain Behav. 2020;10(12).
231. Gan C, Wang L, Ji M, Ma K, Sun H, Zhang K, et al. Abnormal interhemispheric resting state functional connectivity in Parkinson's disease patients with impulse control disorders. NPJ Parkinsons Dis. 2021;7(1):60.
232. Ibarretxe-Bilbao N, Junque C, Marti MJ, Valldeoriola F, Vendrell P, Bargallo N, et al. Olfactory impairment in Parkinson's disease and white matter abnormalities in central olfactory areas: A voxel-based diffusion tensor imaging study. Movement Disorders. 2010;25(12):1888-94.
233. Wen MC, Xu Z, Lu Z, Chan LL, Tan EK, Tan LCS. Microstructural network alterations of olfactory dysfunction in newly diagnosed Parkinson's disease. Sci Rep. 2017;7(1).
234. Haehner A, Schopf V, Loureiro A, Linn J, Reichmann H, Hummel T, et al. Substantia nigra fractional anisotropy changes confirm the PD at-risk status of patients with idiopathic smell loss. Parkinsonism & Related Disorders. 2018;50:113-6.
235. Hummel T, Haehner A, Thaploo D, Georgiopoulos C, Falkenburger B, Whitcroft K. Advancement of pd is reflected by white matter changes in olfactory areas: A pilot study. Medicina. 2021;57(11).
236. Scherfler C, Esterhammer R, Nocker M, Mahlknecht P, Stockner H, Warwitz B, et al. Correlation of dopaminergic terminal dysfunction and microstructural abnormalities of the basal ganglia and the olfactory tract in Parkinson's disease. Brain: A Journal of Neurology. 2013;136(10):3028-37.
237. Georgiopoulos C, Warntjes M, Dizdar N, Zachrisson H, Engström M, Haller S, et al. Olfactory impairment in Parkinson's disease studied with diffusion tensor and magnetization transfer imaging. Journal of Parkinson's Disease. 2017;7(2):301-11.
238. Roy HA, Griffiths DJ, Aziz TZ, Green AL, Menke RAL. Investigation of urinary storage symptoms in Parkinson's disease utilizing structural MRI techniques. Neurourol Urodyn. 2019;38(4):1168-75.
239. Polli A, Weis L, Biundo R, Thacker M, Turolla A, Koutsikos K, et al. Anatomical and functional correlates of persistent pain in Parkinson's disease. Movement Disorders. 2016;31(12):1854-64.

240. Chen MH, Chen PC, Lu CH, Chen HL, Chao YP, Li SH, et al. Plasma DNA Mediate Autonomic Dysfunctions and White Matter Injuries in Patients with Parkinson's Disease. Oxidative Med Cell Longevity. 2017;2017.

Appendix A

Table A1: DTI literature on cognitive impairment in PD.

Cognitive Impairment							
Measure	Author	Groups	Regions Analyzed	FA	FA-Location	MD	MD-Location
Global Cognition – Group Comparisons							
PD-MCI (vs. HC)	Melzer (2013)(67)	28 PD-MCI, 32 HC	Whole-brain WM	↓	Entire WM^{avg}, ATR^{b}, CC^{b} (body, genu, and splenium), cerebral peduncle^{b}, CB^{b} (at CG and hippocampus), CR^{b} (anterior, posterior, and superior), CST^{b}, EC^{b}, IC^{b} (anterior and posterior limb), IFOF^{b}, ILF^{b}, medial lemniscus^{l}, SCP^{b}, SLF^{b}, UF^{b}	↑	Entire WM^{avg}, ATR^{b}, CC^{b} (body, genu, and splenium), cerebral peduncle^{l}, CB^{b} (at CG), CR^{b} (anterior, posterior, and superior), CST^{b}, EC^{b}, IC^{b} (anterior and posterior limb), IFOF^{b}, ILF^{b}, SLF^{b}, UF^{l}
	Galantucci (2017)(68)	54 PD-MCI, 41 HC		↓	Entire brain^{avg}, associative frontoparietal tracts^{b}, CC^{b} (genu and anterior), WM^{b} (frontal, parietal, and temporal), WM networks (connections between brainstem^{r}, caudate^{b}, frontal pole^{r}, frontotemporoparietal regions^{r}, fusiform gyrus^{l}, GP^{l}, IFG-pars orbitalis^{r}, insula^{r}, IPG^{r}, OFC^{r} (lateral), temporal gyrus^{r} (middle), paracentral gyrus^{r}, putamen^{r}, MFG^{r} (rostral), superior parietal gyrus^{r}, temporal pole^{l}, temporoparietooccipital regions^{l}, thalamus^{b})	↑	Entire brain^{avg}, associative frontoparietal tracts^{b}, CC^{b} (genu and anterior), WM^{b} (frontal, parietal, temporal, midbrain, pontine), WM networks (connections between BG^{l}, caudate^{r}, frontal lobe^{r} [orbital and lateral], insula^{l}, occipital lobe^{b}, pallidum^{b}, parietal lobe^{b}, precentral gyrus^{l}, putamen^{r}, thalamus^{r})
	Minett (2018)(51)	27 PD-MCI, 48 HC		↓	CB^{uns}, CST^{uns}, FMa^{uns}, IFOF^{uns}, SFOF^{uns}	↑	CC^{b}, CB^{b},CR^{b}, EC^{b}, FMi^{b}, IC^{b}, IFOF^{b}, ILF^{b}, SFOF^{b}, SLF^{b}
	Gorges (2019)(69)	67 PD-MCI, 72 HC		↓	CC^{uns}, CB^{uns}, CR^{uns} (anterior and superior), CST^{uns}, fasciculi^{uns} (anterior, inferior, and superior), insular connections^{uns}, striatum^{uns}, thalamus^{uns}	↑	CC^{uns}, thalamus^{uns}
	Inguanzo(a) (2021)(70)	27 PD-MCI, 51 HC		↓	CST^{l}, FMa^{l},IFOF^{l}, ILF^{l}, SLF^{l}	n.s.	-
	Hattori (2012)(71)	28 PD-MCI, 40 HC		↓	CC^{uns}, CB^{uns}, IFOF^{uns}, ILF^{uns}, SLF^{uns}, UF^{uns}	N/A	-
	Deng (2013)(72)	30 PD-MCI, 21 HC	CB, CC, CST, frontal WM, occipital WM, parietal WM, SLF, temporal WM	↓	CB^{r} (anterior), frontal WM^{l}, temporal WM^{r}	N/A	-
	Hanganu (2018)(194)	19 PD-MCI, 16 HC	BG tracts, frontal WM, thalamic tracts	n.s.	-	N/A	-
	Garcia-Diaz (2018)(195)	10 PD-MCI, 20 HC	Whole-brain WM	?	CC^{r} (posterior)	N/A	-
PD-MCI (vs. PD-CogU)	Melzer (2013)(67)	28 PD-MCI, 63 PD-CogU	Whole-brain WM	↓	Entire WM^{avg}, and CC (body^{r} and genu^{b}), EC^{r}, IC^{b} (anterior limb)	↑	Entire WM^{avg}, CR^{l} (anterior and superior), EC^{b} , IC^{b} (anterior limb), IFOF^{l}, SLF^{l}, UF^{b}
	Galantucci (2017)(68)	54 PD-MCI, 116 PD-CogU		↓	WM networks (connections between BG^{r}, WM^{b} [frontal, parietal, temporal], thalamus^{l})	n.s.	-
	Gorges (2019)(69)	67 PD-MCI, 56 PD-CogU		↓	ILF^{uns}	n.s.	-
	Deng (2013)(72)	30 PD-MCI, 24 PD-CogU	CB, CC, CST, frontal WM, occipital WM, parietal WM, SLF, temporal WM	↓	CB^{l} (anterior), temporal WM^{r}	N/A	-
	Minett (2018)(51)	27 PD-MCI, 93 PD-CogU	Whole-brain WM	n.s.	-	↑	Frontal lobe^{b}
	Bledsoe (2018)(79)	35 PD-MCI, 23 PD-CogU	CC	n.s.	-	n.s.	-

Table A1: DTI literature on cognitive impairment in PD.

Cognitive Impairment							
Measure	Author	Groups	Regions Analyzed	FA	FA-Location	MD	MD-Location
	Inguanzo(a) (2021)(70)	27 PD-MCI, 35 PD-CogU	Whole-brain WM	n.s.	-	n.s.	-
	Hattori (2012)(71)	28 PD-MCI, 32 PD-CogU		n.s.	-	N/A	-
	Rossi (2014)(196)	Numbers unspecified		n.s.	-	N/A	-
	Hanganu (2018)(194)	19 PD-MCI, 16 PD-CogU	BG tracts, frontal WM, thalamic tracts	n.s.	-	N/A	-
	Garcia-Diaz (2018)(195)	10 PD-MCI, 26 PD-CogU	Whole-brain WM	?	CC^{r} (posterior)	N/A	-
PD with amnestic MCI (vs. PD-CogU)	Chen (2019)(197)	17 PD with amnestic MCI, 19 PD-CogU	Whole-brain WM	↓	CC^{b} (body and splenium), CB^{b} (at CG), CR (posterior^{b} and superior^{l}), fornix^{l} (crux), $IFOF^{b}$, ILF^{b}, PTR^{b}, SLF^{b}, tapetum^{b}	N/A	-
PD with MCI earlier (vs. PD-CogU)	Shin (2016)(198)	16 PD with MCI earlier, 15 PD-CogU	Whole-brain WM	n.s.	-	↑	CC^{uns} (body and genu), CB^{r}, CR^{b} (anterior and superior), SLF^{r}
PD with MCI later (vs. PD-CogU)	Shin (2016)(198)	43 PD with MCI later, 15 PD-CogU	Whole-brain WM	n.s.	-	n.s.	-
PD with MCI earlier (vs. PD with MCI later)	Shin (2016)(198)	16 PD with MCI earlier, 43 PD with MCI later	Whole-brain WM	↓	CST^{uns}, SLF^{r}	↑	CC^{uns} (body and genu), CB^{r}, CR^{b}, IC^{r} (anterior and posterior limbs), SLF^{b}
PD with Frontostriatal MCI (vs. PD-CogU)	Devignes (2021)(96)	16 PD with Frontostriatal MCI, 41 PD-CogU	Whole-brain WM	n.s.	-	n.s.	-
PD with Posterior Cortical MCI (vs. PD-CogU)	Devignes (2021)(96)	25 PD with Posterior Cortical MCI, 41 PD-CogU	Whole-brain WM	↓	$IFOF^{r}$, tract from isthmus to parieto-temporal cortex^{l}	n.s.	-
PD with Posterior Cortical MCI (vs. PD with Frontostriatal MCI)	Devignes (2021)(96)	25 PD with Posterior Cortical MCI, 16 PD with Frontostriatal MCI	Whole-brain WM	n.s.	-	n.s.	-
PD with Mixed MCI (vs. PD-CogU)	Devignes (2021)(96)	32 PD with Mixed MCI, 41 PD-CogU	Whole-brain WM	↓	$IFOF^{r}$, striato-parietal tract^{l}, tract from CC (genu) to frontal cortex^{r}, tract from isthmus to parieto-temporal cortex^{l}	↑	Tract from CC (posterior midbody) to postcentral cortex^{l}
PD with Mixed MCI (vs. PD with Frontostriatal MCI)	Devignes (2021)(96)	32 PD with Mixed MCI, 16 PD with Frontostriatal MCI	Whole-brain WM	n.s.	-	n.s.	-
PD with Mixed MCI (vs. PD with Posterior Cortical MCI)	Devignes (2021)(96)	32 PD with Mixed MCI, 25 PD with Posterior Cortical MCI	Whole-brain WM	n.s	-	n.s	-
PD with MoCA <=25 (vs. PD with MoCA >=26)	Schulz (2018)(62)	72 PD with MoCA <=25, 232 PD with MoCA >=26	Amygdala, entorhinal cortex, hippocampus, insula, NBM, primary somatosensory cortex, thalamus	↓	$Amygdala^{avg}$, $hippocampus^{avg}$, $thalamus^{avg}$	↑	$Entorhinal\ cortex^{avg}$, $hippocampus^{avg}$, $insula^{avg}$, NBM^{avg}, $thalamus^{avg}$
PDD (vs. HC)	Kamagata(b) (2013)(73)	20 PDD, 20 HC	Whole-brain WM	↓	CB^{b}, IC^{b} (anterior limb), $IFOF^{b}$, ILF^{b}, SLF^{b}, SN^{b}, UF^{b}	↑	CB^{b}, IC^{b} (anterior and posterior limb), $IFOF^{b}$, ILF^{b}, SLF^{b}, SN^{b}, UF^{b}
	Melzer (2013)(67)	18 PDD, 32 HC		↓	Entire WM^{avg}, ATR^{b}, CC^{b} (body, genu, and splenium), cerebral peduncle^{b}, CB^{l} (at CG and hippocampus), CR^{b} (anterior, posterior, and superior), CST^{b}, EC^{b}, IC^{b} (anterior and posterior limb), ICP^{r},	↑	Entire WM^{avg}, ATR^{b}, CC^{b} (body, genu, and splenium), cerebral peduncle^{r}, CB^{b} (at CG), CR^{b} (anterior, posterior, and superior), CST^{b}, EC^{b}, IC^{b} (anterior and

Table A1: DTI literature on cognitive impairment in PD.

Cognitive Impairment							
Measure	Author	Groups	Regions Analyzed	FA	FA-Location	MD	MD-Location
					IFOF^{b}, ILF^{b}, medial lemniscus^{b}, SCP^{b}, SLF^{b}, UF^{b}		posterior limb), IFOF^{b}, ILF^{b}, SCP^{r}, SLF^{b}, UF^{b}
	Gorges (2019)(69)	11 PDD, 72 HC		↓	CC^{uns}, CB^{uns}, CR^{uns} (anterior and superior), CST^{uns}, fasciculi^{uns} (anterior, inferior, and superior), insular connections^{uns}, striatum^{uns}, thalamus^{uns}	↑	CC^{uns}, CR^{uns} (superior), thalamus^{uns}
	Kamagata (2012)(74)	15 PDD, 15 HC	CB, CST	↓	CB^{avg} (anterior and posterior)	n.s.	-
	Matsui(a) (2007)(75)	11 PDD, 10 HC	CB, frontal WM, occipital WM, parietal WM, temporal WM	↓	CB^{r} (posterior), frontal WM^{l}, occipital WM^{b}, temporal WM^{b}	N/A	-
	Lee (2010)(76)	19 PDD, 18 HC	Whole-brain WM	↓	Cingulate^{b} (anterior and middle), OFC^{b}, parietal WM^{l}, prefrontal WM^{r} (dorsolateral), temporal WM^{l} (anterior)	N/A	-
	Hattori (2012)(71)	25 PDD, 40 HC		↓	CC^{uns}, CB^{uns}, IC^{uns} (anterior limb), IFOF^{uns}, ILF^{uns}, SLF^{uns}, SN^{uns}, UF^{uns}	N/A	-
	Deng (2013)(72)	10 PDD, 21 HC	CB, CC, CST, frontal WM, occipital WM, parietal WM, SLF, temporal WM	↓	CB^{l} (anterior), CC^{uns} (splenium), frontal WM^{l}, temporal WM^{r}	N/A	-
	Chen (2015)(77)	11 PDD, 21 HC	CB, CC, fornix, IFOF, ILF, SFOF, SLF, UF	n.s.	-	↑	CC^{uns} (body and splenium), SFOF^{r}, SLF^{l}, UF^{b}
	Wiltshire (2010)(199)	6 PDD, 15 HC	CB, CC	n.s.	-	n.s.	-
PDD (vs. PD-CogU)	Kamagata(b) (2013)(73)	20 PDD, 20 PD-CogU	Whole-brain WM	↓	CC^{uns} (genu), IFOF^{uns} (anterior)	↑	CC^{uns} (genu), IFOF^{uns} (anterior)
	Melzer (2013)(67)	18 PDD, 63 PD-CogU		↓	Entire WM^{avg}, CR^{r} (superior), CST^{r}	↑	Entire WM^{avg}, ATR^{l}, CC (body^{r} and genu^{b}), CR^{b} (anterior and superior), CST^{r}, EC^{r}, IC (anterior^{b} and posterior^{r} limb), IFOF^{b}, UF^{l}
	Chen (2015)(77)	11 PDD, 19 PD-CogU	CB, CC, fornix, IFOF, ILF, SFOF, SLF, UF	↓	CB^{l} (at hippocampus)	↑	CB^{r} (at CG), ILF^{l}, SFOF^{r}, SLF^{l}, UF^{b}
	Chondrogiorgi (2019)(78)	21 PDD, 40 PD-CogU	Whole-brain WM	↓	ATR^{l}, CC^{uns} (body), CB^{b} (at CG), CR^{b} (anterior and superior), FMi^{l}, IFOF^{l}, UF^{l}	n.s.	-
	Gorges (2019)(69)	11 PDD, 56 PD-CogU	Whole-brain WM	↓	SLF^{uns}	n.s.	-
	Matsui(a) (2007)(75)	11 PDD, 26 PD-CogU	CB, frontal WM, occipital WM, parietal WM, temporal WM	↓	CB^{b} (posterior)	N/A	-
	Hattori (2012)(71)	25 PDD, 32 PD-CogU	Whole-brain WM	↓	CC^{uns}, CB^{uns}, IFOF^{uns}, ILF^{uns}, SLF^{uns}, UF^{uns}	N/A	-
	Deng (2013)(72)	10 PDD, 24 PD-CogU	CB, CC, CST, frontal WM, occipital WM, parietal WM, SLF, temporal WM	↓	CB^{l} (anterior), CC^{uns} (splenium), occipital WM^{l}	N/A	-
	Bledsoe (2018)(79)	17 PDD, 23 PD-CogU	CC	n.s.	-	↑	CC^{uns} (segments 1 and 2)
	Wiltshire (2010)(199)	6 PDD, 29 PD-CogU	CB, CC	n.s.	-	n.s.	-
	Kamagata (2012)(74)	15 PDD, 15 PD-CogU	CB, CST	n.s.	-	n.s.	-
PDD (vs. PD-MCI)	Deng (2013)(72)	10 PDD, 30 PD-MCI	CB, CC, CST, frontal WM, occipital WM, parietal WM, SLF, temporal WM	↓	CB^{l} (anterior), CC^{uns} (splenium)	N/A	-
	Bledsoe (2018)(79)	17 PDD, 35 PD-MCI	CC	n.s.	-	↑	CC^{uns} (segment 1)
	Melzer (2013)(67)	18 PDD, 28 PD-MCI	Whole-brain WM	n.s.	-	n.s.	-

Table A1: DTI literature on cognitive impairment in PD.

Cognitive Impairment							
Measure	Author	Groups	Regions Analyzed	FA	FA-Location	MD	MD-Location
	Hattori (2012)(71)	25 PDD, 28 PD-MCI		n.s.	-	N/A	-
DLB (vs. HC)	Ota (2009)(200)	14 DLB, 13 HC	CC, ILF, visual pathway	↓	ILF^{avg}	↑	ILF^{avg}
	Nicastro (2020)(201)	19 DLB, 20 HC	Whole-brain WM	↓	CC^{uns} (body and splenium), CG^{l}, CR^{r} (anterior and posterior), SLF^{r}	↑	CC^{uns} (body and splenium)
	Lee (2010)(76)	18 DLB, 18 HC		↓	Cingulate^{b}, insula^{b}, OFC^{b}, parietal WM^{l}, prefrontal WM^{r} (dorsolateral), temporal WM^{l}, visual association regions^{b}	N/A	-
	Hattori (2012)(71)	29 DLB, 40 HC		↓	CC^{uns}, CB^{uns}, IFOF^{uns}, ILF^{uns}, SLF^{uns}, UF^{uns}	N/A	-
	Pardini (2020)(202)	18 DLB, 12 HC	CST, nigroputaminal tracts	↑	Nigroputaminal tracts^{avg}	n.s.	-
	Nedelska (2015)(203)	30 DLB, 60 HC	Whole-brain WM	n.s.	-	N/A	-
	Delli Pizzi (2014)(204)	15 DLB, 13 HC	Amygdala, frontal WM, occipital WM, parietal WM, precentral gyrus, premotor cortex, sensory cortex, temporal WM, thalamus	N/A	N/A	↑	Thalamus^{b}
	Delli Pizzi (2015)(205)	16 DLB, 13 HC	Frontal WM, occipital WM, parietal WM, sensorimotor cortex, temporal WM, thalamus	N/A	N/A	↑	Thalamus^{b}
DLB (vs. PDD)	Lee (2010)(76)	18 DLB, 18 HC	Whole-brain WM	↓	Cingulate^{b} (posterior), temporal lobe^{b} (posterior), visual association fibres extending into occipital areas^{b}	N/A	-
	Hattori (2012)(71)	29 DLB, 25 PDD		n.s.	-	N/A	-
Global Cognition – Rating Scales							
Addenbrooke's Cognitive Examination - Total Score	Agosta (2013)(206)	29 PD	CB, CC, CR, EC, IC, olfactory tract, PTR, SLF	n.s.	-	N/A	-
Cambridge Cognitive Examination - Total Score	Jonkman (2021)(109)	53 PD	Tract from insula (dorsal anterior) to ACC	n.s.	-	n.s.	-
	Hepp (2017)(125)	55 PD	Tracts from NBM to occipital lobe, tracts from NBM to parietal lobe	N/A	N/A	n.s.	-
CERAD Total Score	Gorges (2019)(69)	134 PD	Whole-brain WM	⊕	CC^{r} (body), cingulate^{r}, CB^{uns}, CR^{uns} (posterior and superior), CST^{r}, frontal lobe^{r}, IC^{r}, insular cortex^{uns,} pons^{r}, SLF^{uns}, striatum^{r}	⊖	CC^{r}, CST^{r}, IC^{r}, optic tract^{l}
Clinical Dementia Rating - Sum of Boxes	Nedelska (2015)(203)	30 DLB	Whole-brain WM	n.s.	-	N/A	-
Cognitive Status Indicators (1 = PD-cogU, 2 = PD-MCI, and 3 = PDD)	Deng (2013)(72)	24 PD-CogU, 30 PD-MCI, 10 PDD	CB, CC, CST, frontal WM, occipital WM, parietal WM, SLF, temporal WM	⊖	CB^{b}, CC^{uns} (splenium), frontal WM^{l}, occipital WM^{l}, temporal WM^{r}	N/A	-
Cumming's Neuropsychiatric Inventory	Inguanzo(a) (2021)(70)	62 PD	Global mean FA	n.s.	-	N/A	-
Global Cognition Composite Score	Melzer (2013)(67)	109 PD	Whole-brain WM	n.s.	-	⊖	ATR^{b}, CC^{b} (body and genu), CB^{l} (at CG), CR^{b} (anterior and superior),

Table A1: DTI literature on cognitive impairment in PD.

Cognitive Impairment							
Measure	Author	Groups	Regions Analyzed	FA	FA-Location	MD	MD-Location
							EC^{b}, IC^{b} (anterior and posterior limb), IFOF^{b}, ILF^{r}, SLF^{r}, UF^{b}
	Koshimori (2015)(98)	26 PD		N/A	N/A	⊖	Frontal lobe^{uns}, temporal lobe^{uns}
Hasegawa's Dementia Scale - Revised	Matsui(a) (2007)(75)	37 PD	CB, frontal WM, occipital WM, parietal WM, temporal WM	⊕	CB^{l} (posterior)	N/A	-
Investigator Diagnosis	Caspell-Garcia (2017)(83)	423 PD	Cortical GM, whole-brain WM	n.s.	-	⊖	ICP^{avg}
Mattis Dementia Rating Scale - Total Score	Matsui(a) (2007)(75)	37 PD	CB, frontal WM, occipital WM, parietal WM, temporal WM	⊕	CB^{l} (posterior)	N/A	-
	Nedelska (2015)(203)	30 DLB	Whole-brain WM	n.s.	-	N/A	-
MMSE	Youn (2015)(207)	42 PD	PPN	⊖	PPN^{l}	⊕	PPN^{l}
	Liu (2022)(87)	41 PD	BG, cerebellum, red nucleus, SN, subthalamic nucleus, thalamus	⊕	Cerebellum^{uns}	⊖	Cerebellum^{l}
	Kamagata (2012)(74)	15 PDD	CB, CST	⊕	CB^{avg} (anterior)	n.s.	-
	Kamagata(b) (2013)(73)	40 PD	Whole-brain WM	⊕	CC^{b} (genu) IFOF^{uns} (anterior), SLF (anterior^{r} and posterior^{l})	n.s.	-
	Matsui(a) (2007)(75)	37 PD	CB, frontal WM, occipital WM, parietal WM, temporal WM	⊕	CB^{l} (posterior)	N/A	-
	Zhang (2022)(208)	34 PD	Bundles connecting the posterior parietal cortex	⊕	Bundles^{uns} connecting the posterior parietal cortex	N/A	-
	Hattori (2012)(71)	32 PD-CogU	Whole-brain WM	?	CC^{uns}, CB^{uns}, IFOF^{uns}, ILF^{uns}, SLF^{uns}, UF^{uns}	N/A	-
		85 PD + 29 DLB combined		?	CC^{uns}, CB^{uns}, IFOF^{uns}, ILF^{uns}, parietal WM^{b}, SLF^{uns}, UF^{uns}	N/A	-
	Wiltshire (2010)(199)	35 PD	CB, CC	n.s.	-	⊖	CC^{uns} (all regions)
	Guttuso (2018)(84)	19 PD	CB, CC, fornix, frontal WM, occipital WM, parietal WM, SN, temporal WM, thalamus	n.s.	-	⊖	Temporal WM^{b}
	Bingbing (2020)(209)	35 PD	BG, red nucleus, SN, thalamus	n.s.	-	⊖	Caudate^{avg} (head), thalamus^{avg}
	Lim (2016)(119)	38 PD	PPN, thalamus	n.s.	-	n.s.	-
	Lu^{a} (2016)(64)	126 PD	Whole-brain GM	n.s.	-	n.s.	-
	Surova (2016)(210)	105 PD	BG, brainstem, CB, CC, CST, fornix, IFOF, ILF, SLF, SN, thalamus, UF	n.s.	-	n.s.	-
	Surova (2018)(211)	76 PD	BG, thalamus, whole-brain WM	n.s.	-	n.s.	-
	Gargouri (2019)(108)	52 PD	Basal forebrain, fornix	n.s.	-	n.s.	-
	Wu (2020)(122)	39 PD	CC	n.s.	-	n.s.	-
	Minett (2018)(51)	93 PD-CogU	Whole-brain WM	n.s.	-	n.s.	-
		27 PD-MCI		n.s.	-	n.s.	-
	Agosta (2013)(206)	29 PD	CB, CC, CR, EC, IC, olfactory tract, PTR, SLF	n.s.	-	N/A	-
	Huang (2014)(103)	15 PD with Depression	Whole-brain WM	n.s.	-	N/A	-

Table A1: DTI literature on cognitive impairment in PD.

Cognitive Impairment							
Measure	Author	Groups	Regions Analyzed	FA	FA-Location	MD	MD-Location
	Nedelska (2015)(203)	30 DLB		n.s.	-	N/A	-
	Wei (2016)(121)	43 PD	BG, frontal WM, hippocampus, occipital WM, parietal WM, SN, temporal WM	n.s.	-	N/A	-
	Wu (2018)(105)	31 PD with Depression	Whole-brain WM	n.s.	-	N/A	-
	Inguanzo(a) (2021)(70)	62 PD	Global mean FA	n.s.	-	N/A	-
	Tang (2021)(212)	90 PD	Whole-brain WM	n.s.	-	N/A	-
MoCA	Chen (2015)(77)	30 PD	CB, CC, fornix, IFOF, ILF, SFOF, SLF, UF	⊕	CB^{l} (at hippocampus), SLF^{b}	⊖	ILF^{l}, SLF^{l}, UF^{r}
	Liu (2022)(87)	41 PD	BG, cerebellum, red nucleus, SN, subthalamic nucleus, thalamus	⊕	$Cerebellum^{uns}$	⊖	$Cerebellum^{uns}$
	Guttuso (2018)(84)	19 PD	CB, CC, fornix, frontal WM, occipital WM, parietal WM, SN, temporal WM, thalamus	n.s.	-	⊖	Temporal WM^{b}
	Abbasi (2020)(80)	144 PD	BG, frontal lobe, precentral gyrus, postcentral gyrus, temporal lobe, lateral occipital gyrus	n.s.	-	⊖	GP^{b}
	Langley (2016)(85)	20 PD	SN	n.s.	-	n.s.	-
	Caspell-Garcia (2017)(83)	423 PD	Cortical GM, whole-brain WM	n.s.	-	n.s.	-
	Arribarat (2019)(81)	18 PD	SN	n.s.	-	n.s.	-
	Pelizzari (2019)(88)	26 PD	BG, red nucleus, SN, subthalamic nucleus, thalamus	n.s.	-	n.s.	-
	Le (2020)(86)	23 PD	BG, SN, thalamus	n.s.	-	n.s.	-
	Surkont (2021)(91)	21 PD with Gait Impairment	BG, mesencephalic locomotion center, thalamus	n.s.	-	n.s.	-
	Zhang (2016)(93)	122 PD	Midbrain, SN, thalamus	n.s.	-	N/A	-
	Wen (2018)(92)	65 PD	ATR, CB, CC, CR, CST, EC, FMa, FMi, fornix, IFOF, ILF, IC, sagittal stratum, SLF, UF	n.s.	-	N/A	-
	Baumeister (2019)(82)	29 PD	Arcuate fasciculus, ATR, CB, CC, CST, IFOF, ILF, SLF, UF	n.s.	-	N/A	-
	Sampedro (2019)(89)	64 PD	Frontal cortex, occipital cortex	N/A	-	n.s.	-
	Sampedro (2020)(90)	133 PD	Cortical GM	N/A	-	n.s.	-
PD-CRS Total Score	Chondrogiorgi (2019)(78)	61 PD	Whole-brain WM	⊕	CC^{uns} (body, genu, and splenium), CB^{b} (at CG and hippocampus), CR^{b} (anterior, posterior, and superior), FMa^{uns}, FMi^{uns}, $IFOF^{b}$, ILF^{b}, SLF^{b}, UF^{b}	⊕	ATR^{b}, CC^{uns} (body, genu, and splenium), CB^{b} (at CG), CR^{b} (anterior, posterior, and superior), CST^{b}, FMa^{uns}, fornix (cres)/stria terminalis^{b}, IC^{l} (anterior, posterior, and retrolenticular), ICP^{b}, $IFOF^{b}$, ILF^{b}, MCP^{b}, medial lemniscus^{b}, SLF^{b}
	Grothe (2021)(54)	73 PD	Basal forebrain, hippocampus	N/A	N/A	⊖	$Hippocampus^{avg}$

Table A1: DTI literature on cognitive impairment in PD.

Cognitive Impairment							
Measure	Author	Groups	Regions Analyzed	FA	FA-Location	MD	MD-Location
Scales for Outcomes in PD - Cognition	Guimaraes (2018)(213)	132 PD	CB, CC, CST	⊕	CB^{avg}	N/A	-
Test-based Cognitive Impairment	Caspell-Garcia (2017)(83)	423 PD	Cortical GM, whole-brain WM	n.s.	-	n.s.	-
UPDRS-I - Cognitive Impairment	Andica (2019)(52)	20 PD	Whole-brain WM and GM	n.s.	-	n.s.	-
Memory							
Memory (Mattis Dementia Rating Scale)	Matsui(a) (2007)(75)	37 PD	CB, frontal WM, occipital WM, parietal WM, temporal WM	⊕	CB^{l} (posterior)	N/A	-
Memory Composite	Bledsoe (2018)(79)	75 PD	CC	⊕	CC^{uns} (segment 5)	⊖	CC^{uns} (segment 1)
	Melzer (2013)(67)	109 PD	Whole-brain WM	n.s.	-	⊖	ATR^{b}, CC (body^{l} and genu^{b}), CR^{b} (anterior and superior), CST^{b}, EC^{b}, IC^{b} (anterior and posterior limb), IFOF^{b}, SLF^{r}, UF^{b}
	Minett (2018)(51)	93 PD-CogU		n.s.	-	n.s.	-
		27 PD-MCI		n.s.	-	n.s.	-
Memory Composite: Long-Term Memory	Zheng (2014)(94)	16 PD	Whole-brain WM	n.s.	-	⊖	CR^{r} (anterior)
Memory Composite: Short-Term Memory	Zheng (2014)(94)	16 PD	Whole-brain WM	n.s.	-	⊖	Fornix^{uns}
Delayed Free Recall (FCSRT)	Gargouri (2019)(108)	52 PD	Basal forebrain, fornix	n.s.	-	n.s.	-
Delayed Memory (RBANS)	Chen (2019)(197)	36 PD	Whole-brain WM	⊕	CC^{b} (body and splenium), CB^{b} (at CG), CR (posterior^{b} and superior^{l}), fornix^{l}, PTR^{r}, SLF^{r}, tapetum^{b}	N/A	-
Delayed Recall (15-Word List)	Carlesimo (2012)(39)	25 PD	Hippocampus	N/A	N/A	⊖	Hippocampus^{b}
Delayed Recall (Alzheimer's Disease Assessment Scale-Cognitive Subscale)	Surova (2016)(210)	105 PD	BG, brainstem, CB, CC, CST, fornix, IFOF, ILF, SLF, SN, thalamus, UF	n.s.	-	⊕	SLF^{avg}
Delayed Recall	Lenka (2020)(126)	42 PD with Psychosis	CC, CST, IFOF, ILF, occipitoparietal WM	⊕	IFOF^{l}, ILF^{l}	N/A	-
	Auning (2014)(95)	18 PD	Entorhinal WM, parahippocampal WM	n.s.	-	N/A	-
	Inguanzo(a) (2021)(70)	62 PD	Global mean FA	n.s.	-	N/A	-
Delayed Recall (RCFT)	Lenka (2020)(126)	42 PD with Psychosis	CC, CST, IFOF, ILF, occipitoparietal WM	n.s.	-	N/A	-
Delayed Verbal Memory (PD-CRS)	Chondrogiorgi (2019)(78)	61 PD	Whole-brain WM	n.s.	-	n.s.	-
	Grothe (2021)(54)	73 PD	Basal forebrain, hippocampus	N/A	N/A	⊖	Hippocampus^{avg}
Delayed Word List Recall (CERAD)	Gorges (2019)(69)	134 PD	Whole-brain WM	n.s.	-	n.s.	-
Immediate Free Recall (FCSRT)	Gargouri (2019)(108)	52 PD	Basal forebrain, fornix	n.s.	-	n.s.	-
Immediate Memory (RBANS)	Chen (2019)(197)	36 PD	Whole-brain WM	n.s.	-	N/A	-
Immediate Recall (15-Word List)	Carlesimo (2012)(39)	25 PD	Hippocampus	N/A	N/A	⊖	Hippocampus^{r}

Table A1: DTI literature on cognitive impairment in PD.

Cognitive Impairment							
Measure	Author	Groups	Regions Analyzed	FA	FA-Location	MD	MD-Location
Immediate Verbal Memory (PD-CRS)	Chondrogiorgi (2019)(78)	61 PD	Whole-brain WM	⊕	ATR^{b}, CC^{uns} (genu, body, and splenium), cerebral peduncle^{b}, CB^{l} (at CG), CR^{b} (anterior, posterior, and superior), CST^{b}, EC^{b}, FMa^{uns}, FMi^{uns}, fornix (cres)/stria terminalis^{b}, IC^{b} (anterior, posterior, and retrolenticular), ICP^{b}, IFOF^{b}, ILF^{b}, MCP^{b}, PTR^{b}, SCP^{b}, SLF^{b}, UF^{b}	n.s.	-
	Grothe (2021)(54)	73 PD	Basal forebrain, hippocampus	N/A	N/A	n.s.	-
Paired Associates Learning (CANTAB)	Duncan (2016)(214)	125 PD	Whole-brain WM	n.s.	-	n.s.	-
	Yao (2016)(59)	12 PD with VH	Hippocampus	N/A	N/A	n.s.	-
Pattern Recognition Memory	Jonkman (2021)(109)	53 PD	Tract from insula (dorsal anterior) to ACC	n.s.	-	n.s.	-
Pattern Recognition Memory (CANTAB)	Duncan (2016)(214)	125 PD	Whole-brain WM	n.s.	-	n.s.	-
Recognition Abilities (RAVLT)	Inguanzo(a) (2021)(70)	62 PD	Global mean FA	n.s.	-	N/A	-
Spatial Recognition Memory (CANTAB)	Duncan (2016)(214)	125 PD	Whole-brain WM	n.s.	-	n.s.	-
Spatial Span	Jonkman (2021)(109)	53 PD	Tract from insula (dorsal anterior) to ACC	n.s.	-	⊖	Tract from insula (dorsal anterior) to ACC^{b}
Total Free Recall (FCSRT)	Gargouri (2019)(108)	52 PD	Basal forebrain, fornix	⊕	Fornix^{avg}	⊖	Basal forebrain^{avg} (ch1-ch2)
Total Learning Recall (RAVLT)	Inguanzo(a) (2021)(70)	62 PD	Global mean FA	n.s.	-	N/A	N/A
Total Recall (FCSRT)	Gargouri (2019)(108)	52 PD	Basal forebrain, fornix	n.s.	-	n.s.	-
Verbal Learning (Hopkins Verbal Learning Test-Revised)	Devignes (2021)(96)	114 PD	Whole-brain WM	n.s.	-	n.s.	-
Verbal Learning (Hopkins Verbal Learning Test)	Sampedro (2019)(89)	64 PD	Frontal cortex, occipital cortex	N/A	N/A	n.s.	-
	Sampedro (2020)(90)	133 PD	Cortical GM	N/A	N/A	n.s.	-
Verbal Memory (fMRI Paradigm)	Lucas-Jiménez (2015)(215)	37 PD	CB, UF	n.s.	-	N/A	N/A
Word List Learning (CERAD)	Gorges (2019)(69)	134 PD	Whole-brain WM	n.s.	-	n.s.	-
Attention/Working Memory							
Attention (Mattis Dementia Rating Scale)	Matsui(a) (2007)(75)	37 PD	CB, frontal WM, occipital WM, parietal WM, temporal WM	⊕	CB^{r} (posterior)	N/A	N/A
Attention (RBANS)	Chen (2019)(197)	36 PD	Whole-brain WM	⊕	CC^{r} (splenium), CR^{r} (posterior)	N/A	N/A
Attention Composite	Zheng (2014)(94)	16 PD	Whole-brain WM	⊕	CB^{b} (at CG), IC^{l} (retrolenticular), PTR^{b}, sagittal stratum^{l}, SFOF^{b}	⊖	CC^{uns} (splenium), CB^{l} (at CG and hippocampus), CR (anterior^{r}, posterior^{b}, and superior^{b}), CST^{l}, IC^{l} (anterior limb and retrolenticular), PTR^{l}, sagittal stratum^{l}, SFOF^{b}
	Nazmuddin (2021)(216)	98 PD	NBM-associated WM tract	⊕	NBM-associated WM tract^{b}	n.s.	-

Table A1: DTI literature on cognitive impairment in PD.

Cognitive Impairment							
Measure	Author	Groups	Regions Analyzed	FA	FA-Location	MD	MD-Location
	Melzer (2013)(67)	109 PD	Whole-brain WM	?	ATR^{r}, CC^{r} (body), CR^{r} (anterior and superior), CST^{r}, EC^{r}, IFOF^{r}, ILF^{r}, SLF^{r}, UF^{b}	?	ATR^{b}, CC^{b} (body and genu), CB^{l} (at CG), CR (anterior^{b}, posterior^{r}, and superior^{b}), CST^{b}, EC^{b}, IC^{b} (anterior and posterior limb), IFOF^{b}, ILF^{r}, SLF^{b}, UF^{b}
	Minett (2018)(51)	27 PD-MCI		n.s.	-	⊖	Entire brain^{avg}
		93 PD-CogU		n.s.	-	n.s.	-
Attention/Memory (NMSS)	Wei (2016)(121)	43 PD	BG, frontal WM, hippocampus, occipital WM, parietal WM, SN, temporal WM	n.s.	-	N/A	N/A
Attention/Working Memory Composite	Bledsoe (2018)(79)	75 PD	CC	⊕	CC^{uns} (segment 1)	⊕	CC^{uns} (segments 4 and 5)
				N/A	N/A	⊖	CC^{uns} (segment 1)
	Devignes (2021)(96)	114 PD	Whole-brain WM	n.s.	-	n.s.	-
Working Memory (PD-CRS)	Chondrogiorgi (2019)(78)	61 PD	Whole-brain WM	⊕	CC^{uns} (body, genu, and splenium), CB^{b} (at CG and hippocampus), CR^{b} (anterior, posterior, and superior), FMa^{uns}, FMi^{uns}, fornix (cres)/stria terminalis^{l}, IFOF^{b}, ILF^{b}, SLF^{b}, UF^{b}	n.s.	-
	Grothe (2021)(54)	73 PD	Basal forebrain, hippocampus	N/A	N/A	⊖	Hippocampus^{avg}
Working Memory - Spatial	Jonkman (2021)(109)	53 PD	Tract from insula (dorsal anterior) to ACC	n.s.	-	⊕	Tract from insula (dorsal anterior) to ACC^{b}
Digit Cancellation Task	Zorzi (2021)(123)	23 DLB	IFOF, ILF, SLF, UF	n.s.	-	⊖	ILF^{r}, SLF^{r}
Digit Span Backward (WAIS-III)	Inguanzo(a) (2021)(70)	62 PD	Global mean FA	n.s.	-	N/A	N/A
	Theilmann (2013)(217)	25 PD	ACC, CC, CR, EC, frontal WM, IC, occipital WM paracentral WM, pars opercularis, pars triangularis, parietal WM, pericalcarine	⊕	CC^{uns} (mid-anterior), CR^{l} (superior), EC^{l}, frontal cortex^{l} (rostral middle), paracentral cortex^{l}	N/A	N/A
Digit Span Forward (WAIS-III)	Inguanzo(a) (2021)(70)	62 PD	Global mean FA	n.s.	-	N/A	N/A
	Theilmann (2013)(217)	25 PD	ACC, CC, CR, EC, frontal WM, IC, occipital WM paracentral WM, pars opercularis, pars triangularis, parietal WM, pericalcarine	⊕	CC^{uns} (mid-anterior), EC^{l}	N/A	N/A
Letter Number Sequencing	Sampedro (2019)(89)	64 PD	Frontal cortex, occipital cortex	N/A	N/A	⊖	Frontal cortex^{l}
	Sampedro (2020)(90)	133 PD	Cortical GM	N/A	N/A	⊖	Parahippocampal-entorhinal cortex^{uns}, temporo-occipital cortex^{avg}
Power of Attention (Cognitive Drug Research Battery)	Duncan (2016)(214)	125 PD	Whole-brain WM	n.s.	-	n.s.	-
Sustained Attention (PD-CRS)	Chondrogiorgi (2019)(78)	61 PD	Whole-brain WM	n.s.	-	n.s.	-
	Grothe (2021)(54)	73 PD	Basal forebrain, hippocampus	N/A	N/A	n.s.	-
TMT-A	Pelizzari (2019)(88)	26 PD	BG, red nucleus, SN, subthalamic nucleus, thalamus	n.s.	-	n.s.	-

Table A1: DTI literature on cognitive impairment in PD.

Cognitive Impairment							
Measure	Author	Groups	Regions Analyzed	FA	FA-Location	MD	MD-Location
	Inguanzo(a) (2021)(70)	62 PD	Global mean FA	n.s.	-	N/A	N/A
Executive Function – Group Comparisons							
PD with Low Categories Achieved (vs. PD with High Categories Achieved)	Matsui(c) (2007)(218)	6 PD with Low Categories Achieved, 15 PD with High Categories Achieved	Frontal WM, occipital WM, parietal WM, temporal WM	↓	Parietal WM^{l}	N/A	N/A
Executive Function – Rating Scales							
Executive Function Composite	Zheng (2014)(94)	16 PD	Whole-brain WM	⊕	CC^{uns} (genu), CR^{r} (anterior), IC^{l} (anterior limb), PTR^{r}	⊖	CC^{uns} (genu), CR (anterior^{b} and posterior^{l}), IC^{l} (anterior limb), sagittal stratum^{l}, SFOF^{l}
	Bledsoe (2018)(79)	75 PD	CC	⊕	CC^{uns} (segment 1)	⊖	CC^{uns} (segment 1)
	Gallagher (2013)(97)	15 PD	Frontal-subcortical WM	⊕	Frontal-subcortical WM^{avg}	n.s.	Frontal-subcortical WM^{avg}
	Minett (2018)(51)	27 PD-MCI	Whole-brain WM	n.s.	-	⊖	Entire brain^{avg}
		93 PD-CogU		n.s.	-	n.s.	-
	Devignes (2021)(96)	114 PD		n.s.	-	n.s.	-
	Auning (2014)(95)	18 PD	MFG WM, orbitofrontal WM	n.s.	-	N/A	N/A
	Lucas-Jiménez (2016)(99)	37 PD	CB, CC, IFOF, ILF	n.s.	-	N/A	N/A
	Melzer (2013)(67)	109 PD	Whole-brain WM	n.s.	-	⊖	ATR^{b}, CC^{b} (body and genu), CR^{b} (anterior, posterior^{r}, and superior), CST^{l}, EC^{b}, IC^{b} (anterior and posterior limb), IFOF^{b}, ILF^{b}, SLF^{r}, UF^{b}
	Koshimori (2015)(98)	26 PD		N/A	N/A	⊖	Frontal lobe^{uns} , temporal lobe^{uns}
Arithmetic (WAIS-III)	Chen(a) (2017)(219)	24 Early-Onset PD	ATR, BG, CST, IFOF, occipital WM, parietal WM, SLF, temporal WM	n.s.	-	⊖	ATR^{r}
Categories Achieved (Wisconsin Card Sorting Test)	Matsui(c) (2007)(218)	21 PD	Frontal WM, occipital WM, parietal WM, temporal WM	⊕	Parietal WM^{l}	N/A	N/A
Color-Word Interference Test (D-KEFS)	Auning (2014)(95)	18 PD	MFG WM, orbitofrontal WM	n.s.	-	N/A	N/A
Controlled Oral Word Association Test	Auning (2014)(95)	18 PD	MFG WM, orbitofrontal WM	n.s.	-	N/A	N/A
Frontal Assessment Battery	Agosta (2013)(206)	29 PD	CB, CC, CR, EC, IC, olfactory tract, PTR, SLF	n.s.	-	N/A	N/A
	Delli Pizzi (2015)(205)	16 DLB	Frontal WM, occipital WM, parietal WM, sensorimotor cortex, temporal WM, thalamus	N/A	N/A	n.s.	-
Initiation/Perseveration (Mattis Dementia Rating Scale)	Matsui(a) (2007)(75)	37 PD	CB, frontal WM, occipital WM, parietal WM, temporal WM	n.s.	-	N/A	N/A
Intra-Extra Dimensional Set Shift Test	Jonkman (2021)(109)	53 PD	Tract from insula (dorsal anterior) to ACC	n.s.	-	n.s.	-
Letter Fluency Test (D-KEFS)	Theilmann (2013)(217)	25 PD	ACC, CC, CR, EC, frontal WM, IC, occipital WM	⊕	ACC^{b} (caudal), CC^{uns} (mid-anterior), CR^{l} (anterior), frontal cortex^{l} (rostral	N/A	N/A

Table A1: DTI literature on cognitive impairment in PD.

Cognitive Impairment							
Measure	Author	Groups	Regions Analyzed	FA	FA-Location	MD	MD-Location
			paracentral WM, pars opercularis, pars triangularis, parietal WM, pericalcarine		middle), paracentral cortex[l], pars opercularis[l]		
Matrix Reasoning (WAIS-III)	Chen(a) (2017)(219)	24 Early-Onset PD	ATR, BG, CST, IFOF, occipital WM, parietal WM, SLF, temporal WM	n.s.	-	n.s.	-
Perseverative Errors of Nelson (Wisconsin Card Sorting Test)	Matsui(c) (2007)(218)	21 PD	Frontal WM, occipital WM, parietal WM, temporal WM	⊖	Parietal WM[l]	N/A	N/A
Stop-Signal Reaction Time	Peterson (2021)(220)	39 PD	IFG, pre-supplementary motor area, subthalamic nucleus	n.s.	-	N/A	N/A
Stroop Color	Inguanzo(a) (2021)(70)	62 PD	Global mean FA	n.s.	-	N/A	N/A
Stroop Denomination Score	Gargouri (2019)(108)	52 PD	Basal forebrain, fornix	n.s.	-	⊖	Basal forebrain[avg] (ch3-ch4)
Stroop Effect Score	Lenka (2020)(126)	42 PD with Psychosis	CC, CST, IFOF, ILF, occipitoparietal WM	⊖	CC[uns], CST[r], IFOF[b], ILF[b], occipitoparietal WM[r]	N/A	N/A
Stroop Interference Score	Gallagher (2013)(97)	15 PD	Frontal-subcortical WM	⊕	Frontal-subcortical WM[avg]	⊖	Frontal-subcortical WM[avg]
	Theilmann (2013)(217)	25 PD	ACC, CC, CR, EC, frontal WM, IC, occipital WM paracentral WM, pars opercularis, pars triangularis, parietal WM, pericalcarine	⊕	EC[l]	N/A	N/A
	Gargouri (2019)(108)	52 PD	Basal forebrain, fornix	n.s.	-	n.s.	-
Stroop Reading Score	Gargouri (2019)(108)	52 PD	Basal forebrain, fornix	n.s.	-	n.s.	-
Stroop Word	Inguanzo(a) (2021)(70)	62 PD	Global mean FA	n.s.	-	N/A	N/A
Stroop Word-Color	Inguanzo(a) (2021)(70)	62 PD	Global mean FA	n.s.	-	N/A	N/A
TMT B-A	Theilmann (2013)(217)	25 PD	ACC, CC, CR, EC, frontal WM, IC, occipital WM paracentral WM, pars opercularis, pars triangularis, parietal WM, pericalcarine	⊖	EC[l], pars triangularis[l], pericalcarine[r]	N/A	N/A
	Gargouri (2019)(108)	52 PD	Basal forebrain, fornix	n.s.	-	n.s.	-
	Inguanzo(a) (2021)(70)	62 PD	Global mean FA	n.s.	-	N/A	N/A
TMT-B	Pelizzari (2019)(88)	26 PD	BG, red nucleus, SN, subthalamic nucleus, thalamus	n.s.	-	n.s.	-
	Auning (2014)(95)	18 PD	MFG WM, orbitofrontal WM	n.s.	-	N/A	N/A
	Lenka (2020)(126)	42 PD with Psychosis	CC, CST, IFOF, ILF, occipitoparietal WM	n.s.	-	N/A	N/A
	Inguanzo(a) (2021)(70)	62 PD	Global mean FA	n.s.	-	N/A	N/A
Tower of London (CANTAB)	Duncan (2016)(214)	125 PD	Whole-brain WM	n.s.	-	⊖	Regions unspecified
Vienna Perseveration Test	Jonkman (2021)(109)	53 PD	Tract from insula (dorsal anterior) to ACC	n.s.	-	n.s.	-

Table A1: DTI literature on cognitive impairment in PD.

Cognitive Impairment							
Measure	Author	Groups	Regions Analyzed	FA	FA-Location	MD	MD-Location
Processing Speed							
Processing Speed Composite	Lucas-Jiménez (2016)(99)	37 PD	CB, CC, IFOF, ILF	n.s.	-	N/A	N/A
Digit Symbol Coding (WAIS-III)	Chen(a) (2017)(219)	24 Early-Onset PD	ATR, BG, CST, IFOF, occipital WM, parietal WM, SLF, temporal WM	n.s.	-	n.s.	-
	Gargouri (2019)(108)	52 PD	Basal forebrain, fornix	n.s.	-	n.s.	-
Quick Test of Cognitive Speed	Surova (2016)(210)	105 PD	BG, brainstem, CB, CC, CST, fornix, IFOF, ILF, SLF, SN, thalamus, UF	n.s.	-	⊕	Putamen^{avg}, SLF^{avg}
	Jalakas (2019)(221)	125 PD	CB, CST, fornix, IFOF, ILF, SLF, UF	N/A	N/A	⊕	CB (dorsal^{b} and ventral^{r}), IFOF^{r}, ILF^{b}
Symbol Digit Modalities Test	Garcia-Diaz (2018)(195)	36 PD	Whole-brain WM	?	FMi^{r}, UF^{r}	N/A	N/A
	Inguanzo(a) (2021)(70)	62 PD	Global mean FA	n.s.	-	N/A	N/A
	Sampedro (2020)(90)	133 PD	Cortical GM	N/A	N/A	⊖	Parahippocampal-entorhinal cortex^{uns}, temporal cortex^{uns} (inferior), temporo-occipital cortex^{uns}
	Sampedro (2019)(89)	64 PD	Frontal cortex, occipital cortex	N/A	N/A	n.s.	-
Verbal/Language – Group Comparisons							
PD with Impaired Semantic Fluency (vs. HC)	Duncan (2016)(214)	19 PD with Impaired Semantic Fluency, 50 HC	Whole-brain WM	n.s.	-	↑	CC^{b}, CB^{b}, CST^{b}, FMi^{b}, IC^{b}., IFOF^{b}, ILF^{b}, SLF^{b}
PD with Impaired Semantic Fluency (vs. PD without Impaired Semantic Fluency)	Duncan (2016)(214)	19 PD with Impaired Semantic Fluency, 106 PD without Impaired Semantic Fluency	Whole-brain WM	n.s.	-	↑	CC^{b}, CB^{b}, CST^{b}, FMi^{b}, IC^{b}., IFOF^{b}, ILF^{b}, SLF^{b}
Verbal/Language – Rating Scales							
Language (RBANS)	Chen (2019)(197)	36 PD	Whole-brain WM	n.s.	-	N/A	N/A
Language Composite	Zheng (2014)(94)	16 PD	Whole-brain WM	⊕	IC^{l} (anterior limb), sagittal stratum^{r}	⊖	CR^{b} (anterior), sagittal stratum^{b}, SFOF^{l}
	Bledsoe (2018)(79)	75 PD	CC	⊕	CC^{uns} (segment 1)	⊖	CC^{uns} (segments 1)
	Minett (2018)(51)	93 PD-CogU	Whole-brain WM	n.s.	-	n.s.	-
		27 PD-MCI		n.s.	-	n.s.	-
Action Verbal Fluency (PD-CRS)	Chondrogiorgi (2019)(78)	61 PD	Whole-brain WM	n.s.	-	n.s.	-
	Grothe (2021)(54)	73 PD	Basal forebrain, hippocampus	N/A	N/A	⊖	Hippocampus^{avg}
Alternating Verbal Fluency (PD-CRS)	Chondrogiorgi (2019)(78)	61 PD	Whole-brain WM	n.s.	-	n.s.	-
	Grothe (2021)(54)	73 PD	Basal forebrain, hippocampus	N/A	N/A	⊖	Hippocampus^{avg}
Boston Naming Test	Gorges (2019)(69)	134 PD	Whole-brain WM	n.s.	-	n.s.	-
	Devignes (2021)(96)	114 PD		n.s.	-	n.s.	-
	Inguanzo(a) (2021)(70)	62 PD	Global mean FA	n.s.	-	N/A	N/A
	Chondrogiorgi (2019)(78)	61 PD	Whole-brain WM	⊕	ATR^{b}, CC^{uns} (body, genu, and splenium), cerebral peduncle^{b}, CB^{b} (at	n.s.	-

Table A1: DTI literature on cognitive impairment in PD.

Cognitive Impairment							
Measure	Author	Groups	Regions Analyzed	FA	FA-Location	MD	MD-Location
Confrontation Naming (PD-CRS)					CG and hippocampus), CR[b] (anterior, posterior, and superior), CST[b], EC[b], FMa[uns], FMi[uns], fornix (cres)/stria terminalis[b], IC[b] (anterior, posterior, and retrolenticular), ICP[b], IFOF[b], ILF[b], MCP[b], medial lemniscus[b], SCP[b], SLF[b], UF[b]		
	Grothe (2021)(54)	73 PD	Basal forebrain, hippocampus	N/A	N/A	n.s.	-
Global Word Accuracy (Generation Morphology Task)	Di Tella (2020)(222)	10 PD with Right-Side Dominant Symptoms	CC, IFOF, UF	⊕	UF[l]	⊖	UF[l]
		9 PD with Left-Side Dominant Symptoms		⊕	UF[b]	n.s.	-
		19 PD		⊕	UF[b]	n.s.	-
Noun Accuracy (Generation Morphology Task)	Di Tella (2020)(222)	10 PD with Right-Side Dominant Symptoms	CC, IFOF, UF	⊕	UF[l]	n.s.	-
		9 PD with Left-Side Dominant Symptoms		⊕	UF[b]	n.s.	-
		19 PD		⊕	UF[b]	n.s.	-
Phonemic Fluency	Duncan (2016)(214)	125 PD	Whole-brain WM	n.s.	-	n.s.	-
	Pelizzari (2019)(88)	26 PD	BG, red nucleus, SN, subthalamic nucleus, thalamus	n.s.	-	n.s.	-
	Di Tella (2020)(222)	10 PD with Right-Side Dominant Symptoms	CC, IFOF, UF	n.s.	-	n.s.	-
		9 PD with Left-Side Dominant Symptoms		n.s.	-	n.s.	-
		19 PD		n.s.	-	n.s.	-
	Inguanzo(a) (2021)(70)	62 PD	Global mean FA	n.s.	-	N/A	N/A
Semantic Fluency	Di Tella (2020)(222)	19 PD	CC, IFOF, UF	⊕	UF[l]	n.s.	-
	Duncan (2016)(214)	125 PD	Whole-brain WM	n.s.	-	⊖	Regions unspecified
	Jonkman (2021)(109)	53 PD	Tract from insula (dorsal anterior) to ACC	n.s.	-	⊖	Tract from insula (dorsal anterior) to ACC[b]
	Pelizzari (2019)(88)	26 PD	BG, red nucleus, SN, subthalamic nucleus, thalamus	n.s.	-	n.s.	-
	Di Tella (2020)(222)	10 PD with Right-Side Dominant Symptoms	CC, IFOF, UF	n.s.	-	n.s.	-
		9 PD with Left-Side Dominant Symptoms		n.s.	-	n.s.	-
	Inguanzo(a) (2021)(70)	62 PD	Global mean FA	n.s.	-	N/A	N/A

Table A1: DTI literature on cognitive impairment in PD.

Cognitive Impairment							
Measure	Author	Groups	Regions Analyzed	FA	FA-Location	MD	MD-Location
	Sampedro (2019)(89)	64 PD	Frontal cortex, occipital cortex	N/A	N/A	⊖	Occipital cortex^{l}
Verb Accuracy (Generation Morphology Task)	Di Tella (2020)(222)	10 PD with Right-Side Dominant Symptoms	CC, IFOF, UF	⊕	UF^{l}	⊖	UF^{l}
		9 PD with Left-Side Dominant Symptoms		⊕	UF^{r}	n.s.	-
		19 PD		n.s.	-	n.s.	-
Verbal Fluency	Agosta (2013)(206)	29 PD	CB, CC, CR, EC, IC, olfactory tract, PTR, SLF	⊕	CC^{uns} (body and genu), EC^{b}, olfactory tract^{b}	N/A	N/A
	Gorges (2019)(69)	134 PD	Whole-brain WM	n.s.	-	⊖	CC^{r}, CST^{r}, IC^{r}
	Yang (2021)(223)	34 PD	Whole-brain WM tracts connecting GM structures	n.s.	-	⊕	Tracts from fusiform gyrus to hippocampal gyrus^{r}, tracts from insula to postcentral cortex and pallidum^{b}, tracts from MFG (caudal) to SFG and precentral cortex^{r}, tracts from OFC (medial) to ACC^{r} (rostral), tracts from pars triangularis to MFG (rostral) and insula^{r}, tracts from pericalcarine cortex to cuneus and precuneus^{b}, tracts from precentral cortex to insula, postcentral cortex, and parietal cortex^{b} (superior), tracts from supramarginal gyrus to parietal cortex (superior) and insula^{r}, tracts from temporal gyrus (inferior) to insula and temporal gyrus^{r} (superior)
	Lucas-Jiménez (2016)(99)	37 PD	CB, CC, IFOF, ILF	n.s.	-	N/A	N/A
Word List Discrimination	Gorges (2019)(69)	134 PD	Whole-brain WM	n.s.	-	n.s.	-
Visuospatial							
Visuospatial Composite	Bledsoe (2018)(79)	75 PD	CC	⊕	CC^{uns} (segment 5)	⊕	CC^{uns} (segment 4)
				n.s.	-	⊖	CC^{uns} (segment 1)
	Melzer (2013)(67)	109 PD	Whole-brain WM	n.s.	-	n.s.	-
	Zheng (2014)(94)	16 PD		n.s.	-	n.s.	-
	Lucas-Jiménez (2016)(99)	37 PD	CB, CC, IFOF, ILF	n.s.	-	N/A	N/A
Visuospatial Function (RBANS)	Chen (2019)(197)	36 PD	Whole-brain WM	n.s.	-	N/A	N/A
Picture Completion (WAIS-III)	Chen(a) (2017)(219)	24 Early-Onset PD	ATR, BG, CST, IFOF, occipital WM, parietal WM, SLF, temporal WM	n.s.	-	n.s.	-
Block Design (WAIS-III)	Chen(a) (2017)(219)	24 Early-Onset PD	ATR, BG, CST, IFOF, occipital WM, parietal WM, SLF, temporal WM	n.s.	-	n.s.	-
Clock Copying Task	Garcia-Diaz (2018)(195)	36 PD	Whole-brain WM	?	FMa^{l}, FMi^{l}	N/A	N/A
	Chondrogiorgi (2019)(78)	61 PD		n.s.	-	n.s.	-
	Grothe (2021)(54)	73 PD	Basal forebrain, hippocampus	N/A	N/A	⊖	Hippocampus^{avg}

Table A1: DTI literature on cognitive impairment in PD.

Cognitive Impairment							
Measure	Author	Groups	Regions Analyzed	FA	FA-Location	MD	MD-Location
Clock Drawing Task	Chondrogiorgi (2019)(78)	61 PD	Whole-brain WM	n.s.	-	n.s.	-
	Grothe (2021)(54)	73 PD	Basal forebrain, hippocampus	N/A	N/A	⊖	Hippocampus^{avg}
	Chen(a) (2017)(219)	24 Early-Onset PD	ATR, BG, CST, IFOF, occipital WM, parietal WM, SLF, temporal WM	⊕	Parietal WM^{l} (superior)	⊖	ATR^{l}
Construction (Mattis Dementia Rating Scale)	Matsui(a) (2007)(75)	37 PD	CB, frontal WM, occipital WM, parietal WM, temporal WM	n.s.	-	N/A	N/A
Constructional Praxis (CERAD)	Gorges (2019)(69)	134 PD	Whole-brain WM	n.s.	-	⊖	CC^{r}, CST^{r}, IC^{r}, optic tract^{l}
Farnsworth–Munsell 100 Hue Color Vision test - Sqrt(Total Error Scores)	Bertrand (2012)(224)	26 PD	Whole-brain WM	⊕	SLF^{b}, tracts from cortico-cortical to cortico-subcortical regions^{b}, U-fibres from MFG (caudal) to SFG and precentral cortex^{r}	n.s.	-
Judgment of Line Orientation Test	Theilmann (2013)(217)	25 PD	ACC, CC, CR, EC, frontal WM, IC, occipital WM paracentral WM, pars opercularis, pars triangularis, parietal WM, pericalcarine	⊕	CR^{l} (anterior)	N/A	N/A
	Garcia-Diaz (2018)(195)	36 PD	Whole-brain WM	?	ATR^{r}, IFOF^{r}, UF^{r}	N/A	N/A
	Devignes (2021)(96)	114 PD		n.s.	-	⊖	Tract from CC (posterior midbody) to postcentral cortex^{l}
	Inguanzo(a) (2021)(70)	62 PD	Global mean FA	n.s.	-	N/A	N/A
	Sampedro (2020)(90)	133 PD	Cortical GM	N/A	N/A	⊖	Frontal clusters^{uns}, parahippocampal-entorhinal cortex^{uns}, temporal clusters^{uns} (superior), temporo-occipital cortex^{uns}
	Sampedro (2019)(89)	64 PD	Frontal cortex, occipital cortex	N/A	N/A	n.s.	-
Pentagon Copying Test	Garcia-Diaz (2018)(195)	36 PD	Whole-brain WM	?	CC^{r} (genu), FMi^{r}	N/A	N/A
	Minett (2018)(51)	93 PD-CogU		n.s.	-	n.s.	-
		27 PD-MCI		n.s.	-	n.s.	-
Rey Complex Figure Test	Gargouri (2019)(108)	52 PD	Basal forebrain, fornix	n.s.	-	⊖	Basal forebrain^{avg} (ch1-ch2)
	Auning (2014)(95)	18 PD	Occipital WM, parietal WM	n.s.	-	N/A	N/A
	Carlesimo (2012)(39)	25 PD	Hippocampus	N/A	N/A	⊖	Hippocampus^{r}
Visual Form Discrimination Test	Garcia-Diaz (2018)(195)	36 PD	Whole-brain WM	?	CC^{r} (splenium), FMa^{r}	N/A	N/A
	Inguanzo(a) (2021)(70)	62 PD	Global mean FA	n.s.	-	N/A	N/A
Visual Verbal Test - Total Number of Shifts	Koshimori (2015)(98)	26 PD	Whole-brain WM	N/A	N/A	n.s.	-
Cognition - Other							
Conceptualization (Mattis Dementia Rating Scale)	Matsui(a) (2007)(75)	37 PD	CB, frontal WM, occipital WM, parietal WM, temporal WM	⊕	CB^{l} (posterior)	N/A	N/A
Facial Recognition Test	Garcia-Diaz (2018)(195)	36 PD	Whole-brain WM	?	CC^{r} (splenium), FMa^{r}	N/A	N/A
	Inguanzo(a) (2021)(70)	62 PD	Global mean FA	n.s.	-	N/A	N/A
Fluctuating Cognition	Delli Pizzi (2015)(205)	16 DLB	Frontal WM, occipital WM, parietal WM,	N/A	N/A	n.s.	-

Table A1: DTI literature on cognitive impairment in PD.

Cognitive Impairment							
Measure	Author	Groups	Regions Analyzed	FA	FA-Location	MD	MD-Location
			sensorimotor cortex, temporal WM, thalamus				

WM: white matter; CB: Cingulate bundle; ILF: inferior longitudinal fasciculus; SLF: superior longitudinal fasciculus, IFOF: inferior fronto-occipital fasciculus, UF: uncinate fasciculus, CC: corpus callosum; IC: internal capsule; SN: substantia nigra; EC: external capsule; CST: corticospinal tract; SCP: superior cerebellar peduncle; CR: corona radiata; ATR: anterior thalamic radiation; CG: cingulate gyrus; SFOF: superior fronto-occipital fasciculus; FMi: forceps minor; MFG: middle frontal gyrus; IFG: inferior frontal gyrus; OFC: orbitofrontal cortex; IPG: inferior parietal gyrus; GP: globus pallidus; BG: basal ganglia; FMa: forceps major; NBM: nucleus basalis of Meynert; PTR: posterior thalamic radiation; ACC: anterior cingulate cortex; PPN: pedunculopontine nucleus; ICP: inferior cerebellar peduncle; MCP: middle cerebellar peduncle.

↓ = significant decrease; ↑ = significant increase; ⊕ = significant positive association; ⊖ = significant positive association; ? = significant finding, but direction unspecified; N/A = the study did not report or measure the parameter.

Table A2: DTI literature on other non-motor symptoms in PD

Other Non-Motor Symptoms							
Measure	Author	Groups	Regions Analyzed	FA	FA-Location	MD	MD-Location
Overall Non-Motor Scores							
NMSS-Total	Wei (2016)(121)	43 PD	BG, frontal WM, hippocampus, occipital WM, parietal WM, SN, temporal WM	⊖	Hippocampus (contralateral to more symptomatic side)	N/A	N/A
	Guimaraes (2018)(213)	132 PD	CB, CC, CST	n.s.	-	N/A	N/A
UPDRS-I	Tsai (2020)(65)	82 PD	Whole-brain GM	⊖	IFG (orbital^{r}), IPG^{r}, Rolandic operculum^{l}, temporal pole^{r} (superior)	⊖	Cerebellum^{uns}, SFG (medial^{r} and orbital^{l})
	Lorio (2019)(225)	44 PD On Medication	Whole-brain WM	⊖	Putamen^{uns}	⊕	Operculum^{uns}, pons^{uns}
	Wei (2016)(121)	43 PD	BG, frontal WM, hippocampus, occipital WM, parietal WM, SN, temporal WM	⊖	Hippocampus^{avg} (and contralateral to more symptomatic side)	N/A	N/A
	Tsai (2020)(65)	82 PD	Whole-brain GM	⊕	Cerebellum^{r}, olfactory cortex^{r}	⊕	Hippocampus^{l}, thalamus^{r}
	Lenfeldt (2013)(226)	64 PD	BG, brainstem, CC, EC, frontal WM, MCP, SN, thalamus	n.s.	-	⊕	GP^{uns}, putamen^{uns}
	Lim (2016)(119)	38 PD	PPN, thalamus	n.s.	-	n.s.	-
	Taylor (2018)(227)	71 PD	Brainstem, cerebellum, CC, CR, CST, IFOF, ILF, insula, motor regions, occipital cortex, optic radiation, parietal cortex, prefrontal cortex, temporal cortex, thalamus	n.s.	-	n.s.	-
	Andica (2019)(52)	20 PD	Whole-brain WM and GM	n.s.	-	n.s.	-
	Lorio (2019)(225)	205 PD	Whole-brain WM	n.s.	-	n.s.	-
		56 PD Off Medication		n.s.	-	n.s.	-
	Xiao (2021)(107)	62 PD with Left-Side Dominant Symptoms		N/A	N/A	n.s.	-
		79 PD with Right-Side Dominant Symptoms		N/A	N/A	n.s.	-
Depression – Group Comparisons							
PD with Depression (vs. HC)	Surdhar (2012)(100)	6 PD with Depression, 6 HC	CC, UF	n.s.	-	n.s.	-
	Li (2020)(101)	30 PD with Depression, 91 HC	Whole-brain WM	n.s.	-	↑	CC^{uns} (body and splenium), CB^{b} (at hippocampus), CR^{b} (superior), EC^{b}, fornix (cres)/stria terminalis^{b}, IFOF^{b}, SFOF^{b}, UF^{b}
PD with Depression (vs. PD without Depression)	Surdhar (2012)(100)	6 PD with Depression, 6 PD without Depression	CC, UF	n.s.	-	n.s.	-
	Gou (2018)(106)	28 PD with Depression, 56 PD without Depression	Whole-brain WM	n.s.	-	n.s.	-
	Li (2020)(101)	30 PD with Depression, 43 PD without Depression		n.s.	-	↑	CB^{l} (at hippocampus)

Table A2: DTI literature on other non-motor symptoms in PD

Other Non-Motor Symptoms							
Measure	Author	Groups	Regions Analyzed	FA	FA-Location	MD	MD-Location
	Li (2010)(102)	14 PD with Depression, 18 PD without Depression	Thalamus	↓	Thalamus^{b} (mediodorsal)	n.s.	-
	Huang (2014)(103)	15 PD with Depression, 15 PD without Depression	Whole-brain WM	↓	ATR^{l}, FMi^{l}, ILF^{l}, SLF^{l}, UF^{l}	n.s.	-
	Matsui(b) (2007)(104)	14 PD with Depression, 14 PD without Depression	CB, frontal WM, occipital WM, parietal WM, temporal WM	↓	ACC^{b}	N/A	N/A
	Wu (2018)(105)	31 PD with Depression, 37 PD without Depression	Whole-brain WM	↓	CB^{l}, CR^{l} (anterior), PTR^{l}, sagittal stratum^{l}, SLF^{l}, UF^{l}	N/A	N/A
PD with Mild-to-Moderate Depression (vs. PD without Depression)	Shen(a) (2022)(111)	22 PD with Mild-to-Moderate Depression, 30 PD without Depression	Whole-brain WM (for FA), regions with significant differences between groups (for MD)	n.s.	-	n.s.	-
PD with Severe Depression (vs. PD with Mild-to-Moderate Depression)	Shen(a) (2022)(111)	15 PD with Severe Depression, 22 PD with Mild-to-Moderate Depression	Whole-brain WM (for FA), regions with significant differences between groups (for MD)	↓	IFOF^{b}, SLF^{l}, UF^{l}	↑	SLF^{l}
PD with Severe Depression (vs. PD without Depression)	Shen(a) (2022)(111)	15 PD with Severe Depression, 30 PD without Depression	Whole-brain WM (for FA), regions with significant differences between groups (for MD)	↓	CR^{l} (anterior), CST^{l}, IFOF^{b}, SLF^{l}, UF^{l}	↑	CR^{l} (anterior), SLF^{l}, UF^{l}
Depression – Rating Scales							
Beck Depression Inventory	Prange (2019)(110)	27 PD	ACC, brainstem, BG, medial frontal cortex, thalamus, whole-brain WM	⊖	ATR^{b}, CC^{uns} (body, genu, and splenium), cerebral peduncle^{b}, CB^{b} (at CG), CR (anterior^{b}, posterior^{b}, and superior^{r}), CST^{b}, EC^{r}, FMa^{r}, FMi^{r}, fornix (cres)/stria terminalis^{r}, IC (anterior limb^{b}, posterior limb^{b}, and retrolenticular^{r}), IFOF^{b}, ILF^{b}, MCP^{uns}, medial lemniscus^{l}, pontine crossing tract^{uns}, PTR^{b}, putamen^{r} (posterior), sagittal stratum^{r}, SCP^{b}, SFOF^{r}, SLF^{b}, SN^{r}, UF^{r}	n.s.	-
	Shen(a) (2022)(111)	37 PD with Depression	CR, CST, IFOF, SLF, UF	⊖	SLF^{l}	N/A	N/A
	Jonkman (2021)(109)	53 PD	Tract from insula (dorsal anterior) to ACC	n.s.	-	n.s.	-
	Baumeister (2019)(82)	29 PD	Arcuate fasciculus, ATR, CB, CC, CST, IFOF, ILF, SLF, UF	n.s.	-	N/A	N/A
	Inguanzo(a) (2021)(70)	62 PD	Global mean FA	n.s.	-	N/A	N/A
GDS-15	Gou (2018)(106)	84 PD	Whole-brain WM	n.s.	-	n.s.	-

Table A2: DTI literature on other non-motor symptoms in PD

Other Non-Motor Symptoms							
Measure	Author	Groups	Regions Analyzed	FA	FA-Location	MD	MD-Location
	Wen (2018)(92)	65 PD	ATR, CB, CC, CR, CST, EC, FMa, FMi, fornix, IFOF, ILF, IC, sagittal stratum, SLF, UF	n.s.	-	N/A	N/A
	Xiao (2021)(107)	79 PD with Right-Side Dominant Symptoms	Whole-brain WM	N/A	N/A	⊕	IC^{l} (retrolenticular)
		62 PD with Left-Side Dominant Symptoms		N/A	N/A	n.s.	-
Hamilton Depression Scale	Li (2010)(102)	14 PD with depression, 18 PD without depression	Thalamus	⊖	Thalamus^{b} (mediodorsal)	n.s.	-
	Huang (2014)(103)	15 PD with Depression	Whole-brain WM	⊖	Temporal cortex^{l} (deep)	N/A	N/A
	Wu (2018)(105)	31 PD with Depression		⊖	CB^{l}, SLF^{l}	N/A	N/A
Montgomery Asberg Depression Rating Scale	Gargouri (2019)(108)	52 PD	Basal forebrain, fornix	n.s.	-	n.s.	-
UPDRS-I - Depression	Andica (2019)(52)	20 PD	Whole-brain WM and GM	n.s.	-	n.s.	-
Anxiety							
Beck Anxiety Inventory	Jonkman (2021)(109)	53 PD	Tract from insula (dorsal anterior) to ACC	n.s.	-	⊕	Tract from insula (dorsal anterior) to ACC^{b}
UPDRS-I - Anxiety	Andica (2019)(52)	20 PD	Whole-brain WM and GM	n.s.	-	n.s.	-
Spielberger State-Trait Anxiety Inventory	Prange (2019)(110)	27 PD	ACC, brainstem, BG, medial frontal cortex, thalamus, whole-brain WM	n.s.	-	n.s.	-
Apathy – Group Comparisons							
PD with Apathy (vs. HC)	Prange (2019)(110)	14 PD with Apathy, 15 HC	ACC, brainstem, BG, medial frontal cortex, thalamus, whole-brain WM	n.s.	-	↑	Thalamus^{r} (medial)
PD with Apathy (vs. PD without apathy)	Zhang (2018)(113)	18 PD with Apathy, 21 PD without Apathy	Whole-brain WM	↓	CC^{uns} (body and genu), CB^{l}, CR (anterior^{b} and superior^{l})	N/A	N/A
	Prange (2019)(110)	14 PD with Apathy, 13 PD without Apathy	ACC, brainstem, BG, medial frontal cortex, thalamus, whole-brain WM	↓	Thalamus^{b} (medial)	↑	ACC^{b} (pregenual), MFG^{r}, subcallosal gyrus^{r}, thalamus (medial^{b} and posterior^{r})
PD with High Sub-Clinical Symptoms of Apathy (vs. HC)	Lucas-Jiménez (2018)(112)	14 PD with High Sub-Clinical Symptoms of Apathy, 25 HC	ATR, CB, CC, IC, SLF, thalamus, UF	N/A	N/A	↑	ATR^{l}, CB^{l}, SLF^{l}, UF^{l}
PD with High Sub-Clinical Symptoms of Apathy (vs. PD with Low Sub-Clinical Symptoms of Apathy)	Lucas-Jiménez (2018)(112)	14 PD with High Sub-Clinical Symptoms of Apathy, 18 PD with Low-Subclinical	ATR, CB, CC, IC, SLF, thalamus, UF	N/A	N/A	n.s.	-

Table A2: DTI literature on other non-motor symptoms in PD

Other Non-Motor Symptoms							
Measure	Author	Groups	Regions Analyzed	FA	FA-Location	MD	MD-Location
		Symptoms of Apathy					
Apathy – Rating Scales							
Lille Apathy Rating Scale - Emotion	Lucas-Jiménez (2018)(112)	14 PD with High Sub-Clinical Symptoms of Apathy	Average MD of: ATR, CB, SLF, UF	N/A	N/A	n.s.	-
		18 PD with Low-Subclinical Symptoms of Apathy		N/A	N/A	n.s.	-
Lille Apathy Rating Scale - Intellectual Curiosity	Lucas-Jiménez (2018)(112)	14 PD with High Sub-Clinical Symptoms of Apathy	Average MD of: ATR, CB, SLF, UF	N/A	N/A	n.s.	-
		18 PD with Low-Subclinical Symptoms of Apathy		N/A	N/A	n.s.	-
Lille Apathy Rating Scale - Lack of Concern	Lucas-Jiménez (2018)(112)	14 PD with High Sub-Clinical Symptoms of Apathy	Average MD of: ATR, CB, SLF, UF	N/A	N/A	⊖	ATR^{l}, CB^{l}, SLF^{l}, UF^{l}
		18 PD with Low-Subclinical Symptoms of Apathy		N/A	N/A	n.s.	-
Lille Apathy Rating Scale - Self-Awareness	Lucas-Jiménez (2018)(112)	14 PD with High Sub-Clinical Symptoms of Apathy	Average MD of: ATR, CB, SLF, UF	N/A	N/A	n.s.	-
		18 PD with Low-Subclinical Symptoms of Apathy		N/A	N/A	n.s.	-
Lille Apathy Rating Scale - Total Score	Prange (2019)(110)	27 PD	ACC, brainstem, BG, medial frontal cortex, thalamus, whole-brain WM	⊖	ATR^{b}, caudate^{b}, CC^{uns} (body, genu, and splenium), cerebral peduncle^{b}, CG^{b}, CB^{b} (at CG), CR (anterior^{b}, posterior^{r}, superior^{b}), CST^{b}, EC^{b}, FMi (no side), fornix (body, column, and cres)/stria terminalis^{r}, GP^{l} (internal and external), IC (anterior limb^{b}, posterior limb^{b}, and retrolenticular^{r}), IFG^{l}, IFOF^{b}, MFG^{l}, SFOF^{r}, SLF^{b}, subcallosal gyrus^{l}, UF^{b}	⊕	ACC^{r} (pregenual), IFG^{l}, subcallosal gyrus^{l}, uncus^{r}
	Zhang (2018)(113)	18 PD with Apathy	Whole-brain WM	⊖	CC^{uns} (body and genu), CB^{l}, CR (anterior^{b}, posterior^{l}, and superior^{l}), SFOF^{r}, SLF^{r}	N/A	N/A
	Baumeister (2019)(82)	29 PD	Arcuate fasciculus, ATR, CB, CC, CST, IFOF, ILF, SLF, UF	n.s.	-	N/A	N/A
Starkstein Apathy Scale	Baumeister (2019)(82)	29 PD	Arcuate fasciculus, ATR, CB, CC, CST, IFOF, ILF, SLF, UF	n.s.	-	N/A	N/A
	Inguanzo(a) (2021)(70)	62 PD	Global mean FA	n.s.	-	N/A	N/A

Table A2: DTI literature on other non-motor symptoms in PD

Other Non-Motor Symptoms							
Measure	Author	Groups	Regions Analyzed	FA	FA-Location	MD	MD-Location
UPDRS-I - Apathy	Andica (2019)(52)	20 PD	Whole-brain WM and GM	n.s.	-	n.s.	-
Other Mood							
Ekman 60 Test - Anger	Baggio (2012)(228)	39 PD	Whole-brain WM	n.s.	-	N/A	N/A
Ekman 60 Test - Disgust	Baggio (2012)(228)	39 PD	Whole-brain WM	n.s.	-	N/A	N/A
Ekman 60 Test - Fear	Baggio (2012)(228)	39 PD	Whole-brain WM	n.s.	-	N/A	N/A
Ekman 60 Test - Happiness	Baggio (2012)(228)	39 PD	Whole-brain WM	n.s.	-	N/A	N/A
Ekman 60 Test - Sadness	Baggio (2012)(228)	39 PD	Whole-brain WM	⊕	CC (body) to centrum semiovale^{l}, FMi^{r}, IFOF^{r}, ILF^{r}	N/A	N/A
Ekman 60 Test - Surprise	Baggio (2012)(228)	39 PD	Whole-brain WM	n.s.	-	N/A	N/A
Mean of HAMD and HAMA z-scores	Wu (2020)(122)	39 PD	CC	?	CC^{avg} (temporal–parietal–occipital subsection)	n.s.	-
NMSS - Mood	Wei (2016)(121)	43 PD	BG, frontal WM, hippocampus, occipital WM, parietal WM, SN, temporal WM	⊖	Hippocampus^{avg} (and hemisphere contralateral to more symptomatic side, and hemisphere contralateral to less symptomatic side)	N/A	N/A
Sleep/Fatigue – Group Comparisons							
PD with EDS (vs. HC)	Matsui (2006)(120)	11 PD with EDS, 10 HC	Fornix, frontal WM, occipital WM, parietal WM, temporal WM	↓	Fornix^{avg}, frontal WM^{avg}, occipital WM^{avg}, parietal WM^{avg}, temporal WM^{avg}	N/A	N/A
PD with EDS (vs. PD without EDS)	Chondrogiorgi (2016)(114)	17 PD with EDS, 17 PD without EDS	Whole-brain WM	n.s.	-	n.s.	-
	Matsui (2006)(120)	11 PD with EDS, 26 PD without EDS	Fornix, frontal WM, occipital WM, parietal WM, temporal WM	↓	Fornix^{avg}, frontal WM^{avg}, occipital WM^{avg}, temporal WM^{avg}	N/A	N/A
PD with Fatigue (vs. PD without Fatigue)	Kang (2020)(117)	16 PD with Fatigue, 31 PD without Fatigue	ATR, CB, CST, FMa, FMi, IFOF, ILF, SLF, UF	↑	ATR^{b}, CB^{b} (at CG), CST^{b}, FMa^{uns}, FMi^{uns}, IFOF^{b}, ILF^{b}, SLF^{l}, UF^{b}	↓	ATR^{b}, CB^{b} (at CG), CST^{b}, FMa^{uns}, FMi^{uns}, IFOF^{b}, ILF^{b}, SLF^{b}, UF^{r}
PD with High Fatigue (vs. PD with Low Fatigue)	Kluger (2019)(118)	29 PD with High Fatigue, 31 PD with Low Fatigue	Whole-brain WM	n.s.	-	N/A	N/A
PD with RBD (vs. HC)	Holtbernd (2021)(116)	30 PD with RBD, 56 HC	GM in the brainstem and midbrain, whole-brain WM	↓	CC^{b} (body and splenium), tapetum^{l}	n.s.	-
	Lim (2016)(119)	24 PD with RBD, 25 HC	Whole-brain WM	↓	Frontal regions^{b}	↑	Widespread^{uns}
	Pyatigorskaya (2021)(57)	34 PD with RBD, 25 HC	Amygdala, brainstem, hippocampus, NBM, PPN, prefrontal cortex, SN	N/A	N/A	↑	Medulla oblongata^{avg}, NBM^{avg}
	Holtbernd (2021)(116)	30 PD with RBD, 56 HC	GM in the brainstem and midbrain, whole-brain WM	↑	ATR^{r}, CST^{b}, ICP^{b}, locus coeruleus^{b}, MCP^{b}, medulla oblongata^{b}, medullary reticularis formation^{b}, PPN^{b}, raphe nuclei^{b} (dorsal and median), red nucleus^{b}, SCP^{b}, SLF^{r} (temporal), SN^{b}, UF^{l}	n.s.	-
	Dolatshahi (2021)(115)	39 PD with RBD, 30 HC	Whole-brain WM	↑	Putamen (contralateral to side of putamen with decreased dopamine)	↑	Fornix/stria terminalis (ipsilateral to side of putamen with decreased dopamine)
PD with RBD (vs. PD without RBD)	Lim (2016)(119)	24 PD with RBD, 14 PD without RBD	Whole-brain WM	n.s.	-	n.s.	-
	Dolatshahi (2021)(115)	39 PD with RBD, 18 PD without RBD		↓	Fornix/stria terminalis (ipsilateral to side of putamen with decreased dopamine)	↑	Fornix/stria terminalis (ipsilateral to side of putamen with decreased dopamine)

Table A2: DTI literature on other non-motor symptoms in PD

Other Non-Motor Symptoms							
Measure	Author	Groups	Regions Analyzed	FA	FA-Location	MD	MD-Location
	Pyatigorskaya (2021)(57)	34 PD with RBD, 20 PD without RBD	Amygdala, brainstem, hippocampus, NBM, PPN, prefrontal cortex, SN	N/A	N/A	n.s.	-
	Holtbernd (2021)(116)	30 PD with RBD, 29 PD without RBD	GM in the brainstem and midbrain, whole-brain WM	↑	ICP^{r}, locus coeruleus^{b}, medulla oblongata^{b}, PPN^{b}, raphe nuclei^{b} (dorsal and median), red nucleus^{r}, SCP^{b}, SN^{b}	n.s.	-
Sleep/Fatigue – Rating Scales							
Epworth Sleepiness Scale	Matsui (2006)(120)	37 PD	Fornix, frontal WM, occipital WM, parietal WM, temporal WM	⊖	Fornix^{avg}	N/A	N/A
	Gargouri (2019)(108)	52 PD	Basal forebrain, fornix	n.s.	-	n.s.	-
Fatigue Severity Scale	Kang (2020)(117)	32 PD	Whole-brain WM	⊕	ATR^{b}, CB (at CG^{b} and hippocampus^{r}), CST^{b}, FMa^{uns}, FMi^{uns}, IFOF^{b}, ILF^{b}, SLF^{l}, UF^{b}	⊖	ATR^{b}, CB (at CG^{r} and hippocampus^{r}), CST^{b}, FMa^{uns}, FMi^{uns}, IFOF^{b}, ILF^{b}, SLF^{b}, UF^{r}
	Baumeister (2019)(82)	29 PD	Arcuate fasciculus, ATR, CB, CC, CST, IFOF, ILF, SLF, UF	n.s.	-	N/A	N/A
Mean of ESS z-score and PDSS negative z-score	Wu (2020)(122)	39 PD	CC	n.s.	-	n.s.	-
NMSS - Sleep/Fatigue	Wei (2016)(121)	43 PD	BG, frontal WM, hippocampus, occipital WM, parietal WM, SN, temporal WM	n.s.	-	N/A	N/A
RBD Screening Questionnaire	Xiao (2021)(107)	62 PD with Left-Side Dominant Symptoms	Whole-brain WM	N/A	N/A	n.s.	-
		79 PD with Right-Side Dominant Symptoms		N/A	N/A	n.s.	-
UPDRS-I - Daytime Sleepiness	Andica (2019)(52)	20 PD	Whole-brain WM and GM	n.s.	-	n.s.	-
UPDRS-I - Fatigue	Andica (2019)(52)	20 PD	Whole-brain WM and GM	n.s.	-	n.s.	-
UPDRS-I - Sleep Problems	Andica (2019)(52)	20 PD	Whole-brain WM and GM	n.s.	-	n.s.	-
QoL/ADL							
Instrumental Activities of Daily Living Scale	Inguanzo(a) (2021)(70)	62 PD	Global mean FA	n.s.	-	N/A	N/A
PDQ-39 SI	Tsai (2020)(65)	82 PD	Whole-brain GM	⊕	Cerebellum^{r}, Rolandic operculum^{r}, SFG^{r} (medial)	⊕	Cerebellum^{uns}, CB^{r} (anterior and posterior), paracentral lobule^{l}, temporal gyrus^{r} (superior)
	Tsai (2020)(65)	82 PD		n.s.	-	⊖	Caudate^{l}, cerebellum^{l}, insula^{r}, occipital gyrus^{l} (middle)
S&E	Chiang (2017)(229)	66 PD	Cerebellum, IFOF, ILF, SLF	⊕	ILF^{l}	⊖	Cerebellum^{l}, IFOF^{l}
	Lenfeldt (2013)(226)	64 PD	BG, brainstem, CC, EC, frontal WM, MCP, SN, thalamus	n.s.	-	⊖	GP^{uns}, putamen^{uns}, thalamus^{uns}
	Lu^{a} (2016)(64)	126 PD	Whole-brain GM	n.s.	-	⊖	CG (posterior) (ipsilateral to side of disease onset)
	Surova (2016)(210)	105 PD	BG, brainstem, CB, CC, CST, fornix, IFOF, ILF, SLF, SN, thalamus, UF	n.s.	-	n.s.	-
Psychosis/Hallucinations – Group Comparisons							

Table A2: DTI literature on other non-motor symptoms in PD

Other Non-Motor Symptoms							
Measure	Author	Groups	Regions Analyzed	FA	FA-Location	MD	MD-Location
DLB with VH (vs. DLB without VH)	Zorzi (2021)(123)	10 DLB with VH, 13 DLB without VH	Whole-brain WM	↓	IFOF^{r} (frontal), ILF^{r} (temporo-parietal), UF^{r}	↑	IFOF^{r} (frontal), ILF^{r} (temporo-parietal), SLF^{r}, UF^{r}
PD with VH (vs. HC)	Hepp (2017)(125)	15 PD with VH, 15 HC	NBM-whole-brain WM tracts	n.s.	-	↑	Tracts from NBM to cortex^{avg}
	Lee (2016)(124)	10 PD with VH,15 HC	Optic chiasm, optic nerve, optic radiation, primary visual cortex, thalamus	↓	Optic nerve^{l}	↑	Optic radiation^{l}
	Yao (2016)(59)	12 PD with VH, 14 HC	Hippocampus	N/A	N/A	↑	Hippocampus (entire^{b}, body^{b}, and posterior^{r})
PD with VH (vs. PD without VH)	Lee (2016)(124)	10 PD with VH, 14 PD without VH	Optic chiasm, optic nerve, optic radiation, primary visual cortex, thalamus	n.s.	-	↑	Optic radiation^{l}
	Hepp (2017)(125)	15 PD with VH, 40 PD without VH	NBM-whole-brain WM tracts	n.s.	-	↑	Tracts from NBM to occipital lobe^{avg}, tracts from NBM to parietal lobe^{avg}
	Yao (2016)(59)	12 PD with VH, 15 PD without VH	Hippocampus	N/A	N/A	↑	Hippocampus^{r} (entire and posterior)
	Yuki (2020)(230)	17 PD with VH, 43 PD without VH	IFOF, ILF	n.s.	-	n.s.	-
PD with Psychosis (vs. PD without Psychosis)	Lenka (2020)(126)	42 PD with Psychosis, 48 PD without Psychosis	Whole-brain WM	↓	CC^{uns}, CST^{r}, IFOF^{b}, ILF^{b}, occipitoparietal WM^{r}	n.s.	-
	Zhong (2013)(56)	18 PD with Psychosis, 48 PD without Psychosis	BG, CG, frontal lobe, hippocampus, occipital lobe, SN	↓	CG^{b}, frontal lobe^{b}, hippocampus^{l}, occipital lobe^{b}	N/A	N/A
Psychosis/Hallucinations – Rating Scales							
NPI Hallucinations – Frequency	Delli Pizzi (2014)(204)	15 DLB	Amygdala, frontal WM, occipital WM, parietal WM, precentral gyrus, premotor cortex, sensory cortex, temporal WM, thalamus	N/A	N/A	⊕	Thalamus^{r}
NPI Hallucinations – Severity	Zorzi (2021)(123)	23 DLB	IFOF, ILF, SLF, UF	⊖	SLF^{r}	⊕	IFOF^{r}, ILF^{r}, SLF^{r}, UF^{l}
	Delli Pizzi (2014)(204)	15 DLB	Amygdala, frontal WM, occipital WM, parietal WM, precentral gyrus, premotor cortex, sensory cortex, temporal WM, thalamus	N/A	N/A	⊕	Thalamus^{r}
NPI Hallucinations – Frequency x Severity	Delli Pizzi (2014)(204)	15 DLB	Amygdala, frontal WM, occipital WM, parietal WM, precentral gyrus, premotor cortex, sensory cortex, temporal WM, thalamus	N/A	N/A	⊕	Thalamus^{r}
VH Presence	Yuki (2020)(230)	60 PD	IFOF, ILF	⊖	ILF^{l}	⊕	ILF^{l}
VH Severity	Nedelska (2015)(203)	30 DLB	Whole-brain WM	n.s.	-	N/A	N/A
UPDRS-I - Hallucinations	Andica (2019)(52)	20 PD	Whole-brain WM and GM	n.s.	-	n.s.	-

Table A2: DTI literature on other non-motor symptoms in PD

Other Non-Motor Symptoms							
Measure	Author	Groups	Regions Analyzed	FA	FA-Location	MD	MD-Location
Psychosis Severity	Lenka (2020)(126)	42 PD with Psychosis	CC, CST, IFOF, ILF, occipitoparietal WM	n.s.	-	n.s.	-
Other Psychiatric/Behavioural – Group Comparisons							
PD with ICD (vs. HC)	Dolatshahi (2021)(115)	18 PD with ICD, 30 HC	Whole-brain WM	↑	ICP (ipsilateral to side of putamen with decreased dopamine)	↓	MCP (ipsilateral to side of putamen with decreased dopamine)
	Yoo (2015)(127)	10 PD with ICD, 18 HC		↑	CC^{uns} (anterior and dorsal)	n.s.	-
	Gan (2021)(231)	21 PD with ICD, 37 HC		n.s.	-	n.s.	-
PD with ICD (vs. PD without ICD)	Yoo (2015)(127)	10 PD with ICD, 9 PD without ICD	Whole-brain WM	↑	CC^{uns} (anterior), CB^{r} (dorsal and posterior), IC^{r} (genu and posterior limb), superior temporo-occipital $lobe^{r}$, thalamic $radiation^{b}$	n.s.	-
	Gan (2021)(231)	21 PD with ICD, 33 PD without ICD		n.s.	-	n.s.	-
PD with RBD and ICD (vs. PD without RBD but with ICD)	Dolatshahi (2021)(115)	16 PD with RBD and ICD, 18 PD without RBD but with ICD	Whole-brain WM	↓	ICP (ipsilateral to side of putamen with decreased dopamine)	↑	MCP (ipsilateral to side of putamen with decreased dopamine)
PD with RBD and ICD (vs. PD without RBD or ICD)	Dolatshahi (2021)(115)	16 PD with RBD and ICD, 18 PD without RBD or ICD	Whole-brain WM	↓	ICP (ipsilateral to side of putamen with decreased dopamine)	↑	MCP (ipsilateral to side of putamen with decreased dopamine)
Other Psychiatric/Behavioural – Rating Scales							
Scales for Outcomes in PD - Psychiatric Complications	Guimaraes (2018)(213)	132 PD	CB, CC, CST	n.s.	-	N/A	N/A
Olfaction – Group Comparisons							
PD with Anosmia (vs. HC)	Ibarretxe-Bilbao (2010)(232)	9 PD with Anosmia, 24 HC	Whole-brain WM	↓	WM^{b} adjacent to gyrus rectus, WM^{b} adjacent to primary olfactory cortex and entorhinal cortex	N/A	N/A
PD with Anosmia (vs. PD without Olfactory Dysfunction)	Ibarretxe-Bilbao (2010)(232)	9 PD with Anosmia, 6 PD without Olfactory Dysfunction	Whole-brain WM	↓	WM^{b} adjacent to gyrus rectus	N/A	N/A
PD with Hyposmia (vs. HC)	Wen (2017)(233)	70 PD with Hyposmia, 33 HC	Whole-brain WM	n.s.	-	n.s.	-
PD with Hyposmia (vs. PD without Olfactory Dysfunction)	Wen (2017)(233)	70 PD with Hyposmia, 18 PD without Olfactory Dysfunction	Whole-brain WM	n.s.	-	n.s.	-
PD with Idiopathic Smell Loss (vs. HC)	Haehner (2018)(234)	19 PD with Idiopathic Smell Loss, 17 HC	SN	↓	SN^{avg}	n.s.	-
PD with Idiopathic Smell Loss (vs. PD without Olfactory Dysfunction)	Haehner (2018)(234)	19 PD with Idiopathic Smell Loss, 12 PD without Olfactory Dysfunction	SN	n.s.	-	n.s.	-
PD with Severe Microsmia (vs. HC)	Ibarretxe-Bilbao (2010)(232)	9 PD Severe Microsmia, 24 HC	Whole-brain WM	↓	WM^{b} adjacent to gyrus rectus	N/A	N/A
PD with Severe Microsmia (vs. PD without	Ibarretxe-Bilbao (2010)(232)	9 PD Severe Microsmia, 6 PD without	Whole-brain WM	↓	WM^{b} adjacent to gyrus rectus	N/A	N/A

Table A2: DTI literature on other non-motor symptoms in PD

Other Non-Motor Symptoms							
Measure	Author	Groups	Regions Analyzed	FA	FA-Location	MD	MD-Location
Olfactory Dysfunction)		Olfactory Dysfunction					
Olfaction – Rating Scales							
Duration of Smell Loss	Hummel (2021)(235)	12 PD	Orbitofrontal WM, piriform cortex	n.s.	-	n.s.	-
Five Odor Olfactory Detection Array: Thresholds of Olfactory Detection	Zhang (2011)(55)	25 PD	Whole-brain WM and GM	n.s.	-	⊖	Parietal WM^{l} (inferior)
Five Odor Olfactory Detection Array: Thresholds of Olfactory Identification	Zhang (2011)(55)	25 PD	Whole-brain WM and GM	⊕	Cerebellum^{l} (medial)	⊖	Cerebellum^{r}
Olfactory Test Scores (Unspecified)	Liu (2022)(87)	41 PD	BG, cerebellum, red nucleus, SN, subthalamic nucleus, thalamus	⊕	Putamen^{b}	⊖	Cerebellum^{b}
Sniffin' Sticks: Odour Discrimination	Scherfler (2013)(236)	16 PD	Olfactory tract, SN	n.s.	-	n.s.	-
	Georgiopoulos (2017)(237)	22 PD	Entorhinal cortex, OFC, piriform cortex	n.s.	-	n.s.	-
	Hummel (2021)(235)	12 PD	Orbitofrontal WM, piriform cortex	n.s.	-	n.s.	-
Sniffin' Sticks: Odour Identification	Scherfler (2013)(236)	16 PD	Olfactory tract, SN	n.s.	-	n.s.	-
	Hummel (2021)(235)	12 PD	Orbitofrontal WM, piriform cortex	n.s.	-	n.s.	-
Sniffin' Sticks: Odour Threshold	Hummel (2021)(235)	12 PD	Orbitofrontal WM, piriform cortex	⊕	Piriform cortex^{l} (posterior)	n.s.	-
	Scherfler (2013)(236)	16 PD	Olfactory tract, SN	n.s.	-	n.s.	-
Sniffin' Sticks: Total Odour Score (Threshold, Discrimination, and Identification)	Haehner (2018)(234)	31 PD + 17 HC Combined	SN	⊕	SN^{avg}	⊖	SN^{avg}
	Scherfler (2013)(236)	16 PD	Olfactory tract, SN	n.s.	-	n.s.	-
	Hummel (2021)(235)	12 PD	Orbitofrontal WM, piriform cortex	n.s.	-	n.s.	-
University of Pennsylvania Smell Identification Test	Ibarretxe-Bilbao (2010)(232)	24 PD	UF, WM adjacent to primary olfactory cortex and entorhinal cortex, WM adjacent to gyrus rectus	⊕	WM^{b} adjacent to primary olfactory cortex and entorhinal cortex, WM^{r} adjacent to gyrus rectus	N/A	N/A
Bladder/Urinary Symptoms							
King's Health Questionnaire - Sum of Storage Symptom Questions	Roy (2019)(238)	17 PD	Whole-brain WM	n.s.	-	⊖	Brainstem^{b}
NMSS - Urinary	Wei (2016)(121)	43 PD	BG, frontal WM, hippocampus, occipital WM, parietal WM, SN, temporal WM	n.s.	-	N/A	N/A
UPDRS-I - Urinary problems	Andica (2019)(52)	20 PD	Whole-brain WM and GM	n.s.	-	n.s.	-
Gastrointestinal Symptoms							

Table A2: DTI literature on other non-motor symptoms in PD

Other Non-Motor Symptoms							
Measure	Author	Groups	Regions Analyzed	FA	FA-Location	MD	MD-Location
NMSS - Gastrointestinal	Wei (2016)(121)	43 PD	BG, frontal WM, hippocampus, occipital WM, parietal WM, SN, temporal WM	n.s.	-	N/A	N/A
UPDRS-I - Constipation	Andica (2019)(52)	20 PD	Whole-brain WM and GM	n.s.	-	n.s.	-
Pain – Group Comparisons							
PD with Pain (vs. PD without Pain)	Polli (2016)(239)	20 PD with Pain, 20 PD without Pain	Whole-brain WM	n.s.	-	n.s.	-
Pain – Rating Scales							
UPDRS-I - Pain	Andica (2019)(52)	20 PD	Whole-brain WM and GM	n.s.	-	n.s.	-
Cardiovascular and Respiratory Measures							
Baroreflex Sensitivity	Chen[b] (2017)(240)	29 PD	CB, MCP, parietal WM	n.s.	-	⊕	CB[l]
Heart Rate Variability during REM Sleep: High Frequency Components	Pyatigorskaya (2016)(58)	52 PD	Brainstem, hippocampus	N/A	N/A	⊕	Medulla oblongata[avg]
Heart Rate Variability during REM Sleep: Low Frequency Components	Pyatigorskaya (2016)(58)	52 PD	Brainstem, hippocampus	N/A	N/A	⊖	Medulla oblongata[avg]
Heart Rate Variability during REM Sleep: Low Frequency/High Frequency Ratio	Pyatigorskaya (2016)(58)	52 PD	Brainstem, hippocampus	N/A	N/A	⊖	Medulla oblongata[avg]
Heart Rate Variability during SWS Sleep: High Frequency Components	Pyatigorskaya (2016)(58)	52 PD	Brainstem, hippocampus	N/A	N/A	n.s.	-
Heart Rate Variability during SWS Sleep: Low Frequency Components	Pyatigorskaya (2016)(58)	52 PD	Brainstem, hippocampus	N/A	N/A	n.s.	-
Heart Rate Variability during SWS Sleep: Low Frequency/High Frequency Ratio	Pyatigorskaya (2016)(58)	52 PD	Brainstem, hippocampus	N/A	N/A	n.s.	-
NMSS - Cardiovascular	Wei (2016)(121)	43 PD	BG, frontal WM, hippocampus, occipital WM, parietal WM, SN, temporal WM	n.s.	-	N/A	N/A
Respiratory Variability during REM Sleep	Pyatigorskaya (2016)(58)	52 PD	Brainstem, hippocampus	N/A	N/A	⊖	Medulla oblongata[avg]
Respiratory Variability during SWS Sleep	Pyatigorskaya (2016)(58)	52 PD	Brainstem, hippocampus	N/A	N/A	n.s.	-
Other Non-Motor Symptoms							

Table A2: DTI literature on other non-motor symptoms in PD

Other Non-Motor Symptoms							
Measure	Author	Groups	Regions Analyzed	FA	FA-Location	MD	MD-Location
NMSS - Miscellaneous	Wei (2016)(121)	43 PD	BG, frontal WM, hippocampus, occipital WM, parietal WM, SN, temporal WM	n.s.	-	N/A	N/A
NMSS - Sexual Function	Wei (2016)(121)	43 PD	BG, frontal WM, hippocampus, occipital WM, parietal WM, SN, temporal WM	n.s.	-	N/A	N/A
UPDRS-I - Light-Headedness on Standing	Andica (2019)(52)	20 PD	Whole-brain WM and GM	n.s.	-	n.s.	-

WM: white matter; CB: Cingulate bundle; ILF: inferior longitudinal fasciculus; SLF: superior longitudinal fasciculus, IFOF: inferior fronto-occipital fasciculus, UF: uncinate fasciculus, CC: corpus callosum; IC: internal capsule; SN: substantia nigra; EC: external capsule; CST: corticospinal tract; SCP: superior cerebellar peduncle; CR: corona radiata; ATR: anterior thalamic radiation; CG: cingulate gyrus; SFOF: superior fronto-occipital fasciculus; FMi: forceps minor; MFG: middle frontal gyrus; IFG: inferior frontal gyrus; OFC: orbitofrontal cortex; IPG: inferior parietal gyrus; GP: globus pallidus; BG: basal ganglia; FMa: forceps major; NBM: nucleus basalis of Meynert; PTR: posterior thalamic radiation; ACC: anterior cingulate cortex; PPN: pedunculopontine nucleus; SFG: superior frontal gyrus; ICP: inferior cerebellar peduncle; MCP: middle cerebellar peduncle

↓ = significant decrease; ↑ = significant increase; ⊕ = significant positive association; ⊖ = significant positive association; ? = significant finding, but direction unspecified; N/A = the study did not report or measure the parameter.

Appendix B

Figure B1: Maps of MD (axial view) obtained from hippocampal segmentations of all participants within the healthy control (HC) and Lewy Body groups (Parkinson's Disease [PD], Parkinson's Disease with Mild Cognitive Impairment [PD-MCI], and Dementia with Lewy Bodies [DLB])

	Axial Map	**Axial Map (z-projection of the voxels with the maximum intensity across all slices)**
	Scale ($x10^{-3}$) 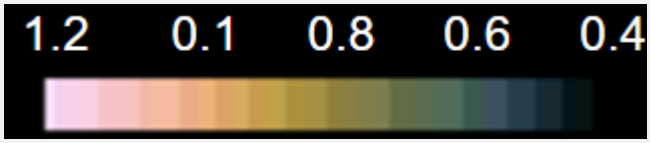	**Scale ($x10^{-3}$)** 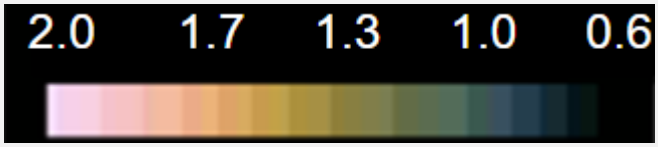
Diagnosis: HC; Age: 50, Sex: Female	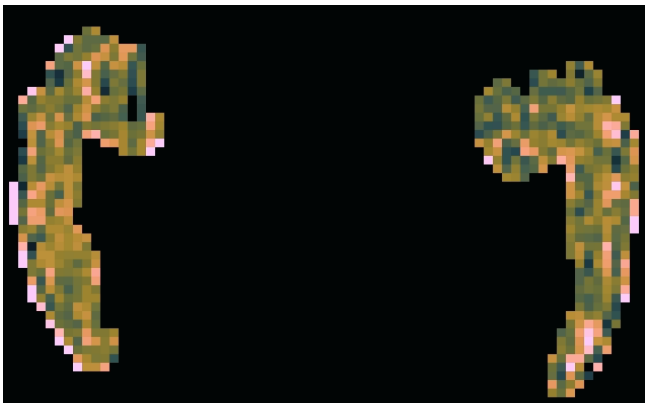	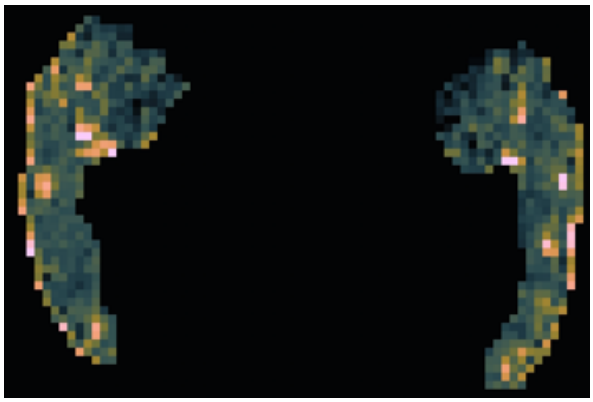
Diagnosis: HC; Age: 57, Sex: Female	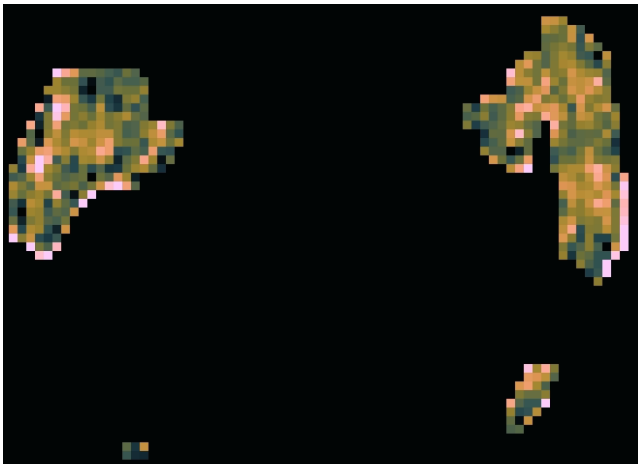	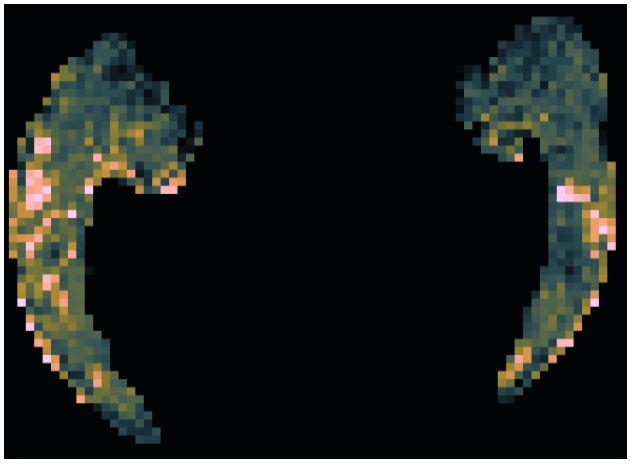

Figure B1: Maps of MD (axial view) obtained from hippocampal segmentations of all participants within the healthy control (HC) and Lewy Body groups (Parkinson's Disease [PD], Parkinson's Disease with Mild Cognitive Impairment [PD-MCI], and Dementia with Lewy Bodies [DLB])

	Axial Map	**Axial Map (z-projection of the voxels with the maximum intensity across all slices)**
	Scale (x10^{-3})	**Scale (x10^{-3})**
	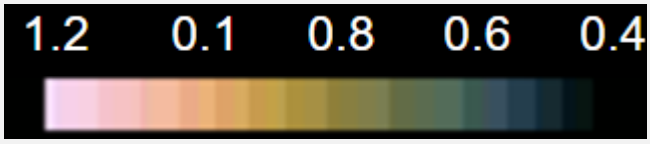	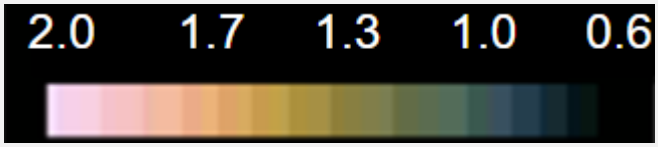
Diagnosis: HC; Age: 58, Sex: Female	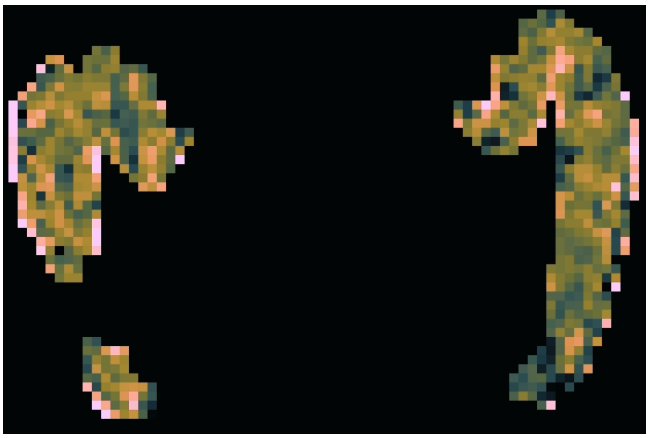	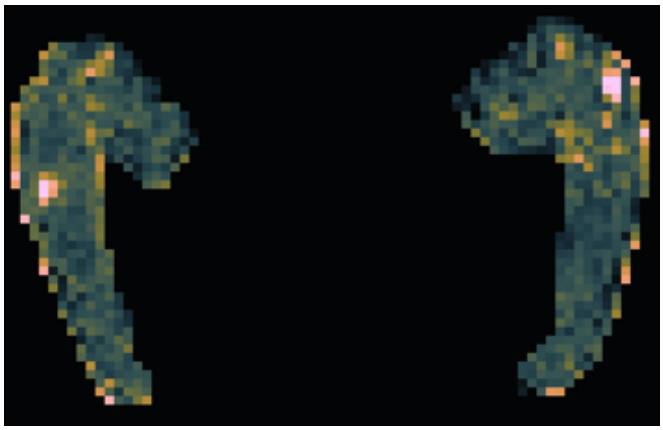
Diagnosis: HC; Age: 58, Sex: Female	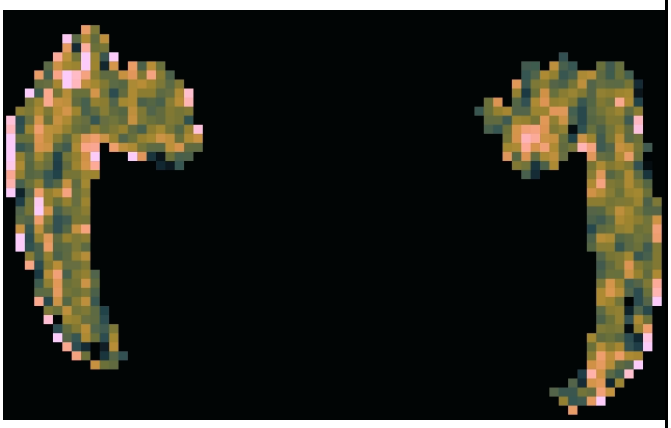	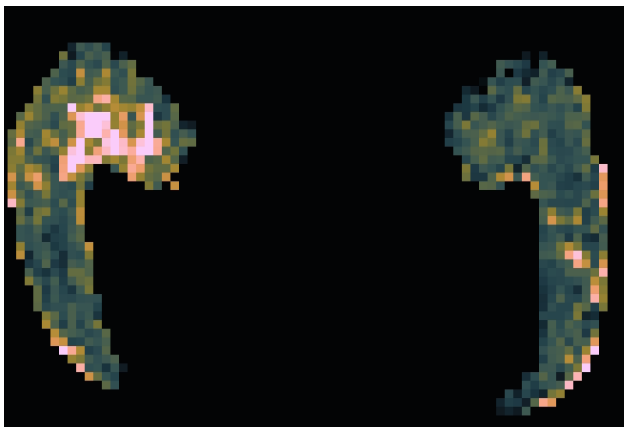

Figure B1: Maps of MD (axial view) obtained from hippocampal segmentations of all participants within the healthy control (HC) and Lewy Body groups (Parkinson's Disease [PD], Parkinson's Disease with Mild Cognitive Impairment [PD-MCI], and Dementia with Lewy Bodies [DLB])

	Axial Map	**Axial Map (z-projection of the voxels with the maximum intensity across all slices)**
	Scale ($x10^{-3}$) 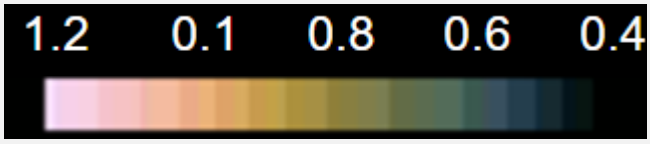	**Scale ($x10^{-3}$)** 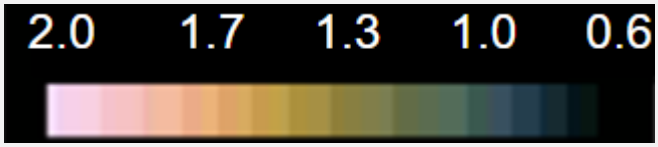
Diagnosis: HC; Age: 58, Sex: Male	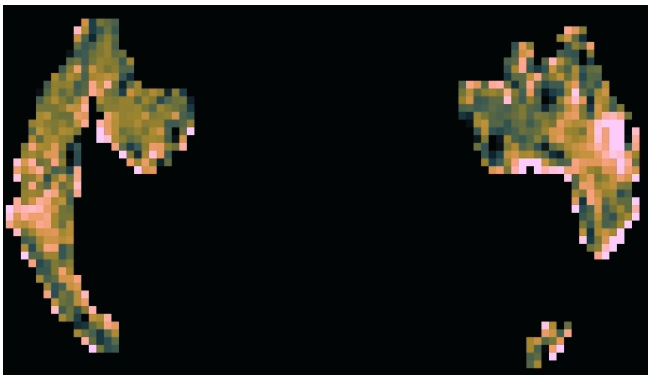	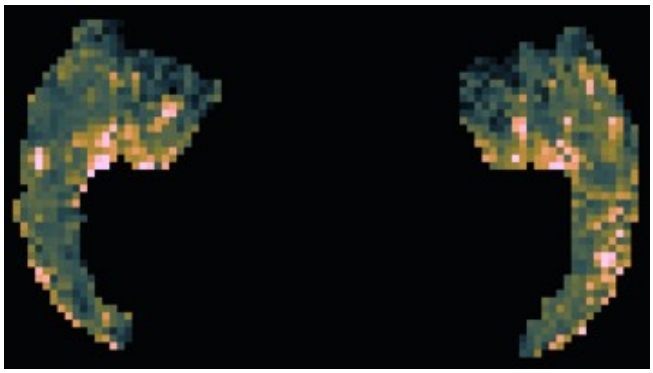
Diagnosis: HC; Age: 60, Sex: Male	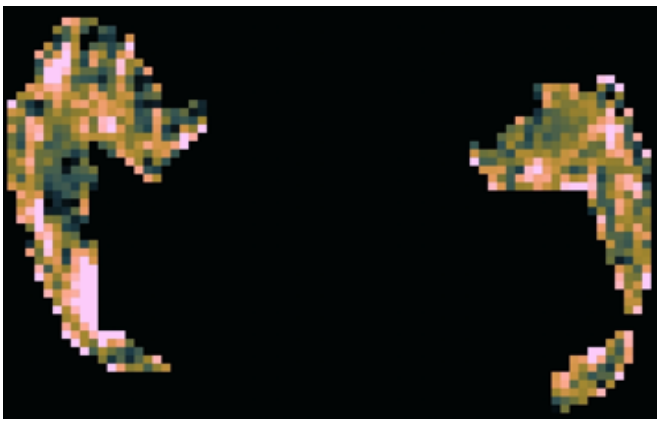	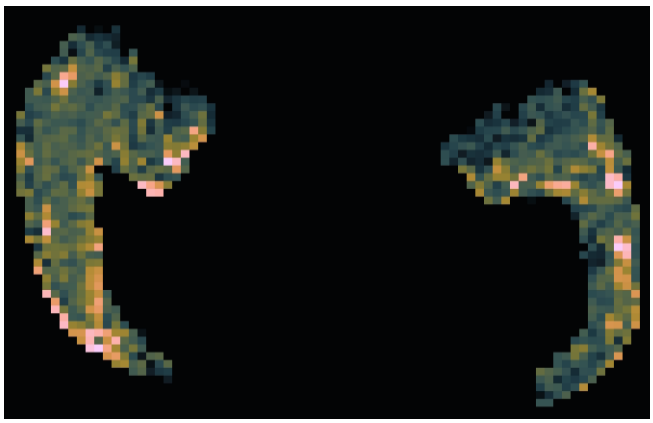
Diagnosis: HC; Age: 60, Sex: Male	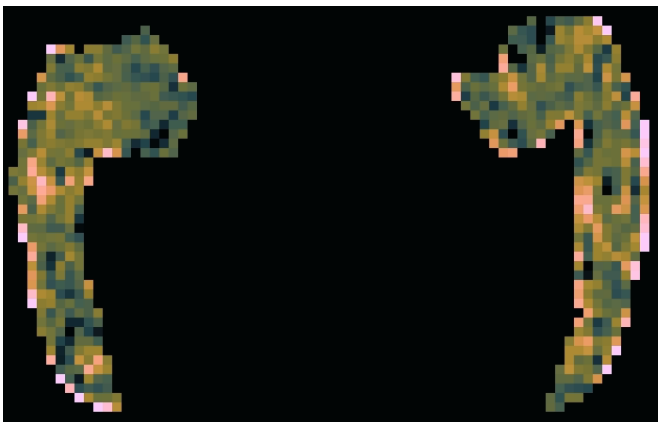	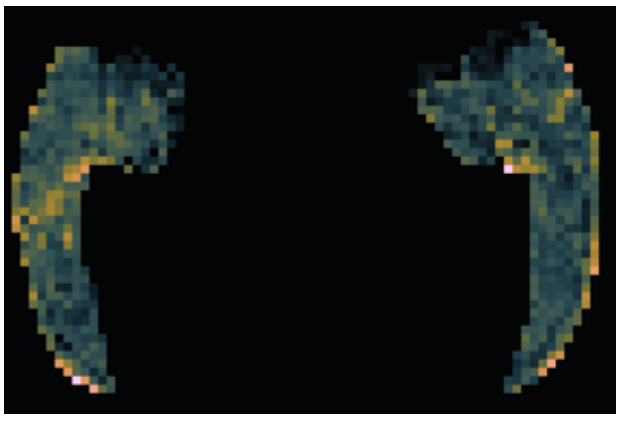

Figure B1: Maps of MD (axial view) obtained from hippocampal segmentations of all participants within the healthy control (HC) and Lewy Body groups (Parkinson's Disease [PD], Parkinson's Disease with Mild Cognitive Impairment [PD-MCI], and Dementia with Lewy Bodies [DLB])

	Axial Map	**Axial Map (z-projection of the voxels with the maximum intensity across all slices)**
	Scale ($x10^{-3}$) 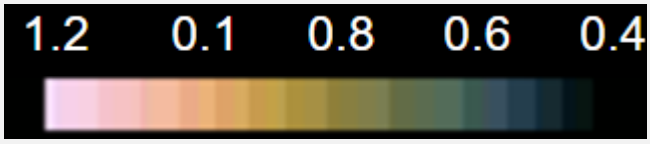	**Scale ($x10^{-3}$)** 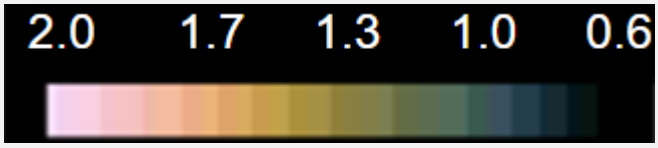
Diagnosis: HC; Age: 61, Sex: Male	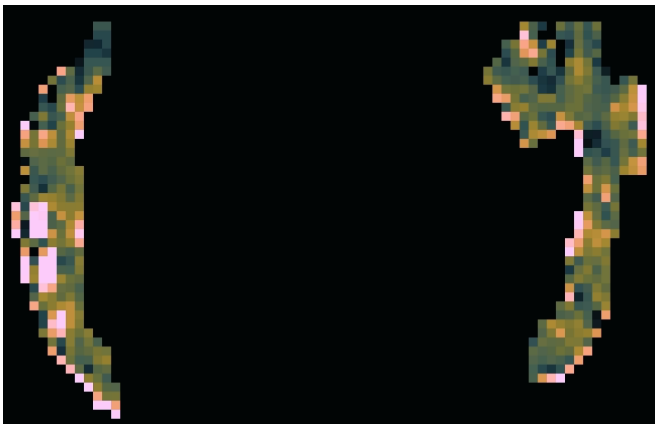	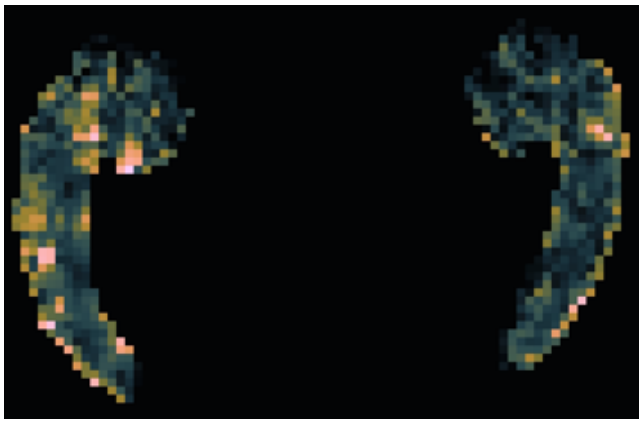
Diagnosis: HC; Age: 62, Sex: Female		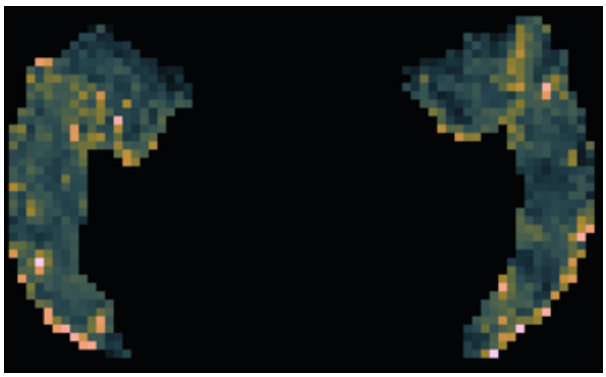
Diagnosis: HC; Age: 62, Sex: Male	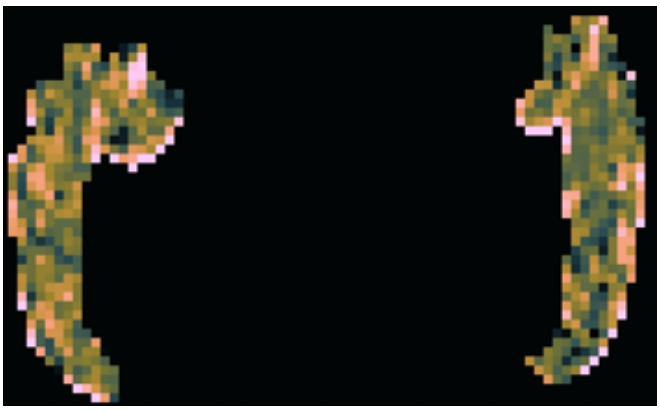	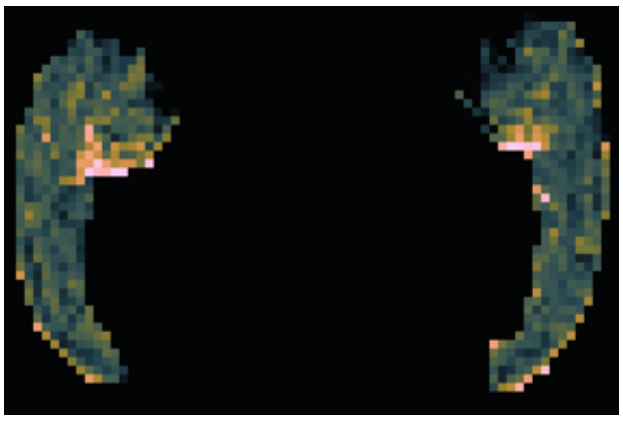

Figure B1: Maps of MD (axial view) obtained from hippocampal segmentations of all participants within the healthy control (HC) and Lewy Body groups (Parkinson's Disease [PD], Parkinson's Disease with Mild Cognitive Impairment [PD-MCI], and Dementia with Lewy Bodies [DLB])

	Axial Map	**Axial Map (z-projection of the voxels with the maximum intensity across all slices)**
	Scale (x10^{-3}) 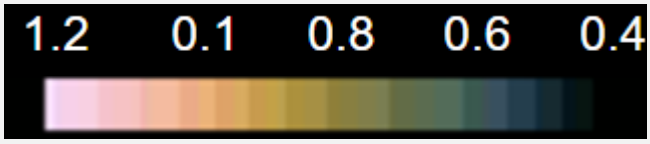	**Scale (x10^{-3})** 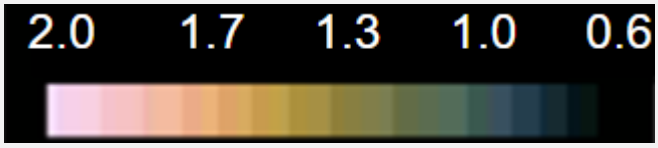
Diagnosis: HC; Age: 62, Sex: Male	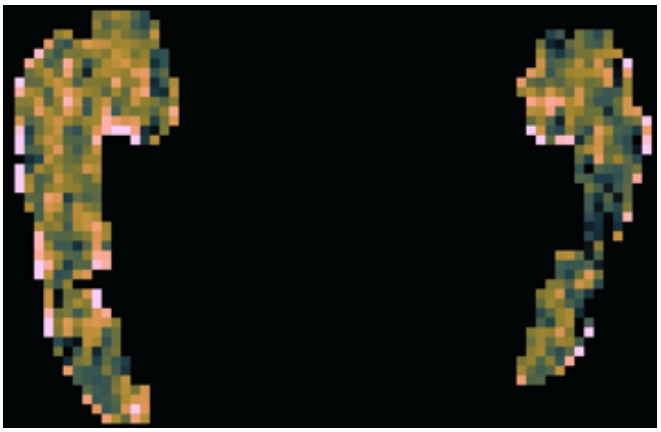	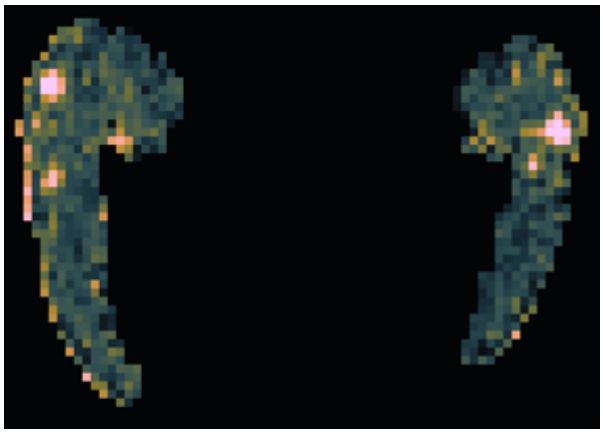
Diagnosis: HC; Age: 62, Sex: Male	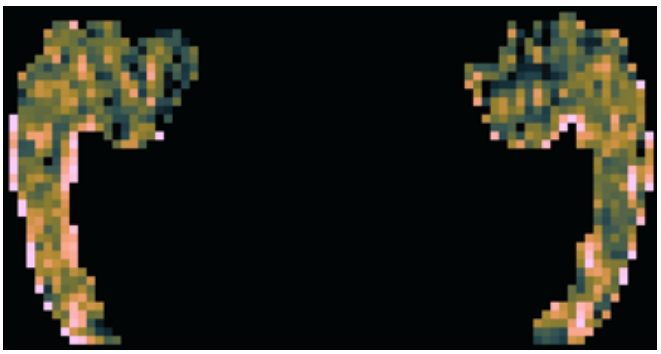	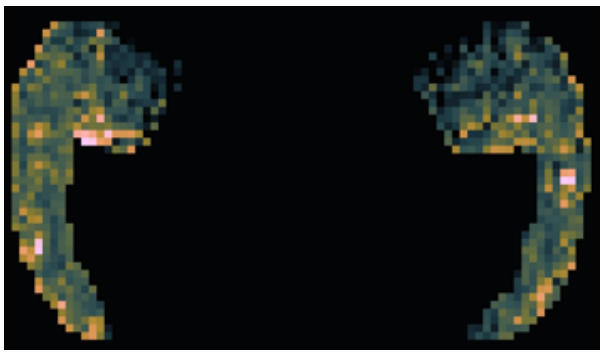
Diagnosis: HC; Age: 63, Sex: Female	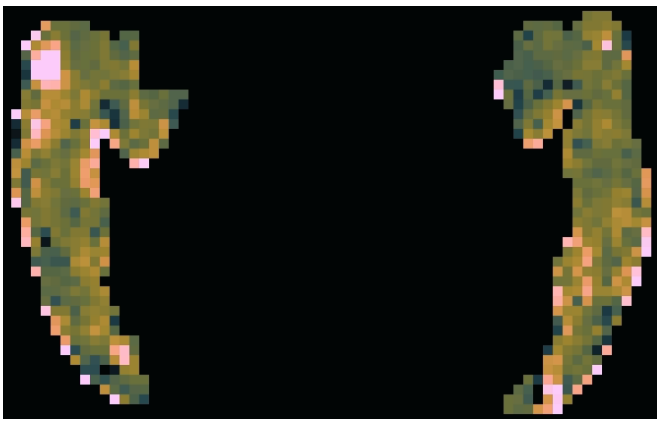	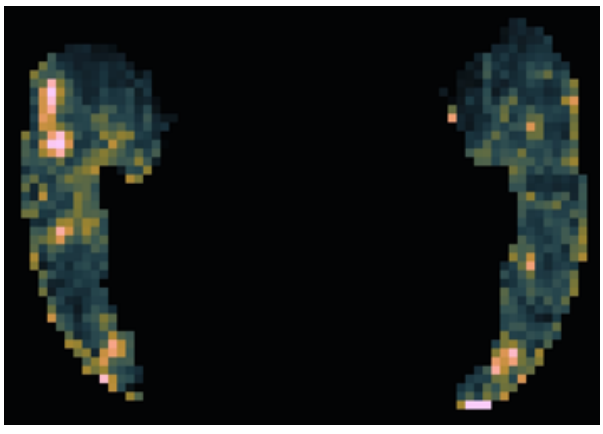

Figure B1: Maps of MD (axial view) obtained from hippocampal segmentations of all participants within the healthy control (HC) and Lewy Body groups (Parkinson's Disease [PD], Parkinson's Disease with Mild Cognitive Impairment [PD-MCI], and Dementia with Lewy Bodies [DLB])

	Axial Map	**Axial Map (z-projection of the voxels with the maximum intensity across all slices)**
	Scale (x10^{-3}) 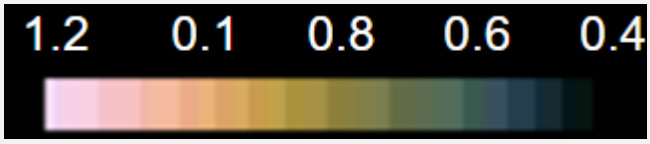	**Scale (x10^{-3})** 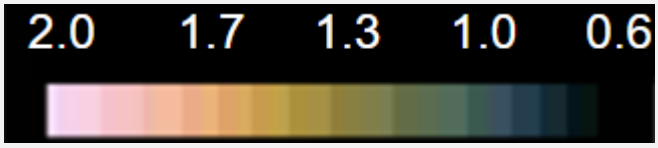
Diagnosis: HC; Age: 65, Sex: Female	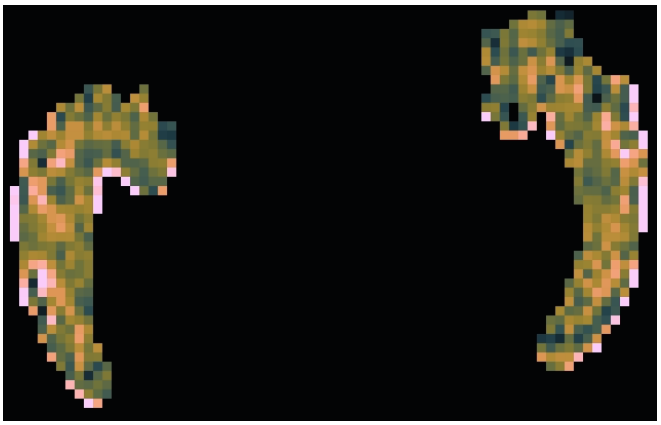	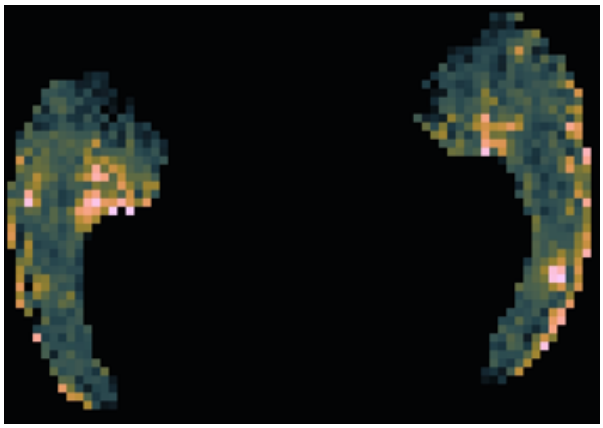
Diagnosis: HC; Age: 65, Sex: Female	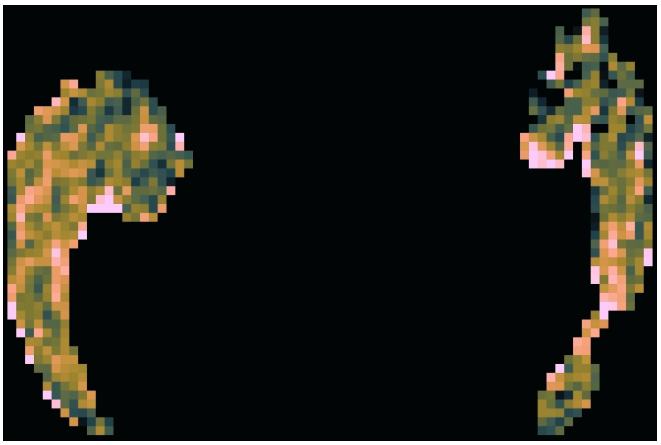	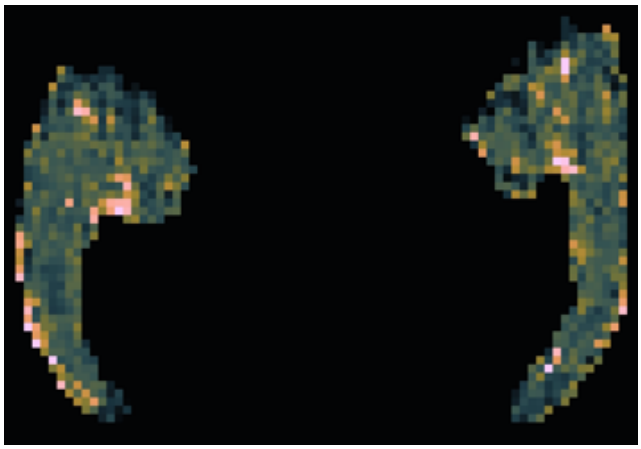

Figure B1: Maps of MD (axial view) obtained from hippocampal segmentations of all participants within the healthy control (HC) and Lewy Body groups (Parkinson's Disease [PD], Parkinson's Disease with Mild Cognitive Impairment [PD-MCI], and Dementia with Lewy Bodies [DLB])

	Axial Map	**Axial Map (z-projection of the voxels with the maximum intensity across all slices)**
	Scale ($x10^{-3}$) 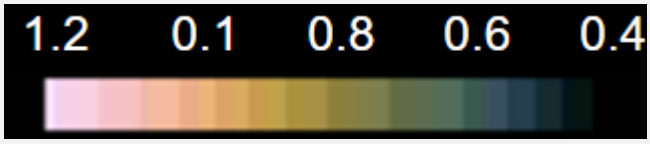	**Scale ($x10^{-3}$)** 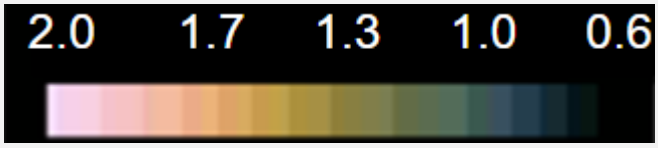
Diagnosis: HC; Age: 66, Sex: Male	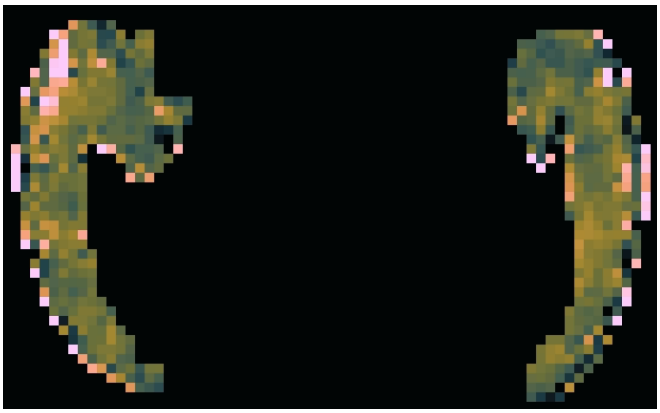	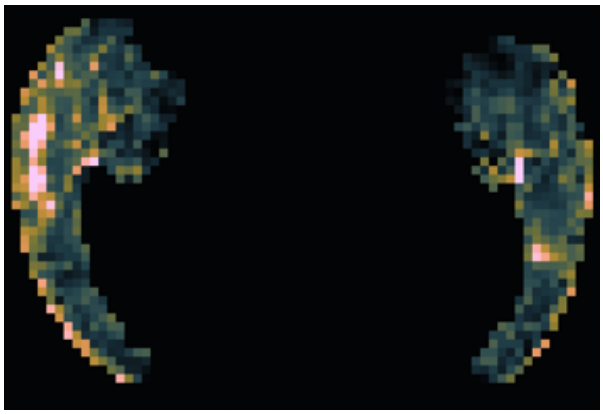
Diagnosis: HC; Age: 68, Sex: Male	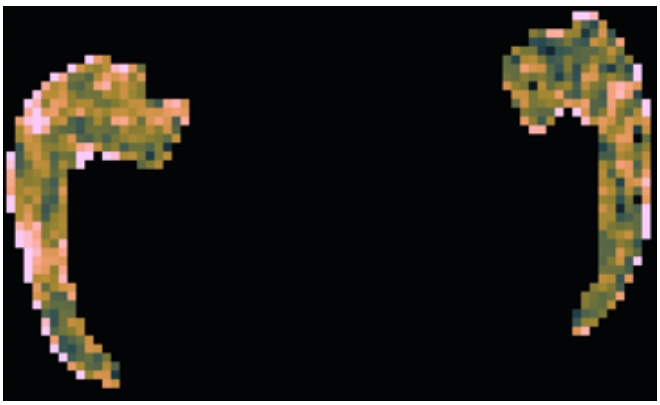	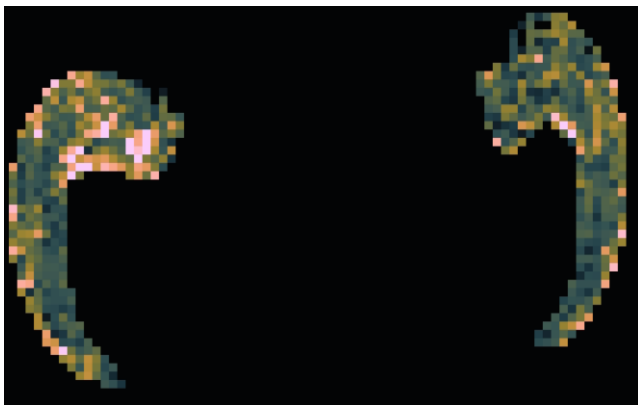

Figure B1: Maps of MD (axial view) obtained from hippocampal segmentations of all participants within the healthy control (HC) and Lewy Body groups (Parkinson's Disease [PD], Parkinson's Disease with Mild Cognitive Impairment [PD-MCI], and Dementia with Lewy Bodies [DLB])

	Axial Map	**Axial Map (z-projection of the voxels with the maximum intensity across all slices)**
	Scale ($x10^{-3}$) 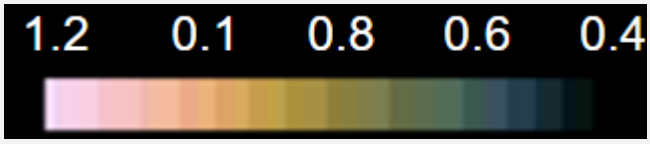	**Scale ($x10^{-3}$)** 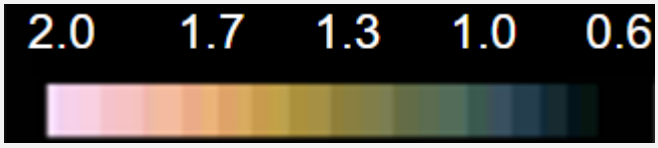
Diagnosis: HC; Age: 69, Sex: Female	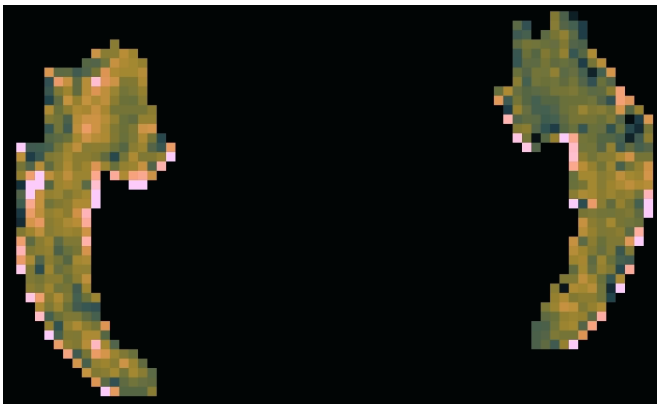	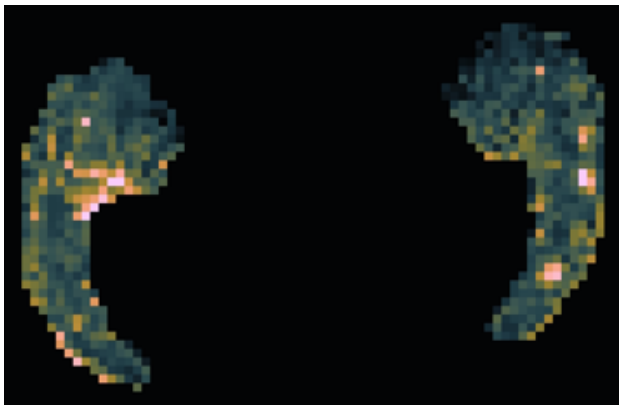
Diagnosis: HC; Age: 69, Sex: Male	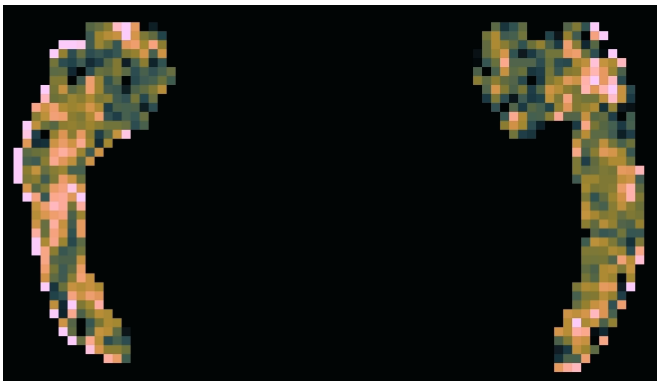	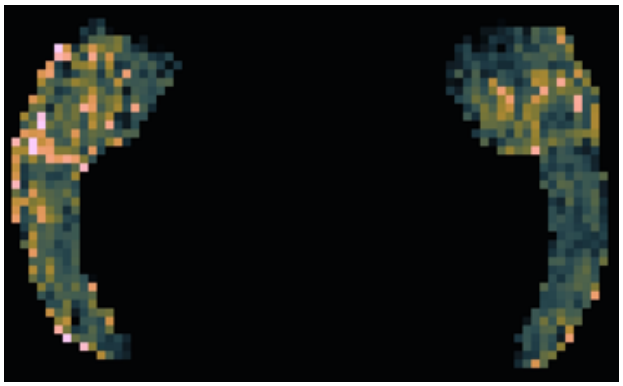
Diagnosis: HC; Age: 69, Sex: Male		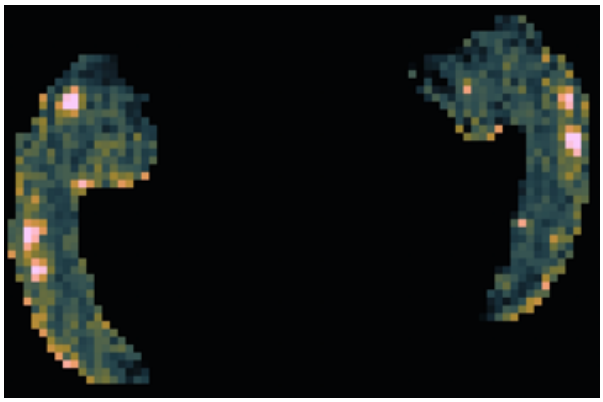

Figure B1: Maps of MD (axial view) obtained from hippocampal segmentations of all participants within the healthy control (HC) and Lewy Body groups (Parkinson's Disease [PD], Parkinson's Disease with Mild Cognitive Impairment [PD-MCI], and Dementia with Lewy Bodies [DLB])

	Axial Map	**Axial Map (z-projection of the voxels with the maximum intensity across all slices)**
	Scale (x10^{-3}) 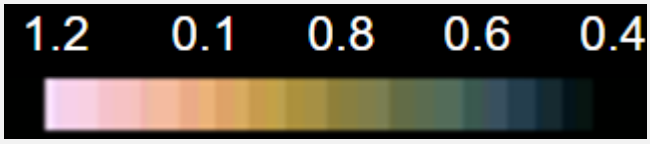	**Scale (x10^{-3})** 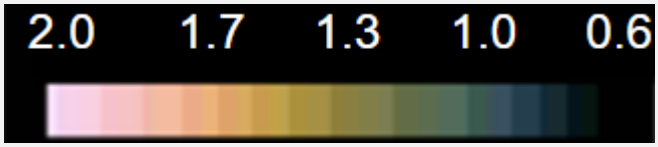
Diagnosis: HC; Age: 70, Sex: Female	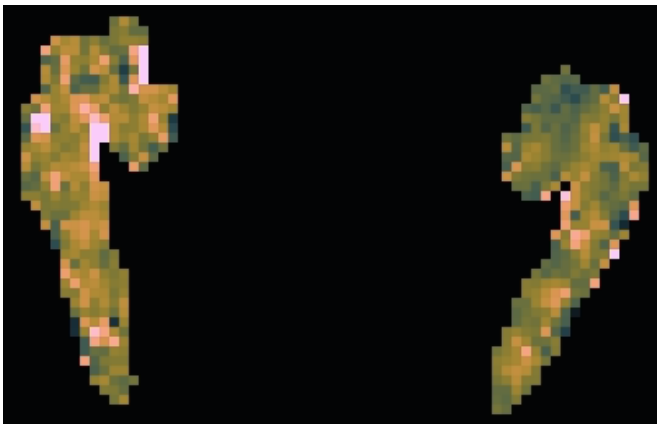	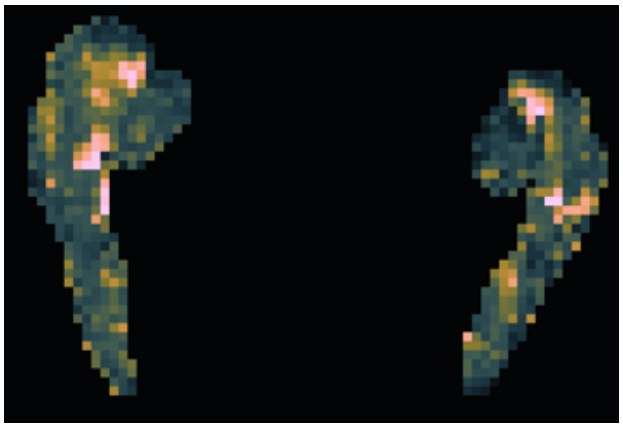
Diagnosis: HC; Age: 70, Sex: Female	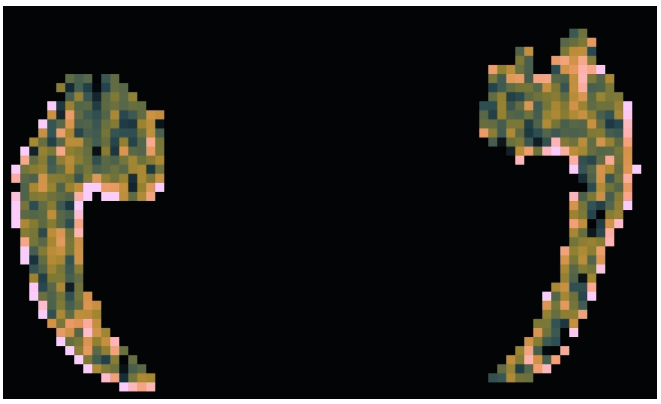	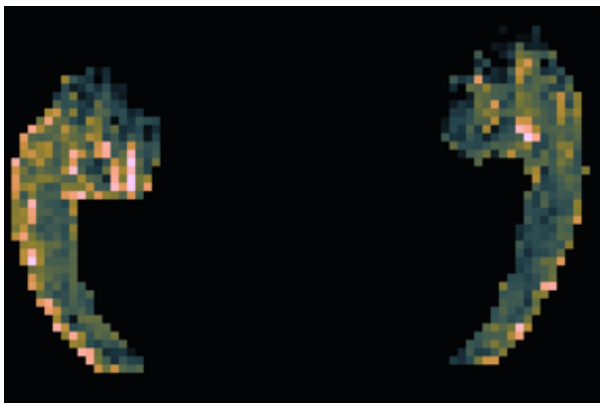

Figure B1: Maps of MD (axial view) obtained from hippocampal segmentations of all participants within the healthy control (HC) and Lewy Body groups (Parkinson's Disease [PD], Parkinson's Disease with Mild Cognitive Impairment [PD-MCI], and Dementia with Lewy Bodies [DLB])

	Axial Map	**Axial Map (z-projection of the voxels with the maximum intensity across all slices)**
	Scale (x10^{-3}) 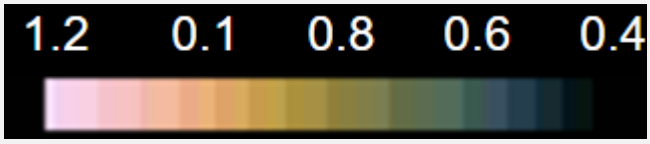	**Scale (x10^{-3})** 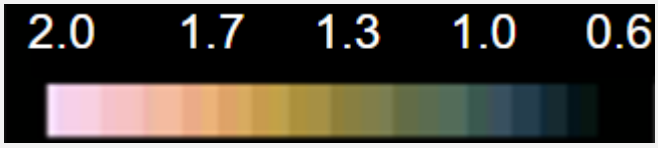
Diagnosis: HC; Age: 70, Sex: Female	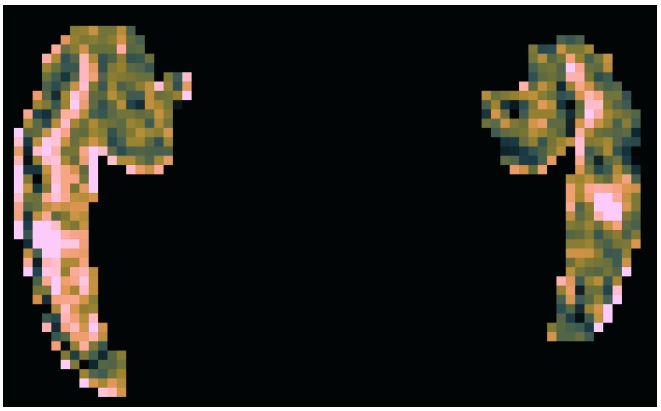	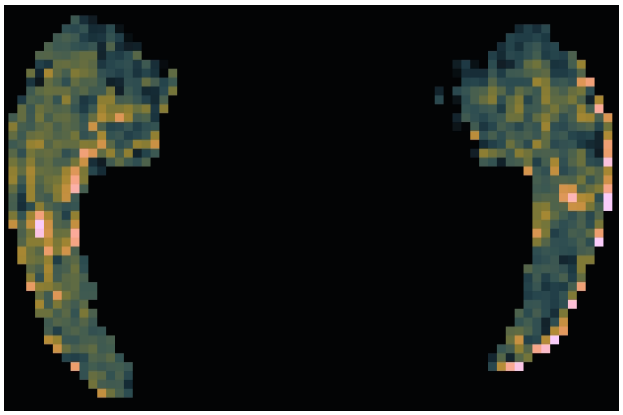
Diagnosis: HC; Age: 70, Sex: Female	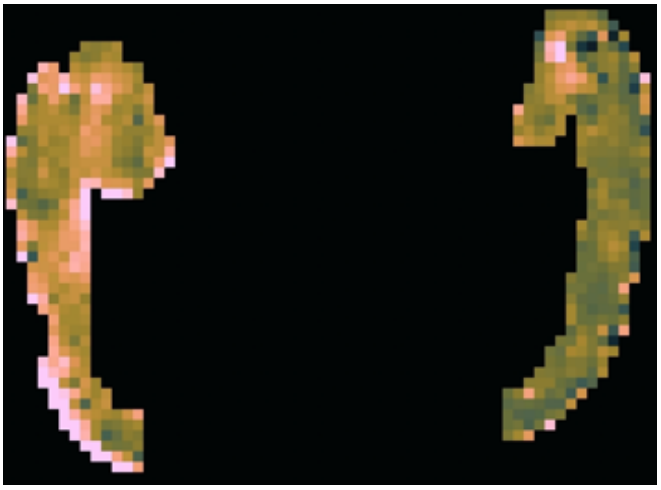	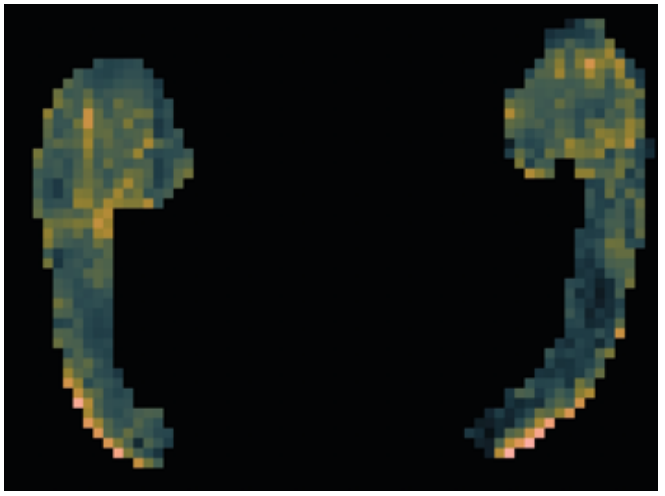

Figure B1: Maps of MD (axial view) obtained from hippocampal segmentations of all participants within the healthy control (HC) and Lewy Body groups (Parkinson's Disease [PD], Parkinson's Disease with Mild Cognitive Impairment [PD-MCI], and Dementia with Lewy Bodies [DLB])

	Axial Map	**Axial Map (z-projection of the voxels with the maximum intensity across all slices)**
	Scale (x10^{-3}) 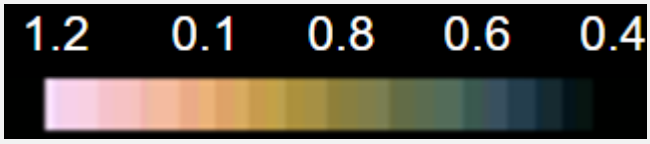	**Scale (x10^{-3})** 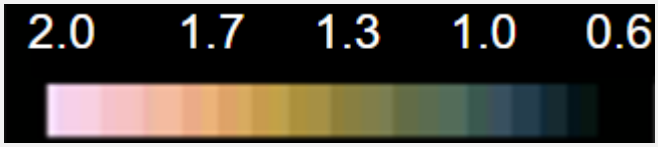
Diagnosis: HC; Age: 70, Sex: Female	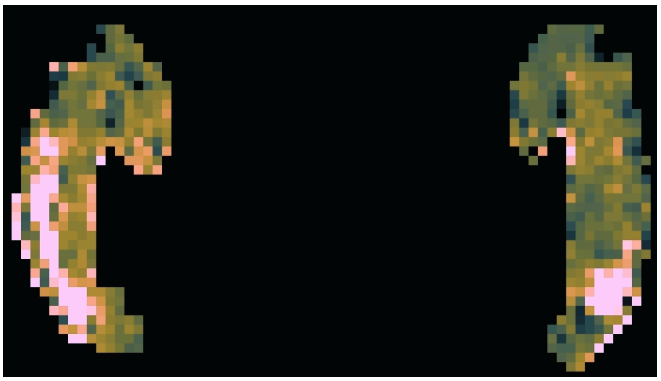	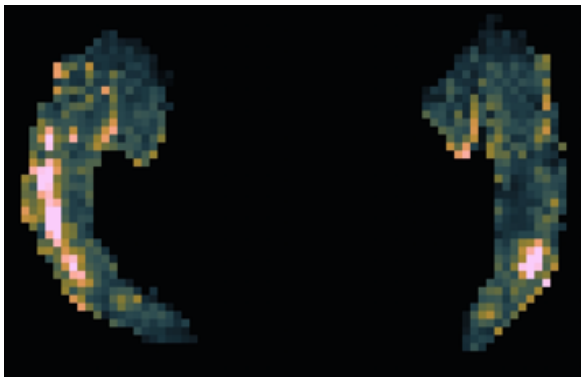
Diagnosis: HC; Age: 70, Sex: Male		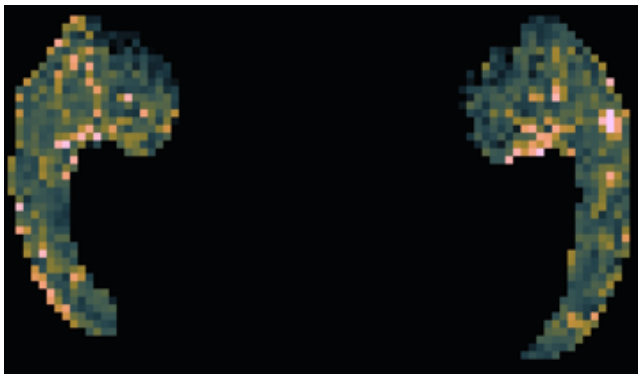
Diagnosis: HC; Age: 70, Sex: Male	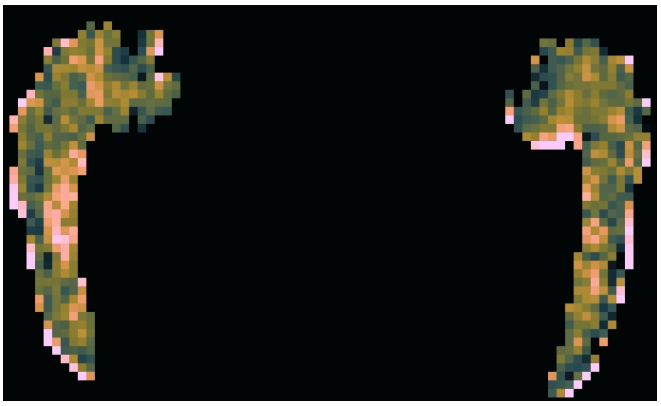	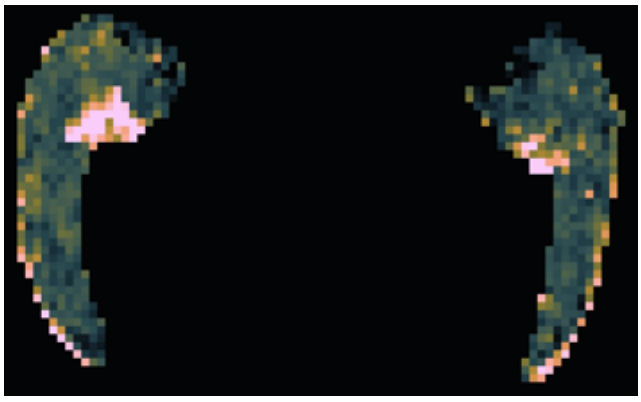

Figure B1: Maps of MD (axial view) obtained from hippocampal segmentations of all participants within the healthy control (HC) and Lewy Body groups (Parkinson's Disease [PD], Parkinson's Disease with Mild Cognitive Impairment [PD-MCI], and Dementia with Lewy Bodies [DLB])

	Axial Map	**Axial Map (z-projection of the voxels with the maximum intensity across all slices)**
	Scale (x10^{-3})	**Scale (x10^{-3})**
	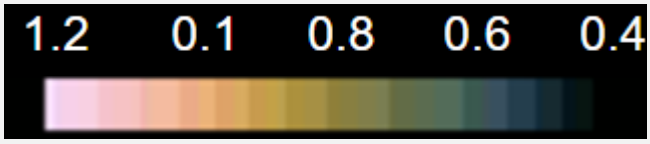	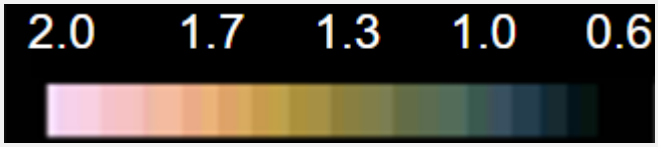
Diagnosis: HC; Age: 71, Sex: Female	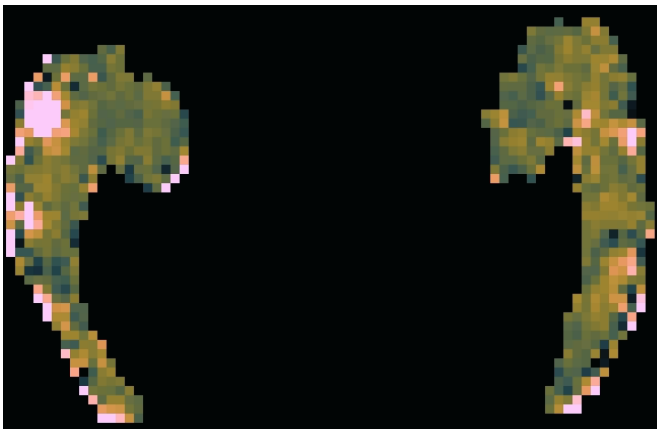	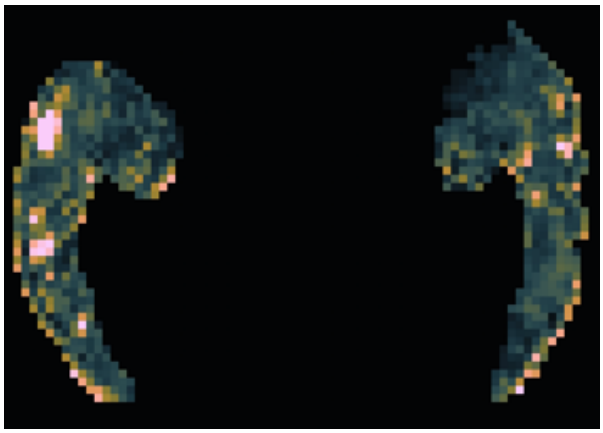
Diagnosis: HC; Age: 71, Sex: Male	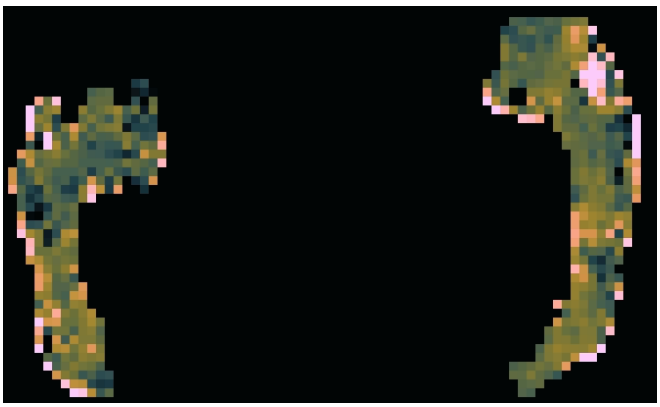	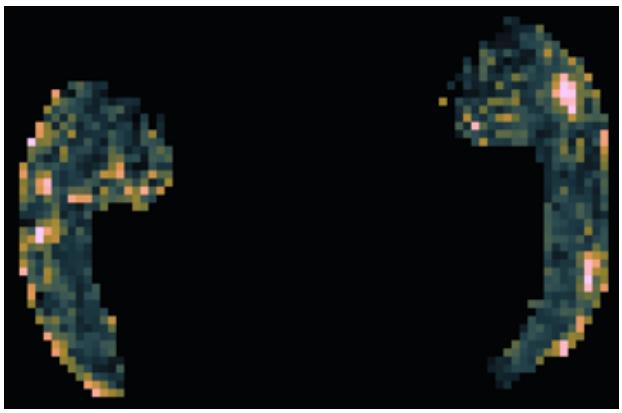

Figure B1: Maps of MD (axial view) obtained from hippocampal segmentations of all participants within the healthy control (HC) and Lewy Body groups (Parkinson's Disease [PD], Parkinson's Disease with Mild Cognitive Impairment [PD-MCI], and Dementia with Lewy Bodies [DLB])

	Axial Map	**Axial Map (z-projection of the voxels with the maximum intensity across all slices)**
	Scale (x10^{-3}) 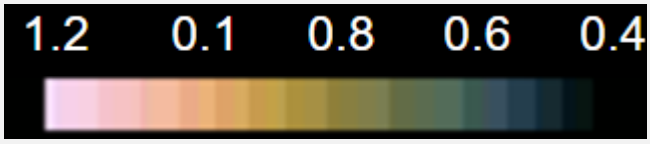	**Scale (x10^{-3})** 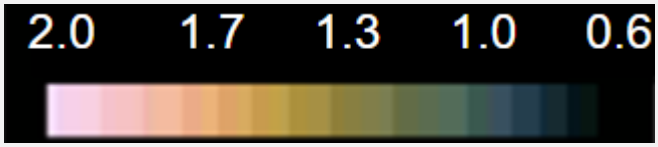
Diagnosis: HC; Age: 73, Sex: Male	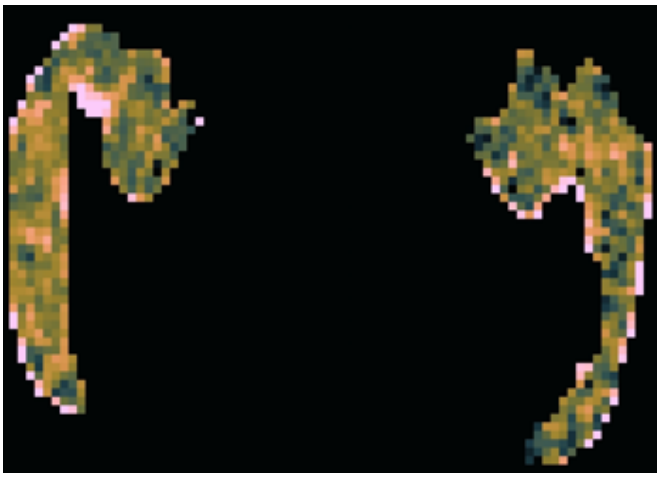	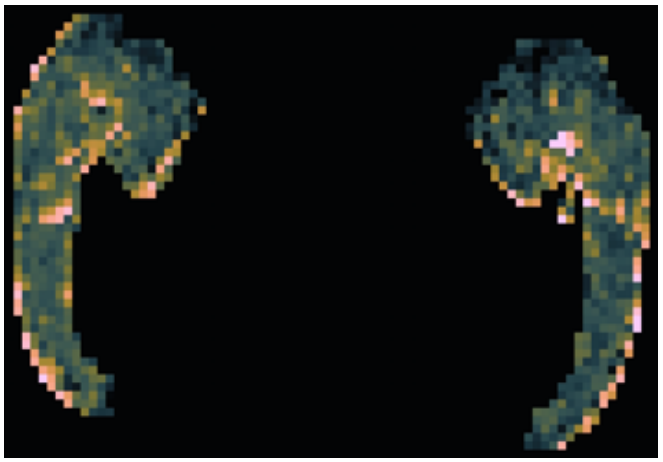
Diagnosis: HC; Age: 74, Sex: Female	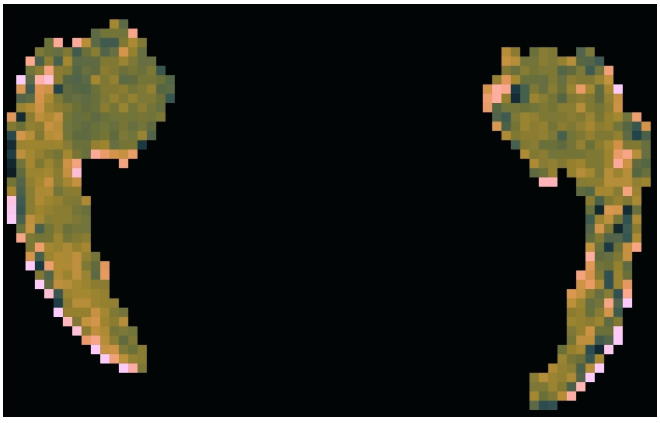	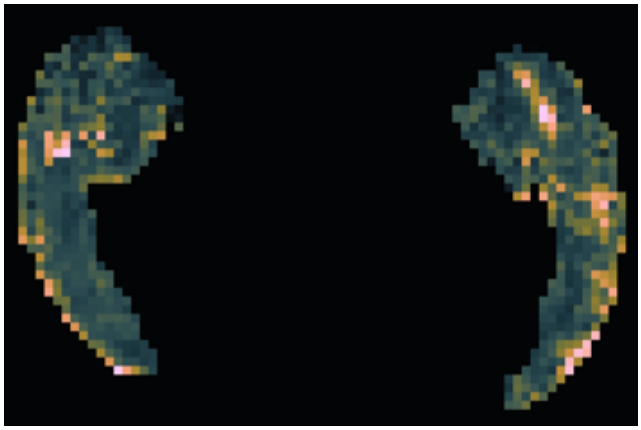

Figure B1: Maps of MD (axial view) obtained from hippocampal segmentations of all participants within the healthy control (HC) and Lewy Body groups (Parkinson's Disease [PD], Parkinson's Disease with Mild Cognitive Impairment [PD-MCI], and Dementia with Lewy Bodies [DLB])

	Axial Map	**Axial Map (z-projection of the voxels with the maximum intensity across all slices)**
	Scale (x10^{-3}) 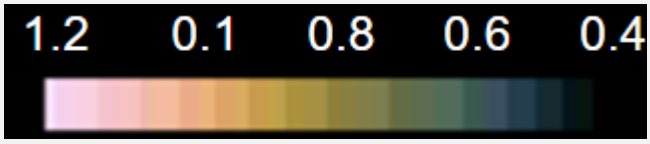	**Scale (x10^{-3})** 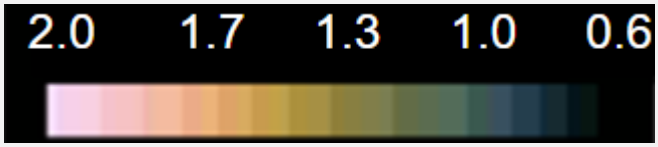
Diagnosis: HC; Age: 74, Sex: Male		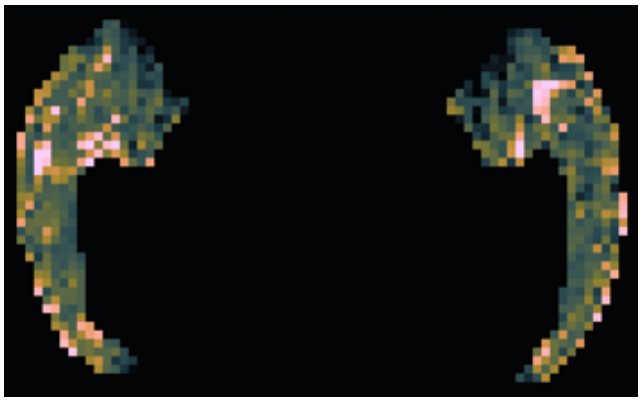
Diagnosis: HC; Age: 75, Sex: Female	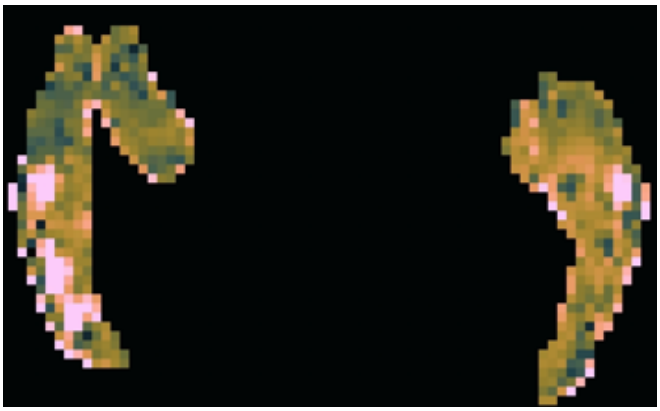	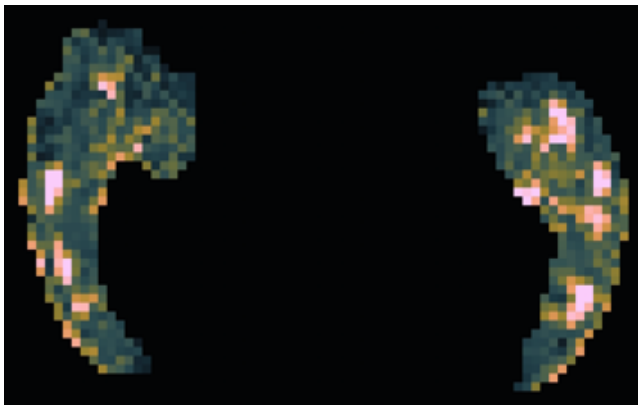
Diagnosis: HC; Age: 78, Sex: Female	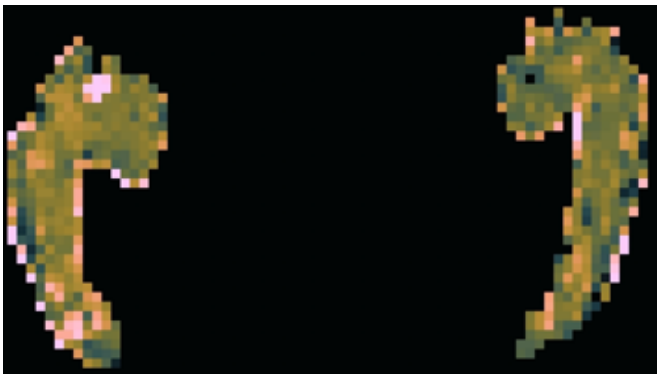	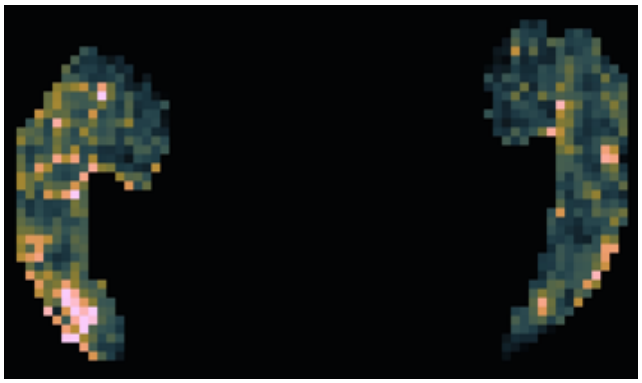

Figure B1: Maps of MD (axial view) obtained from hippocampal segmentations of all participants within the healthy control (HC) and Lewy Body groups (Parkinson's Disease [PD], Parkinson's Disease with Mild Cognitive Impairment [PD-MCI], and Dementia with Lewy Bodies [DLB])

	Axial Map	**Axial Map (z-projection of the voxels with the maximum intensity across all slices)**
	Scale ($x10^{-3}$) 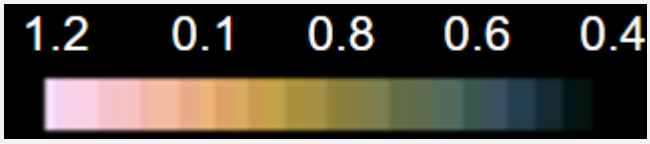	**Scale ($x10^{-3}$)** 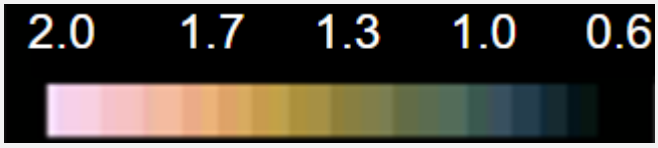
Diagnosis: HC; Age: 83, Sex: Female	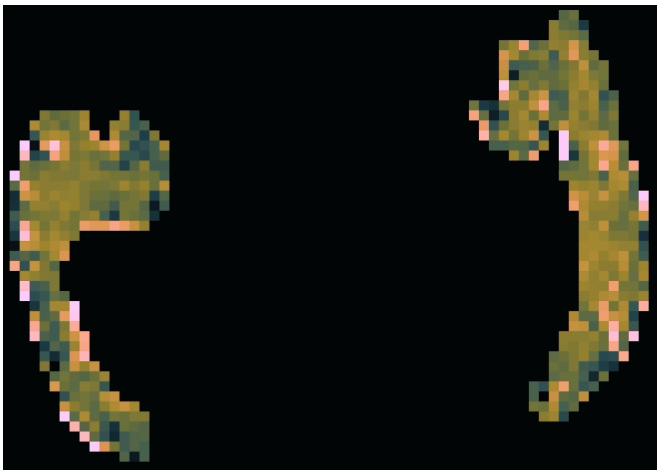	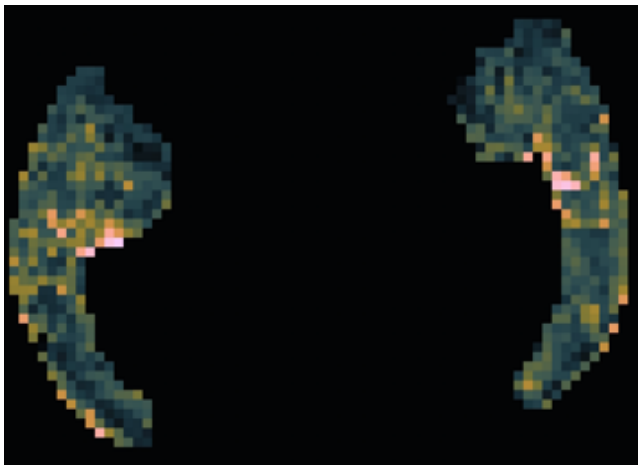
Diagnosis: PD; Age: 58, Sex: Female	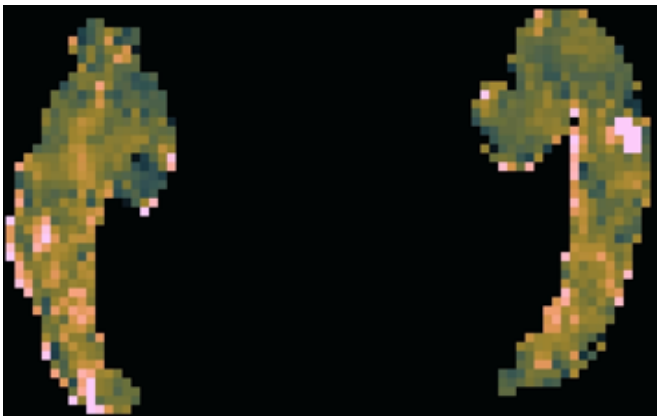	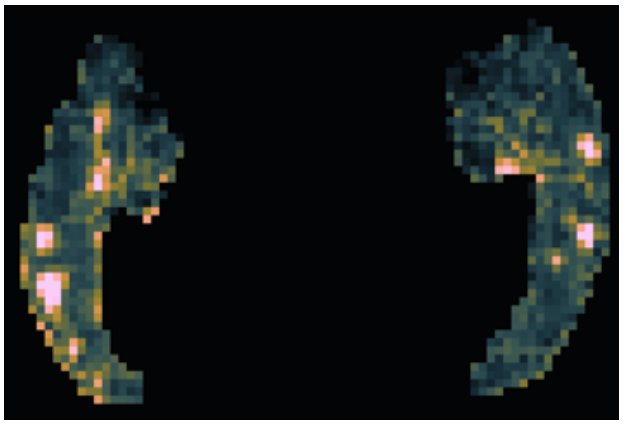

Figure B1: Maps of MD (axial view) obtained from hippocampal segmentations of all participants within the healthy control (HC) and Lewy Body groups (Parkinson's Disease [PD], Parkinson's Disease with Mild Cognitive Impairment [PD-MCI], and Dementia with Lewy Bodies [DLB])

	Axial Map	**Axial Map (z-projection of the voxels with the maximum intensity across all slices)**
	Scale ($x10^{-3}$) 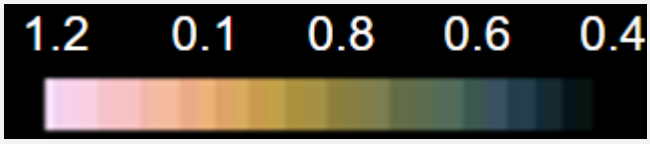	**Scale ($x10^{-3}$)** 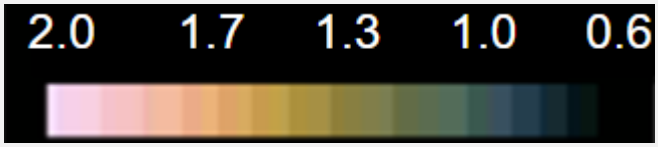
Diagnosis: PD; Age: 58, Sex: Female	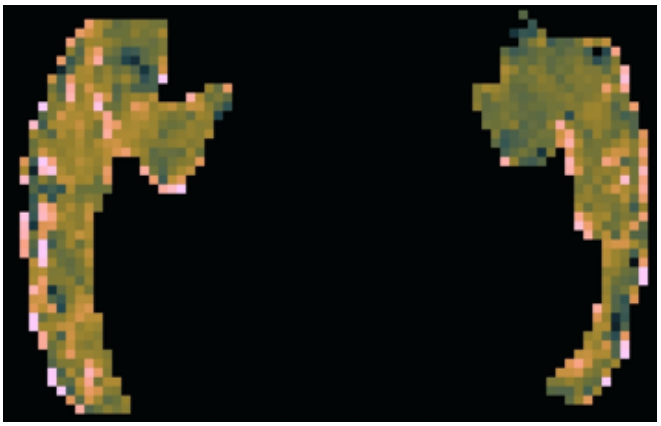	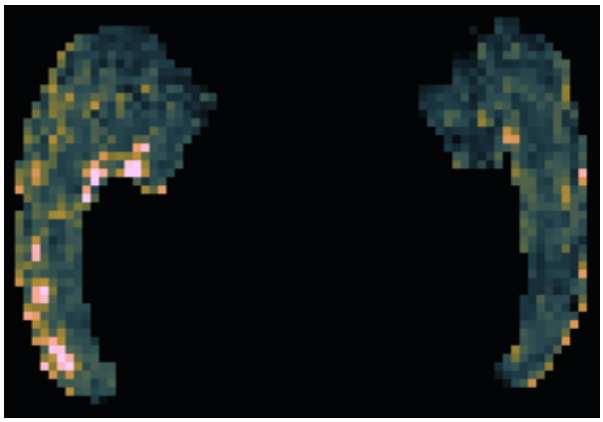
Diagnosis: PD; Age: 58, Sex: Male	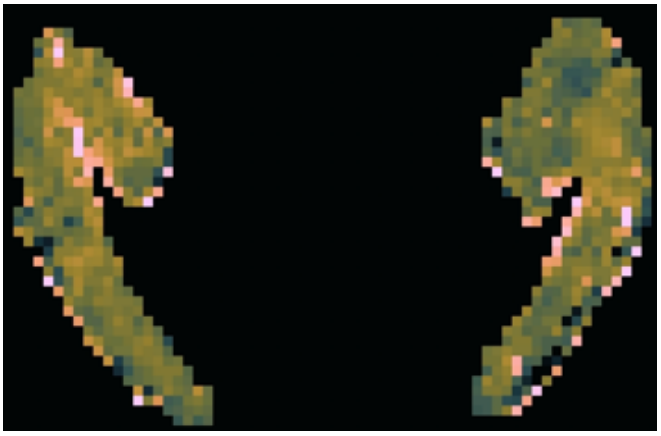	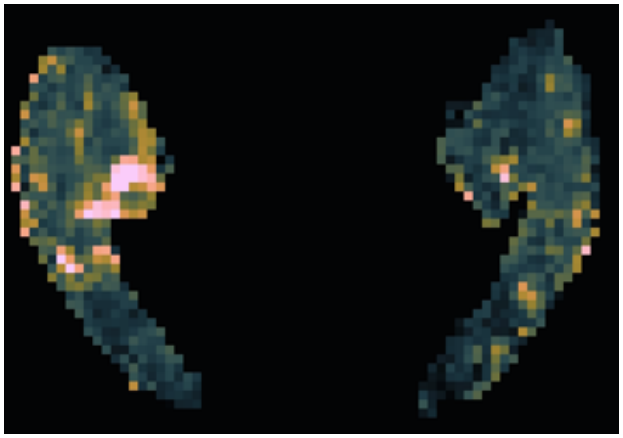

Figure B1: Maps of MD (axial view) obtained from hippocampal segmentations of all participants within the healthy control (HC) and Lewy Body groups (Parkinson's Disease [PD], Parkinson's Disease with Mild Cognitive Impairment [PD-MCI], and Dementia with Lewy Bodies [DLB])

	Axial Map	**Axial Map (z-projection of the voxels with the maximum intensity across all slices)**
	Scale ($x10^{-3}$) 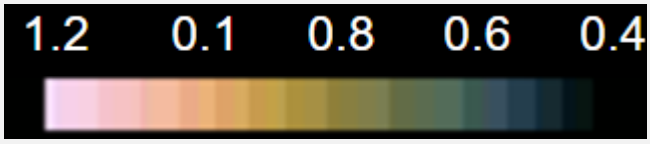	**Scale ($x10^{-3}$)** 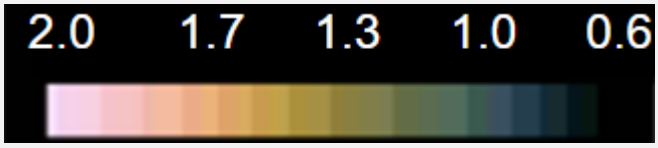
Diagnosis: PD; Age: 59, Sex: Female	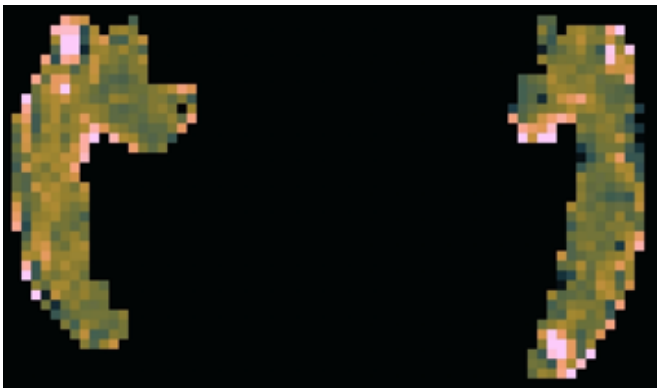	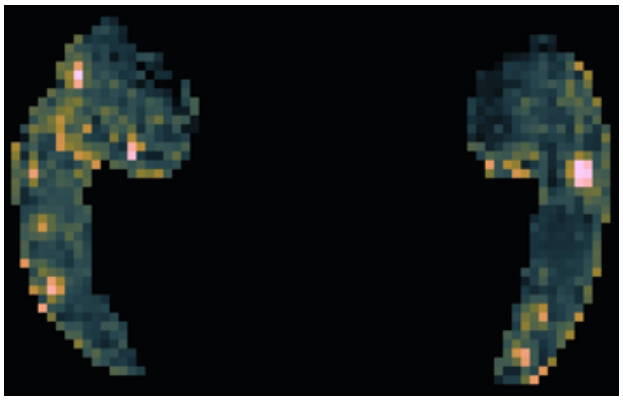
Diagnosis: PD; Age: 61, Sex: Male		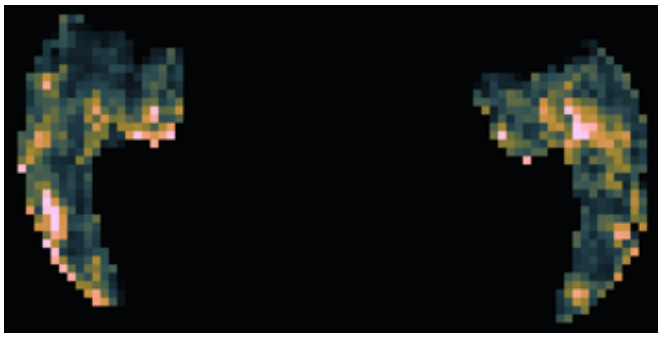
Diagnosis: PD; Age: 63, Sex: Male	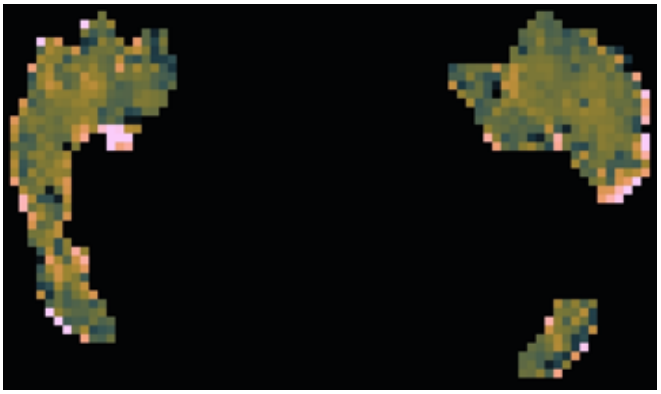	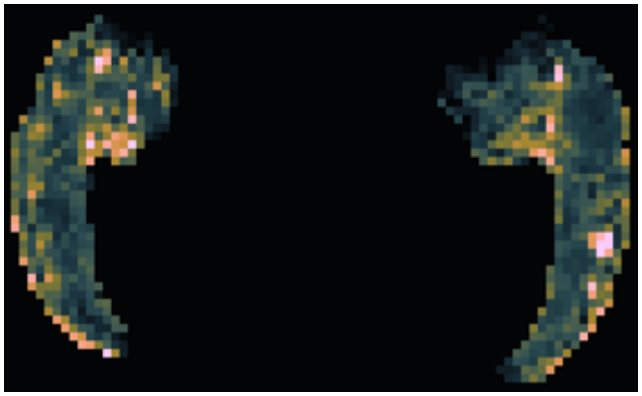

Figure B1: Maps of MD (axial view) obtained from hippocampal segmentations of all participants within the healthy control (HC) and Lewy Body groups (Parkinson's Disease [PD], Parkinson's Disease with Mild Cognitive Impairment [PD-MCI], and Dementia with Lewy Bodies [DLB])

	Axial Map	**Axial Map (z-projection of the voxels with the maximum intensity across all slices)**
	Scale (x10^{-3}) 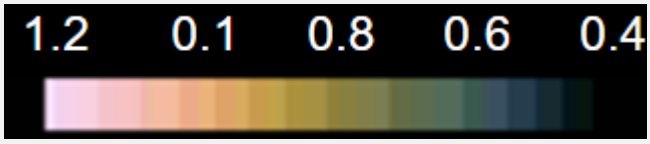	**Scale (x10^{-3})** 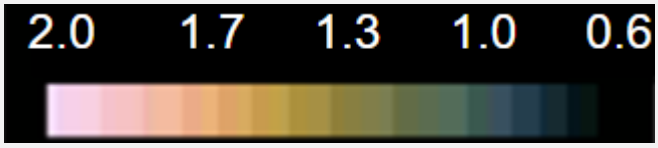
Diagnosis: PD; Age: 63, Sex: Male	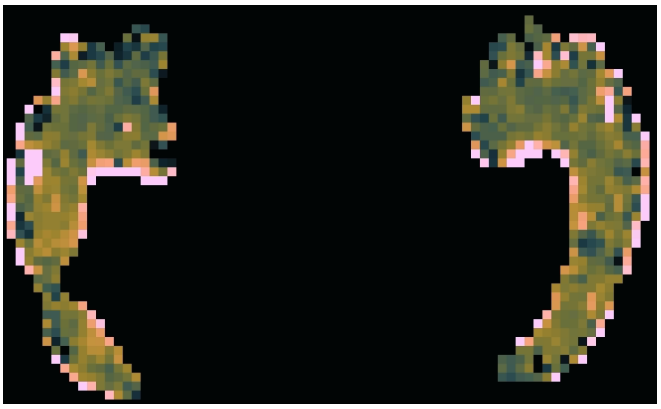	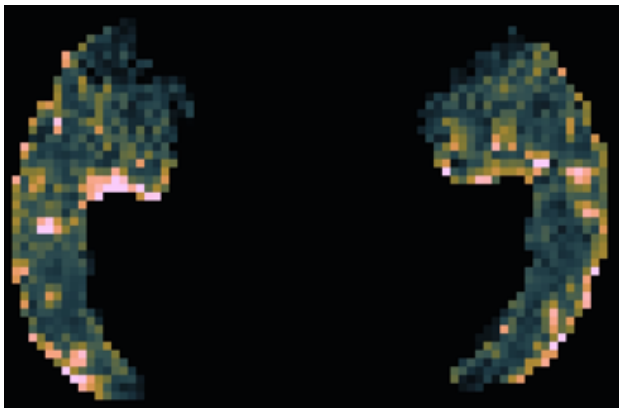
Diagnosis: PD; Age: 64, Sex: Female	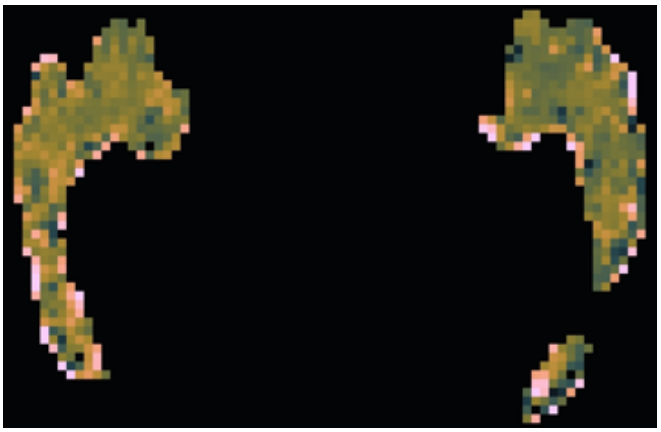	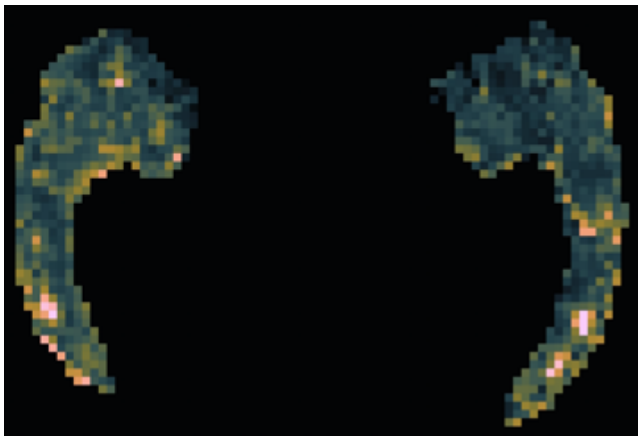

Figure B1: Maps of MD (axial view) obtained from hippocampal segmentations of all participants within the healthy control (HC) and Lewy Body groups (Parkinson's Disease [PD], Parkinson's Disease with Mild Cognitive Impairment [PD-MCI], and Dementia with Lewy Bodies [DLB])

	Axial Map	**Axial Map (z-projection of the voxels with the maximum intensity across all slices)**
	Scale ($x10^{-3}$) 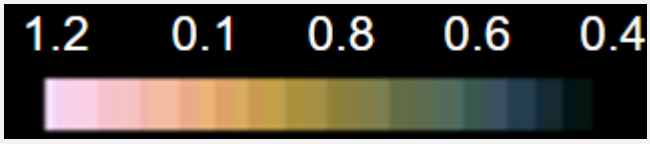	**Scale ($x10^{-3}$)** 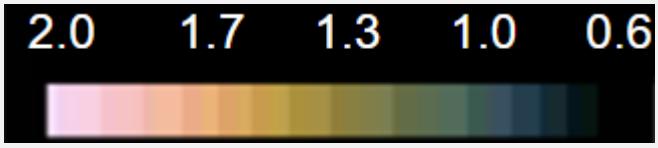
Diagnosis: PD; Age: 64, Sex: Female	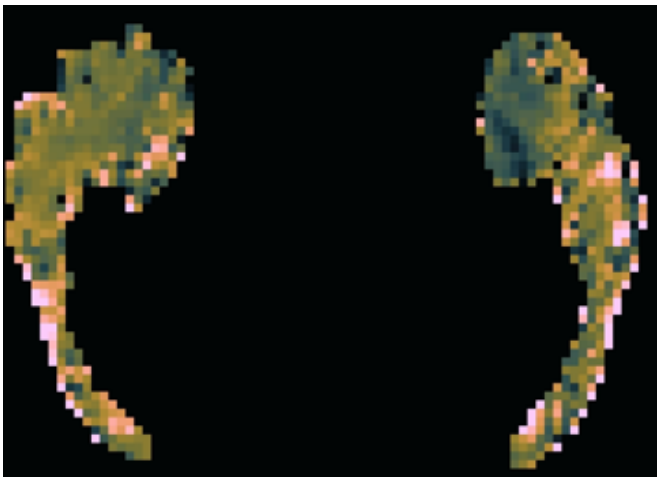	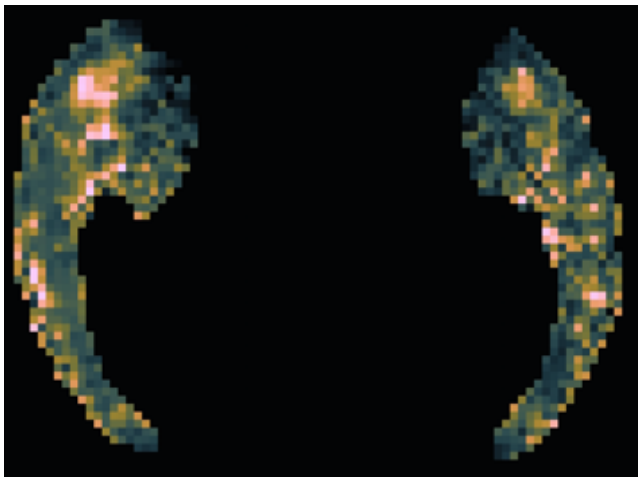
Diagnosis: PD; Age: 65, Sex: Female	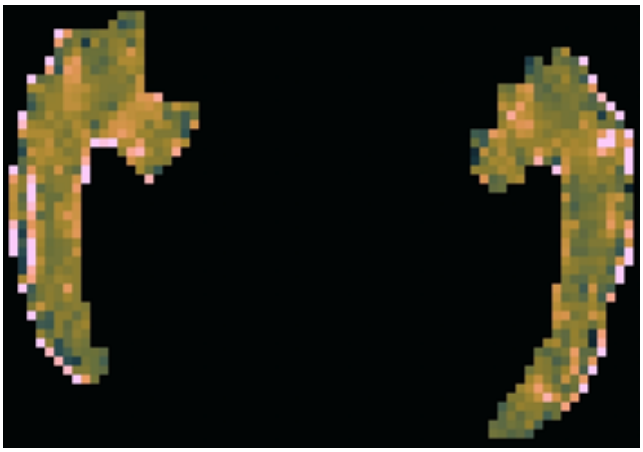	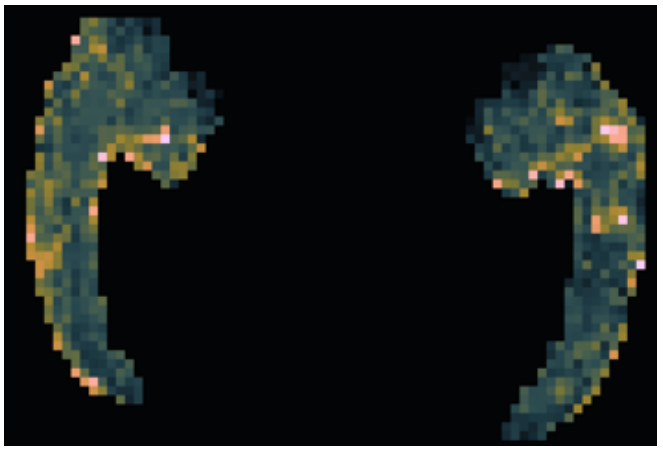

Figure B1: Maps of MD (axial view) obtained from hippocampal segmentations of all participants within the healthy control (HC) and Lewy Body groups (Parkinson's Disease [PD], Parkinson's Disease with Mild Cognitive Impairment [PD-MCI], and Dementia with Lewy Bodies [DLB])

	Axial Map	**Axial Map (z-projection of the voxels with the maximum intensity across all slices)**
	Scale ($x10^{-3}$) 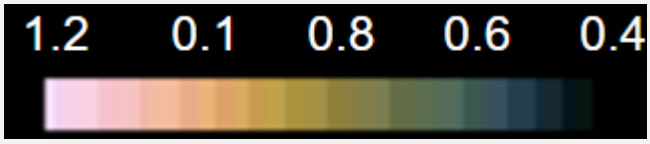	**Scale ($x10^{-3}$)** 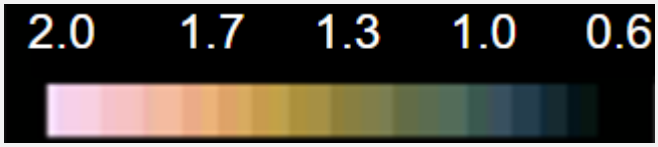
Diagnosis: PD; Age: 65, Sex: Male	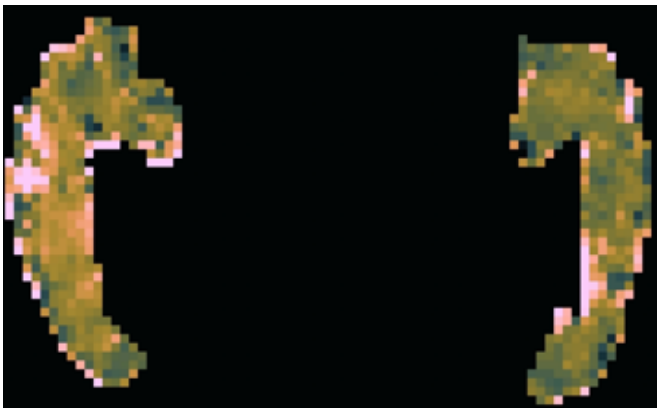	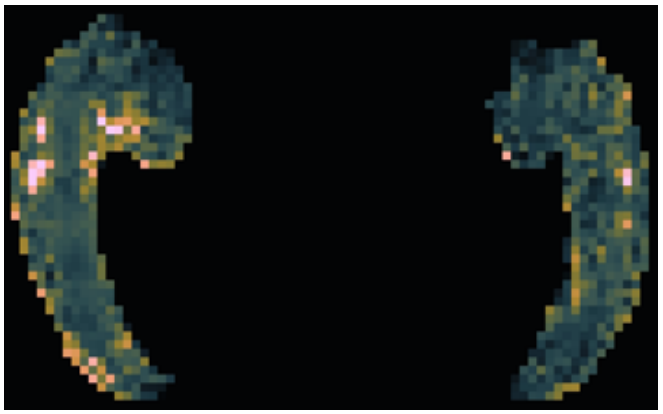
Diagnosis: PD; Age: 66, Sex: Male	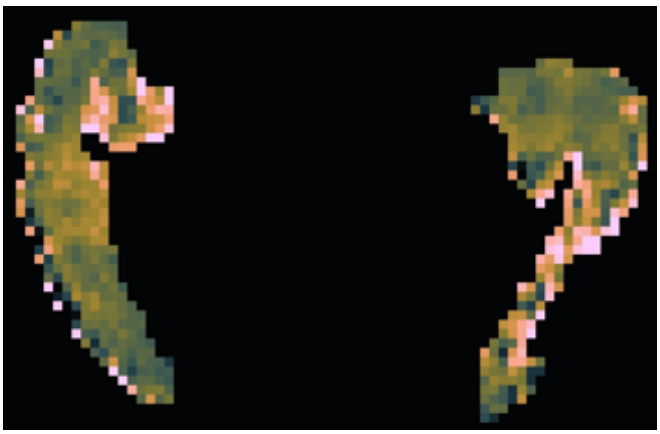	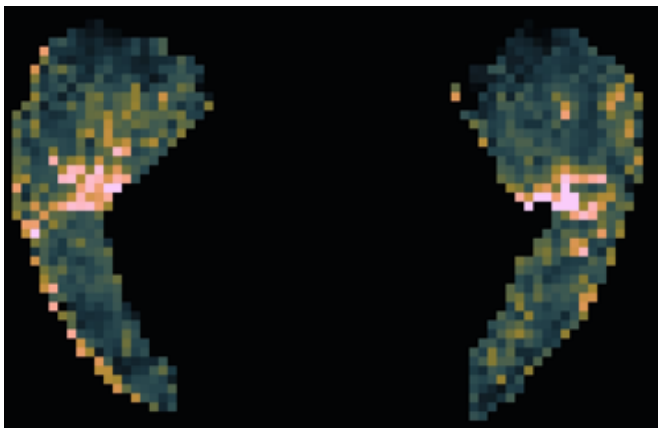

Figure B1: Maps of MD (axial view) obtained from hippocampal segmentations of all participants within the healthy control (HC) and Lewy Body groups (Parkinson's Disease [PD], Parkinson's Disease with Mild Cognitive Impairment [PD-MCI], and Dementia with Lewy Bodies [DLB])

	Axial Map	**Axial Map (z-projection of the voxels with the maximum intensity across all slices)**
	Scale ($x10^{-3}$) 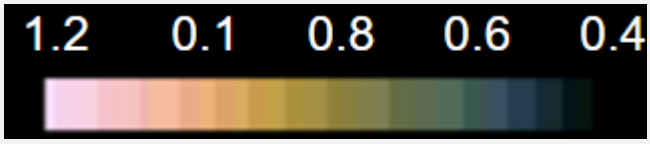	**Scale ($x10^{-3}$)** 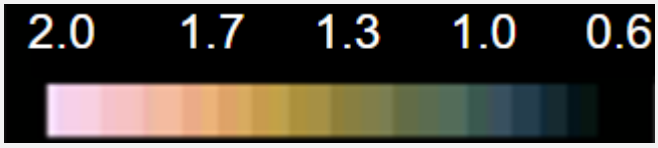
Diagnosis: PD; Age: 68, Sex: Male	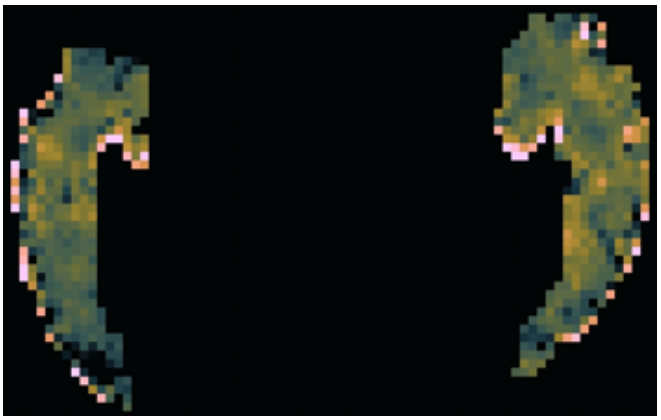	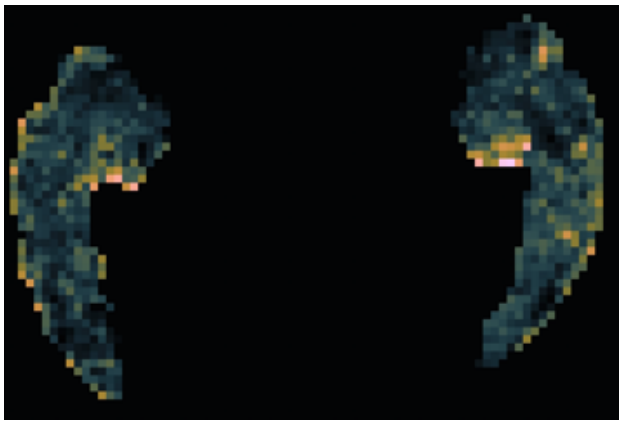
Diagnosis: PD; Age: 69, Sex: Male	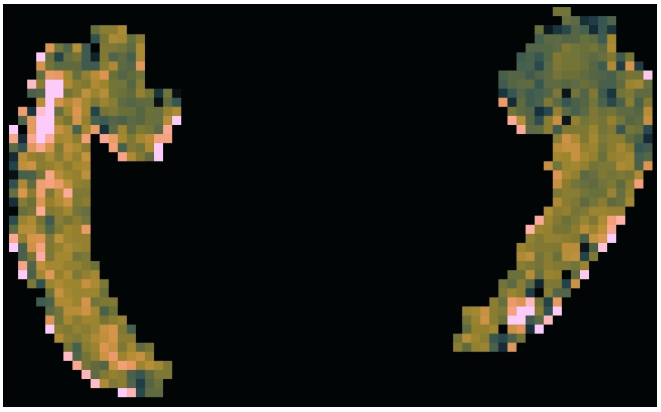	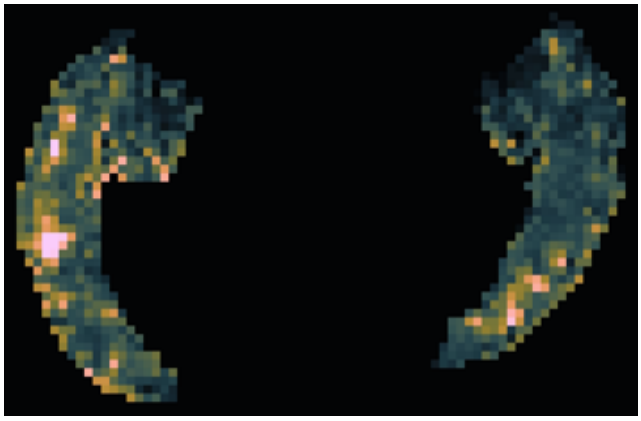
Diagnosis: PD; Age: 71, Sex: Male		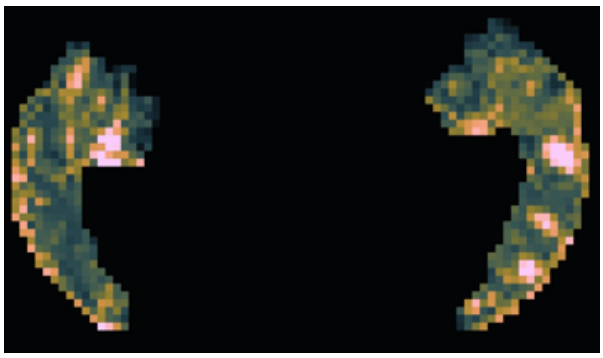

Figure B1: Maps of MD (axial view) obtained from hippocampal segmentations of all participants within the healthy control (HC) and Lewy Body groups (Parkinson's Disease [PD], Parkinson's Disease with Mild Cognitive Impairment [PD-MCI], and Dementia with Lewy Bodies [DLB])

	Axial Map	**Axial Map (z-projection of the voxels with the maximum intensity across all slices)**
	Scale ($x10^{-3}$) 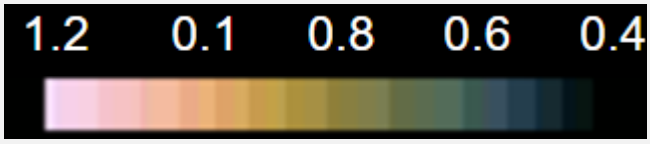	**Scale ($x10^{-3}$)** 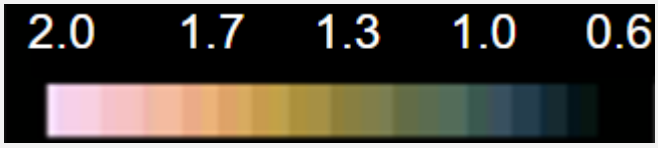
Diagnosis: PD; Age: 72, Sex: Female		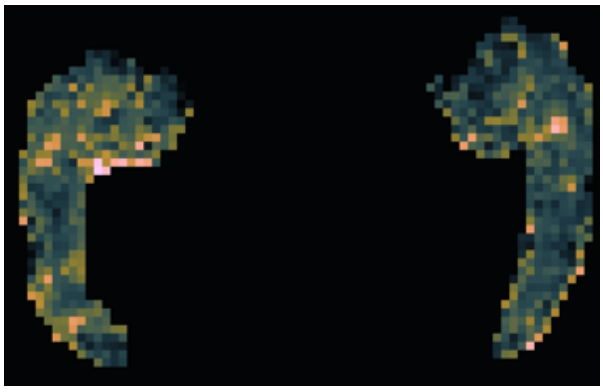
Diagnosis: PD; Age: 72, Sex: Female	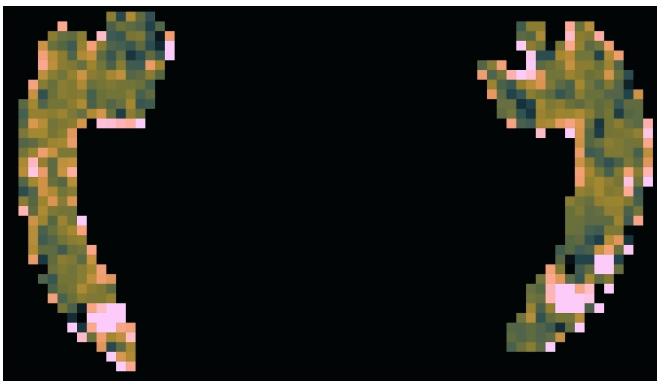	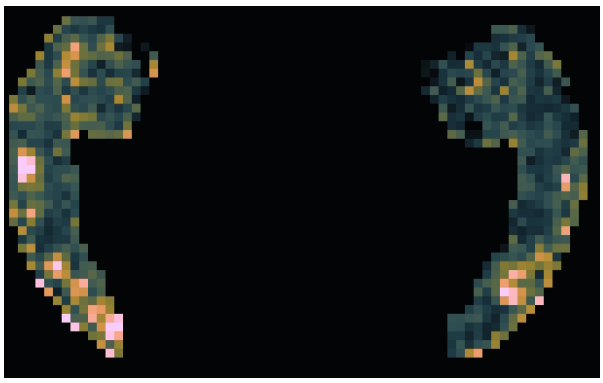
Diagnosis: PD; Age: 73, Sex: Female	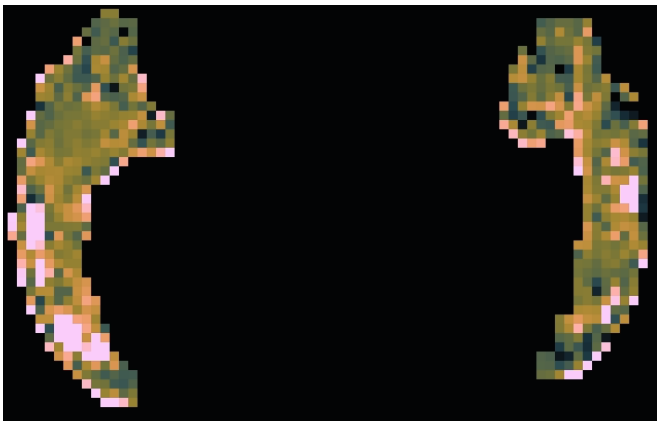	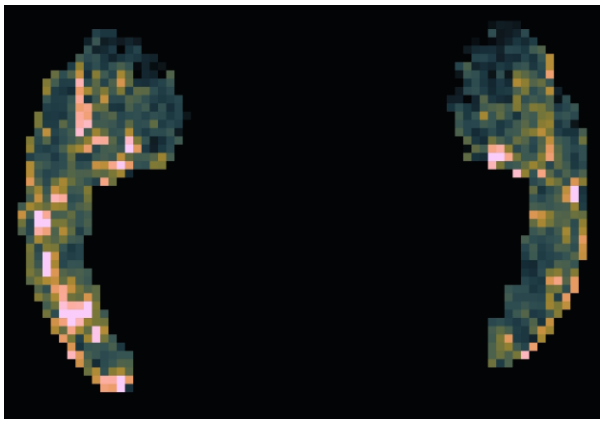

Figure B1: Maps of MD (axial view) obtained from hippocampal segmentations of all participants within the healthy control (HC) and Lewy Body groups (Parkinson's Disease [PD], Parkinson's Disease with Mild Cognitive Impairment [PD-MCI], and Dementia with Lewy Bodies [DLB])

	Axial Map	**Axial Map (z-projection of the voxels with the maximum intensity across all slices)**
	Scale (x10^{-3}) 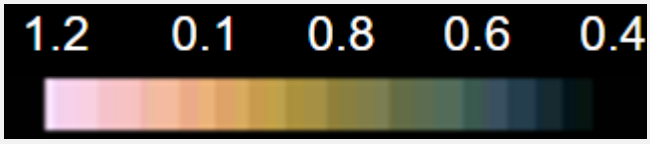	**Scale (x10^{-3})** 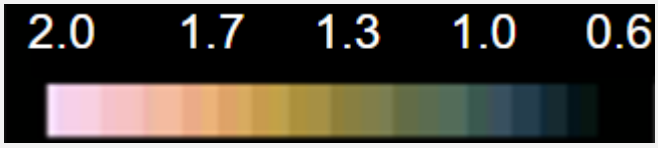
Diagnosis: PD; Age: 73, Sex: Female	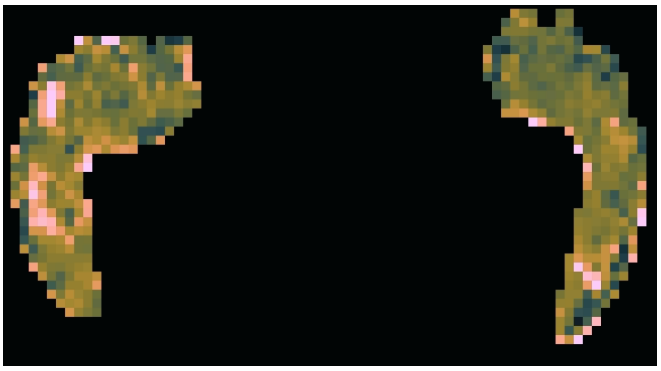	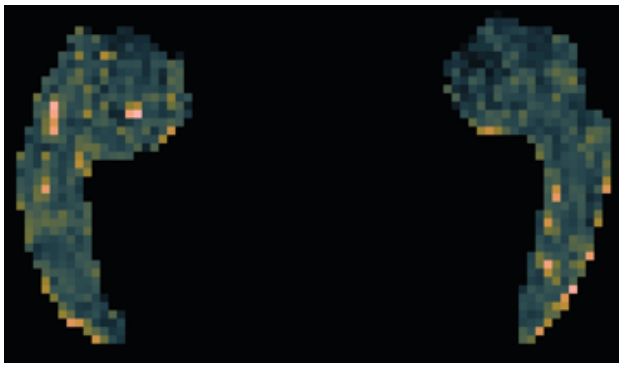
Diagnosis: PD; Age: 74, Sex: Male	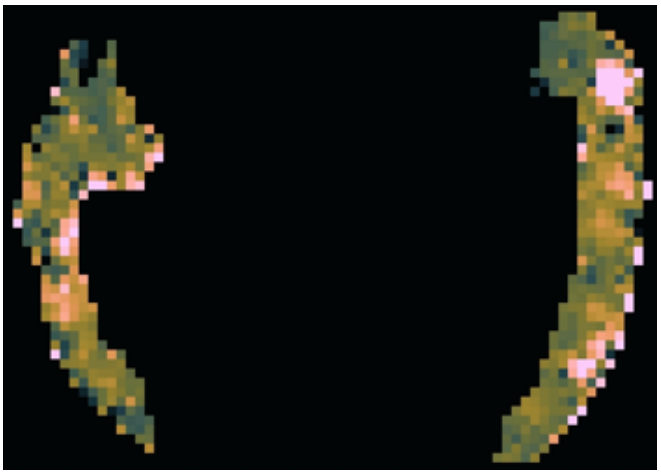	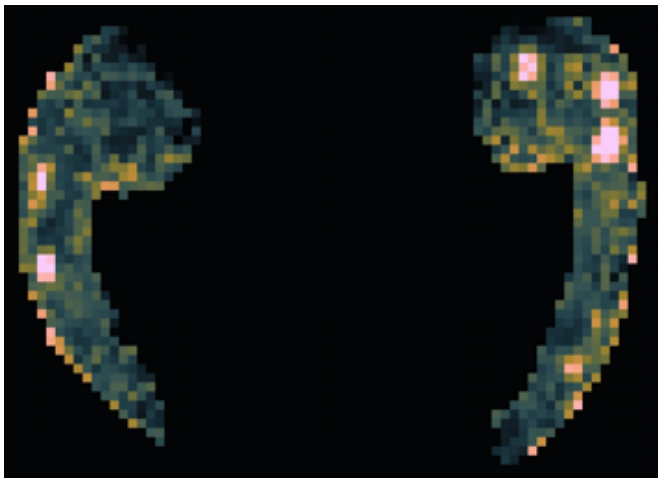

Figure B1: Maps of MD (axial view) obtained from hippocampal segmentations of all participants within the healthy control (HC) and Lewy Body groups (Parkinson's Disease [PD], Parkinson's Disease with Mild Cognitive Impairment [PD-MCI], and Dementia with Lewy Bodies [DLB])

	Axial Map	**Axial Map (z-projection of the voxels with the maximum intensity across all slices)**
	Scale (x10^{-3}) 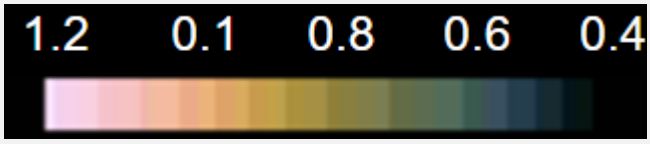	**Scale (x10^{-3})** 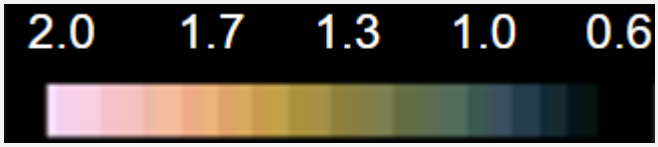
Diagnosis: PD; Age: 76, Sex: Male	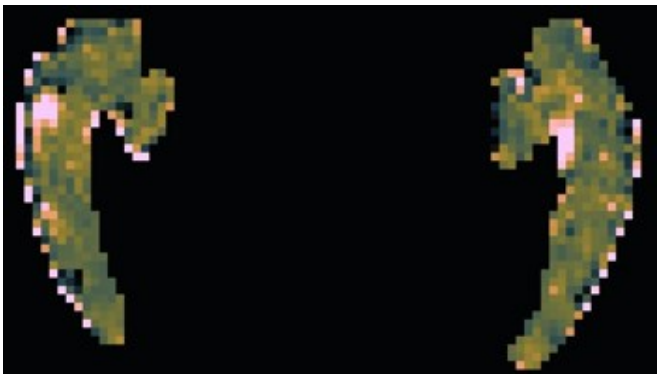	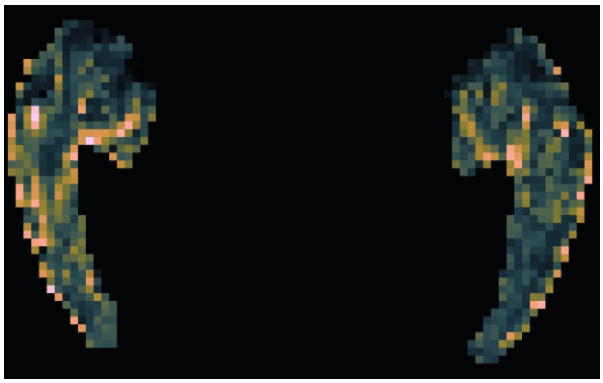
Diagnosis: PD; Age: 78, Sex: Male	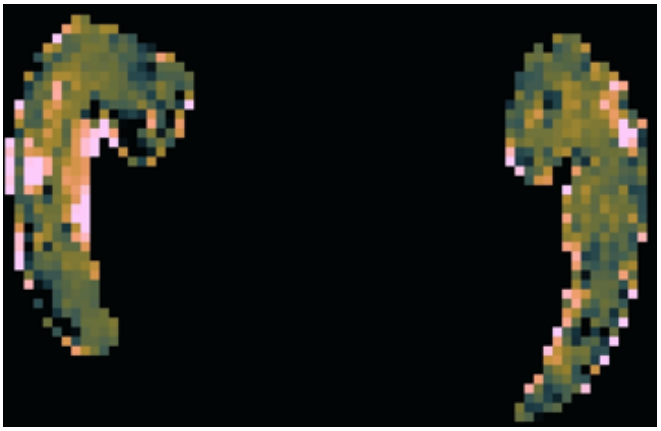	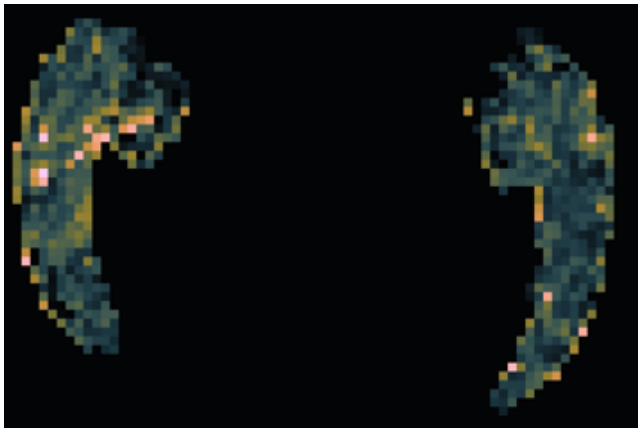
Diagnosis: PD-MCI; Age: 67, Sex: Male	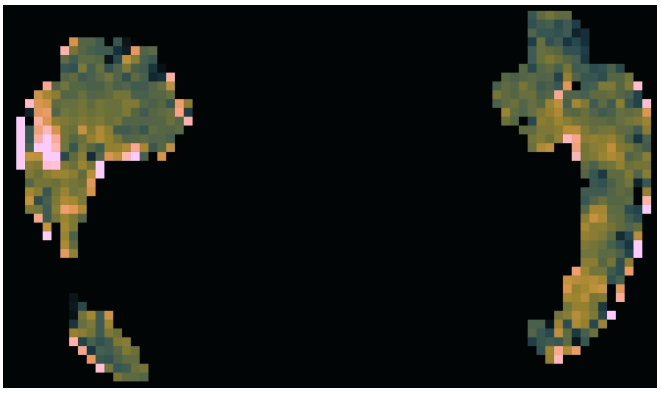	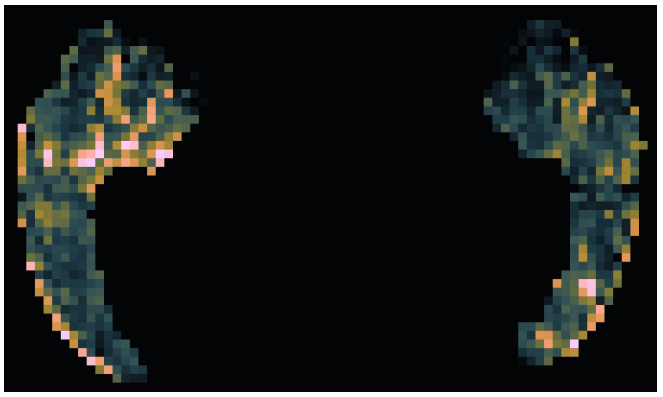

Figure B1: Maps of MD (axial view) obtained from hippocampal segmentations of all participants within the healthy control (HC) and Lewy Body groups (Parkinson's Disease [PD], Parkinson's Disease with Mild Cognitive Impairment [PD-MCI], and Dementia with Lewy Bodies [DLB])

	Axial Map	**Axial Map (z-projection of the voxels with the maximum intensity across all slices)**
	Scale ($x10^{-3}$) 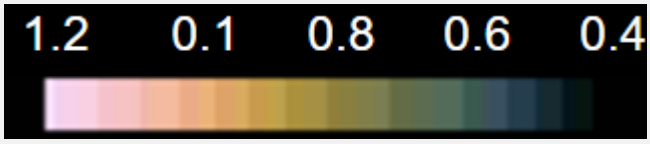	**Scale ($x10^{-3}$)** 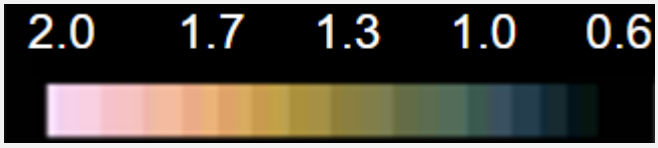
Diagnosis: PD-MCI; Age: 68, Sex: Male	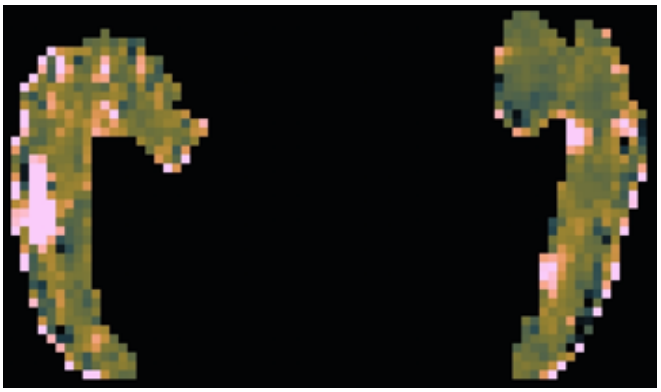	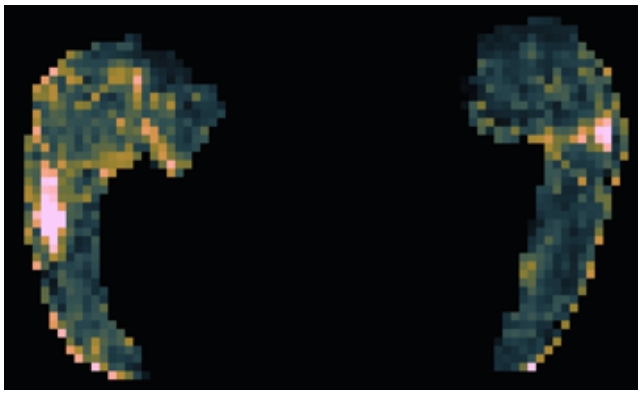
Diagnosis: PD-MCI; Age: 69, Sex: Male		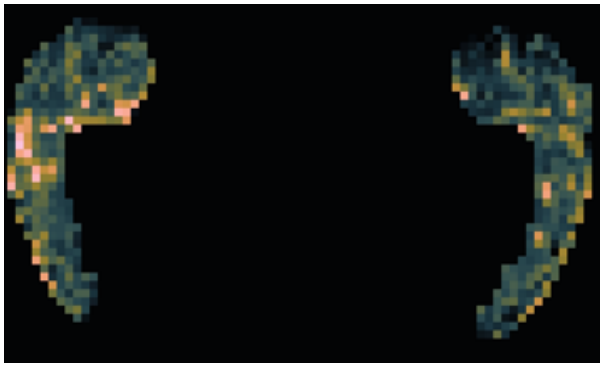
Diagnosis: PD-MCI; Age: 71, Sex: Male		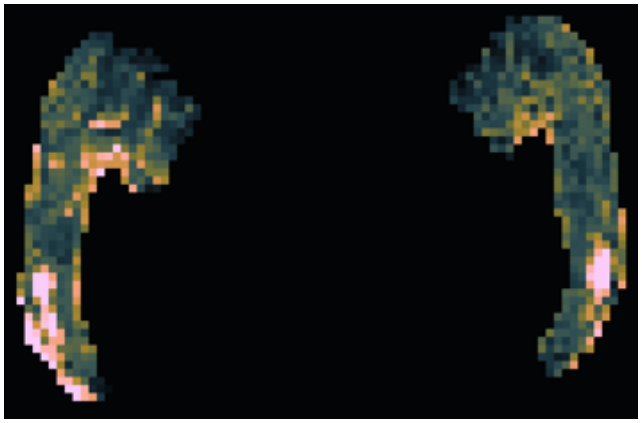

Figure B1: Maps of MD (axial view) obtained from hippocampal segmentations of all participants within the healthy control (HC) and Lewy Body groups (Parkinson's Disease [PD], Parkinson's Disease with Mild Cognitive Impairment [PD-MCI], and Dementia with Lewy Bodies [DLB])

	Axial Map	**Axial Map (z-projection of the voxels with the maximum intensity across all slices)**
	Scale (x10^{-3}) 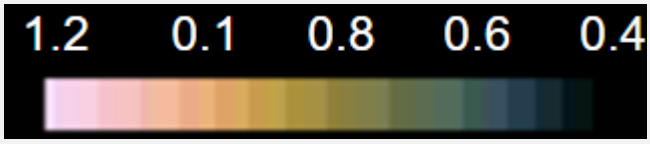	**Scale (x10^{-3})** 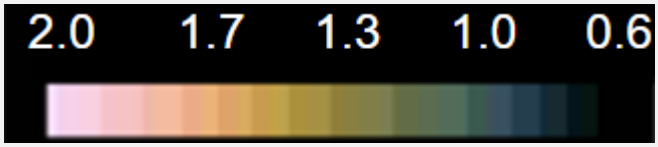
Diagnosis: PD-MCI; Age: 72, Sex: Male	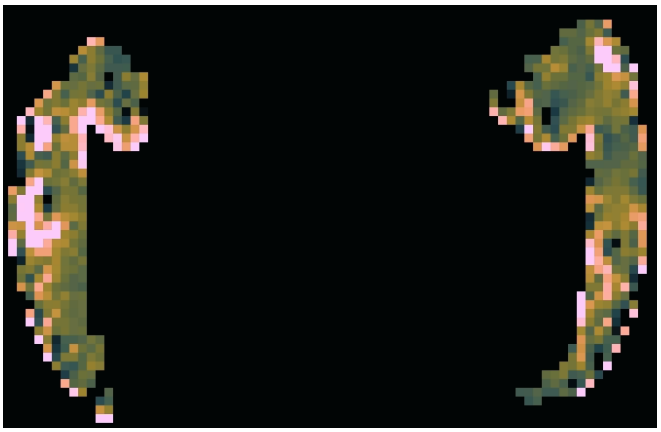	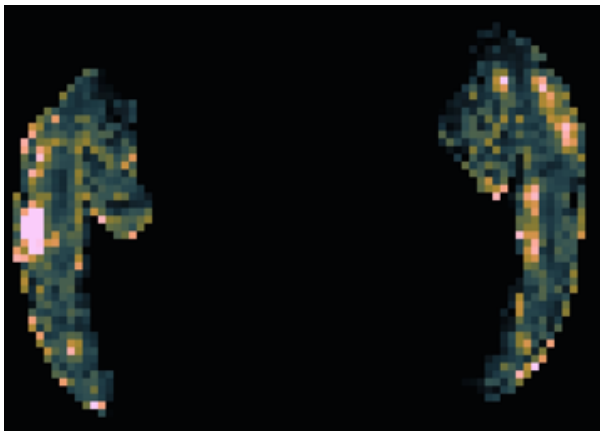
Diagnosis: PD-MCI; Age: 73, Sex: Male	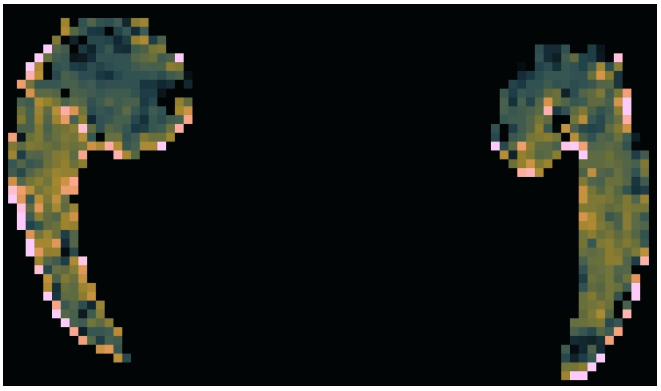	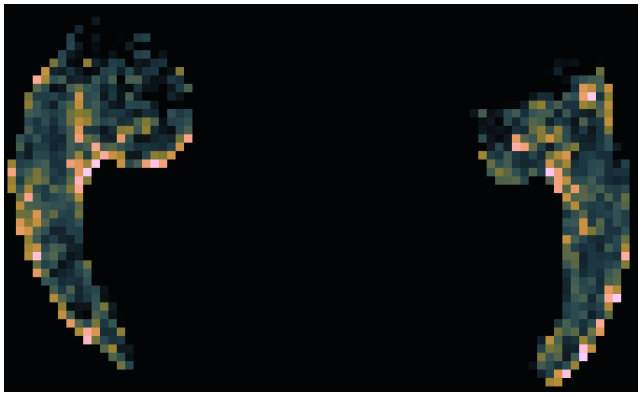

Figure B1: Maps of MD (axial view) obtained from hippocampal segmentations of all participants within the healthy control (HC) and Lewy Body groups (Parkinson's Disease [PD], Parkinson's Disease with Mild Cognitive Impairment [PD-MCI], and Dementia with Lewy Bodies [DLB])

	Axial Map	**Axial Map (z-projection of the voxels with the maximum intensity across all slices)**
	Scale (x10^{-3}) 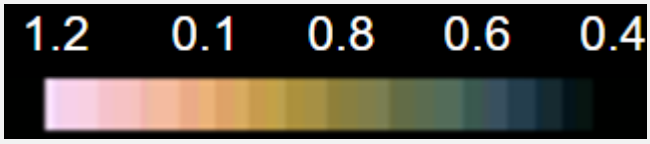	**Scale (x10^{-3})** 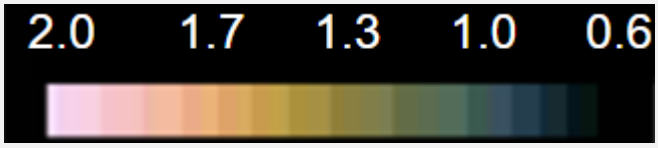
Diagnosis: PD-MCI; Age: 78, Sex: Male		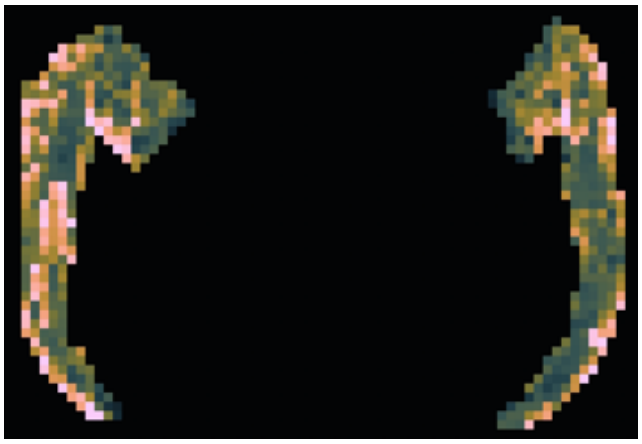
Diagnosis: PD-MCI; Age: 84, Sex: Female	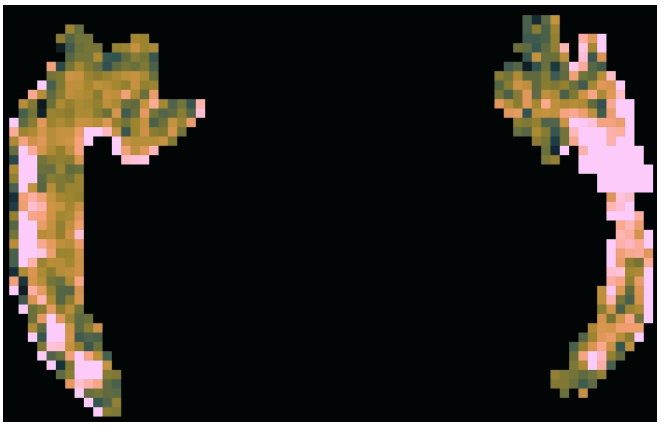	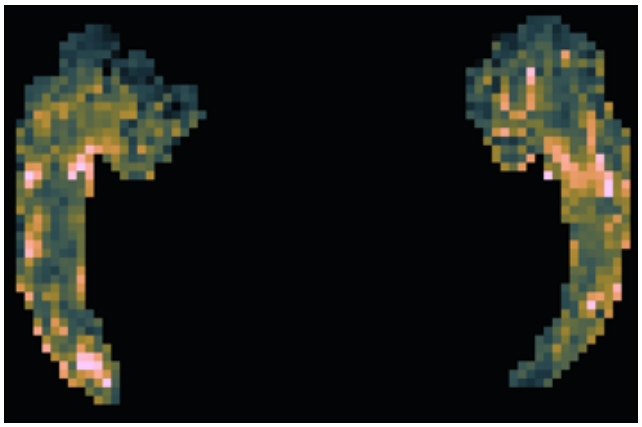

Figure B1: Maps of MD (axial view) obtained from hippocampal segmentations of all participants within the healthy control (HC) and Lewy Body groups (Parkinson's Disease [PD], Parkinson's Disease with Mild Cognitive Impairment [PD-MCI], and Dementia with Lewy Bodies [DLB])

	Axial Map	**Axial Map (z-projection of the voxels with the maximum intensity across all slices)**
	Scale ($x10^{-3}$) 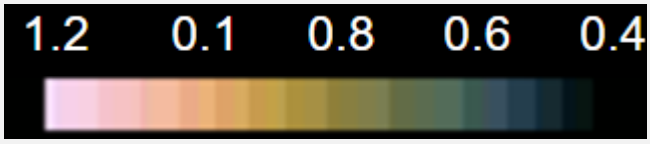	**Scale ($x10^{-3}$)** 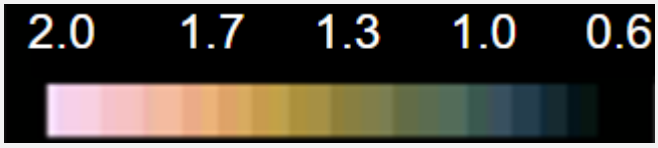
Diagnosis: PD-MCI; Age: 87, Sex: Male	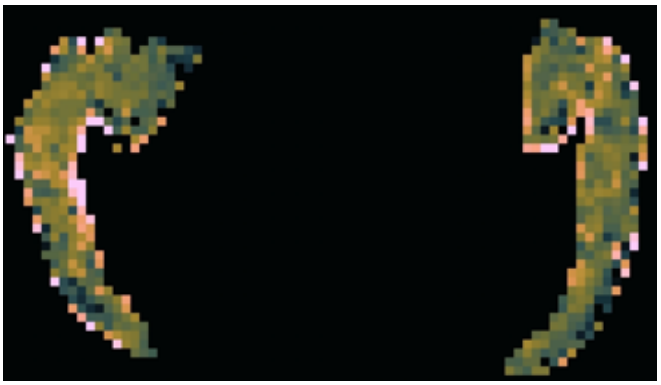	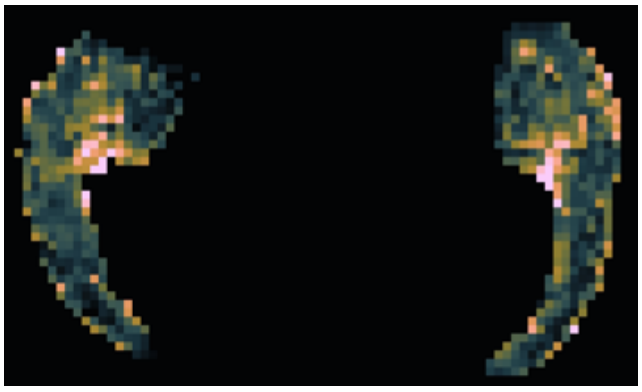
Diagnosis: PDD; Age: 62, Sex: Male	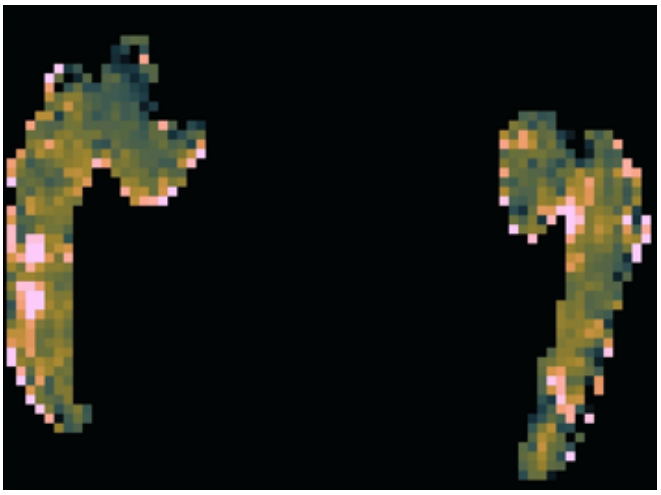	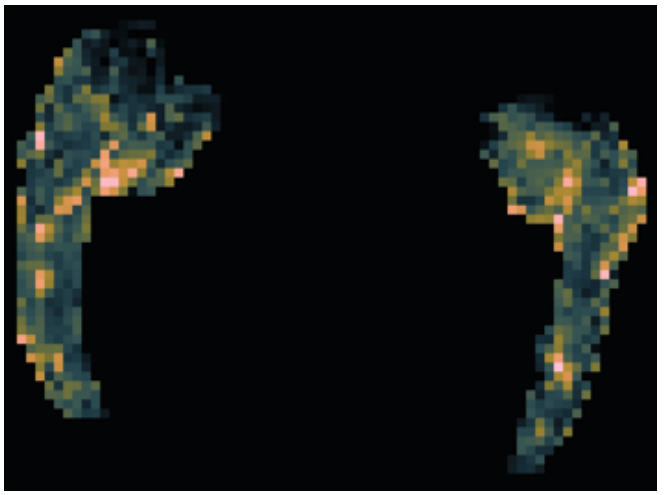

Figure B1: Maps of MD (axial view) obtained from hippocampal segmentations of all participants within the healthy control (HC) and Lewy Body groups (Parkinson's Disease [PD], Parkinson's Disease with Mild Cognitive Impairment [PD-MCI], and Dementia with Lewy Bodies [DLB])

	Axial Map	**Axial Map (z-projection of the voxels with the maximum intensity across all slices)**
	Scale (x10^{-3}) 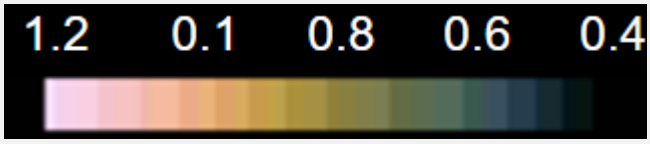	**Scale (x10^{-3})** 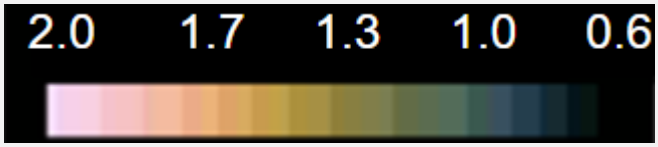
Diagnosis: PDD; Age: 78, Sex: Male	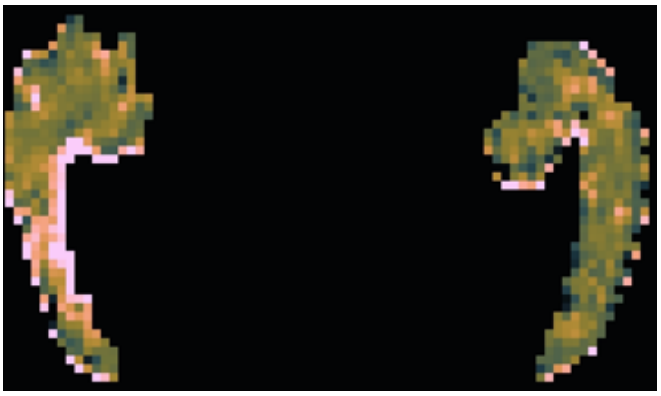	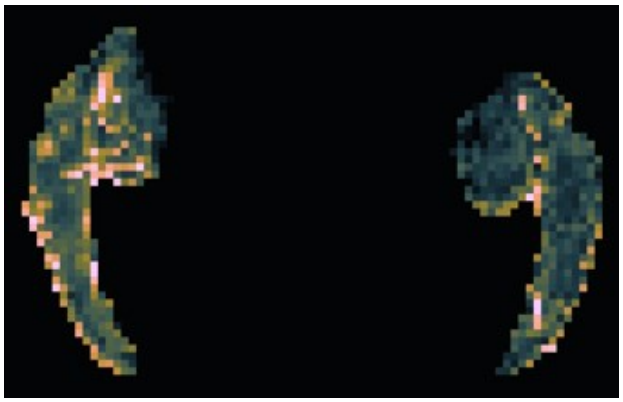
Diagnosis: PDD; Age: 82, Sex: Male	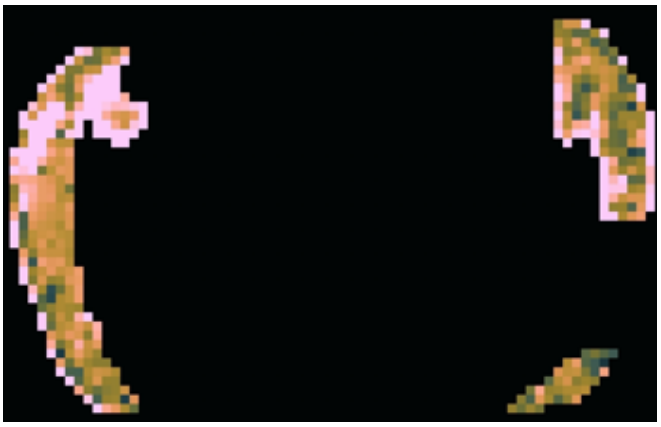	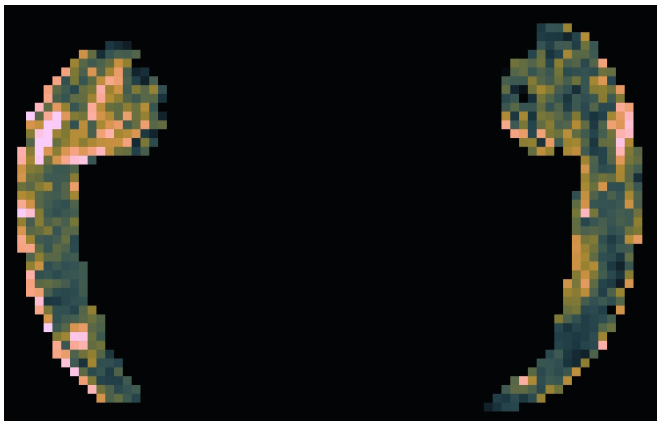

Figure B1: Maps of MD (axial view) obtained from hippocampal segmentations of all participants within the healthy control (HC) and Lewy Body groups (Parkinson's Disease [PD], Parkinson's Disease with Mild Cognitive Impairment [PD-MCI], and Dementia with Lewy Bodies [DLB])

	Axial Map	**Axial Map (z-projection of the voxels with the maximum intensity across all slices)**
	Scale (x10^{-3}) 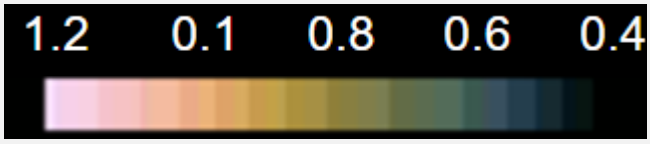	**Scale (x10^{-3})** 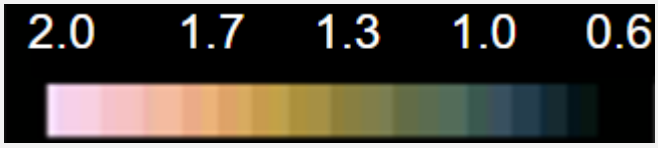
Diagnosis: DLB; Age: 65, Sex: Male	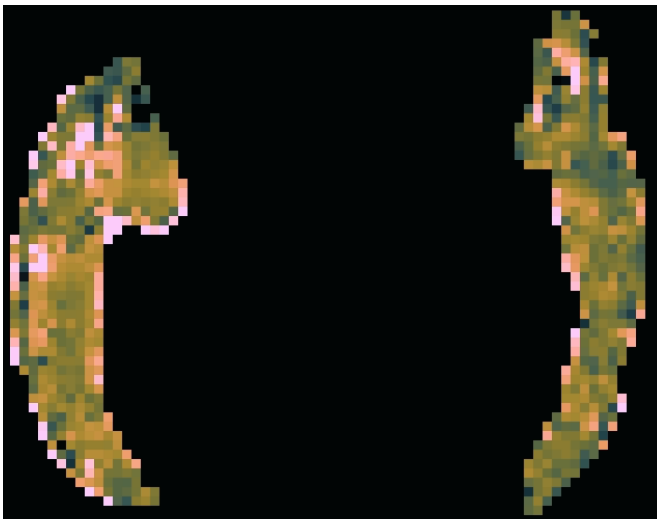	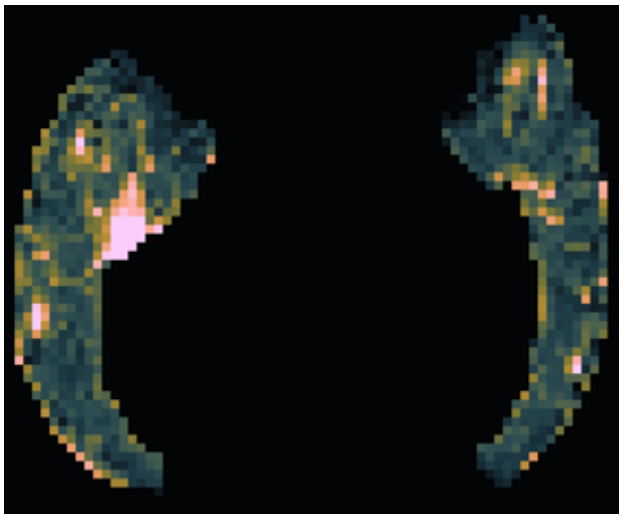
Diagnosis: DLB; Age: 69, Sex: Male	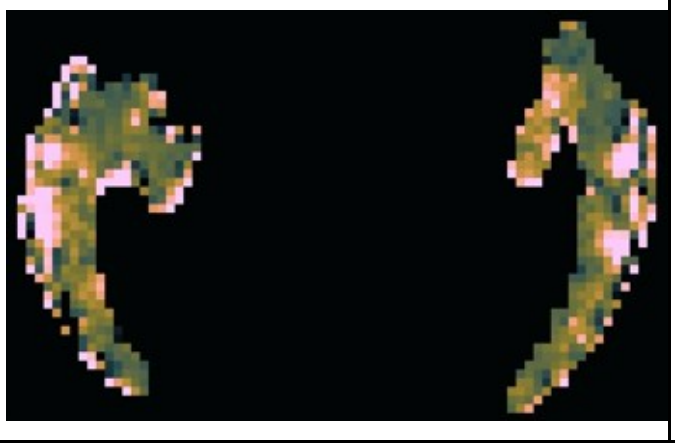	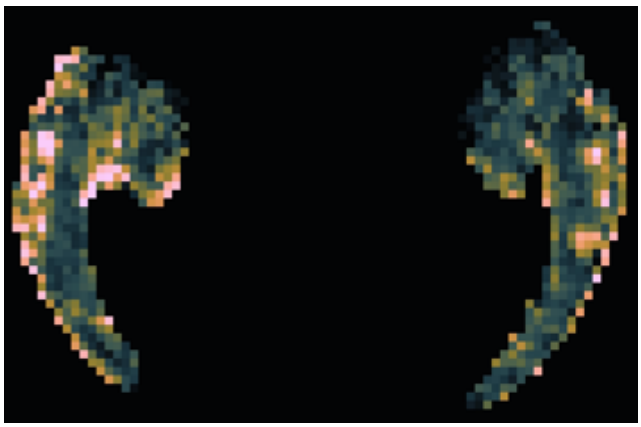

Figure B1: Maps of MD (axial view) obtained from hippocampal segmentations of all participants within the healthy control (HC) and Lewy Body groups (Parkinson's Disease [PD], Parkinson's Disease with Mild Cognitive Impairment [PD-MCI], and Dementia with Lewy Bodies [DLB])

	Axial Map	**Axial Map (z-projection of the voxels with the maximum intensity across all slices)**
	Scale (x10^{-3}) 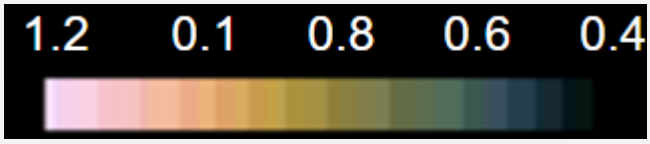	**Scale (x10^{-3})** 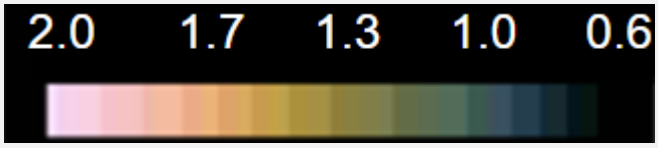
Diagnosis: DLB; Age: 73, Sex: Female	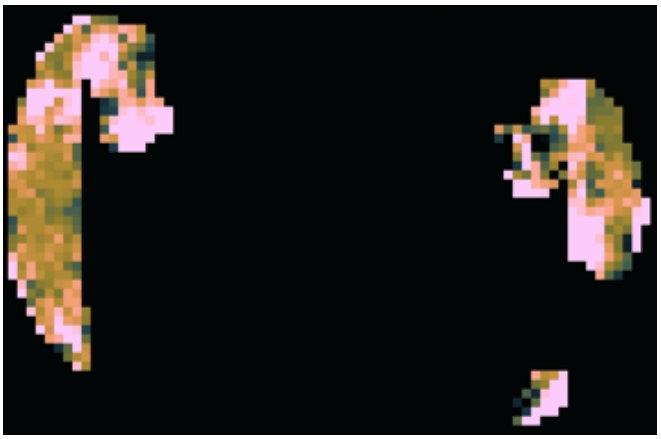	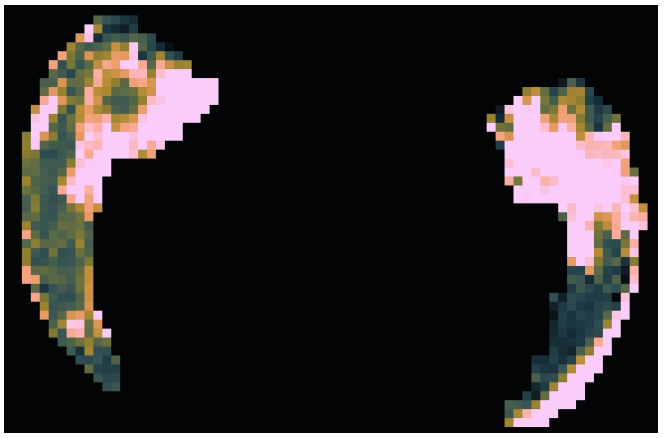
Diagnosis: DLB; Age: 74, Sex: Male		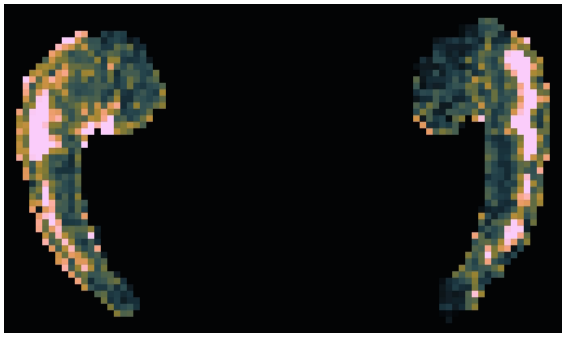

Figure B2: Sagittal and coronal MD maps obtained from hippocampal segmentations of all participants within the healthy control (HC) and Lewy Body groups (Parkinson's Disease [PD], Parkinson's Disease with Mild Cognitive Impairment [PD-MCI], and Dementia with Lewy Bodies [DLB])

	Sagittal Map - Right (Z-Project - Max intensity)	**Sagittal Map - Left (Z-Project - Max intensity)**	**Coronal Map (z-projection of the voxels with the maximum intensity across all slices) [RIGHT/LEFT]**
	Scale ($x10^{-3}$) 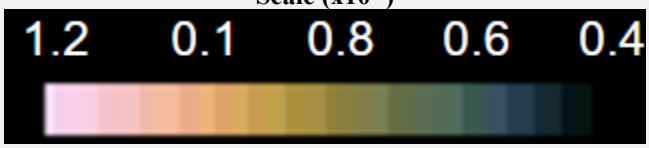		
Diagnosis: HC; Age: 50, Sex: Female			
Diagnosis: HC; Age: 57, Sex: Female			
Diagnosis: HC; Age: 58, Sex: Female			
Diagnosis: HC; Age: 58, Sex: Female		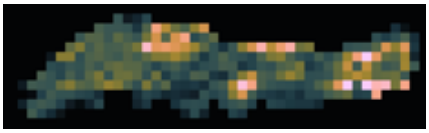	
Diagnosis: HC; Age: 58, Sex: Male			
Diagnosis: HC; Age: 60, Sex: Male		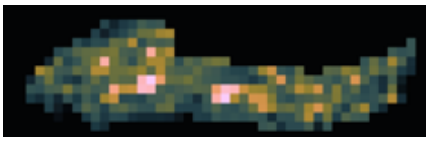	
Diagnosis: HC; Age: 60, Sex: Male			
Diagnosis: HC; Age: 61, Sex: Male		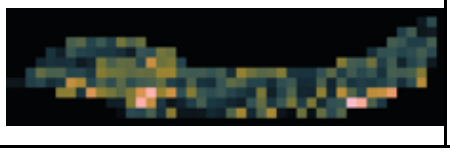	

Figure B2: Sagittal and coronal MD maps obtained from hippocampal segmentations of all participants within the healthy control (HC) and Lewy Body groups (Parkinson's Disease [PD], Parkinson's Disease with Mild Cognitive Impairment [PD-MCI], and Dementia with Lewy Bodies [DLB])

	Sagittal Map - Right (Z-Project - Max intensity)	**Sagittal Map - Left (Z-Project - Max intensity)**	**Coronal Map (z-projection of the voxels with the maximum intensity across all slices) [RIGHT/LEFT]**
	Scale ($x10^{-3}$) 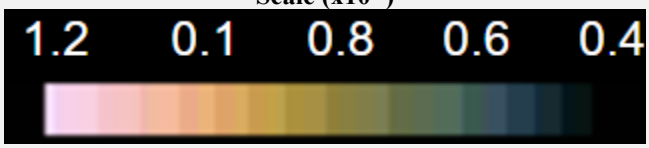		
Diagnosis: HC; Age: 62, Sex: Female	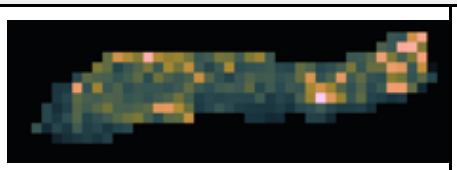	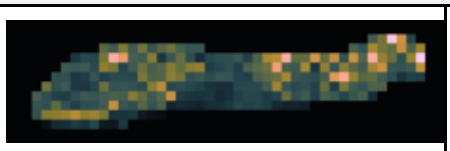	
Diagnosis: HC; Age: 62, Sex: Male		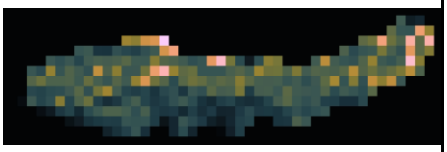	
Diagnosis: HC; Age: 62, Sex: Male		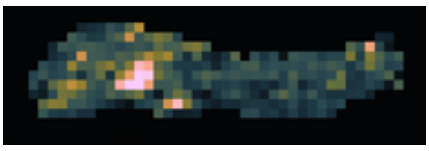	
Diagnosis: HC; Age: 62, Sex: Male			
Diagnosis: HC; Age: 63, Sex: Female			
Diagnosis: HC; Age: 65, Sex: Female	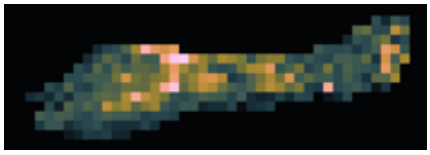		
Diagnosis: HC; Age: 65, Sex: Female			

Figure B2: Sagittal and coronal MD maps obtained from hippocampal segmentations of all participants within the healthy control (HC) and Lewy Body groups (Parkinson's Disease [PD], Parkinson's Disease with Mild Cognitive Impairment [PD-MCI], and Dementia with Lewy Bodies [DLB])

	Sagittal Map - Right (Z-Project - Max intensity)	**Sagittal Map - Left (Z-Project - Max intensity)**	**Coronal Map (z-projection of the voxels with the maximum intensity across all slices) [RIGHT/LEFT]**
	Scale ($x10^{-3}$) 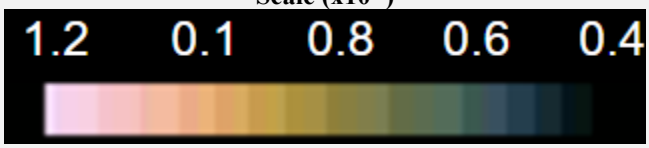		
Diagnosis: HC; Age: 66, Sex: Male	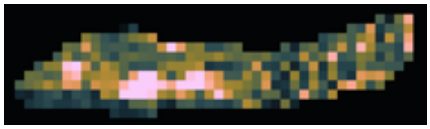		
Diagnosis: HC; Age: 68, Sex: Male			
Diagnosis: HC; Age: 69, Sex: Female			
Diagnosis: HC; Age: 69, Sex: Male			
Diagnosis: HC; Age: 69, Sex: Male			
Diagnosis: HC; Age: 70, Sex: Female			
Diagnosis: HC; Age: 70, Sex: Female	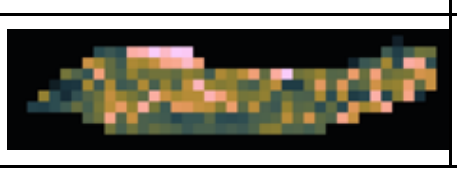		

Figure B2: Sagittal and coronal MD maps obtained from hippocampal segmentations of all participants within the healthy control (HC) and Lewy Body groups (Parkinson's Disease [PD], Parkinson's Disease with Mild Cognitive Impairment [PD-MCI], and Dementia with Lewy Bodies [DLB])

	Sagittal Map - Right (Z-Project - Max intensity)	**Sagittal Map - Left (Z-Project - Max intensity)**	**Coronal Map (z-projection of the voxels with the maximum intensity across all slices) [RIGHT/LEFT]**
	Scale ($x10^{-3}$) 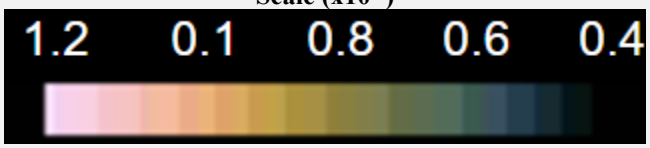		
Diagnosis: HC; Age: 70, Sex: Female	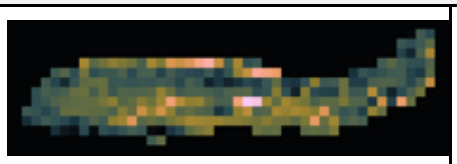	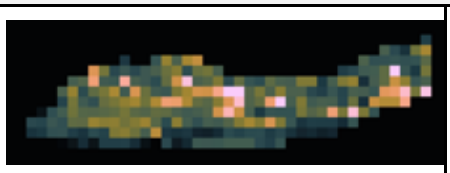	
Diagnosis: HC; Age: 70, Sex: Female	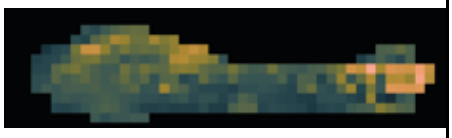		
Diagnosis: HC; Age: 70, Sex: Female			
Diagnosis: HC; Age: 70, Sex: Male			
Diagnosis: HC; Age: 70, Sex: Male			
Diagnosis: HC; Age: 71, Sex: Female			
Diagnosis: HC; Age: 71, Sex: Male			

Figure B2: Sagittal and coronal MD maps obtained from hippocampal segmentations of all participants within the healthy control (HC) and Lewy Body groups (Parkinson's Disease [PD], Parkinson's Disease with Mild Cognitive Impairment [PD-MCI], and Dementia with Lewy Bodies [DLB])

	Sagittal Map - Right (Z-Project - Max intensity)	**Sagittal Map - Left (Z-Project - Max intensity)**	**Coronal Map (z-projection of the voxels with the maximum intensity across all slices) [RIGHT/LEFT]**
	Scale ($x10^{-3}$) 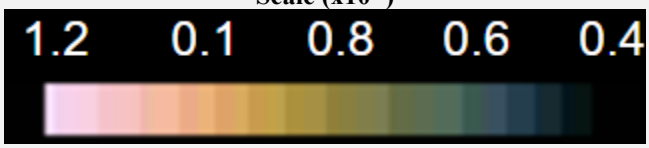		
Diagnosis: HC; Age: 73, Sex: Male			
Diagnosis: HC; Age: 74, Sex: Female			
Diagnosis: HC; Age: 74, Sex: Male			
Diagnosis: HC; Age: 75, Sex: Female			
Diagnosis: HC; Age: 78, Sex: Female			
Diagnosis: HC; Age: 83, Sex: Female			
Diagnosis: PD; Age: 58, Sex: Female			
Diagnosis: PD; Age: 58, Sex:		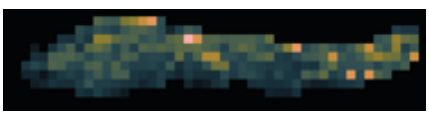	

Figure B2: Sagittal and coronal MD maps obtained from hippocampal segmentations of all participants within the healthy control (HC) and Lewy Body groups (Parkinson's Disease [PD], Parkinson's Disease with Mild Cognitive Impairment [PD-MCI], and Dementia with Lewy Bodies [DLB])

	Sagittal Map - Right (Z-Project - Max intensity)	**Sagittal Map - Left (Z-Project - Max intensity)**	**Coronal Map (z-projection of the voxels with the maximum intensity across all slices) [RIGHT/LEFT]**
	Scale ($x10^{-3}$) 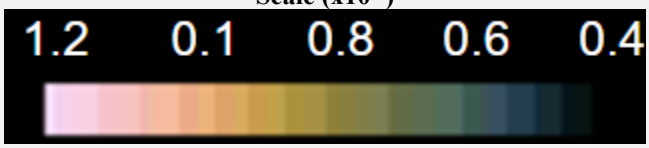		
Female			
Diagnosis: PD; Age: 58, Sex: Male		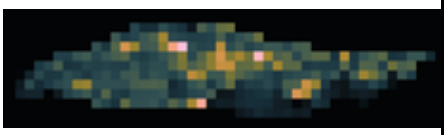	
Diagnosis: PD; Age: 59, Sex: Female		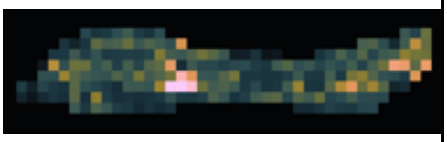	
Diagnosis: PD; Age: 61, Sex: Male			
Diagnosis: PD; Age: 63, Sex: Male			
Diagnosis: PD; Age: 63, Sex: Male			
Diagnosis: PD; Age: 64, Sex: Female			
Diagnosis: PD; Age: 64, Sex: Female			

Figure B2: Sagittal and coronal MD maps obtained from hippocampal segmentations of all participants within the healthy control (HC) and Lewy Body groups (Parkinson's Disease [PD], Parkinson's Disease with Mild Cognitive Impairment [PD-MCI], and Dementia with Lewy Bodies [DLB])

	Sagittal Map - Right (Z-Project - Max intensity)	**Sagittal Map - Left (Z-Project - Max intensity)**	**Coronal Map (z-projection of the voxels with the maximum intensity across all slices) [RIGHT/LEFT]**
	Scale ($x10^{-3}$) 1.2 0.1 0.8 0.6 0.4		
Diagnosis: PD; Age: 65, Sex: Female	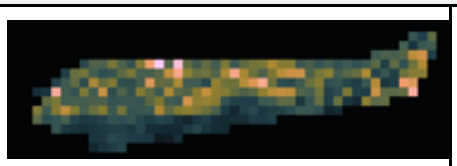	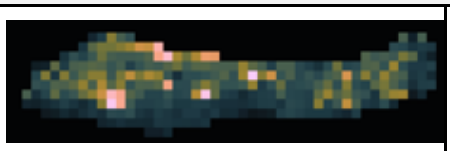	
Diagnosis: PD; Age: 65, Sex: Male			
Diagnosis: PD; Age: 66, Sex: Male			
Diagnosis: PD; Age: 68, Sex: Male	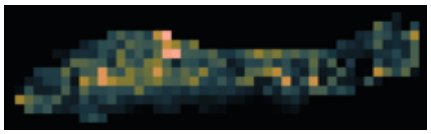		
Diagnosis: PD; Age: 69, Sex: Male			
Diagnosis: PD; Age: 71, Sex: Male			
Diagnosis: PD; Age: 72, Sex: Female		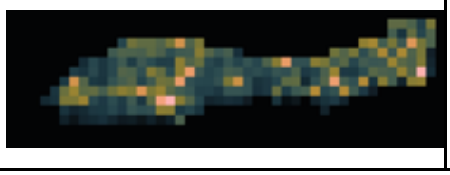	

Figure B2: Sagittal and coronal MD maps obtained from hippocampal segmentations of all participants within the healthy control (HC) and Lewy Body groups (Parkinson's Disease [PD], Parkinson's Disease with Mild Cognitive Impairment [PD-MCI], and Dementia with Lewy Bodies [DLB])

	Sagittal Map - Right (Z-Project - Max intensity)	**Sagittal Map - Left (Z-Project - Max intensity)**	**Coronal Map (z-projection of the voxels with the maximum intensity across all slices) [RIGHT/LEFT]**
	Scale ($x10^{-3}$) 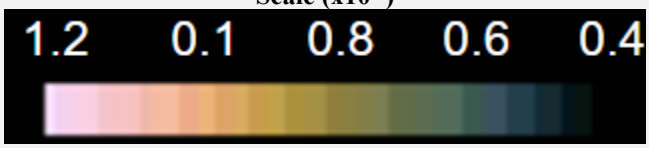		
Diagnosis: PD; Age: 72, Sex: Female	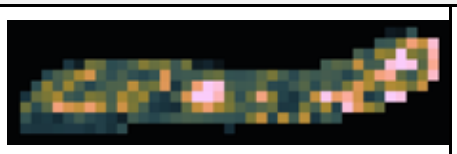	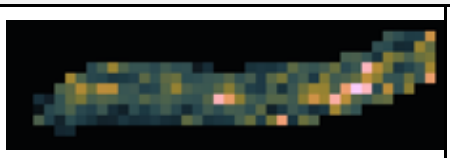	
Diagnosis: PD; Age: 73, Sex: Female			
Diagnosis: PD; Age: 73, Sex: Female	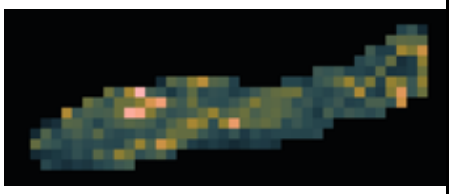		
Diagnosis: PD; Age: 74, Sex: Male			
Diagnosis: PD; Age: 76, Sex: Male			
Diagnosis: PD; Age: 78, Sex: Male		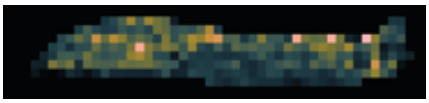	
Diagnosis: PD-MCI; Age: 67, Sex: Male		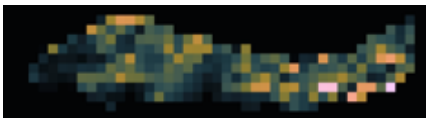	

Figure B2: Sagittal and coronal MD maps obtained from hippocampal segmentations of all participants within the healthy control (HC) and Lewy Body groups (Parkinson's Disease [PD], Parkinson's Disease with Mild Cognitive Impairment [PD-MCI], and Dementia with Lewy Bodies [DLB])

	Sagittal Map - Right (Z-Project - Max intensity)	**Sagittal Map - Left (Z-Project - Max intensity)**	**Coronal Map (z-projection of the voxels with the maximum intensity across all slices) [RIGHT/LEFT]**
	Scale ($x10^{-3}$) 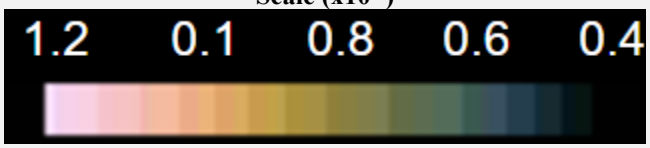		
Diagnosis: PD-MCI; Age: 68, Sex: Male	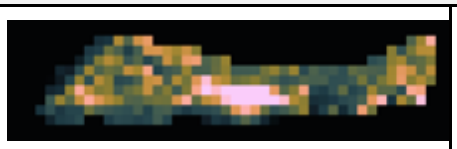		
Diagnosis: PD-MCI; Age: 69, Sex: Male			
Diagnosis: PD-MCI; Age: 71, Sex: Male		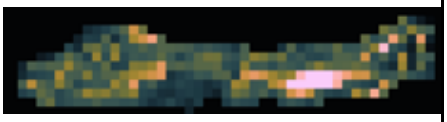	
Diagnosis: PD-MCI; Age: 72, Sex: Male			
Diagnosis: PD-MCI; Age: 73, Sex: Male		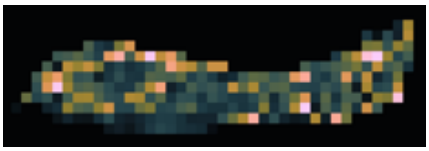	
Diagnosis: PD-MCI; Age: 78, Sex: Male			
Diagnosis: PD-MCI; Age: 84, Sex: Female			

Figure B2: Sagittal and coronal MD maps obtained from hippocampal segmentations of all participants within the healthy control (HC) and Lewy Body groups (Parkinson's Disease [PD], Parkinson's Disease with Mild Cognitive Impairment [PD-MCI], and Dementia with Lewy Bodies [DLB])

	Sagittal Map - Right (Z-Project - Max intensity)	**Sagittal Map - Left (Z-Project - Max intensity)**	**Coronal Map (z-projection of the voxels with the maximum intensity across all slices) [RIGHT/LEFT]**
	Scale ($x10^{-3}$) 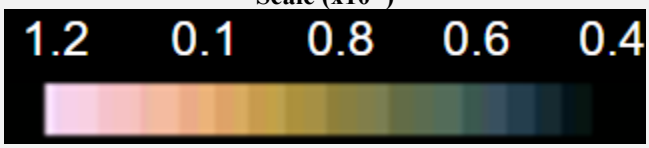		
Diagnosis: PD-MCI; Age: 87, Sex: Male			
Diagnosis: PDD; Age: 62, Sex: Male			
Diagnosis: PDD; Age: 78, Sex: Male		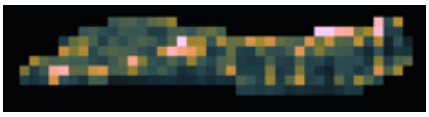	
Diagnosis: PDD; Age: 82, Sex: Male			
Diagnosis: DLB; Age: 65, Sex: Male			
Diagnosis: DLB; Age: 69, Sex: Male			
Diagnosis: DLB; Age: 73, Sex: Female		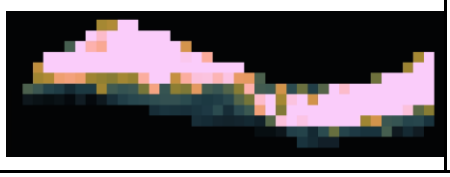	

Figure B2: Sagittal and coronal MD maps obtained from hippocampal segmentations of all participants within the healthy control (HC) and Lewy Body groups (Parkinson's Disease [PD], Parkinson's Disease with Mild Cognitive Impairment [PD-MCI], and Dementia with Lewy Bodies [DLB])

	Sagittal Map - Right (Z-Project - Max intensity)	**Sagittal Map - Left (Z-Project - Max intensity)**	**Coronal Map (z-projection of the voxels with the maximum intensity across all slices) [RIGHT/LEFT]**
	Scale ($x10^{-3}$) 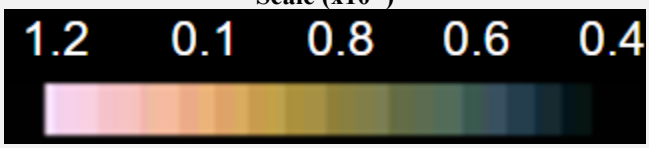		
Diagnosis: DLB; Age: 74, Sex: Male	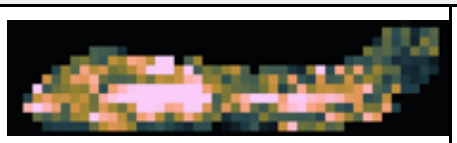	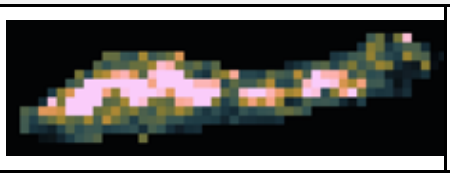	

Appendix C

Table C1: Kendall rank correlations between potential confounders and hippocampal MRI measures for participants in the LB group (n=38).

	Average Volume (mm^3)	*Right Volume (mm^3)*	*Left Volume (mm^3)*	*Average MD (mm^2/s)*	*Right MD (mm^2/s)*	*Left MD (mm^2/s)*	*Average FA*	*Right FA*	*Left FA*	*Age (years)*	*Sex (M: 0, F: 1)*	*Disease Duration (years)*
Average Volume (mm^3)												
Right Volume (mm^3)	0.83 *(<.001)*											
Left Volume (mm^3)	0.87 *(<.001)*	0.71 *(<.001)*										
Average MD (mm^2/s)	-0.00 *(1.0)*	0.03 *(.78)*	-0.02 *(.84)*									
Right MD (mm^2/s)	-0.01 *(.92)*	0.05 *(.63)*	-0.04 *(.71)*	0.81 *(<.001)*								
Left MD (mm^2/s)	0.00 *(1.0)*	-0.02 *(.84)*	0.00 *(.98)*	0.63 *(<.001)*	0.43 *(<.001)*							
Average FA	0.08 *(.50)*	0.10 *(.37)*	0.07 *(.56)*	-0.47 *(<.001)*	-0.42 *(<.001)*	-0.39 *(<.001)*						
Right FA	0.05 *(.65)*	0.08 *(.50)*	0.03 *(.80)*	-0.49 *(<.001)*	-0.43 *(<.001)*	-0.38 *(<.001)*	0.79 *(<.001)*					
Left FA	0.06 *(.64)*	0.07 *(.51)*	0.08 *(.50)*	-0.41 *(<.001)*	-0.35 *(<.001)*	-0.37 *(<.001)*	0.77 *(<.001)*	0.56 *(<.001)*				
Age (years)	-0.32 § *(<.001)*	-0.33 § *(<.001)*	-0.29 *(.01)*	0.16 *(.17)*	0.19 *(.10)*	0.18 *(.12)*	-0.13 *(.24)*	-0.08 *(.50)*	-0.16 *(.16)*			
Sex (M: 0, F: 1)	-0.09 *(.49)*	-0.05 *(.69)*	-0.11 *(.41)*	0.33 *(.02)*	0.23 *(.08)*	0.24 *(.08)*	-0.27 *(.04)*	-0.23 *(.08)*	-0.26 *(.06)*	-0.12 *(.39)*		
Disease Duration (years)	-0.14 *(.21)*	-0.17 *(.14)*	-0.09 *(.41)*	-0.12 *(.30)*	-0.08 *(.47)*	-0.17 *(.14)*	0.04 *(.72)*	-0.02 *(.84)*	0.09 *(.42)*	0.04 *(.73)*	-0.19 *(.17)*	

Computed correlation used kendall-method with pairwise-deletion.

§ Correlations between MRI measures and potential confounders remained significant after FDR correction (when run on average, right, and left hippocampal values separately).

Table C2: Kendall rank correlations between potential confounders and hippocampal MRI measures for participants in the control group (n=35).

	Average Volume (mm^3)	*Right Volume (mm^3)*	*Left Volume (mm^3)*	*Average MD (mm^2/s)*	*Right MD (mm^2/s)*	*Left MD (mm^2/s)*	*Average FA*	*Right FA*	*Left FA*	*Age (years)*	*Sex (M: 0, F: 1)*
Average Volume (mm^3)											
Right Volume (mm^3)	0.85 *(<.001)*										
Left Volume (mm^3)	0.84 *(<.001)*	0.69 *(<.001)*									
Average MD (mm^2/s)	-0.08 *(.50)*	-0.09 *(.43)*	-0.09 *(.48)*								
Right MD (mm^2/s)	-0.14 *(.26)*	-0.11 *(.33)*	-0.17 *(.17)*	0.74 *(<.001)*							
Left MD (mm^2/s)	-0.01 *(.98)*	-0.02 *(.84)*	0.03 *(.84)*	0.65 *(<.001)*	0.40 *(<.001)*						
Average FA	0.23 *(.05)*	0.23 *(.06)*	0.20 *(.09)*	-0.24 *(.05)*	-0.19 *(.11)*	-0.20 *(.09)*					
Right FA	0.23 *(.05)*	0.23 *(.06)*	0.24 *(.05)*	-0.16 *(.17)*	-0.17 *(.16)*	-0.11 *(.35)*	0.80 *(<.001)*				
Left FA	0.17 *(.17)*	0.17 *(.15)*	0.11 *(.37)*	-0.24 *(.04)*	-0.14 *(.23)*	-0.32 *(.01)*	0.77 *(<.001)*	0.57 *(<.001)*			
Age (years)	-0.21 *(.08)*	-0.19 *(.13)*	-0.16 *(.19)*	0.18 *(.13)*	0.12 *(.32)*	0.11 *(.35)*	-0.24 *(.05)*	-0.16 *(.18)*	-0.25 *(.04)*		
Sex (M: 0, F: 1)	-0.11 *(.43)*	-0.16 *(.26)*	-0.07 *(.62)*	0.29 *(.04)*	0.18 *(.20)*	0.28 *(.05)*	-0.18 *(.21)*	-0.17 *(.23)*	-0.13 *(.37)*	0.11 *(.45)*	

Computed correlation used kendall-method with pairwise-deletion.

§ Correlations between MRI measures and potential confounders remained significant after FDR correction (when run on average, right, and left hippocampal values separately).

Table C3: Kendall rank correlations between general health measures and hippocampal volume and MD for participants in the LB group (n=38).

	Average Adjusted Volume	*Right Adjusted Volume*	*Left Adjusted Volume*	*Average Adjusted MD*	*Right Adjusted MD*	*Left Adjusted MD*	*Framingham Risk Score*	*Olfactory Score*	*Age of Onset (years)*	*MDS-UPDRS Axial Score*
Average Adjusted Volume										
Right Adjusted Volume	0.83 *(<.001)*									
Left Adjusted Volume	0.77 *(<.001)*	0.60 *(<.001)*								
Average Adjusted MD	0.13 *(.26)*	0.13 *(.26)*	0.08 *(.47)*							
Right Adjusted MD	0.12 *(.29)*	0.13 *(.27)*	0.06 *(.58)*	0.82 *(<.001)*						
Left Adjusted MD	0.16 *(.15)*	0.14 *(.24)*	0.14 *(.22)*	0.74 *(<.001)*	0.56 *(<.001)*					
Framingham Risk Score	0.07 *(.52)*	0.08 *(.46)*	0.03 *(.77)*	0.06 *(.57)*	0.05 *(.64)*	0.10 *(.39)*				
Olfactory Score	-0.04 *(.71)*	-0.05 *(.66)*	-0.03 *(.83)*	-0.12 *(.30)*	-0.15 *(.21)*	-0.07 *(.57)*	-0.20 *(.10)*			
Age of Onset (years)	0.07 *(.53)*	0.07 *(.53)*	0.03 *(.78)*	-0.13 *(.25)*	-0.08 *(.50)*	-0.15 *(.19)*	0.19 *(.09)*	-0.19 *(.11)*		
MDS-UPDRS Axial Score	-0.05 *(.67)*	-0.07 *(.58)*	-0.05 *(.67)*	0.04 *(.77)*	0.01 *(.95)*	0.09 *(.48)*	0.37 *(<.001)*	-0.33 *(.01)*	0.27 *(.03)*	

Computed correlation used kendall-method with pairwise-deletion.

Table C4: Kendall rank correlations between cognitive measures and hippocampal volume and MD for participants in the LB group (n=38).

	Average Adjusted Volume	*Right Adjusted Volume*	*Left Adjusted Volume*	*Average Adjusted MD*	*Right Adjusted MD*	*Left Adjusted MD*	*MoCA Score*	*Memory Z-Score*	*Executive Function Z-Score*	*Cognitive Speed Z-Score*
Average Adjusted Volume										
Right Adjusted Volume	0.83 *(<.001)*									
Left Adjusted Volume	0.77 *(<.001)*	0.60 *(<.001)*								
Average Adjusted MD	0.13 *(.26)*	0.13 *(.26)*	0.08 *(.47)*							
Right Adjusted MD	0.12 *(.29)*	0.13 *(.27)*	0.06 *(.58)*	0.82 *(<.001)*						
Left Adjusted MD	0.16 *(.15)*	0.14 *(.24)*	0.14 *(.22)*	0.74 *(<.001)*	0.56 *(<.001)*					
MoCA Score	0.05 *(.65)*	0.00 *(1.0)*	0.11 *(.36)*	-0.16 *(.16)*	-0.19 *(.10)*	-0.15 *(.21)*				
Memory Z-Score	0.10 *(.39)*	0.14 *(.21)*	0.02 *(.84)*	-0.02 *(.88)*	-0.01 *(.96)*	-0.03 *(.80)*	0.50 *(<.001)*			
Executive Function Z-Score	0.04 *(.75)*	0.02 *(.83)*	0.02 *(.87)*	0.02 *(.89)*	-0.03 *(.79)*	0.04 *(.70)*	0.51 *(<.001)*	0.36 *(<.001)*		
Cognitive Speed Z-Score	-0.03 *(.79)*	-0.03 *(.77)*	-0.04 *(.72)*	-0.05 *(.68)*	-0.10 *(.36)*	-0.05 *(.66)*	0.47 *(<.001)*	0.42 *(<.001)*	0.44 *(<.001)*	

Computed correlation used kendall-method with pairwise-deletion.

Table C5: Kendall rank correlations between non-cognitive measures and hippocampal volume and MD for participants in the LB group (n=38 for all variables except for sleep score [n=37]).

	Average Adjusted Volume	*Right Adjusted Volume*	*Left Adjusted Volume*	*Average Adjusted MD*	*Right Adjusted MD*	*Left Adjusted MD*	*GDS Score*	*GAD Score*	*Apathy Inventory Score*	*NPI Severity Score*	*PDQ-39 SI Score*	*Sleep Score*
Average Adjusted Volume												
Right Adjusted Volume	0.83 *(<.001)*											
Left Adjusted Volume	0.77 *(<.001)*	0.60 *(<.001)*										
Average Adjusted MD	0.13 *(.26)*	0.13 *(.26)*	0.08 *(.47)*									
Right Adjusted MD	0.12 *(.29)*	0.13 *(.27)*	0.06 *(.58)*	0.82 *(<.001)*								
Left Adjusted MD	0.16 *(.15)*	0.14 *(.24)*	0.14 *(.22)*	0.74 *(<.001)*	0.56 *(<.001)*							
GDS Score	-0.19 *(.10)*	-0.19 *(.11)*	-0.14 *(.23)*	-0.13 *(.25)*	-0.11 *(.34)*	-0.12 *(.32)*						
GAD Score	-0.12 *(.30)*	-0.10 *(.41)*	-0.16 *(.18)*	0.05 *(.68)*	0.03 *(.81)*	0.11 *(.37)*	0.42 *(<.001)*					
Apathy Inventory Score	-0.07 *(.59)*	-0.06 *(.65)*	0.02 *(.85)*	0.09 *(.47)*	0.09 *(.46)*	0.06 *(.61)*	0.26 *(.05)*	0.12 *(.36)*				
NPI Severity Score	-0.18 *(.13)*	-0.09 *(.46)*	-0.25 *(.03)*	-0.05 *(.65)*	-0.02 *(.84)*	-0.04 *(.74)*	0.14 *(.24)*	0.26 *(.04)*	0.32 *(.01)*			
PDQ-39 SI Score	-0.02 *(.83)*	0.01 *(.92)*	0.00 *(1.0)*	-0.13 *(.26)*	-0.09 *(.45)*	-0.12 *(.28)*	0.47 *(<.001)*	0.32 *(.01)*	0.40 *(<.001)*	0.27 *(.02)*		
Sleep Score	-0.13 *(.26)*	-0.14 *(.23)*	-0.17 *(.15)*	0.04 *(.70)*	0.11 *(.36)*	-0.05 *(.69)*	0.24 *(.05)*	0.25 *(.04)*	0.18 *(.16)*	0.30 *(.01)*	0.29 *(.02)*	

Computed correlation used kendall-method with pairwise-deletion.

§ Correlations between MRI measures and non-cognitive measures remained significant after FDR correction (when run on average, right, and left hippocampal values separately).

Table C6: Hippocampal volume comparisons between LB participants (n=38) with clinically significant non-cognitive symptoms.

Clinically Significant Symptom	Average Volume (x10^3 mm^3)			Right-Sided Volume (x10^3 mm^3)			Left-Sided Volume (x10^3 mm^3)		
	With	**Without**	***t* (p)**	**With**	**Without**	***t* (p)**	**With**	**Without**	***t* (p)**
Depression	2.08 (0.35)	2.15 (0.34)	0.6 (.6)	2.16 (0.4)	2.21 (0.35)	0.41 (.7)	2 (0.31)	2.09 (0.35)	0.7 (.5)
Anxiety	2.01 (0.3)	2.15 (0.34)	1.0 (.3)	2.1 (0.3)	2.22 (0.37)	0.7 (.5)	1.91 (0.31)	2.09 (0.34)	1.3 (.2)
Apathy	2.11 (0.41)	2.14 (0.29)	0.2 (.8)	2.16 (0.45)	2.22 (0.3)	0.5 (.6)	2.07 (0.39)	2.06 (0.32)	-0.1 (.9)
MBI Symptoms									
Abnormal Thoughts	2.04 (0.32)	2.14 (0.34)	0.7 (.5)	2.14 (0.34)	2.21 (0.36)	0.4 (.7)	1.93 (0.31)	2.08 (0.34)	0.9 (.4)
Decreased Motivation	2.11 (0.32)	2.14 (0.35)	0.2 (.8)	2.19 (0.36)	2.2 (0.37)	0.1 (.9)	2.04 (0.31)	2.08 (0.36)	0.4 (.7)
Emotional Dysregulation	2.02 (0.33)	2.35 (0.24)	3.2 (**.003**)‡	2.1 (0.36)	2.39 (0.27)	2.6 (**.02**)‡	1.94 (0.31)	2.31 (0.25)	3.7 (**.001**)‡§
Impulse Dyscontrol	2.14 (0.35)	2.12 (0.33)	-0.1 (.9)	2.24 (0.35)	2.17 (0.37)	-0.6 (.5)	2.04 (0.38)	2.08 (0.32)	0.4 (.7)
Social Inappropriateness	2.23 (0.4)	2.12 (0.33)	-0.6 (.6)	2.31 (0.43)	2.18 (0.35)	-0.7 (.5)	2.14 (0.38)	2.05 (0.34)	-0.5 (.6)

Note: Participants were determined as having clinically significant symptoms if questionnaire scores were: above 11 on the GDS-30 (for clinically significant depression; *n*=10 participants), above 10 on the GAD-7 (for clinically significant anxiety; *n*=6 participants), and 1 or higher on the Apathy Inventory (for clinically significant apathy; *n*=14 participants). Responses to questions on the NPI were used to determine the presence of behavioural symptoms in the five MBI domains: Abnormal thoughts (*n*=5 participants), decreased motivation (*n*=15 participants), emotional dysregulation (*n*=25 participants), impulse dyscontrol (*n*=15 participants), and social inappropriateness (*n*=4 participants).
Values of $p < .05$ are bolded.
LB: Lewy Body; MBI: Mild Behavioral Impairment; GDS-30: Geriatric Depression Scale (30 items); GAD-7: Generalized Anxiety Disorder (7 items); NPI: Neuropsychiatric Inventory.
‡ Comparison is significant when comparing age- and sex-adjusted standardized FA values.
§ Comparison between age- and sex-adjusted standardized MRI measures remained significant after FDR correction (when run separately across each set of *p*-values obtained for average, right-sided, and left-sided volume).

Table C7: Hippocampal MD comparisons between LB participants with clinically significant non-cognitive symptoms.

Clinically Significant Symptom	Average MD (x10^{-3} mm^2/s)			Right-Sided MD (x10^{-3} mm^2/s)			Left-Sided MD (x10^{-3} mm^2/s)		
	With	**Without**	***W* (p)**	**With**	**Without**	***W* (p)**	**With**	**Without**	***W* (p)**
Depression	0.81 (0.1)	0.8 (0.05)	155 (.6)	0.82 (0.1)	0.82 (0.05)	156 (.6)	0.8 (0.12)	0.78 (0.05)	143 (.9)
Anxiety	0.83 (0.15)	0.8 (0.04)	120 (.4)	0.83 (0.14)	0.82 (0.04)	120 (.4)	0.84 (0.17)	0.78 (0.04)	109 (.6)
Apathy	0.81 (0.08)	0.8 (0.05)	188 (.6)	0.83 (0.07)	0.81 (0.06)	157 (.8)	0.8 (0.1)	0.78 (0.06)	180 (.7)
MBI Symptoms									
Abnormal Thoughts	0.78 (0.03)	0.81 (0.07)	91 (.7)	0.81 (0.04)	0.82 (0.07)	80 (.9)	0.76 (0.02)	0.79 (0.08)	118 (.1)
Decreased Motivation	0.8 (0.09)	0.81 (0.05)	230 (.09)	0.81 (0.09)	0.82 (0.05)	199 (.4)	0.78 (0.1)	0.79 (0.05)	246 (**.03**)
Emotional Dysregulation	0.81 (0.08)	0.80 (0.03)	181 (.6)‡	0.82 (0.08)	0.82 (0.03)	193 (.4)‡	0.79 (0.09)	0.78 (0.05)	164 (1)
Impulse Dyscontrol	0.82 (0.09)	0.79 (0.04)	149 (.5)	0.84 (0.08)	0.81 (0.05)	151 (.5)	0.81 (0.11)	0.77 (0.03)	151 (.5)
Social Inappropriateness	0.86 (0.15)	0.8 (0.05)	69 (1)	0.86 (0.11)	0.82 (0.06)	56 (.6)	0.85 (0.18)	0.78 (0.05)	74 (.8)

Note: Participants were determined as having clinically significant symptoms if questionnaire scores were: above 11 on the GDS-30 (for clinically significant depression; *n*=10 participants), above 10 on the GAD-7 (for clinically significant anxiety; *n*=6 participants), and 1 or higher on the Apathy Inventory (for clinically significant apathy; *n*=14 participants). Responses to questions on the NPI were used to determine the presence of behavioural symptoms in the five MBI domains: Abnormal thoughts (*n*=5 participants), decreased motivation (*n*=15 participants), emotional dysregulation (*n*=25 participants), impulse dyscontrol (*n*=15 participants), and social inappropriateness (*n*=4 participants).

Values of p <.05 are bolded. MD: Mean Diffusivity; LB: Lewy Body; MBI: Mild Behavioral Impairment; GDS-30: Geriatric Depression Scale (30 items); GAD-7: Generalized Anxiety Disorder (7 items); NPI: Neuropsychiatric Inventory.

‡ Comparison is significant when comparing age- and sex-adjusted standardized FA values.

§ Comparison between age- and sex-adjusted standardized MRI measures remained significant after FDR correction (when run separately across each set of *p*-values obtained for average, right-sided, and left-sided MD).